

## The Role of Algae in Fine Cohesive Sediment Flocculation

Deng, Z.

**DOI**

[10.4233/uuid:07ed19ec-52a8-4abb-ad7f-64eaace73f3a](https://doi.org/10.4233/uuid:07ed19ec-52a8-4abb-ad7f-64eaace73f3a)

**Publication date**

2022

**Document Version**

Final published version

**Citation (APA)**

Deng, Z. (2022). *The Role of Algae in Fine Cohesive Sediment Flocculation*. [Dissertation (TU Delft), Delft University of Technology]. <https://doi.org/10.4233/uuid:07ed19ec-52a8-4abb-ad7f-64eaace73f3a>

**Important note**

To cite this publication, please use the final published version (if applicable).  
Please check the document version above.

**Copyright**

Other than for strictly personal use, it is not permitted to download, forward or distribute the text or part of it, without the consent of the author(s) and/or copyright holder(s), unless the work is under an open content license such as Creative Commons.

**Takedown policy**

Please contact us and provide details if you believe this document breaches copyrights.  
We will remove access to the work immediately and investigate your claim.

# **The Role of Algae in Fine Cohesive Sediment Flocculation**

生物作用下的粘性细颗粒泥沙絮凝



# **The Role of Algae in Fine Cohesive Sediment Flocculation**

生物作用下的粘性细颗粒泥沙絮凝

## **Dissertation**

for the purpose of obtaining the degree of doctor

at Delft University of Technology

by the authority of the Rector Magnificus, Prof.dr.ir. T.H.J.J. van der Hagen

chair of the Board for Doctorates

to be defended publicly on

Monday 21 February 2022 at 10:00 o'clock

by

**Zhirui DENG**

Bachelor of Science in Marine Resources of Biology and Environment

Sun Yat-Sen University, China

born in Guangxi, China

This dissertation has been approved by the promotor.

Composition of the doctoral committee:

Rector Magnificus	chairman
Prof.dr.ir. Z.B. Wang	Delft University of Technology, promotor
Prof.dr. Q. He	East China Normal University, promotor
Dr. C. Chassagne	Delft University of Technology, promotor

Independent members:

Prof.dr. P.M.J. Herman,	Delft University of Technology
Prof.dr. A.J. Manning,	University of Plymouth, United Kingdom
Prof.dr. Q. Liu,	East China Normal University, China
Dr. M. Fettweis,	Royal Belgian Institute of Natural Sciences, Belgium
Prof.dr. J.D. Pietrzak,	Delft University of Technology, reserve member

The doctoral research has been carried out in the context of an agreement on joint doctoral supervision between East China Normal University, China and Delft University of Technology, the Netherlands.



Keywords: Sediment, Flocculation, Algae, Biological effects, Hydrodynamics

Cover: Changjiang estuary sunset

Copyright © 2022 by Zhirui Deng (Email: [Z.Deng-1@tudelft.nl](mailto:Z.Deng-1@tudelft.nl))

Printed by: ProefschriftMaken.nl

ISBN: 978-94-6423-679-8

An electronic version of this dissertation is available at

<http://repository.tudelft.nl/>.

All rights reserved. No part of the material protected by this copyright notice may be reproduced or utilized in any form or by any mean, electronic or mechanical, including photocopying, recording or by any information storage and retrieval system, without the prior permission of the author.

*To my family for patience and encouragement*



# Contents

<b>Summary</b>	<b>xi</b>
<b>Samenvatting</b>	<b>xvii</b>
<b>摘要</b>	<b>xxiii</b>
<b>1 Introduction</b>	<b>1</b>
1.1 Background . . . . .	1
1.2 Goals and approach . . . . .	5
1.3 Outline . . . . .	6
<b>2 Literature survey</b>	<b>9</b>
2.1 Flocculation mechanisms . . . . .	9
2.1.1 Collision frequency . . . . .	9
2.1.2 Collision efficiency . . . . .	12
2.2 Flocculation by organic matter . . . . .	15
2.3 Break-up mechanisms . . . . .	17
2.3.1 The Kolmogorov microscale . . . . .	19
2.4 Characteristics of Floccs . . . . .	21
2.4.1 Floc sizes and shapes . . . . .	21
2.4.2 Floc density and settling velocity . . . . .	23
2.4.3 Floc composition . . . . .	25
2.5 Other influence factors . . . . .	29
2.6 Discussion . . . . .	30
<b>3 Methodology</b>	<b>33</b>
3.1 Laboratory measurements . . . . .	34
3.1.1 Experimental samples . . . . .	34
3.1.2 Static Light Scattering (SLS) . . . . .	36

3.1.3	Settling columns . . . . .	38
3.1.4	Microscopy . . . . .	38
3.1.5	Zeta potential and Conductivity . . . . .	39
3.1.6	LabsFLOC-2 camera system (Laboratory Spectral Flocculation Characteristics, version 2) . . . . .	40
3.1.7	Experimental setup . . . . .	42
3.2	In-situ observations . . . . .	44
3.2.1	Changjiang Estuary Hydrodynamics . . . . .	44
3.2.2	Instruments . . . . .	47
3.2.3	Monitoring campaigns . . . . .	50
3.3	Data processes . . . . .	51
3.3.1	Laboratory measurements data processes . . . . .	51
3.3.2	Hydrodynamics data processes . . . . .	51
3.3.3	Flocculation data processes . . . . .	52
3.3.4	Chlorophyll data processes . . . . .	53
3.3.5	Others . . . . .	54
<b>4</b>	<b>A laboratory study on the behavior of estuarine sediment flocculation as function of salinity, EPS and living algae</b>	<b>55</b>
4.1	Introduction . . . . .	56
4.2	Sediment, EPS and algae flocs . . . . .	57
4.3	Salinity and EPS effects . . . . .	60
4.3.1	Evolution of the flocculation with salinity . . . . .	60
4.3.2	Evolution of sediment flocculation with EPS and salinity . . . . .	60
4.3.3	Experiments with sea water . . . . .	62
4.3.4	Electrokinetic studies . . . . .	65
4.4	Experiments with living algae . . . . .	67
4.4.1	Flocculation with living algae in demi-water . . . . .	67
4.4.2	Flocculation with living algae in salt water . . . . .	72
4.4.3	Comparisons between EPS and living algae influences on flocculation . . . . .	74
4.5	Evolutions of the algae-sediment flocculation . . . . .	76
4.6	Conclusions . . . . .	82

<b>5</b>	<b>The role of algae in fine sediment flocculation: in-situ and laboratory measurements</b>	<b>85</b>
5.1	Introduction . . . . .	86
5.2	Hydrodynamics and flocculation in a tidal period. . . . .	90
5.2.1	In-situ versus laboratory OBS and chlorophyll estimations. . . . .	90
5.2.2	Hydrodynamics, and salinity . . . . .	91
5.2.3	Suspended sediment, floc and chlorophyll characteristics . . . . .	91
5.3	Shear rate influence on the floc size and its density . . . . .	93
5.4	Evolution of the particle size distribution at different . . . . .	95
5.4.1	At Maximum Flood Velocity (MFV) and Maximum Ebb Velocity (MEV). . . . .	95
5.4.2	At High Water Slack (HWS) and Low Water Slack (LWS) . . . . .	98
5.5	Role of algae in the particle size distribution . . . . .	98
5.5.1	Algae-sediment ratio in in-situ conditions . . . . .	101
5.5.2	Algae-sediment flocculation process in laboratory . . . . .	102
5.5.3	Link between in-situ observations and laboratory measurements . . . . .	107
5.6	Conclusions . . . . .	108
<b>6</b>	<b>Seasonal variation of floc population influenced by the presence of algae in the Changjiang (Yangtze River) Estuary</b>	<b>111</b>
6.1	Introduction . . . . .	112
6.2	Seasonal variations. . . . .	115
6.3	Mean floc properties in winter and in summer surveys . . . . .	118
6.3.1	Variations with shear rate, salinity and SSC. . . . .	120
6.3.2	Variation with CC and CC/SSC in the tidal cycle. . . . .	120
6.4	Particle Size Distributions (PSDs) in winter and summer surveys . . . . .	123
6.4.1	Variation within the tidal cycle . . . . .	123
6.4.2	Particle characteristics at the top of the water column . . . . .	124

---

6.5	Floc classes . . . . .	126
6.5.1	Variation with CC/SSC . . . . .	126
6.5.2	Transfer between classes . . . . .	127
6.6	Conclusions . . . . .	131
<b>7</b>	<b>Conclusions and recommendations</b>	<b>135</b>
7.1	Findings of this study . . . . .	135
7.2	Applications . . . . .	142
7.3	Recommendations for future work . . . . .	143
	<b>References</b>	<b>145</b>
	<b>List of symbols</b>	<b>173</b>
	<b>List of acronyms</b>	<b>175</b>
	<b>Acknowledgements</b>	<b>177</b>
	<b>List of Publications</b>	<b>181</b>
	<b>Curriculum Vitæ</b>	<b>183</b>

# Summary

Flocculation is an important process in fine cohesive sediment transport that still requires investigation as it is a complex process, involving the aggregation, break-up and reformation of mineral and biological particles.

Fine cohesive sediments are found in rivers, estuaries and their adjacent areas. With the rapid economic development in the Changjiang (Yangtze River) estuary, human activities have intensified, including the development of shipping, and the exploitation of water and soil resources. The erosion and deposition problems in waterways and tidal flats have become increasingly prominent, affecting the evolution of geomorphology and ecological environment.

In estuaries under combined action of fluvial and marine processes, flocculation of cohesive sediment has many influencing factors involving complex mechanisms. At present, the occurrence of flocculation, the transport and settling processes of sediment flocs cannot be accurately predicted. Up to now, the research on sediment flocculation in estuaries mainly focuses on the influence of physical factors such as hydrodynamics, suspended sediment concentration and salinity, while the research on the influence of biological factors is insufficient. Fully understanding sediment flocculation and its effect on sediment transport is not only beneficial to sediment transport modelling, but also for the research on the transport of the material carried by sediment particles, such as heavy metals, organic pollutants and nutrient substances. Better understanding flocculation can help to solve many engineering problems associated to river channel management, channel siltation, mudflat evolution, and the corresponding ecological problems which are ongoing with changes in climate and environment.

In this study, the influence of biology on sediment flocculation and the characteristics of flocs and transport processes of flocculated sediment under different conditions are investigated by combining laboratory experiments and in-situ observations.

In the laboratory experiments, grab sediment samples from the Changjiang Estuary were analyzed by Static Light Scattering (SLS). This study was mainly meant to

understand the characteristics of flocculation processes (timescales, floc sizes) for different environmental conditions at constant shear. These conditions were adapted by changing salinity and studying the effect of the presence of the microalgae *Skeletonema costatum* which is one the dominant algae species in the Changjiang estuary. The effect of extracellular polymeric substances (EPS) on flocculation was also studied. EPS is usually secreted by microorganisms. Mean floc particle size, particle size distributions, zeta potential and conductivity were recorded and correlated to each other.

During the in-situ survey, the characteristics of flocculation in different tidal cycles, seasons and locations in the maximum turbidity zone of the Changjiang estuary were observed. In-situ laser diffraction technique (by means of a LISST-100C) was used to obtain in-situ volume concentration and particle size distribution. Combined with hydrodynamic data recorded synchronously, the effects of biology under different hydrodynamic conditions on sediment flocculation and transport was analyzed and discussed.

The key conclusions obtained are as follows:

### **1. The effects and mechanisms of algae, extracellular polymers (EPS) and salinity (Chapter 4).**

In the laboratory experiments, sediment flocculation is different in the presence of algae, EPS and dissolved salt: (1) Algae particles can form large flocs by themselves, the floc size distribution (PSD) presents a bimodal curve when algae and sediment particles are mixed. With the progress of flocculation, the bimodal curve gradually merged into a unimodal curve, and the overall floc size increased. (2) The effect of EPS needs the participation of cations. The floc size changes little with EPS in fresh water, while the flocculation is remarkable under the influence of salinity. (3) Salinity can promote sediment flocculation, and the flocculation effect of divalent cations ( $\text{MgCl}_2$  and  $\text{CaCl}_2$ ) is greater than that of monovalent cations ( $\text{NaCl}$ ).

Algae and EPS can significantly promote the flocculation of sediment, and the flocculation time is short, while salinity has a weak influence, with smaller flocs and longer flocculation time. The presence of salt ions in the water changes the surface potential of sediment particles and the flocs are formed by the DLVO interaction force between sediment particles.

The algae change the floc's composition and form large algae-sediment mixed

flocs by combining algae-formed flocs with sediment particles. EPS, as a connecting medium, has bridging effect between sediment particles under the action of cations.

## **2. Coupling effect of algae and suspended sediment in flocculation process (Chapter 4, Chapter 5 and Chapter 6).**

Both in-situ observations and laboratory experiments show that algae and sediment are coupled. In field observations, a correlation was found between algae concentration and suspended sediment concentration (SSC) in estuary area. In this study, the ratio of chlorophyll concentration (CC) to suspended sediment concentration is taken as the parameter to represent the algae effects, which is abbreviated as algae-sediment ratio (CC/SSC). Both chlorophyll concentration and suspended sediment concentration show a trend that increases with the increase of water depth in an estuarine area. The algae-sediment ratio not only reflects the role played by algae in the formation of flocs, and therefore can help to study sediment flocculation in the water column.

In laboratory experiments, increasing algae-sediment ratio promotes the flocculation process, and the flocs formed have larger particle size and faster flocculation rate. In the field observations, the algae-sediment ratio increases significantly in the middle and bottom layers of the water column during the short period after high water slack in summer, which reflects the fact that algae are settling during the sediment flocculation process (differential settling).

## **3. Biological effects on sediment flocculation in estuarine area (Chapter 5 and Chapter 6).**

Most of the algae particles in the Changjiang Estuary are distributed in the part where the floc population has an average size larger than 100  $\mu\text{m}$ . When the concentration of algae is high with respect to the sediment concentration (the algae-sediment ratio is high), the floc particle size distribution (PSD) will display a bimodal curve with one peak associated to sediment particles and one to algae particles. The bimodal PSD and unimodal PSD are interchangeable due to variation of tidal hydrodynamics and the main peaks are located in the range 10–100  $\mu\text{m}$ . The effective density and settling velocity of flocs in this size range are related to the flocculation time. Flocculation time influences settling velocity, as particles grow and have a time-dependent density upon flocculation. This is very important for sediment transport models. Instead of using constant sediment settling velocity, sediment transport models should account for

a change in settling velocity of flocs. In line with previous studies, it was found that flocs can be divided into three components according to their particle size distribution: Single-grain ( $< 5 \mu\text{m}$ ), Microflocs ( $5\text{--}200 \mu\text{m}$ ) and Macroflocs ( $> 200 \mu\text{m}$ ). The main flocculation mechanism is related to the change of microflocs into macroflocs.

The algae-sediment flocculation process in estuaries is mainly affected by shear rate. During the high water slack period, a low shear rate is maintained for about 2–3 hours, and the algae particles and sediment particles are fully mixed under relatively stable hydrodynamic conditions to form unimodal large flocs with a particle size of about  $40\text{--}80 \mu\text{m}$ . Flocculation is then close to steady-state. Salinity and other factors have no significant influence on algae-sediment flocculation process in estuarine area.

#### **4. Temporal and spatial variation of biological effects and tidal asymmetry of sediment settling (Chapter 6).**

The effect of algae is of more importance in summer due to higher algae concentration than in winter. The variation of flood and ebb tide indicates different flocculation processes in summer: during flood tide, the algae-sediment ratio increases in the upper layer of the water column and algae-sediment flocculation occurs in the early flood period, forming large flocs with low density and high settling velocity. In the following 2–3 hours, the large flocs gradually settled to the middle and bottom layers of the water column, and the floc size distribution changes from bimodal to unimodal. In the short period after high water slack (within 1–2 hours), the suspended sediment concentration decreases significantly as many sediment particles have settled to the bed. During ebb, the flocculation efficiency decreases due to the decrease in suspended sediment concentration and seawater retreat (which contains most algae), so there are no double peak PSDs and the mean floc size and settling velocity is smaller than that during flood. Consequently, it can be concluded that algae promote the asymmetry of sediment settling during ebb and flood tide, which is an important factor causing sediment transport toward the estuary in a tidal cycle.

To sum up, the combination of laboratory experiment and in-situ observation results is helpful to deeply understand flocculation kinetics. This study establishes the relationship between sediment transport and ecological cycle in estuarine area. The

coupling phenomenon between biology and sediment showed that sediment flocculation not only affects the evolution of estuarine geomorphology, but is also an important process in estuarine ecological cycle.



# Samenvatting

Flocculatie is een belangrijk proces bij het transport van slib dat nog steeds onderzoek vereist. Het is een complex proces waarbij minerale en organische deeltjes aggregeren, opbreken en opnieuw worden gevormd.

Slib wordt aangetroffen in rivieren, estuaria en de aangrenzende gebieden. De ontwikkeling van het getij en de bodemligging in het estuarium van de Changjiang (Yangtze-rivier) worden beïnvloed door een combinatie van klimaat- en milieuverandering en de snelle economische ontwikkeling in het estuarium met bijbehorende menselijke activiteiten zoals scheepvaart. De erosie- en depositieproblemen in waterwegen en droogvallende platen zijn steeds belangrijker geworden en beïnvloeden de ontwikkeling van de geomorfologie en ecologie.

Flocculatie wordt door veel complexe mechanismen en factoren zoals rivier- en zeestromingen beïnvloed. Het optreden van flocculatie, het transport en de bezinkingsprocessen van vlokken kunnen niet nauwkeurig worden voorspeld. Het optreden van flocculatie, het transport en de bezinkingsprocessen van sedimentvlokken niet nauwkeurig te voorspellen. Momenteel richt het onderzoek naar flocculatie in estuaria zich vooral op de invloed van fysische processen zoals hydrodynamica, gesuspendeerde sedimentconcentratie en saliniteit, terwijl het onderzoek naar de invloed van biologische factoren onvoldoende is. Een beter begrip van de invloed van flocculatie op sedimenttransport is niet alleen gunstig voor de voorspellingen van sedimentmodellen, maar ook voor het onderzoek naar het transport van stoffen die geboden zijn aan sedimentdeeltjes, zoals zware metalen, organische verontreinigingen en nutriënten. Een beter begrip van flocculatie kan helpen bij het oplossen van veel technische problemen die verband houden met het beheer van riviergeulen, het aanslibben van vaargeulen, de ontwikkeling van intergetijdengebieden en de bijbehorende ecologische problemen die zich voordoen bij veranderingen in klimaat en milieu.

In deze studie wordt de invloed van biologie op sedimentflocculatie en de kenmerken van vlokken en transportprocessen van geflocculeerd sediment onder invloed

van verschillende omstandigheden bestudeerd door laboratoriumexperimenten en in-situ observaties te combineren.

In de laboratoriumexperimenten werden bodemonsters uit het Changjiang-estuarium geanalyseerd met Static Light Scattering (SLS). Deze studie werd voornamelijk gebruikt om de kenmerken van flocculatieprocessen (tijdschalen, vloggroottes) voor verschillende omgevingscondities bij constante afschuiving te begrijpen. Deze omstandigheden werden aangepast door het zoutgehalte te veranderen en het effect te bestuderen van de aanwezigheid van de microalg *Skeletonema costatum*, één van de dominante algensoorten in het Changjiang-estuarium. Ook werd het effect van extracellulaire polymere stoffen (EPS) op flocculatie bestudeerd. EPS wordt meestal uitgescheiden door micro-organismen. Gemiddelde vlokdeeltjesgrootte, deeltjesgrootteverdelingen, zèta-potentiaal en geleidbaarheid werden geregistreerd en aan elkaar gecorreleerd.

Tijdens het in-situ onderzoek werden de kenmerken van flocculatie in verschillende getijcycli, seizoenen en locaties in de zone met maximale troebelheid van het Changjiang estuarium bestudeerd. In-situ laserdiffractietechniek (door middel van een LISST-100C) werd gebruikt om in-situ volumeconcentratie en deeltjesgrootteverdeling te bepalen. Gecombineerd met synchroon geregistreerde hydrodynamische gegevens, werden de effecten van biologie onder verschillende hydrodynamische omstandigheden op flocculatie en transport geanalyseerd en besproken.

De belangrijkste conclusies zijn als volgt:

### **1. De effecten en mechanismen van algen, extracellulaire polymeren (EPS) en saliniteit (Hoofdstuk 4).**

In de laboratoriumexperimenten is sedimentflocculatie anders in aanwezigheid van algen, EPS en opgelost zout: (1) Algendeeltjes kunnen zelf grote vlokken vormen, de vloggrootteverdeling (PSD) vertoont een bimodale curve wanneer algen en sedimentdeeltjes worden gemengd. Met de voortgang van de flocculatie, ging de bimodale curve geleidelijk over in een unimodale curve en nam de totale vloggrootte toe. (2) Het effect van EPS vereist de deelname van kationen. De vloggrootte verandert weinig met EPS in zoet water, terwijl de uitvlokking sterk is onder invloed van het zoutgehalte. (3) Het zoutgehalte kan de uitvlokking van sedimenten bevorderen en het uitvlokkingseffect van tweewaardige kationen ( $MgCl_2$  en  $CaCl_2$ ) is groter dan dat van eenwaardige kationen ( $NaCl$ ).

Algen en EPS kunnen de flocculatie van sediment aanzienlijk bevorderen, en de flocculatietijd is kort, terwijl het zoutgehalte een zwakke invloed heeft, met kleinere vlokken en een langere flocculatietijd. De aanwezigheid van zoutionen in het water verandert de oppervlaktepotentiaal van sedimentdeeltjes en de vlokken worden gevormd door de DLVO-interactiekraft tussen sedimentdeeltjes.

De algen veranderen de vloksamenstelling en vormen grote samengestelde vlokken die bestaan uit zowel algen als sediment door vlokken met algen te combineren met sedimentdeeltjes. EPS heeft als verbindend medium een overbruggende werking tussen sedimentdeeltjes onder invloed van kationen.

## **2. Koppelingseffect van algen en zwevend sediment in flocculatieproces (Hoofdstuk 4, Hoofdstuk 5 en Hoofdstuk 6).**

Zowel in-situ waarnemingen als laboratoriumexperimenten laten zien dat algen en sediment gekoppeld zijn. In veldwaarnemingen werd een correlatie gevonden tussen de algenconcentratie en de gesuspenderde sedimentconcentratie (SSC) in het estuariumgebied. In deze studie wordt de verhouding tussen de chlorofylconcentratie en de gesuspenderde sedimentconcentratie gebruikt als indicator om de algeneffecten weer te geven. Deze verhouding wordt afgekort als algen-sedimentverhouding (CC/SSC). Zowel de chlorofylconcentratie als de gesuspenderde sedimentconcentratie vertonen een trend die toeneemt met de toename van de waterdiepte. De algen-sedimentverhouding weerspiegelt niet alleen de rol die algen spelen bij de vorming van vlokken, maar kan ook helpen bij het bestuderen van sedimentflocculatie in de waterkolom, die wordt gedomineerd door algeneffecten.

In laboratoriumexperimenten bevordert een toenemende algen-sedimentverhouding het flocculatieproces, en de gevormde vlokken hebben een grotere deeltjesgrootte en een snellere flocculatiesnelheid. In de veldwaarnemingen neemt de algen-sedimentverhouding aanzienlijk toe in de middelste en onderste lagen van de waterkolom tijdens de late vloedperiode in de zomer, wat een weerspiegeling is van het feit dat algen bezinken tijdens het sedimentflocculatieproces (differentiële bezinking).

## **3. Biologische effecten op sedimentflocculatie in estuariene gebieden (Hoofdstuk 5 en Hoofdstuk 6).**

De meeste algendeeltjes in het Changjiang-estuarium zijn verspreid in het deel waar de vlokpopulatie gemiddeld groter is dan 100  $\mu\text{m}$ . Wanneer de concentratie van al-

gen hoog is ten opzichte van de sedimentconcentratie (de algen-sedimentverhouding is hoog), zal de vlokdeeltjesgrootteverdeling (PSD) een bimodale curve vertonen met één piek geassocieerd met sedimentdeeltjes en één met algendeeltjes. De bimodale PSD- en unimodale PSD-curves wisselen elkaar af afhankelijk van de getijfase en bevinden zich in het bereik van 10–100  $\mu\text{m}$ . De effectieve dichtheid en bezinkingssnelheid van vlokken in dit groottebereik zijn gerelateerd aan de uitvlokkingsstijd. De uitvlokkingsstijd beïnvloedt de bezinkingssnelheid, aangezien deeltjes groeien en een tijdsafhankelijke dichtheid hebben bij uitvlokkingsproces. Dit is erg belangrijk voor sedimenttransportmodellen. Deze modellen moeten rekening houden met een verandering in de bezinkingssnelheid van vlokken over het getij; de bezinkingssnelheid mag dus niet constant worden verondersteld. In overeenstemming met eerdere studies werd gevonden dat vlokken kunnen worden onderverdeeld in drie componenten op basis van hun deeltjesgrootteverdeling: enkelkorrelige ( $< 5 \mu\text{m}$ ), microvlokken (5–200  $\mu\text{m}$ ) en macrovlokken ( $> 200 \mu\text{m}$ ). Het belangrijkste uitvlokkingsmechanisme houdt verband met de verandering van microvlokken in macrovlokken.

Het uitvlokkingsproces van algen en sedimenten in estuaria wordt voornamelijk beïnvloed door de afschuifsnelheid. Tijdens de periode van hoogwaterkentering treedt gedurende ongeveer 2–3 uur een lage afschuifsnelheid op en worden de algendeeltjes en sedimentdeeltjes volledig gemengd onder relatief stabiele hydrodynamische omstandigheden om unimodale grote vlokken te vormen met een deeltjesgrootte van ongeveer 40–80  $\mu\text{m}$ . Uitvlokkingsproces is dan dicht bij dynamisch evenwicht. Het zoutgehalte en andere factoren hebben geen significante invloed op het flocculatieproces van algen en sediment in estuariene gebieden.

#### **4. Temporele en ruimtelijke variatie van biologische effecten en getijdenasymmetrie van sedimentafzetting (Hoofdstuk 6).**

De werking van algen is in de zomer belangrijker vanwege de hogere algenconcentratie dan in de winter. De variatie van vloed en eb wijst op verschillende flocculatieprocessen in de zomer: in de vloedperiode neemt de algen-sedimentverhouding in de bovenste waterlaag toe en algen-sedimentflocculatie treedt op in de vroege vloedperiode, waarbij grote vlokken met een lage dichtheid en hoge valsnelheid worden gevormd. In de volgende 2 tot 3 uur ontwikkelen er zich geleidelijk grote vlokken in de middelste en onderste waterlagen en verandert de verdeling van de vloggrootte

van bimodaal in unimodaal. Aan het einde van de vloedperiode (binnen 1 à 2 uur na de periode van laagwater) neemt de gesuspendeerde sedimentconcentratie aanzienlijk af omdat veel sedimentdeeltjes zijn bezonken. In de ebperiode neemt de flocculatie-efficiëntie af door de afname van de concentratie van gesuspendeerd sediment en de terugtrekking van zeewater (waarin zich de meeste algen bevinden), dus er zijn geen bimodale PSD's en de gemiddelde vlok grootte en bezinkingssnelheid is kleiner dan bij vloed. Als gevolg hiervan kan worden geconcludeerd dat algen de asymmetrie van sedimentbezinking tijdens eb en vloed vergroten, wat een belangrijke invloed heeft op het residuele sedimenttransport naar het estuarium over een getijcyclus.

Samenvattend kan worden gesteld dat de combinatie van laboratoriumexperimenten en in-situ waarnemingen nuttig is om de kinetiek en mechanismen van flocculatie te doorgronden. Deze studie legt de relatie vast tussen sedimenttransport en de ecologische cyclus in estuaria. De koppeling tussen biologie en sedimenttransport toonde aan dat sedimentflocculatie niet alleen de ontwikkeling van de estuariene geomorfologie beïnvloedt, maar ook een belangrijk proces is in de ecologische cyclus van het estuarium.



# 摘要

絮凝 (Flocculation) 是粘性细颗粒泥沙 (Fine cohesive sediment) 运动中的一个重要过程。在天然水体中, 大部分的粘性细颗粒泥沙以絮团 (Floc) 的形式进行运动, 由于絮团具有不同于分散泥沙颗粒的特殊性质, 其对泥沙悬浮、输运、沉降、固结以及再悬浮等过程有显著影响。絮凝涉及矿物和生物颗粒的聚集、分散和重构等复杂过程, 目前仍未得到充分的解释。因此, **对泥沙絮凝的研究, 是泥沙运动力学中的重要科学问题, 不仅有利于泥沙模型的预测, 而且有利于研究泥沙颗粒所携带的重金属、有机污染物和营养物等物质迁移过程, 更有助于解决生态环境的保护等问题。**

粘性细颗粒泥沙广泛存在于河流、河口及其邻近区域。在气候和环境不断变化的背景下, 随着长江河口地区经济快速发展, 人类活动对于河口航运、水土资源的开发力度不断加大, 航道和潮滩等地区的冲淤问题日益凸显, 并影响着地貌和生态环境的演化。在河口径潮流作用下, 絮凝影响因素多, 机制复杂, 其发育、输运及沉降过程仍无法准确预测。因此, **对河口地区泥沙絮凝的研究, 具有理论和应用方面的迫切需求, 不仅有利于改进只考虑恒定流速泥沙模型, 而且有利于解决河道治理、航道淤积、水库和港口的维护和深化、潮滩演变等工程问题。**

目前对河口地区泥沙絮凝的研究主要集中在水动力、含沙量和盐度等物理过程的影响, 生物因素的影响研究不足。尤其在长江口区域, 浮游生物丰度高、分布广、种类多, 具有丰富的时空变化, 并时常爆发藻华等危害。此外, 长江口泥沙运动复杂, 水体混合强烈, 泥沙运动和生物活动必然会相互影响, 且生物活动和泥沙絮凝均受多种因素的综合作用。因此, **生物作用下的泥沙絮凝过程是个具有挑战性的问题, 了解生物因素在泥沙絮凝中的作用机制, 是全面理解河口泥沙运动的必要环节, 更是连接粘性细颗粒泥沙运动与生物地球化学循环之间的关键纽带。**

本研究的主要目标有: (1) 通过室内实验分析, 探究不同影响因子 (藻类、EPS 和阳离子) 下泥沙絮凝的变化过程和特征, 深入了解生物泥沙絮凝过程中的不同机制; (2) 通过现场观测分析, 获得河口地区泥沙絮凝的特征参数, 包括

絮团粒径 ( $D_{50}$ )、粒度分布 (PSD)、有效密度 ( $\Delta\rho$ ) 和沉速 ( $\omega_s$ ) 等, 结合水文水动力条件, 包括藻类浓度/叶绿素浓度 (CC, Chlorophyll Concentration)、剪切率 ( $G$ , Shear rate)、含沙量 (SSC, Suspended Sediment Concentration)、盐度等, 探究生物作用下河口泥沙絮凝的特性和变化过程; (3) 将室内实验和现场观测的生物絮凝变化特征相结合, 分析生物活动与泥沙变化的耦合关系, 通过参数建立藻类和泥沙的联系, 探究藻类与泥沙共同作用的现象与机制; (4) 通过分析泥沙絮凝特征的时空变化, 剖析生物作用的表征与效应, 阐明生物对河口泥沙絮凝沉降过程的作用。**拟解决的关键科学问题:** 旨在填补河口和沿海地区生物活动对泥沙运动过程影响的认识空白, 特别是研究生物 (如藻类) 在泥沙絮凝中的作用。**拟解决的关键技术**包括: 分别建立室内实验和现场观测中动水条件下絮凝特性及生物等影响因素的观测方法; 合理的生物泥沙絮凝分析模式和参数的选择; 确定生物因子对絮凝过程影响的表征和机制; 泥沙沉降与输沙模式的确定。

河口是河流与海洋相互作用的耦合区, 考虑其动力条件和泥沙运动的复杂性, 本文采用**室内实验**和**现场观测**相结合的方法对泥沙絮凝进行研究:

在室内实验中, 泥沙样品为野外观测时抓取的**长江口南槽表层沉积物泥沙**, 生物样品为室内培养的**中肋骨条藻**(*Skeletonema costatum*)以及**胞外聚合物**(EPS, Extracellular Polymeric Substances)。仪器设备包括静态光散射设备 (Static Light Scattering 和 Malvern Mastersizer 2000)、光学显微镜、马尔文电位仪 (Malvern Zetasizer 1000HS/3000HS) 和沉降筒等。获得连续变化的絮凝粒度曲线、絮团粒径、形态、表面电位 (Zeta Potential) 等参数。通过室内实验研究了恒定剪切条件下絮凝特征 (时间尺度、絮团粒径) 随时间和环境条件 (不同阳离子、胞外聚合物和藻类) 的变化规律, 特别是研究了无法从现场观测中获得的絮凝时间尺度和絮凝效率等参数, 可从机理上解释生物因素对泥沙絮凝的作用。

在现场观测中, 研究站点位于长江口最大浑浊带主槽之一的**南槽**。观测数据主要通过船测方式获得, 利用先进仪器设备, 包括**现场激光粒度仪** (LISST, Laser In Situ Scattering and Transmissometry)、**声学多普勒流速剖面仪** (ADCP, Acoustic Doppler Current Profiler)、**后向散射浊度计** (OBS, Optical Backscatter Sensor)、**多参数水质仪** (Manta 2, Water Quality Multiprobe Manta 2) 等, 获得观测站点的絮团粒径、粒度分布与体积浓度、水动力 (剪切率)、藻类浓度 (叶绿素浓度)、含沙量及盐度等参数。此外, 本研究的野外观测涵盖了不同的时空变化尺度, 包括不同的潮周期、季节、垂向水深以及观测站位等。通过现场观测分析了自然环境下泥沙絮凝和生物变化过程, 结合室内实验结果, 建立泥沙和藻类的相关

联系,明确生物因素在泥沙运动过程中的效应。研究获得的主要结论有:

### 1. 藻类、胞外聚合物 (EPS) 和盐度的影响和机制

在室内实验中,泥沙絮凝在藻类、EPS 和盐度的作用下分别具有不同变化过程:(1)藻类颗粒可以自己形成大絮团,粒径可达  $100\ \mu\text{m}$ ,大于中肋骨条藻的单体长度 ( $30\ \mu\text{m}$ 左右)。当藻类和泥沙颗粒混合时,絮团粒径分布呈现双峰曲线,较小的峰值对应泥沙颗粒粒径 ( $10\ \mu\text{m}$ 左右),较大的峰值对应藻类或藻类絮团粒径 ( $100\ \mu\text{m}$ 左右)。随着絮凝的进行,双峰曲线逐渐合并为单峰曲线,整体絮团粒径增大,达到平衡态的时间约为  $10\sim 40$ 分钟,粒径峰值区域在  $10\sim 100\ \mu\text{m}$ 之间,平衡态絮团粒径变化范围为  $20\sim 70\ \mu\text{m}$ 。(2)EPS 的作用需要有阳离子的参与。EPS 在淡水中对泥沙絮团粒径影响甚微,而在有一定盐度存在的条件下,絮凝效应显著,絮团平衡粒径从大约  $10\ \mu\text{m}$ 增大到  $40\ \mu\text{m}$ ,达到平衡态的絮凝时间约  $10$ 分钟。EPS 与二价盐 ( $\text{MgCl}_2$  和  $\text{CaCl}_2$ ) 或海水共存时的絮凝速率高于一价盐 ( $\text{NaCl}$ ) 的絮凝速率;由 EPS 作用形成的絮团比藻类作用形成的絮团更小。(3)盐度可以促进泥沙絮凝,其中二价阳离子 ( $\text{MgCl}_2$  和  $\text{CaCl}_2$ ) 的絮凝效应大于一价阳离子 ( $\text{NaCl}$ )。由盐度引起的絮凝速率慢,达到平衡状态的时间长,通常需要  $60$ 分钟以上,形成的絮团粒径增加幅度小,变化范围为  $10\sim 20\ \mu\text{m}$ 。由盐度形成的絮团粒径小于藻类和 EPS 作用下的絮团粒径。

总体看来,藻类、EPS 与盐度对絮凝作用的影响和机制显著不同。从影响上看,藻类和 EPS 能显著促进泥沙絮凝,所形成的絮团较大,絮凝时间短;而盐度的影响较弱,其絮团较小,絮凝时间长。从机制上看,藻类通过改变絮凝成分,利用自身形成的聚合体与泥沙颗粒相结合,从而形成混合大絮团;EPS 作为连接介质,在阳离子作用下产生桥联作用,可以形成较大絮团,且抗剪强度高;盐度通过改变泥沙颗粒表面电位,由泥沙颗粒间的相互作用力形成絮团,但形成的絮团较脆弱,在高剪切率下难以形成大絮团。此外,三种因素还可互相结合,共同影响絮凝过程。

### 2. 藻类与悬沙在絮凝过程中的耦合作用

现场观测与室内实验的研究均发现藻类与泥沙有明显的耦合性:在现场观测中,河口地区水体藻类浓度 (CC) 与含沙量 (SSC) 有显著相关性,与其他水域中叶绿素集中在水体上层的分布情况不同,水体叶绿素浓度与含沙量均呈现出随水深增加而增加的分布规律,这是在高含沙量与强水动力条件下,藻类与泥沙颗粒发生絮凝,共同运输所造成的河口地区特有现象。本研究将叶绿素

浓度与含沙量的比值作为代表藻类影响的参数,简称含藻率(CC/SSC)。含藻率不仅可反映生物作用的强度,也可确定泥沙絮凝受藻类作用主导的区域和周期。在室内实验中,较高的含藻率可以促进絮凝过程,形成的絮团粒径更大,絮凝速率更快。含藻率在河口地区的时空分布与生物活动分布相似:夏季含藻率大于冬季,最高可达  $60 \mu\text{g g}^{-1}$ ,且口外区域(靠近海域)整体大于口内区域(靠近流域)。除了季节变化,含藻率在潮周期内的变化也不同——夏季涨落潮期间的水体表层均出现较高含藻率,生物活动较强,而冬季的高含藻率主要由含沙量降低而造成,且仅出现在落潮时期。含藻率的分布总体反映了生物活动强度的季节和潮周期变化。此外,在夏季涨憩时期,水体中下层的含藻率会显著增加,体现了藻类随泥沙絮凝沉降的过程。

含藻率所反映的生物作用需考虑藻类和含沙量的特殊情况:冬季整体藻类浓度低,生物活动强度弱,此时的高含藻率主要由水体表层的低含沙量造成,对泥沙絮凝的作用不显著。此外,在夏季涨憩后 1~2 小时内,含藻率的升高主要是由于藻类的再悬浮作用及含沙量降低而造成,因此高含藻率下没有大絮团产生。

### 3. 河口泥沙絮凝过程中的生物影响

长江口区域藻类颗粒多数分布在絮凝组分大于  $100 \mu\text{m}$  的部分,并且与泥沙颗粒有动态相互作用——当藻类作用较强(含藻率较高)时,絮团粒度曲线会同时出现泥沙颗粒和藻类颗粒双峰,并且在  $10\sim 100 \mu\text{m}$  的范围内在单峰和双峰曲线之间相互转换,同时受径潮流相互作用力的影响随时空变化。在这个尺寸范围内的絮团有效密度、沉速与絮凝时间有关,这对使用恒定泥沙沉速的泥沙运输模型至关重要,这些模型应该考虑水体中絮团沉降速度的变化。生物的作用机制可反映在含藻率对絮团三组分变化的影响:絮团根据其粒径分布可分为三个组分:单颗粒(Single-grain,  $< 5 \mu\text{m}$ )、小絮体(Microflocs,  $5\sim 200 \mu\text{m}$ )和大絮体(Macroflocs,  $> 200 \mu\text{m}$ ),随着含藻率的增加,单颗粒组分频率几乎无变化,而小絮体组分频率占比下降、大絮体组分频率占比增加,即藻类的作用主要为结合小絮体并转换成大絮体,提高大絮体组分占比而形成大絮团。

河口地区生物泥沙絮凝过程主要受水体剪切率的影响:从整体上看,潮周期内水体剪切率控制着絮团粒径的上限,控制区间约为  $\eta/6$  ( $\eta$  为 Kolmogorov microscale)。絮团粒径的整体变化随潮周期变化而变化——在急流时刻水体絮团较小、憩流时刻较大;在涨潮期间,水体剪切率较高,絮团在较强的生物作用下会形成双峰曲线,其中泥沙峰在  $10\sim 30 \mu\text{m}$  区间,生物藻类峰由于其较高的抗剪特性而保留在  $100\sim 200 \mu\text{m}$  区间,此类双峰大絮团出现在随海水带来的较多藻类的涨潮期间,絮团粒径可达  $160 \mu\text{m}$ ,与室内实验中藻类颗粒峰值相近;在涨

憩期间，低水体剪切率维持时间约为 2~3 小时，藻类颗粒与泥沙颗粒在相对稳定的水动力条件下充分混合，形成粒径约为 40~80  $\mu\text{m}$  单峰大絮团，絮凝接近稳定状态。盐度等其他因素对河口生物泥沙絮凝过程的影响不显著。

#### 4. 生物效应的时空变化及泥沙沉降的潮汐不对称

由于夏季藻类浓度高于冬季（叶绿素浓度约为 1~8  $\mu\text{g l}^{-1}$ ），藻类的作用主要体现在夏季。其中涨落潮阶段体现了不同的絮凝过程：在涨潮阶段，随海水带来的大量藻类造成涨潮前期水体上层（水深 2m 以内）含藻率升高并发生生物絮凝，形成密度低、沉速大的双峰大絮团；在随后的 2~3 小时内，大絮团逐渐沉降到水体中层和底层，且絮团粒径分布从双峰转变成单峰，同时受水体中下层较高剪切率影响，絮团粒径减小；在涨憩后 1~2 小时内，由于藻类发生再悬浮效应，水体表层叶绿素浓度没有明显降低，同时大量泥沙颗粒沉降导致含沙量降低，因此水体含藻率升高，但絮团粒径减小。在落潮阶段，虽然也有藻类的参与，但由于海水退却及涨憩后含沙量的减小，絮凝效率下降，生物效应减弱，未出现大量双峰大絮团沉降现象。落潮期的大絮团主要出现在水体剪切率较小的落憩时刻，且絮团粒径小于涨潮期的大絮团，整个落潮阶段的泥沙沉降小于涨潮阶段。因此，藻类的作用促进了涨落潮期间泥沙沉降的不对称性，是潮周期内泥沙向河口运输的重要因素。

冬季长江河口地区藻类浓度相对较低（叶绿素浓度小于 1  $\mu\text{g l}^{-1}$ ），生物作用较弱，因此泥沙絮凝过程由水动力主导，未出现生物泥沙双峰絮团，大絮团出现在憩流时刻，小絮团出现在急流时刻。由于长江口是落潮优势河口，落憩时刻更长，因此在落潮阶段有更多大絮团的形成和泥沙沉降，泥沙形成向口外输送的趋势。长江口生物影响下的泥沙絮凝季节变化和潮周期变化体现了不同的泥沙沉降过程，是影响长江口泥沙运输的重要因素。

**综上所述**，室内实验和现场观测结果的相互结合有助于从机制到特征深入了解絮凝动力学。本研究建立了河口地区泥沙运输与生态循环的联系，生物和泥沙的相互耦合现象表明泥沙絮凝不仅影响河口地貌的演变，而且是河口生态循环中的一个重要过程。

**本文的创新点**有：（1）推动了河口泥沙与生化过程相结合的研究方法的创新：首先，在室内实验中，改进絮凝发生装置，结合激光散射、电位与图像分析等分析技术，突破了絮团与藻类观测的技术难点。其次，在现场观测中，完成了常规水动力与生物等因素的集成观测系统，获取更丰富的观测参数；（2）明确了

藻类、胞外聚合物 (EPS) 和盐度对泥沙絮凝的不同作用机制和效果: 藻类的作用机制为絮团组分结合, 其促进絮凝的效果最强; EPS 的作用机制为桥连作用, 其作用需要有阳离子的参与, 能明显促进絮凝; 盐度的作用机制为颗粒间相互作用力, 促进絮凝的效果较弱; (3) 发现了河口地区藻类与泥沙的相互耦合作用: 藻类和泥沙发生絮凝而共同运输, 二者具有明显相关性, 而含藻率参数可同时考虑藻类和泥沙效应, 为河口生物泥沙絮凝研究提供了关键参数; (4) 发现了河口地区生物因素对絮凝影响的表征: 大粒径、低密度和高沉速絮团的出现, 絮团粒度曲线单双峰形态的相互转化, 以及絮团三组分频率的变化; (5) 发现生物作用在河口泥沙输运过程中有重要作用: 夏季强烈的生物作用促进了涨落潮期间泥沙沉降的不对称性, 涨潮阶段丰富的藻类促进泥沙形成大絮团并大量沉降, 泥沙沉降高于落潮阶段。因此夏季生物作用促进了泥沙向口内输沙的过程。

**今后的工作的展望:** (1) 在室内实验方面, 可改进絮凝观测设备以获得更多絮凝参数, 此外也可设置更多实验条件以研究更多因素对生物泥沙絮凝的影响; (2) 在现场观测方面, 可扩大观测时空尺度, 如长江口其他区域及河流、湖泊、潮滩等其他水生系统, 获得更丰富的生物絮凝资料; (3) 在模型研究方面, 本文的研究成果可应用于考虑不同絮凝组分的泥沙絮凝模型, 进一步研究泥沙絮凝演化过程。

**关键词:** 泥沙, 絮凝, 粒度分布, 生物, 藻类, EPS, 长江口, 潮周期变化, 季节变化, 沉降

# 1

## Introduction

*The secret of getting ahead is getting started.*

Mark Twain

### 1.1. Background

With human's ongoing exploitation of rivers, coastal areas and oceans, sediment management (dredging works, channel siltation), water supply and water pollution are ongoing topics of interest. These topics are related to the erosion, transport and accumulation of sediment (and bound nutrients/contaminants). Sediment particles can be categorized into clay ( $<4\ \mu\text{m}$ ), silt ( $4\text{--}62\ \mu\text{m}$ ) and sand ( $>62\ \mu\text{m}$ ) fractions according to their size. Cohesive sediment refers to a complex mixture mainly composed of mineral clay and silt, a small amount of fine sand, organic matter and water. Even though the proportion of clay and organic matter is only 5 to 10 percent in cohesive sediment, its presence results in remarkable rheological properties (yield stress, viscosity) of the overall sediment and can lead to significant flocculation of suspended sediment through

electrochemical and biochemical processes [Dyer, 1989, Winterwerp & Van Kesteren, 2004].

Cohesive sediment is widely found in estuary, coastal and adjacent sea areas. Cohesive sediment particles can aggregate and these aggregates may break. This dynamical behavior should be accounted for in sediment transport models. Since heavy metals, organic nutrients and pollutants can easily adhere to the surface of cohesive sediment, it makes cohesive sediment an important carrier for these products. The spreading and deposition of cohesive sediment in estuaries and coastal areas ought therefore to be fully understood and modelled.

The study of cohesive sediment transport has therefore two main scientific goals:

- 1— to understand the role of cohesive sediment in the morphological evolution of estuaries and coasts. This type research applies to river channel development, reservoirs and harbours maintenance and deepening, as well as to tidal flats evolution [Chen, 1995, Guo & He, 2011, van Maren & Winterwerp, 2013].
- 2— to understand the impact of cohesive sediment on biogeochemical cycles. This type research applies to among others the evaluation of pollutant and nutrient spreading, the protection and management of aquatic ecological resources [Herbert, 1999, McAnally & Mehta, 2001, Stone, 2000].

Over 90 % of the total volume of fine suspended sediment in an estuary exists in the form of aggregates, also called flocs [Droppo & Ongley, 1994]. Figure 1.1 shows a classical picture of the behavior of cohesive sediment in natural water during the process of suspension, flocculation/break-up, settling and deposition. Mineral clay particles are seen to be suspended by erosion. Then, under the action of microscopic forces which are linked to the particles' surface charge [Gregory, 2005, van Leussen, 1988], particles will flocculate, and form flocs, which can be large in volume. These flocs can be broken into smaller or primary flocs under the action of shear stress or grow larger by collision with other particles. As the environmental factors are changing, flocs in natural water stay in a dynamic process of aggregation and break-up [Burban et al., 1989, Eisma, 1991, Lick et al., 1993]. This classical picture should however be reconsidered in the light of organic matter properties: when organic matter consists of polymeric substances (like proteins, sugars or DNA), flocs can also display elastic properties and show a high resistance to shear [Shakeel et al., 2020]. Increasing shear

rate then does not lead to break-up of flocs but rather to a decrease in volume (the flocs become denser).

So far there have been many studies showing that flocs have a wide range of particle sizes and settling velocity. The average particle size mostly ranges from 10 to 100  $\mu\text{m}$ , and the average settling velocity from 0.01 to 10  $\text{mm s}^{-1}$ , both of which cover several orders of magnitude and are far larger than the average size and settling velocity of the primary particles forming these flocs (e.g., [Chen et al., 1994](#), [Dyer, 1989](#), [Fettweis & Baeye, 2015](#), [Mikkelsen et al., 2007](#), [Uncles et al., 2010](#), [Wang et al., 2013](#), [Xia et al., 2004](#)). Besides, flocs formed in different environmental conditions may greatly differ in composition and structure, but have the same average particle size [[Wells & Goldberg, 1993](#)].

Flocculation is affected by many factors, on which several scholars have done detailed research, mainly focusing on three aspects: physical factors, chemical factors and biological factors. Physical factors include hydrodynamic conditions (such as shear stress, vertical mixing, viscosity) and sediment particle characteristics (such as particle size distribution, sediment concentration); chemical factors consist of environmental conditions (such as salinity, temperature, pH), mineral composition and surface charge of sediment particles; biological factors mainly refer to the biochemical effect caused by biological activity in the water [[Droppo et al., 2015](#), [Dyer & Manning, 1999](#), [Fettweis & Lee, 2017](#), [Gibbs, 1985](#), [Mietta et al., 2009a](#), [Winterwerp & Van Kesteren, 2004](#)]. Physical, chemical and biological processes are all related and their relation is extremely complex. There has not yet been a fully integrated study on them. In the past thirty years, a lot of research has been performed on flocculation but the effect of biological processes were seldom taken into account [[Maggi, 2005](#), [Mietta, 2010](#), [Thomas et al., 1999](#), [Winterwerp, 1999](#)]. This is reflected in the classical picture presented in Figure 1.1, where the action of biology is absent. As there is significant biological activity in estuaries and coastal areas, which generates a large amount of organic matter, this exerts a great impact on flocculation, as has long been recognized [[Avnimelech et al., 1982](#)].

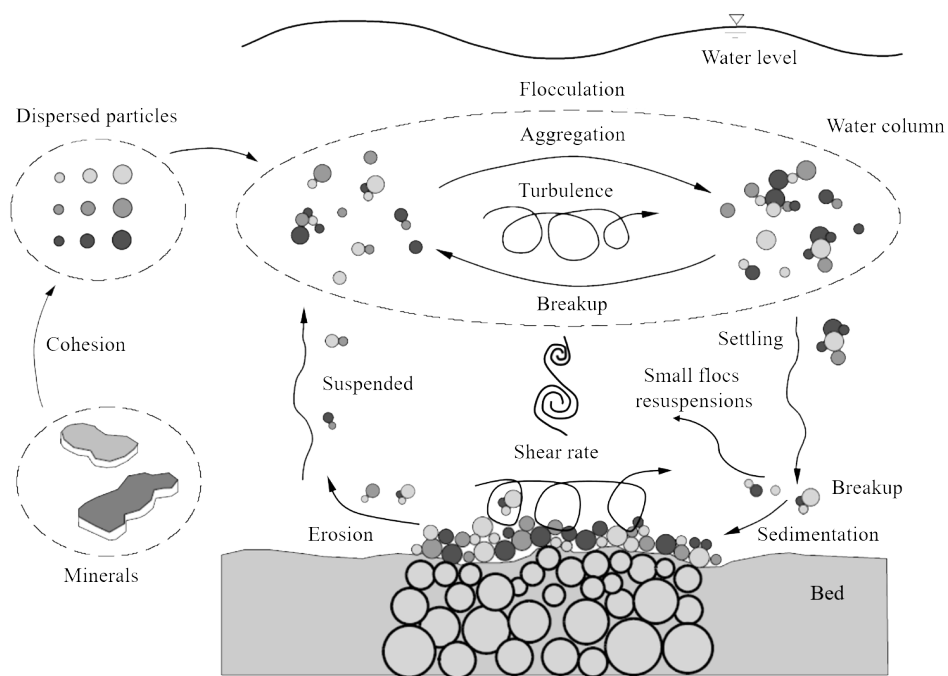


Figure 1.1: Flocculation processes and mechanisms of sediment. Adapted from Guo [2018], Maggi [2005].

## 1.2. Goals and approach

The present thesis is meant to start to fill the knowledge gap regarding the role of biological activity in estuaries and coastal areas on physical processes and aims in particular to study the role of biological microorganisms such as microscopic algae in sediment flocculation. It will be shown that biological effects are essential to understand in-situ sediment dynamics. It is anticipated that current sediment transport models should be revised in order to better correlate fine sediment (clay fraction) spreading to the aquatic biological activity. The results will ultimately lead to a better understanding of the dynamics of estuaries and coasts where suspended bio-mineral particles are found.

The research questions for this thesis are:

- 1. What are the effects of biological components (algae, EPS) and salinity on flocculation? What are the different mechanisms of algae and EPS?**
- 2. How does the algae population interact with hydrodynamics in an estuarine area? How to assess the biological parameters in natural environment?**
- 3. What are the roles of biological parameters on sediment flocculation in an estuarine area?**
- 4. How do the seasonal and tidal variations affect flocculation in the presence of biological activity? How does algae-sediment flocculation affect sediment transport and deposition in the estuarine area?**

In this dissertation sediment flocculation is studied with the help of laboratory experiments and field observations. Different equipment will be used to assess the particles' properties such as light scattering devices (Malvern Mastersizer in the lab and LISST-100C in-situ) and microscopy to assess particle sizes and shapes, Optical Back Scatter (OBS) to assess Suspended Sediment Concentration (SSC) and Chlorophyll Concentrations (CC) will be measured by Water Quality Multiprobe (Manta2-WQM) as a proxy for algae concentrations. Additional measurements will be performed in-situ by temperature and conductivity sensors and Acoustic Doppler Current Profiler (ADCP) to estimate the hydrodynamics and salinity conditions.

Two major paths of research are followed:

1. Laboratory investigation

The laboratory experiments were conducted to study the evolution of floc par-

ticle size as function of time and environmental conditions (different cations, extracellular polymeric substance and algae). Grab sediment samples from the Changjiang Estuary were used in this study. In particular, the timescale and efficiency of flocculation could be estimated –something that cannot be assessed directly from in-situ monitoring.

## 2. In-situ monitoring

The field observations were done for two different seasonal conditions (summer and winter) and measurements are performed to determine various quantities as function of depth and time. The study area of interest lays in the maximum turbidity zone of the Changjiang estuary (China). This enabled in particular to study the changes in sediment properties during settling and highlight the role of biology in the process. The temporal and spatial variations in sediment transport mechanisms in different environmental conditions were carefully analyzed.

### 1.3. Outline

An overview of the thesis content is given in Figure 1.2. The outline of this dissertation is as follows:

**Chapter 2** gives a literature overview and state-of-the-art.

**Chapter 3** details the research material and methods, which consist of laboratory experiments and field recordings. The laboratory experiments consisted of static light scattering (SLS) measurements, whereby flocculation could be followed in time, microscope visualization and sedimentation column experiments. The field survey mainly covered the area of south channel of the Changjiang River estuary. The experiment design, observations and data processing used in the research are described in detail.

**Chapter 4** discusses the results of the laboratory experiments. Different flocculation experiments have been carried out under different conditions of salinity, extracellular polymeric substance (EPS) and microalgae concentration. The correlation between the floc characteristics and these parameters were analyzed.

**Chapter 5** discusses the variation of flocs and living organisms in the turbidity maximum zone of estuaries obtained from field observation in summer. Recordings from an anchored ship were obtained in the South Passage of the Changjiang estuary turbidity maximum zone to study the action of different types of tide on particle

size distribution and composition. The recordings include the variation of chlorophyll concentration, current speed, suspended sediment concentration, salinity and floc size distributions as function of depth.

**Chapter 6** discusses in depth the effect of seasonality on sediment flocculation. The discussion is mostly based on the data acquired during the field observations. The change in biological composition (in winter/summer) is shown to have a large influence on floc development in estuarine areas.

**Chapter 7** gives a summary and outlook. The main findings of the previous four key chapters and the innovative points of this dissertation are highlighted. Recommendations for future research are made.

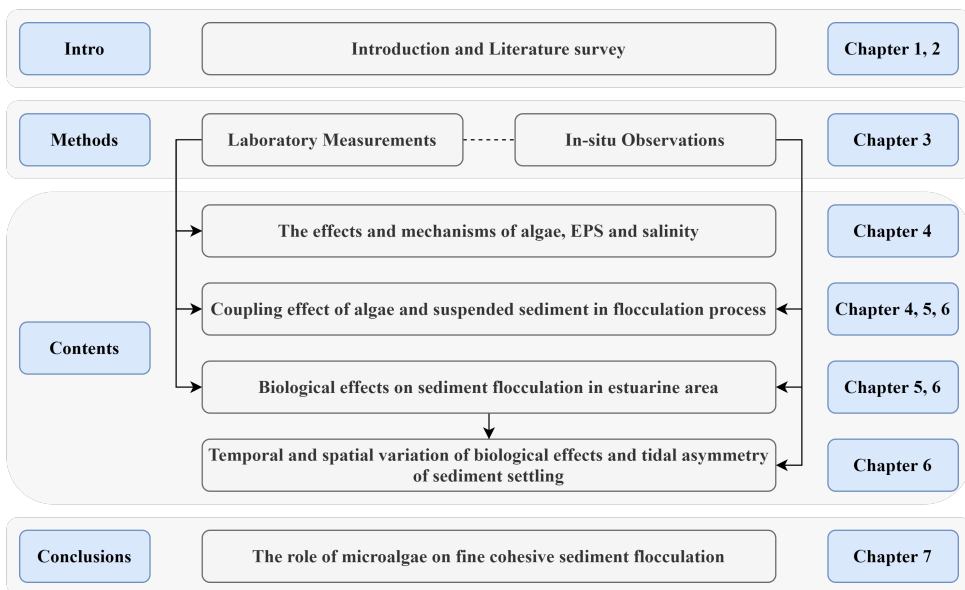


Figure 1.2: Outline of this thesis



# 2

## Literature survey

*It does not matter how slowly you go as long as you do not stop.*

Confucius

In this chapter, a state-of-the-art is given regarding the studies performed so far on flocculation. The main mechanisms leading to floc formation and break-up are discussed. The characteristics of flocs are detailed.

### **2.1. Flocculation mechanisms**

There are two important parameters for fine sediment particles that are related to their flocculation ability. One is the collision frequency and the other the collision efficiency. The aggregation rate of particles depends on both these parameters.

#### **2.1.1. Collision frequency**

There are three main expressions for the collision frequency, based on the different approach mechanisms between particles. Particles can approach one another by

Brownian motion, shear or differential settling [McCave, 1984, Tsai & Hwang, 1995, van Leussen, 1994]. So, if a collision occurs between a particle of diameter  $d_i$  and a particle of diameter  $d_j$ , the collision frequency  $f_{i,j}$  can be expressed as follows [Hunt, 1980]:

Brownian motion (BM):

$$f_{i,j} (BM) = \frac{2}{3} \frac{k \cdot T}{\mu} \cdot \frac{(d_i + d_j)^2}{d_i \cdot d_j} \quad (2.1)$$

Shear (SH):

$$f_{i,j} (SH) = \frac{G}{6} (d_i + d_j)^3 \quad (2.2)$$

Differential settling (DS):

$$f_{i,j} (DS) = \frac{\pi}{4} (d_i + d_j)^2 |\omega_{s,i} - \omega_{s,j}| \quad (2.3)$$

The parameter  $k$  is the Boltzmann constant ( $1.38 \times 10^{-23} \text{ J K}^{-1}$ ),  $T$  is the absolute temperature (293 K),  $\mu$  is the dynamic viscosity of the suspending medium—water ( $1.005 \times 10^{-3} \text{ Pa s}$  when the temperature is 20 °C),  $G$  is the shear rate ( $\text{s}^{-1}$ ),  $g$  is the gravitational acceleration ( $9.8 \text{ m s}^{-2}$ ), and  $\omega_{s,i(j)}$  represents the settling velocity of the flocs.

Brownian motion is caused by the random thermal motion of liquid molecules, so in general it is only effective for sediment particles under the colloidal size of 1–2  $\mu\text{m}$  [Dronkers et al., 1988, Lick et al., 1993, Partheniades, 1993]. Brownian-induced flocculation is a slow process and in estuarine systems, where the water column experiences hydrodynamic mixing, is not expected to be the dominant cause for flocculation.

The effect of shear rate is considered to be primordial on flocculation in estuarine systems. Many studies have provided a better understanding about the relations between shear rate and flocculation [Eisma, 1991, Manning & Dyer, 1999, Mehta & Partheniades, 1975, Mietta et al., 2009a, Partheniades, 1991, 1993, Winterwerp et al., 2006]. As is shown in Eq. (2.2), the collision frequency increases with increase in shear rate, thus promoting flocculation and the growth in particle size. However, when the particle size of flocs reaches the Kolmogorov microscale  $\eta$ , the increase upon shear rate will be limited. Eisma [1986] and van Leussen [1997] in particular argued that the maximum diameter of flocs should be equivalent to the Kolmogorov microscale (minimum turbulent vortex scale). The Kolmogorov microscale is defined in Eq. (2.6).

Polyelectrolyte-induced flocs, on the other hand can achieve sizes much larger than the Kolmogorov microscale, owing to the polyelectrolyte anisotropic size and elastic nature [Ibanez Sanz, 2018, Shakeel et al., 2020].

When a floc has a size larger than the Kolmogorov microscale, it is expected to break up into smaller flocs with a denser structure [Dyer, 1989, Winterwerp, 2002]. The effect of shear rate on floc size can thus be divided into two parts:

(1) under the critical shear rate linked to the Kolmogorov microscale, the collision frequency between particles is increasing with shear rate and therefore large flocs can be formed, with high settling velocity.

(2) above the critical shear rate linked to the Kolmogorov microscale, the shear stress caused the rupture of flocs and hence the settling velocity of the formed (smaller) flocs is smaller than the one of the large flocs that produced them.

In estuarine and coastal areas, the largest shear gradient is close to the channel bed area (10–20% of the water column above bed is affected), where about 80% of turbulence energy is present. This produces a powerful uplift force for particles and the local shear stress controls the maximum size of suspended flocs [Mehta & Partheniades, 1975]. From a modelling perspective, using a model based on Population Balance Equations (PBE) the aggregation and break-up of flocs is a continuous process. In an area with constant shear stress, the strength, size and density of flocs will be in a dynamic equilibrium. When analyzed using PBE, flocs can break up into smaller flocs or individual particles owing to particle collision or shear stress [Burban et al., 1989]. They (re)form larger flocs in the upper water where there is less turbulence.

One can question this standard model in the case of in-situ flocculation, as it has been observed that flocs do not necessarily break under shear, but rather change shape as the organic matter they contain is rather elastic [Shakeel et al., 2020]. In fact, the standard model has been derived primarily for the flocculation of inorganic particles, where aggregation is induced DLVO theory (Derjaguin-Landau-Verwey-Overbeek theory, which will be explained in section 2.1.2).

Differential settling is a phenomenon that occurs when the particle size and density of two particles are different. The particle with faster settling velocity can then collide with the one with slower settling velocity. Therefore, the greater the particle size, the higher the collision probability, see Eq. (2.3). From the analysis of differential settling based on collision frequency of spherical particles in low Reynolds conditions, it was

shown that when there is a great difference in size between two particles, the largest particle, having a larger volume and hence a larger weight, has a faster settling velocity than the smaller one. There is of course a limiting factor, which is density: when one or both particles have a small density (close to water), there is almost no collision between the two particles [Stolzenbach & Elimelech, 1994]. Differential settling is a phenomenon occurring in still water conditions—a condition seldom respected in estuarine conditions. This has led some researchers to emphasize the importance of shear rate on the formation of flocs, and arguing that the effect of differential settling on flocculation can be omitted [Dyer & Manning, 1999, Winterwerp, 1998]. Nonetheless, when the shear rate is small (at slack water for instance), flocculation caused by the differential settling of fine sediment particles cannot be neglected [Chen et al., 1994, Eisma, 1991, Fugate & Friedrichs, 2003]). As is shown by Lick et al. [1993]’s laboratory experiment, with decreasing shear rate the flocculation switches from shear rate induced collision to differential settling induced collision. When dominated by differential settling, the floc size and settling velocity tended to be larger. The effect of differential settling on floc structure and settling in estuarine conditions, especially in presence of organic matter, still needs further research. As organic matter particles (which have a density close to  $1 \text{ g l}^{-1}$ ) populate the whole water column, they can certainly be captured by settling sediment particles at low water shear stress periods.

### 2.1.2. Collision efficiency

The collision efficiency is mainly driven by the interaction forces between particles upon approach. These forces are linked to physical, chemical and biological processes, and include electrostatic forces, Van der Waals’ force (VDW), hydrophobic interactions and entropic forces. In the past decades, researchers have put forward a number of theories and models for sediment flocculation, among which there is the standard electrokinetic theory (named DLVO, for Derjaguin, Landau, Verwey and Overbeek), polymer bridging, cation bridging, sweep flocculation and others [Bolto & Gregory, 2007, Higgins & Novak, 1997, Kruyt, 1949, Lee et al., 2011, van Leussen, 1988, 1994].

## DLVO theory

The DLVO theory models the interaction potential between two approaching colloidal particles in a solvent (usually water). The interaction is made of two terms: a Coulombic repulsion and a van der Waals attraction [Chassagne, 2019, Kruyt et al., 1952]. The two particles have a surface charge and are surrounded by a so-called double layer which is composed, in majority, of counterions. The double layer is the result of the attractive interaction between the surface of sediment particles (usually negatively charged) and the positively charged ions found in water. The  $\zeta$ -potential is used to quantify the surface charge of a particle. It is defined as the electric potential at the surface of shear of the particle (the potential of reference is taken at infinity, where it is defined as zero). Sometimes, this surface of shear is located at the surface of the particle, in which case the  $\zeta$ -potential is identical to the electric surface potential  $\varphi_0$  [Chassagne & Ibanez, 2012]. The potential  $\varphi_0$  depends on the number of ions adsorbed on the particle surface. In most cases, the shear plane is located in the Stern layer [Chassagne et al., 2009], which is the layer between the surface of the particle and the plane of shear. When the concentration of cations increases in the water, there will be a reduction in  $\zeta$ -potential, as more ions will be located between the particle's surface and the shear plane, leading to better screening of the surface charge.

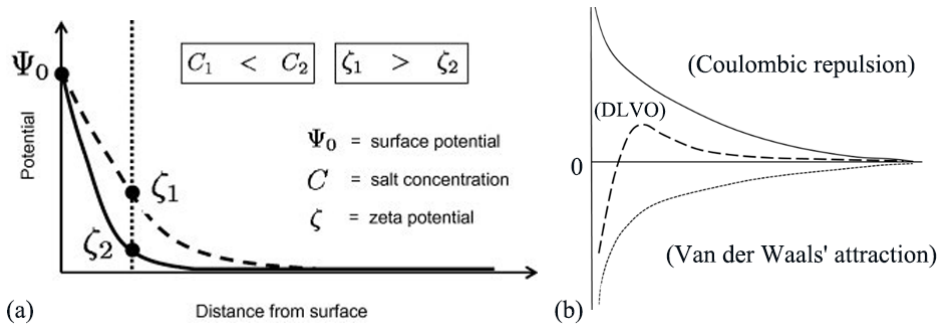


Figure 2.1: (a) Electric potential as function of the distance from the surface of a colloidal particle. The  $\zeta$ -potential of particles is a function of salinity: the higher the salinity, the lower the  $\zeta$ -potential.

Taken from Chassagne et al. [2009] (b) The DLVO interaction energy between two particles is the sum of an attraction (van der Waals) and a repulsion (Coulomb).

As is seen in Figure 2.1a, the electric potential drops from  $\zeta_1$  to  $\zeta_2$  when the salt concentration is increased from  $C_1$  to  $C_2$ . The interaction energy curve displays a max-

imum which indicates that a repulsion force is preventing particles to aggregate when Coulombic repulsion is dominant. This barrier can be overcome by increasing ionic strength or lowering pH but can also be overcome by “pushing” the particles together. This happens in-situ, when the water flow enables particles to collide (see section 2.1.1).

For more details about DLVO theory, the reader is referred to [Chassagne \[2019\]](#). There are a lot of studies about the  $\zeta$ -potential and the surface charge of clays [[Chassagne et al., 2009](#), [Kosmulski & Dahlsten, 2006](#), [Mietta, 2010](#), [Rand & Melton, 1977](#), [Sondi et al., 1996](#), [Tsujiimoto et al., 2013](#)], and the results show that either a decrease in pH or an increase in ionic strength usually decrease the absolute value of the  $\zeta$ -potential. A low  $\zeta$ -potential is synonymous for aggregation ability: particles with a low  $\zeta$ -potential have a weak Coulombic repulsion. For these particles, van der Waals attraction will dominate and lead to flocculation.

In estuarine areas, the suspended sediment particle will, according to DLVO theory, be destabilized and flocculate because of the increase in salinity between the river fresh water and the sea. In the presence of organic matter however, DLVO theory cannot be applied, as the flocculation mechanisms will be driven by the presence of polyelectrolytes and microorganisms which are not accounted for in the DLVO theory.

[Hunter & Liss \[1979, 1982\]](#) already demonstrated in 1979, by analyzing the surface properties of suspended particles in four rivers in the UK by electrophoresis that because of the organic coatings of the particles no major difference could be found in the particles' surface characteristics. The general trend that was found is that the electrophoretic mobility (and hence the  $\zeta$ -potential) is decreasing (in absolute values) with increasing salinity. This behavior is in line with the description given in Figure 2.1a and reflects the surface screening of the charge of the coated particles.

Under the suitable conditions, microbial organisms, such as diatoms, can produce polyelectrolytes (polysaccharides), which is a gelatinous organic matter (OM). These polyelectrolytes are called Transparent Exopolymer Particles (TEP) or Extracellular Polymeric Substances (EPS). They are polymeric chains which include a large amount of anionic polysaccharides like galacturonic acid that is the main component of pectin [[Plude et al., 1991](#)]. The organic polymers can form biofilms on the surface of sediment particles and act as flocculating agent [[Bar-Or & Shilo, 1988a,b](#)]. Because of the ionization of their functional groups (such as carboxylic acid and phosphate), microbial cells and EPS have a high density of negative charge [[Sheng et al., 2010](#)], and

anionic polysaccharides aggregate with negatively charged sediment particles through cationic bonding. These cations are salt ions found in the water, and their concentration is a function of salinity. The mucus secreted from microorganisms can also be a cationic polymer [Plude et al., 1991]. Aly & Letey [1988] have found that flocculation by cationic polymers is different from flocculation by anionic polymers. Flocculation with cationic polymer is done by charge neutralization, while flocculation with anionic polymer is mainly done by bridging mechanism [Shakeel et al., 2020]. Studies have shown that adding divalent cation can enhance flocculation [Park et al., 2010, Yeh, 1988].

## 2.2. Flocculation by organic matter

Organic matter, and more specifically the polyelectrolytes produced by microorganisms bind to sediment particles in different ways, depending on their polymeric chain length (defined by the molecular weight), and charge groups. Their way to bind to sediment particles is also depending on salinity, pH and shear stresses. Depending on the polyelectrolyte, flocculation can occur through bridging [Nabzar et al., 1988, R. F. Hicks, 1988, Riley, 1963, Winterwerp & Van Kesteren, 2004], or patching mechanism [Bergaya & Lagaly, 2013], as see in Figure 2.2.

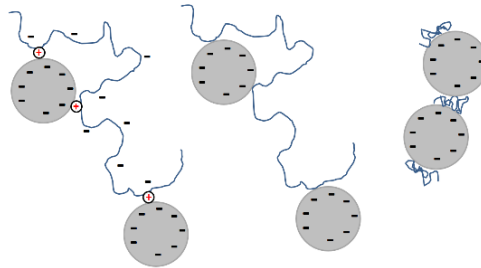


Figure 2.2: The schematic diagram of different types of flocculation. Left and middle: bridging flocculation. The anionic polyelectrolyte on the left needs a cation (in red) to bridge to the clay; right: patching flocculation. Taken from Chassagne [2019].

A polyelectrolyte can stick to certain points of the sediment's surface as trains, separated from one another by loops and for much of its length it is able to extend into the solvent as tails (Figure 2.3). The attraction between the interacting molecular chains should be strong enough to overcome the entropy repulsive force caused by the

decrease in freedom of the chains [Rosen, 2004].

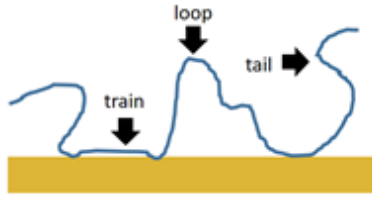


Figure 2.3: Train, loop and tail of a polymer. Taken from Chassagne [2019].

**Bridging aggregation:** the loops and tails of one polymer of one particle will be able to attach to the sediment particle. Usually, one finds that the optimum polymer concentration to achieve flocculation corresponds to half surface coverage for the polymer. Polymeric bridges are changing as function of shear. Bridging aggregation can even occur with polyelectrolytes having surface charges of same sign as the ones of the particles. In that case, aggregation is enabled by the presence of oppositely charged ions in the water. as discussed in section 2.1.1. When polymer bridging flocculation happens, the bridging particles should have an available surface to connect polymer chain segments [Biggs et al., 2000].

**Patching aggregation:** patching aggregation occurs when polyelectrolytes have a charge that is opposite in sign to the one of the sediment particles. The polyelectrolyte then strongly binds to the sediment particle, and its tails do not extend much into the solvent. Aggregation is then made possible between one polymer patch of one particle and the bare surface area of another particle. Floccs formed through patching aggregation have a higher strength than those through other ways, because the floc formed by bridging through polymer chains is flexible and stretchable [Gregory & Barany, 2011, Otsubo, 1992]. The force is dependent on the number of bound segments [Swenson et al., 1998].

**Sweep Flocculation:** As is visible under a microscope, microorganisms can form a polymeric network with holes and channels [Li & Ganczarczyk, 1990] through the bridging of their produced Extracellular Polymeric Substances (EPS) [Jorand et al., 1995, Leppard, 1992]. This network has a large surface area and can absorb pollutants, nutrients and minerals [Costerton et al., 1987]. At the same time, there are large and small interspaces inside the network. When sedimentation of this network occurs, some fine particles can be trapped by it and be embedded. This process is called sweep

flocculation. Although sweep flocculation is usually studied in sewage treatment, a similar process has been observed in estuarine environments [Gregory, 2005, Lee et al., 2011]. Sweep flocculation is a function of electrochemistry and other characteristics of the network. As a result, the network floc gets increasingly larger [Deng et al., 2019].

To summarize, the flocculation of fine sediment under biological action is a complicated dynamic process involving chemistry, physics and biology. Even though the mechanism of bio-sediment flocculation can be partly explained some open questions remain. For example, the DLVO approach, which predicts that the increase of ion concentration is beneficial for flocculation, cannot explain why an increase in sodium concentration will slow-down flocculation [Sobeck & Higgins, 2002]. Physico-chemical models also do not take into consideration the uneven charge distribution on sediment surfaces and the charge distribution of EPS, which most probably have a great influence on bio-sediment flocculation. While the process of bridging flocculation is recognized as one of the mechanisms for bioflocculation, it is not possible to perform a quantitative analysis. Moreover, the colony formation and growth of microorganisms is a dynamic process that will influence bio-sediment flocculation. The microbial activity is a complex process that is hard to quantitatively study, especially in field observation. So far, the biological activity is studied by quantifying the number of microorganisms present, understanding their growth cycle, analyzing their EPS etc. The link between biological activity and sediment flocculation remains a key open question for the study of sediment transport dynamics.

### 2.3. Break-up mechanisms

When shear forces are stronger than the bonding force between particles, it is expected that flocs will break-up.

The break-up rate  $B_i$  is usually used to describe the break-up of flocs and it is traditionally a function of shear and size of particles [Lick & Lick, 1988]. The term break-up can be misleading. Experimentally it implies that one particle breaks in smaller pieces. From a modeling point of view, “break-up” is synonymous of “particles leaving a size class”, which can happen either by break-up or aggregation [Spicer & Pratsinis, 1996]. The break-up term corresponding to the actual breaking of particles is given by  $B_i(TS)$  and is caused by turbulent shear. The break-up term corresponding to particles leaving a size class by aggregation is given by  $B_i(C)$  [Serra & Casamitjana, 1998]. The

expressions for  $B_i(TS)$  and  $B_i(C)$  are:

By break-up it is understood that particles leave a particle size class. Therefore break-up is appropriate to describe the rate  $B_i(TS)$  caused by turbulent shear [Spicer & Pratsinis, 1996] but not the rate  $B_i(C)$  which models the fact that particles are leaving a particle size class by collision [Serra & Casamitjana, 1998]. The rate  $B_i(C)$  should better be named “decay” of the number of particles of a certain size, as these particles leave a size class because they aggregate to form larger particles (which is the contrary to break-up). The expressions for  $B_i(TS)$  and  $B_i(C)$  are:

Caused by turbulent shear (TS):

$$B_i(TS) = EG^b d_i^p \quad (2.4)$$

where  $d_i$  is the size of floc in class  $i$ . The parameter  $p$  is usually taken equal to 1 and  $E$  and  $b$  are fitted to data.

Caused by collision (C):

$$B_i(C) = \sum_{j=1}^N a_{(i,j)} f_{(i,j)} n_j \quad (2.5)$$

where  $a_{(i,j)}$  is the collision efficiency,  $f_{(i,j)}$  represents the frequency of particle collision, and  $n_j$  is the number of flocs of a given size  $L_j$ . Usually  $a$ , which should be between 0 (no aggregation) and 1 (always aggregation), is taken to be constant and equal to  $a = 0.5$  [Mietta, 2010]. It can be seen from Eq. (2.4) that the increase of either shear rate or the floc size will increase the break-up rate of particles.

In general, the floc break-up process is poorly understood [Thill et al., 2001]. The empirical parameters should account for the bonding forces between particles as the stronger the bonds, the more resistant the floc is to any exterior force [Jarvis et al., 2005] or inner tensile stress [Yeung & Pelton, 1996], see Figure 2.4. The ability of flocs to resist damage (floc strength) is closely related to flocculation and the size and structure of flocs [Son & Hsu, 2009]. Floc strength is a function of the electrochemical attraction between clay minerals and the agglutination of organisms and organic matter on particle surface [Bainbridge et al., 2012, Passow, 2002].

Recent studies have however found that sediment flocculation under biological influence is also affected by biological decay and that the strength of bonds is time-

dependent. Flocs can therefore break without the influence of shear, simply by biomat-  
ter degradation [Jeldres et al., 2018, Mikutta et al., 2007].

The rate of microbial degradation depends on the environment and the catabolism [Foree & McCarty, 1970], and the degradation is different for different types of EPS [Comte et al., 2006, Zinkevich et al., 1996]. Living microorganisms (that produce EPS and other types of polyelectrolytes) are function of grazing [Porter, 1973] and water nutrients [Chai et al., 2006, Li et al., 2014]. Further study on the degradation of EPS in combination with its interaction with sediment is required.

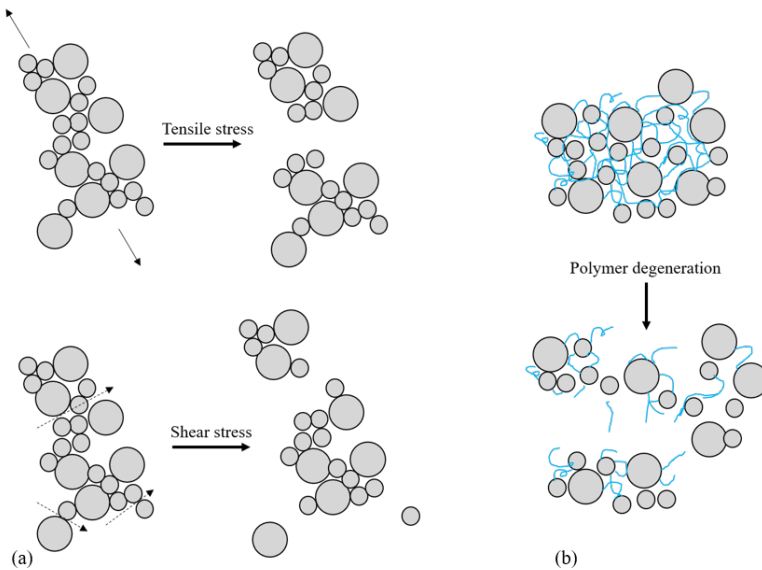


Figure 2.4: Schematic diagram of floc breakup processes, (a) Breakup by stress (b) Breakup by polymer degeneration. Adapted from Jarvis et al. [2005], Lai et al. [2018]

### 2.3.1. The Kolmogorov microscale

Shear stress is one of the most important external factors affecting the flocculation process and has been widely studied (e.g., Dyer & Manning, 1999, Mietta et al., 2009a, Partheniades, 1993, Winterwerp, 1998).

The turbulent shear rate  $G$  is often used to quantitatively describe the turbulent strength:

$$G = \sqrt{\epsilon / \nu} = \nu / \eta^2 \quad (2.6)$$

where  $\epsilon$  is the turbulent energy dissipation rate,  $\nu$  is the kinematic viscosity of water body, and  $\eta$  is the Kolmogorov microscale. The Kolmogorov microscale is the smallest scale of a turbulent eddy.

The increase of turbulent shear stress can increase the collision frequency between sediment particles hereby promoting sediment particle aggregation, whereas high shear stress reduces the Kolmogorov microscale and increases the break-up frequency of flocs. Dyer [1989] first suggested that there exist a critical value of shear stress, below which the floc size increases and after which decreases (Figure 2.5). Many researchers believe that the maximum size of flocs formed in turbulent flow is controlled by  $\eta$ . There is indeed a positive correlation between the floc size and Kolmogorov microscale, which are usually of the same order of magnitude [Kumar et al., 2010, Mietta et al., 2009a, van Leussen, 1997]. This is however not true for organic matter flocs—they can grow larger than the Kolmogorov microscale, as already mentioned above [Shakeel et al., 2020].

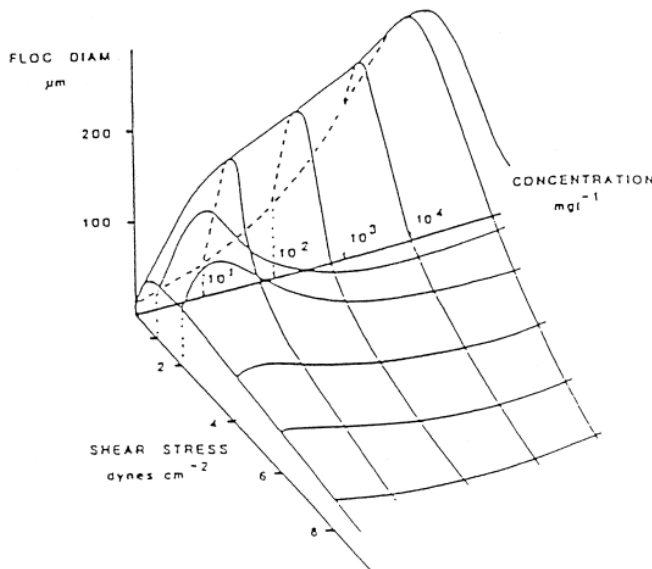


Figure 2.5: The generalized diagram of the relationship between floc size and turbulent shear and suspended sediment concentration [Dyer, 1989].

The fact that floccs follow the Kolmogorov microscale is true for salt-induced floccs [Mietta, 2010], but under the condition that the floccs have reached their equilibrium size. At low shear, it can be shown that for dense particles, not all particles remain in suspension and hence the average mean diameter decreases with the increasing number of particles that are not suspended [Mietta et al., 2009b]. It should be noted that in the case of low turbulent shear stress, the flocculation process may change from being dominated by turbulent shear stress to being dominated by differential settling, thus affecting the flocculation process and the characteristics of the final flocculation [Chen et al., 1994, Fugate & Friedrichs, 2003, Lick et al., 1993].

The characteristic values of shear stress between these two regimes have been obtained in many studies, including laboratory experiments (e.g., Kumar et al., 2010, Manning & Dyer, 1999, Miotta et al., 2009a, Serra et al., 2008) and field observation studies (e.g., Guo et al., 2017, Markussen & Andersen, 2014, Sahin, 2014). Markussen & Andersen [2014] and Guo et al. [2017] showed that the characteristic turbulent shear rate in their in-situ studies was about  $3\text{--}4\text{ s}^{-1}$ , whereas the critical range obtained in other studies [Kumar et al., 2010, Manning & Dyer, 1999, Sahin, 2014, Serra et al., 2008, Zhang et al., 2013] was about  $15\text{--}40\text{ s}^{-1}$ , indicating that the magnitude of the turbulent shear rate may be different in different estuaries.

## 2.4. Characteristics of Floccs

Characteristics of floccs include size, shape, effective density and composition. These parameters are important to understand the cohesion of floccs and their settling velocity.

### 2.4.1. Floc sizes and shapes

Generally, floc size is assessed by laser diffraction techniques (with equipment like Malvern Mastersizer and LISST that are detailed in chapter 3). These techniques convert the raw data (diffracted light) into particle size by making use of the assumption that particles are spherical and represented by their equivalent diameter. The particle sizes are given in logarithmically-spaced size bins, and the particle size distribution (PSD) is given as a volume-% (volume occupied by particles of a sizes within a given bin compared to the volume occupied by all particles). It is usually assumed that the  $D_{50}$  of the distribution is representative for the mean particle size of the distribution

[Maggi, 2005]. Nonetheless it often occurs that a PSD displays multiple size peaks [van Leussen, 1994], which reflects the fact that different types of particles are present in the sample, such as mineral sediment, flocs and microorganisms like algae [Deng et al., 2019, Tang, 2007].

Multiple peaks in PSD also occur because of the shape of particles [Agrawal & Pottsmith, 2000]. For example, Liu et al. [2007b] found by scanning electron microscope technique that the sediment flocs of the Changjiang estuary at different salinities have various shapes. Mhashhash et al. [2018] showed that at different suspended sediment concentrations (SSC) flocs of different shape are found. In high shear stress areas such as estuaries and coasts, flocs are usually small and spherical or ellipsoidal [van Leussen, 1994]. Some typical flocs are given in Figure 2.6. In low shear stress environment, the flocs are usually elongated in a chain-like fashion [Manning et al., 2007]. The drag force on these flocs will be different and this will thus affect the aggregation between particles leading to larger flocs of various shapes [Adachi et al., 2012, Maggi, 2005].

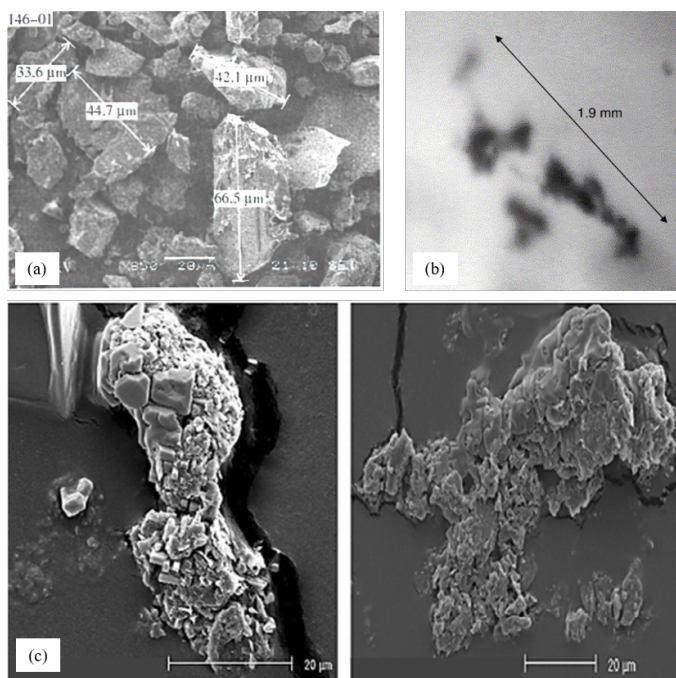


Figure 2.6: Photomicrography of flocs (a) Liu et al. [2007a] (b) Manning et al. [2007] (c) Mhashhash et al. [2018]

### 2.4.2. Floc density and settling velocity

It has been shown that the density of a floc usually decreases with the increase of the floc size [Fennessy et al., 1994]. Figure 2.7 shows the relationship between effective density (floc particle density minus water density) and floc size obtained from several previous studies. The results are for many different rivers and estuaries, such as the upper Tamar River in the UK [Fennessy et al., 1994], the Po River Estuary in Italy [Fox et al., 2004] and the Changjiang River Estuary (e.g., Guo et al., 2017, Wang et al., 2013) and laboratory experiments with natural sediment (e.g., Gibbs, 1985, Manning & Dyer, 1999). The effective density of flocs ranged from ten to several hundred kilograms per cubic meter, but there were quite some large differences between the correlations of the effective density and particle size. Basically, a same floc size may correspond to different effective densities. This is the result of the fact that flocs can have very heterogeneous composition.

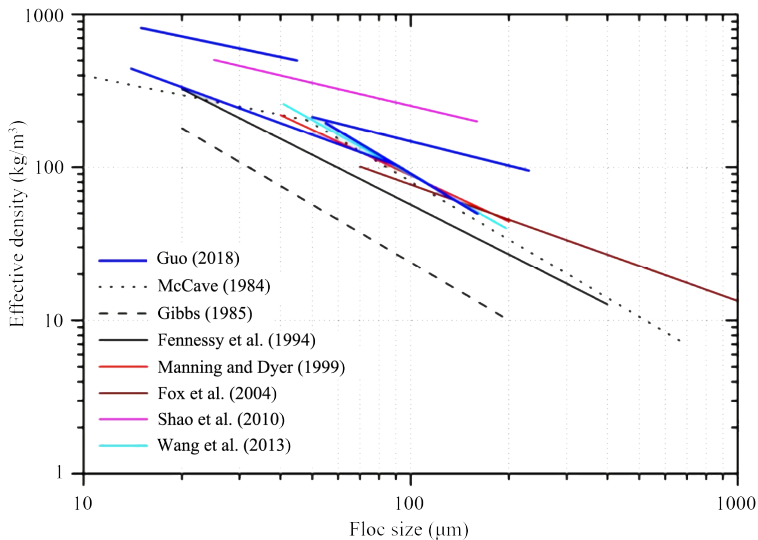


Figure 2.7: Change of effective density of flocs with particle size [Fennessy et al., 1994, Fox et al., 2004, Guo, 2018, Manning & Dyer, 1999, McCave, 1984, Shao et al., 2011, Wang et al., 2013].

To describe quantitatively the relation between floc size and floc effective density, Kranenburg [1994] proposed that the flocs should be treated as fractals. A fractal is defined as a self-similar object [Mandelbrot, 1982]. In existing studies, there are two main descriptions of fractals: one is the two-dimensional fractal dimension  $N_p$  based on

perimeter and area, and the other is the three-dimensional fractal dimension  $N_f$  based on the volume of particles contained inside a floc. It is the latter that is of interest to determine the density of flocs. [Kranenburg \[1994\]](#) derived the following relationship between effective density and particle size:

$$\Delta\rho = \rho_F - \rho_W \propto (\rho_p - \rho_W) \left(\frac{D_F}{d}\right)^{N_f-3} \quad (2.7)$$

where  $\Delta\rho$  is the effective density of floc,  $\rho_F$  and  $\rho_W$  are the density of floc and the density of water, respectively.  $\rho_p$  is the density of mineral sediment particles,  $D_F$  and  $d$  represent the floc size ( $D_{50}$ ) and the mean particle size of the constitutive particles. It can be seen that for a same size of constitutive particles and flocs, different fractal dimensions lead to different effective densities. By tuning the fractal dimension, it is therefore possible to fit the different effective densities as function of floc sizes found in [Figure 2.7](#). Usually the density of flocs is obtained from settling velocities experiments from which, using Stokes settling velocity, the density can be deduced. In general the settling velocity of a sinking object is expressed as:

$$\omega_s = \sqrt{\frac{4}{3} \gamma \frac{\Delta\rho g D_{50}}{C_D \rho_W}} \quad (2.8)$$

$\gamma$  is the coefficients related to particle shape where  $\gamma = \alpha/\beta$  as defined in [Winterwerp \[1998\]](#).  $C_D$  is the drag coefficient and  $\omega_s$  is the settling velocity of flocs. The drag coefficient is a function of particle Reynolds number [[Winterwerp, 1998](#)]:

$$C_D = \frac{24}{Re(1 + 0.15Re^{0.687})} \quad (2.9)$$

Particle Reynolds number  $Re = \omega_s D_{50}/\nu$ ,  $\nu$  is the kinematic viscosity of water. For spherical particles,  $\gamma = 1$ . When the particle Reynolds number  $Re \ll 1$ , the above expression can be simplified to Stokes settling velocity:

$$\omega_s = \frac{\Delta\rho g D_{50}^2}{18\mu} \quad (2.10)$$

In fine sediment transport models, the settling velocity is usually taken to be constant, and its value is about  $0.05\text{--}0.1 \text{ mm s}^{-1}$  (e.g., [Geyer et al., 2004](#), [Hu et al., 2009](#)). This assumption of a constant settling velocity is obviously an approximation, as it was discussed above that flocs can change shape and density as function of shear (and time).

### 2.4.3. Flocc composition

#### Mineral sediment

It is usually assumed that floccs are composed of fine sediment (clay and silt fraction) with some amount of organic matter. However, sand can also sometimes be entrapped in floccs. Manning et al. [2010a] studied the flocculation process with different mud/sand mixtures and demonstrated that different composition ratio of mud and sand can influence the floccs settling velocity.

Different clay minerals with different particle size and surface charges are found in floccs. Goldberg [1991] found that the optimum flocculation salinity for different clay minerals is different. The optimum flocculating salinity of illite and kaolinite is 9–13 PSU, while that of montmorillonite is 20–24 PSU. This result is in line with DLVO theory, as montmorillonite clay, being delaminated, has a larger surface area than kaolinite or illite particles and hence the particles experience a larger Coulombic repulsion. The content of clay minerals in the suspended sediment of the Changjiang estuary is about 26%, of which 65%–70% are illite, and the rest are chlorite, montmorillonite and kaolinite. The settling velocity of illite is 9 times higher than that of montmorillonite when the salinity is 10 PSU. The main types of clay minerals vary as function of the tidal periods because the sediment transport and deposition mechanisms are different [Zhang, 1996]. The laboratory experiments and field observations of the flocculation characteristics of fine sediment in the Changjiang Estuary show that the optimum flocculation salinity ranges from 4 to 16 PSU [Guan et al., 1996, Jiang et al., 2002, Wan et al., 2015].

#### Extracellular Polymeric Substances (EPS) and microbial communities

EPS and other polymeric substances are produced by microorganisms. These microorganisms can be microscopic algae (such as diatoms), which can form large floccs by themselves, and afterwards capture sediment particles [Deng et al., 2019].

In 1968, Walsby [1968] described the aggregation of *N. nutans*, by the mucus this microorganism is secreting. Avnimelech et al. [1982] studied the aggregation process of *Chlamydomonas* and collar algae with clay by electron microscope in 1982 (Figure 2.8). This is the earliest image of algae and sediment flocculation. Besides, Avnimelech et al. [1982] compared the effect of four different forms of algae on clay flocculation and showed that algae can significantly promote the flocculation of clay in the presence

of electrolytes. Therefore, the reason why the growth of algae is restricted in high turbidity areas may not only be due to the limited light supply but also because of the flocculation with sediment particles.

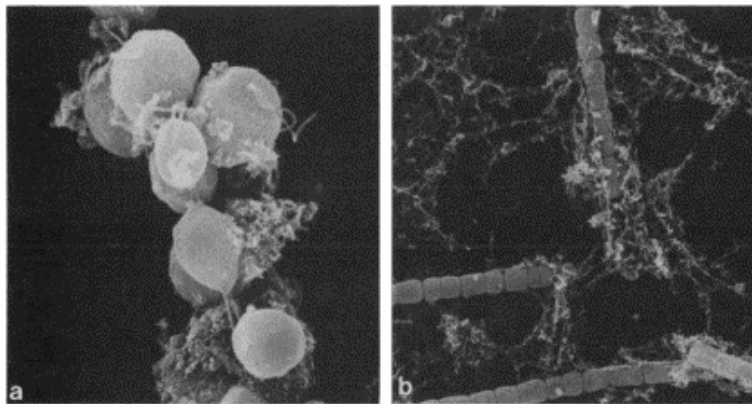


Figure 2.8: Floccs under scanning electron microscope (a *Chlamydomonas* clay cluster, 1470 times; B-ring algae clay cluster, 1200 times), images taken from [Avnimelech et al. \[1982\]](#)

Diatoms are the largest component of microalgae which goes by the name phytoplankton. Therefore, most of the research on the effects of microorganisms on sediment flocculation in estuaries are done with diatoms. Diatoms in healthy state will remain suspended due to turbulence and water current.

Phytoplankton is a large community with strong adaptability. These microorganisms can live under very low nutrient concentration, very weak light intensity and quite low temperature. They can not only grow in rivers, streams, lakes and oceans, but also in short-term ponding or humid places [[Blum, 1956](#), [Round, 1981](#)].

Temperature is the main factor affecting the geographical distribution of algae. Therefore, in the sea area where the water temperature changes greatly, the species changes greatly through the year. In winter, there are cold water algae (the optimum temperature for growth and reproduction is less than 4 °C) and there are warm water algae (the optimum temperature for growth and reproduction is about 20 °C) in summer, which can complete their life cycle in a short time. Most of freshwater microalgae appear in spring and autumn. Some cyanobacteria only appear when the water temperature is high in summer. Light is the decisive factor to determine the vertical distribution of algae. The light absorption capacity of a water body is very strong, so the light in-

tensity at 10 meters depth is only 10% of that of water surface, and the light intensity at 100 meters deep is only 1% that of water surface. Moreover, because seawater can easily absorb long-wave light, it also causes a spectral difference in light at various water depths. Different algae have different requirements for light intensity and spectrum. Green algae generally live at the surface of water, while red algae and brown algae can use short wave light such as green, yellow and orange to live in deep water [Castro & Huber, 2016, Reynolds, 2006, Wood, 2014].

The chemical properties of a water body are also important factors for the appearance and species composition of algae [Pearson et al., 1987, Zou et al., 2011]. For example, *Cyanobacteria* and *Gymnophyta* can live in eutrophic water and often form blooms; *Bacillariophyta* and *Chrysophyta* often exist in lakes with poor nutrition in mountainous areas; *Chlorophyta* and *Cryptophyta* often occur in small ponds. In addition, the interaction between algae living in the same water area also plays an important role in their emergence and growth, as some algae can inhibit the growth of other algae by secretions.

*Skeletonema costatum* (Figure 2.9) of *Bacillariophyta* are the dominant species in the Changjiang Estuary [Gao & Song, 2005, Pan et al., 2007]. *Skeletonema costatum* is a common planktonic species. Its cells are lenticular or cylindrical with an equivalent diameter of 6–22  $\mu\text{m}$ . It can adapt to a wide range of salinity and temperature. The range of survival salinity is 7–50 PSU, the optimum salinity is 15–30 PSU, and the survival temperature is 10–34  $^{\circ}\text{C}$ , with the optimum temperature range being 20–30  $^{\circ}\text{C}$ . It is widely distributed from the arctic to the equator, from the high salt water mass in the open sea to the low salt water mass along the coast, and lives even in brackish water, even though most of organisms are found along the coast [Castro & Huber, 2016, Round, 1981, Wood, 2014]. *Skeletonema costatum* is a common species forming a red tide the Changjiang Estuary, which usually appears in summer when the salinity is 14–20 PSU and temperature is 25  $^{\circ}\text{C}$ . Therefore, in the present thesis, *Skeletonema costatum* is used to study sediment flocculation as being representative of the dominant species in the Changjiang Estuary .

The presence of organic matter like EPS promotes the flocculation of fine sediment (e.g., Droppo & Ongley, 1992, Fettweis & Baeye, 2015, Gratiot & Manning, 2004, Mietta et al., 2009a). It was found that organic matter play a major role in the floc collision rate and floc strength in the observation of seasonal variation of flocs.

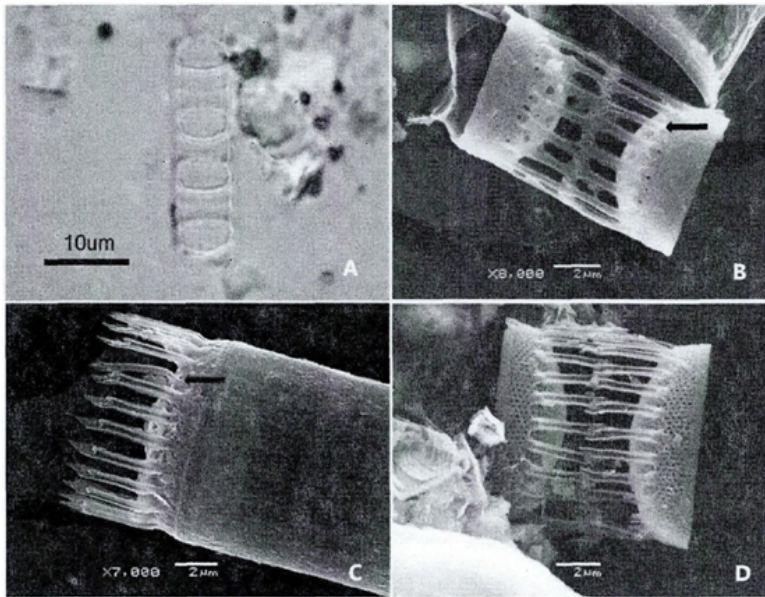


Figure 2.9: Light microscope images (A) and Scanning Electron Microscopic images (B–D) of *Skeletonema costatum* from Changjiang Estuary. Images from Wu [2015].

A: Intercalary valve of colony in girdle view.

B: Intercalary valves of colony with intercalary fultoportula processes (IFPPs), arrow shows the intercalary rimoportula process (IRPP).

C: Terminal valve of colony in girdle view, with claw-shaped tips in the terminal fultoportula process (TFPP) and the terminal rimoportula process (TRPP) (arrow) in a marginal position.

D: Detail of a colony. fultoportula processes (FPPs) are similar to terminal fultoportula processes (TFPPs) of terminal valves, indicating that the colony is dividing in that point.

Large flocs usually appeared at algae bloom seasons due to biologically induced aggregation [Fettweis & Baeye, 2015, Lee et al., 2014, Mikkelsen, 2002, Uncles et al., 2010]. Besides, the biological effects on sediment flocculation also be found in fresh water environment [Guo & He, 2011].

An overview of different studies is given in Table 2.1.

Table 2.1: Some flocculation in-situ observation results which included the organic matter

Authors	Location	Spatial variation	Seasonal variation	Parameters				
				Floc size	Settling velocity	SSC	Salinity	Organic matter
Eisma & Li [1993]	Dollard	o	-	o	-	o	o	o
van der Lee [2000]	Dollard	-	o	o	o	o	-	o
Thill et al. [2001]	Rhone	o	o	o	o	o	o	o
Mikkelsen [2002]	Danish coast	o	o	o	o	o	o	o
Fugate & Friedrichs [2003]	Chesapeake Bay	o	-	o	o	o	o	o
Fox et al. [2004]	Po	o	-	o	o	o	o	o
Xia et al. [2004]	Pearl river	o	-	o	o	o	o	o

“o” means the factor has been measured or taken into account

“-” means it has not been measured or taken into account

Some studies have shown that the presence of humus in estuarine water also has influence on sediment flocculation. When humus, which has a strong negative charge, is adsorbed on suspended particles, it will increase the negative charge of particles, thus enhancing the stability of sediment particles [Bob & Walker, 2001, Lee et al., 2017].

## 2.5. Other influence factors

The effect of shear has already been discussed in section 2.1.1 and the effect of salinity in section 2.1.2. Besides shear stress and salinity, the water property is defined by pH and temperature. The pH value of water has a direct impact on the physiological activities of bacteria and microorganisms on the surface charge of mineral sediment. pH can therefore significantly affect (bio)flocculation by changing the EPS activity [Yokoi, 2002, Yokoi et al., 1995]. With the increase of pH in a water body, the functional groups on the mineral sediment (and EPS) such as carboxyl and amino group will dissociate or not leading to an increase or decrease in surface charge. Different bacterial species have different adaptability to pH and therefore, the effect of pH on sediment flocculation needs further study.

The effect of temperature on the flocculation ability of sediment particles is in principle twofold. An increase in temperature theoretically increases the thickness of electric double layer of particles, leading to an increase in the repulsive force between

two particles. On the other hand, the increase in temperature leads to an increase in Brownian motion of particles which leads to an increase in collision frequency, which is beneficial for flocculation. In general, however, it is found that temperature has little effect on flocculation, and the effect of shear (through turbulence) on flocculation is much greater than the one caused by temperature [Lau, 1994].

However, if microorganisms are involved in the flocculation process, temperature changes have a significant impact on flocculation, because biological activities are closely related to temperature. For example, the highest value of photosynthesis is between 20 °C and 25 °C, when the algae growth reaches the maximum value [Blanchard et al., 1996, Colijn & van Buurt, 1975], and some algae produce EPS with high viscosity [Lupi et al., 1991]. When the temperature drops to 4 °C, both the number of algae and the EPS will decrease [Domozych, 2007, Kiemle et al., 2007], and the activity of EPS will also decrease, thus reducing the effect on flocculation [Wilén et al., 2000].

## 2.6. Discussion

In conclusion, flocculation of cohesive sediment mainly includes two processes: aggregation and decay (break-up by biodegradation or shear—whereby shear can also lead to a densification of flocs (without breakage)). In these two processes, physical, chemical and biological factors will have a role and also interact with each other. These factors can either promote aggregation or decay. For example, turbulent shear stress and suspended sediment concentration can promote particle collision frequency and facilitate flocculation, but a very high shear will limit flocs growth. The effect of salinity (cation concentration) has an optimal range as well, as within a certain range salinity can promote sediment flocculation. Organic matter (such as EPS) will usually enhance the stability of sediment particles, but can also degrade over time and lead to a decay (break-up) of flocs.

Although many studies have been performed in the field of flocculation, floc characteristics and factors affecting sediment flocculation, there are relatively few studies on biological effects on sediment flocculation. Many authors have begun to pay attention to the study of biological factors in recent years, however, in most studies the effects of organic matter and microbial communities are not differentiated, whereas the effects of these two factors should be distinguished in the context of sediment flocculation. Even though it is the microbial community that produces polymeric organic matter

(such as EPS), two types of flocculation can be found: EPS acts on the surface properties of sediment while living microalgae aggregate themselves to form large flocs first, and then catch sediment particles within their network. Hence, the effects of organic matter (EPS) and biological community (algae) on the flocculation process are studied separately in this thesis.

A summary of the different processes involved in flocculation is given in Figure 2.10.

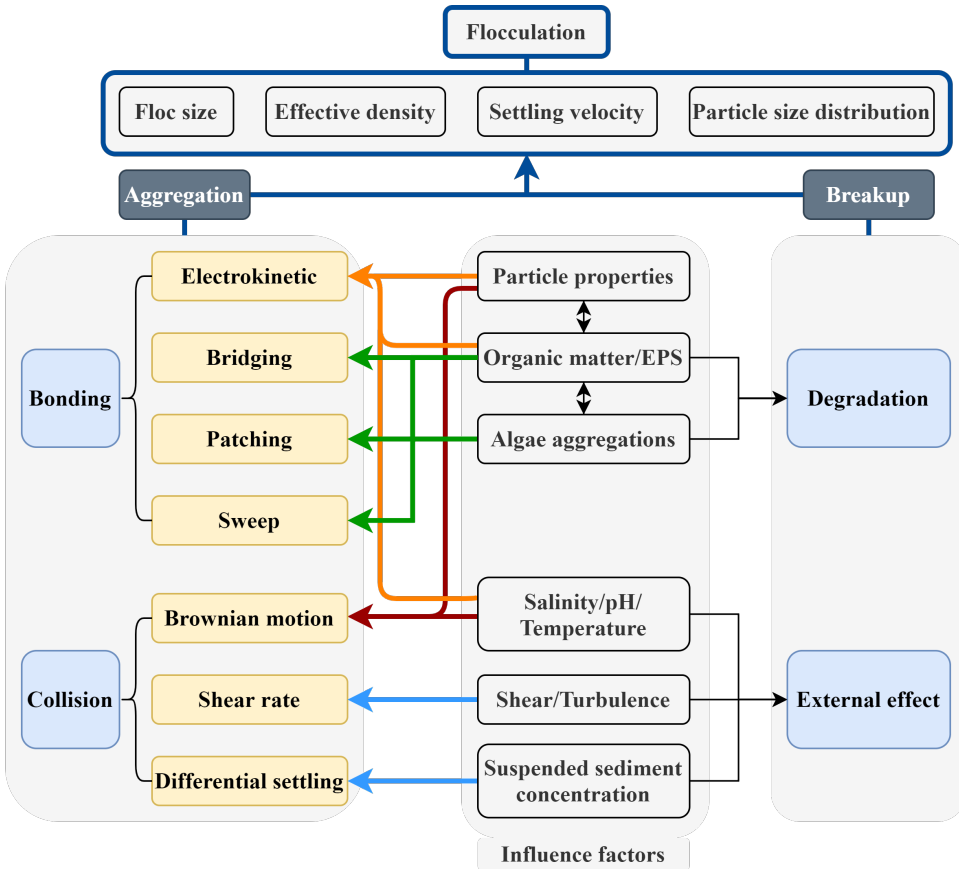


Figure 2.10: Influence factors and their interactions in the flocculation process



# 3

## Methodology

*God gives every bird its food,  
but He does not throw it into its nest.*

Josiah Gilbert Holland

Because sediment flocculation is sensitive to a large number of parameters and conditions and that both laboratory measurements and in-situ observations have their limitations, it is profitable to combine the two methods to investigate the flocculation. The goal of this chapter is to describe the flocculation measurements obtained from both laboratory measurements and in situ observations. From analyzing the results obtained from these two investigation methods, a discussion about the role of biological effects on sediment flocculation in natural environments will be given.

The in-situ observations were realized in the maximum turbidity zone (TM) in Changjiang Estuary.

## 3.1. Laboratory measurements

### 3.1.1. Experimental samples

The laboratory experiments were conducted at Deltares research institute in the Netherlands. The sediment samples used in the experiments were bed surface sediments collected from the maximum turbidity zone in the South Passage (NP) of the Changjiang estuary (the site of in-situ observation in this study). Figure 3.1 shows the particle size distribution of a sediment sample in demi-water water, which was measured by Malvern Mastersizer 2000. It is found that the sediment sample mainly consists of clay (<4  $\mu\text{m}$ ) and silt (4–62  $\mu\text{m}$ ), the proportions being 28% and 70%, respectively. In addition, there is 2% of sand in the sample. The peak of the PSD corresponds to size 7.1  $\mu\text{m}$ , and the median particle size is 7.9  $\mu\text{m}$ . It should be noted that, due to the non-uniformity of the samples, the particle size distributions of sediment samples could vary a little, but the changes were found to be small and do not affect the results of the experiments.

The sediment samples were collected during the in-situ observations, and they were kept at 4 °C to avoid changes in sediment properties. Before the experiment, the samples were taken out and placed at room temperature (about 15–20 °C). It is worth noting that the organic matter of sediment sample was measured by calcination method, and the content of organic matter was less than 3% in mass.

A lot of algae can be found in the water samples collected from the Changjiang estuary, such as *Skeletonema costatum*, *Cyclotella meneghiniana* and *Aulacoseira granulata*, among others (see Figure 3.2).

As *Skeletonema costatum* represents over 90% of the algae species in Changjiang Estuary, especially in the study field station [He & Sun, 2009, Wu, 2015], this species was used in the laboratory tests. The algae were bought from Roem van Yerseke B.V. (The Netherlands) and used within a few days following the purchase. The purchased algae were in good health and sampled during the growing period (Figure 3.3). The concentration of algae was confirmed when purchased, and counted using a high resolution microscope. The average concentration of algae is about  $5 \times 10^6$  cells  $\text{l}^{-1}$  (marked as 100% concentration). During the experiments, the concentration and number of algae were obtained according to the volume of the algae solution added. Finally, to ensure the survival of the algae, each experiment usually lasted no more than three hours. Ev-

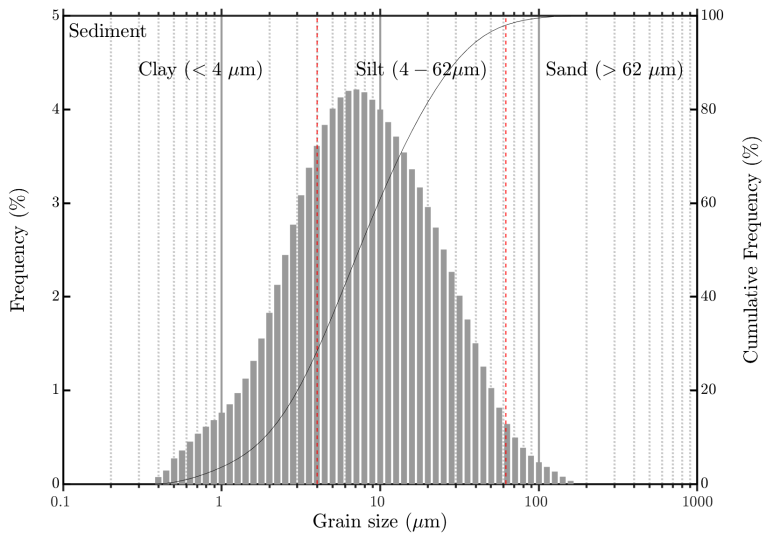


Figure 3.1: The cumulative (black curve) and non-cumulative (grey bar) distributions of the sediment samples for laboratory experiments.

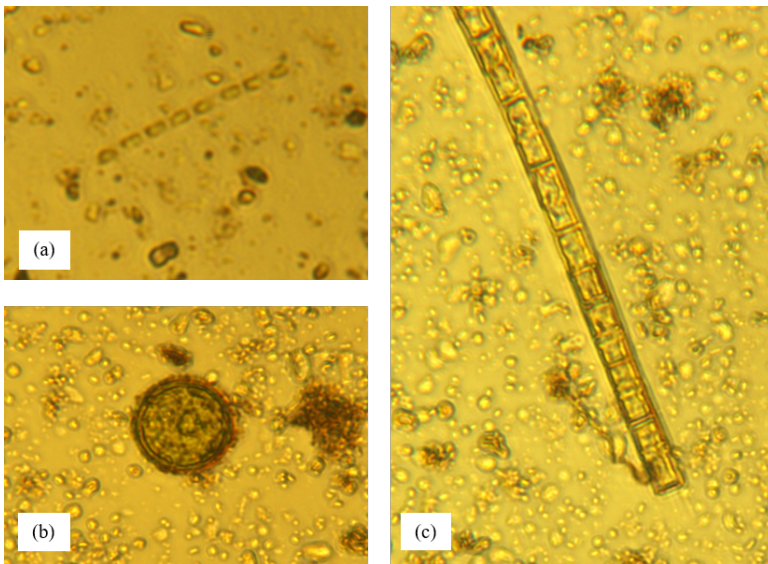


Figure 3.2: *Skeletonema costatum*, *Cyclotella meneghiniana* and *Aulacoseira granulata* in Changjiang estuary, measured in laboratory.

ery two weeks a fresh batch of algae was used to keep the bulk concentration constant. The EPS used in this thesis was obtained from municipal waste water extractions and contained  $200 \mu\text{g l}^{-1}$  proteins,  $40 \mu\text{g l}^{-1}$  humic acids and  $110 \mu\text{g l}^{-1}$  polysaccharides.

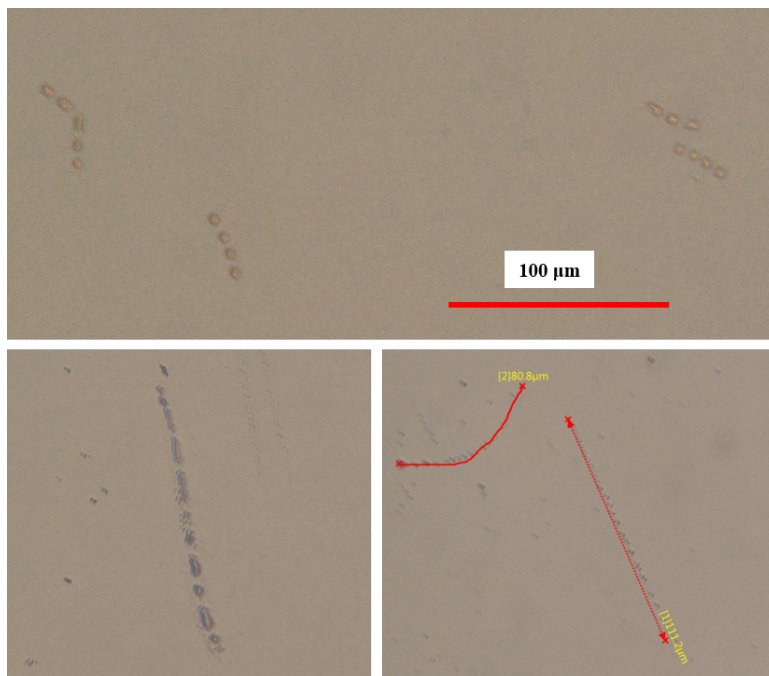


Figure 3.3: The microscope images of algae from Roem van Yerseke B.V.

### 3.1.2. Static Light Scattering (SLS)

The static light scattering experiments were performed using a Malvern MasterSizer [Mietta, 2010]. The experimental device consists of beaker, pipes, agitator, pump and Malvern Mastersizer (Figure 3.4). The principles of the LISST equipment used in-situ and the Malvern MasterSizer are quite similar [Filippa et al., 2011]. From the SLS measurements a full particle size distribution (size range 2 nm–2 mm in 100 log-spaced bins) was recorded every 30 s, enabling to follow flocculation in time. Sediment and algae sample were added to a mixing jar and stirred by a paddle at the lowest speed possible to keep particles suspended. The samples were pumped into instrument and back to mixing jar continuously through two pipes of diameter 6 mm. The mixing jar was 0.125 m wide and 0.185 m high.

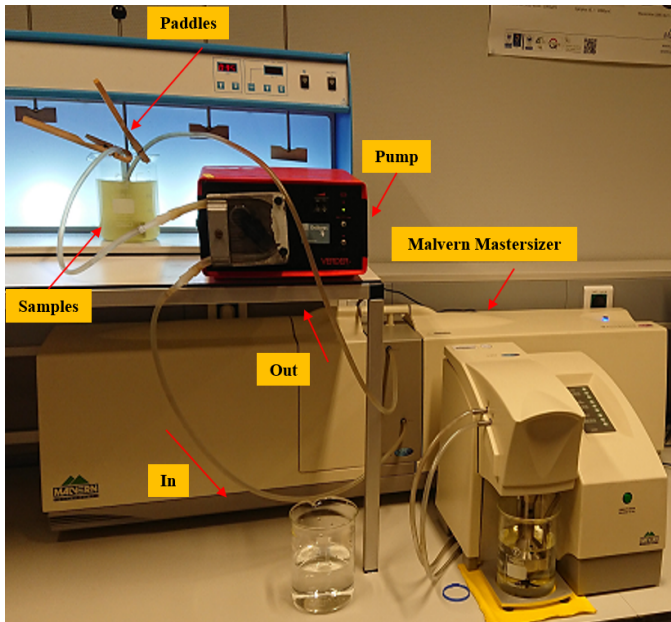


Figure 3.4: The Static Light Scattering device pictures taken at Deltares Laboratory.

In previous studies, the shear rate in the jar was evaluated using  $\log G = -0.849 + 1.5 \log(60s_f)$ , where  $s_f$  is the stirring rotations per second [de Lucas Pardo, 2014, Mietta, 2010]. In the experiments, flocculation is not only affected by the shear forces in the beaker, but also affected by the shear rate in the tubes. The shear rates in the tubes are estimated using:

$$G = 4Q / (\pi r^3) \quad (3.1)$$

where  $Q$  is the discharge ( $\text{m}^3 \text{s}^{-1}$ ) and  $r$  is the radius of the pipe (3 mm).

In general, the minimum pump speed was kept to 10 rotations per minute (RPM) as the pump would sometimes stop working when the pump speed was lower than 10 RPM. 10 RPM corresponds to  $90 \text{ s}^{-1}$ . As shown in Table 3.1 and Table 3.2, the shear rate in the tubes was usually larger than in the jar and is therefore the one we will consider here as limiting factor for aggregation.

The speed of the mixer was adjusted to 30 RPM to keep the samples in suspension. The pump speed was set to 10 RPM. Although there were two different shear rate distribution in jar and tubes, it has been shown that the shear rate distribution in the

Table 3.1: The comparisons of the shear rate in the jar (generated by paddles)

RPM	10	20	30	40	50	60	70	80	90	100	110	120
Shear rate (G)	4	13	23	36	50	66	83	101	121	-	-	-

“-” means the high shear rate led to water sample spilling

Table 3.2: The comparisons of the shear rate in tubes (generated by the pump)

RPM	5	10	20	30	40	50
Shear rate (G)	10	90	203	359	-	-

“-” means the high shear rate led to water sample spilling

jar affects the shape of the floc size distribution but not the mean floc size [Bouyer et al., 2004].

The minimum shear rate used in the experiments was therefore  $90 \text{ s}^{-1}$  which is usually higher than in situ observations, implying that smaller flocs could be created in laboratory experiments compared to in situ. Another difference is the residence time in the jar: as the particles are kept in suspension, their collision probability and frequency will be higher than in-situ.

### 3.1.3. Settling columns

The settling column measurements were performed in 5 cylindrical glass columns (1 L). Each cylinder contained different concentrations of sediment and fresh algae samples in demi-water, as given in Table 3.3. The samples were mixed thoroughly by inverting the columns ten times by hand. The columns were then left to stand for about 24 hours. The water/suspension interface was recorded by camera (Canon 70D) every 2 minutes.

### 3.1.4. Microscopy

The pictures of (flocculated) algae were taken using a Digital Microscope (VHX 5000 Series, Figure 3.5). Flocs were sampled from the mixing jar, put onto a clean glass slide covered by another glass slide and visualized. The required confinement of the flocs between two glass slides affects the structure of the flocs and therefore the

recorded sizes of flocs were smaller than the ones measured in-situ.

Table 3.3: Set-ups of the settling column measurements

Group name	SSC	Volume	Algae concentration		CC/SSC
	$\text{g l}^{-1}$		$\text{cells l}^{-1}$	(Estimated CC) $\mu\text{g l}^{-1}$	$\mu\text{g g}^{-1}$
a	0.7	-	-	-	-
b	-	1%	$5 \times 10^4$	1.25	-
c	-	10%	$5 \times 10^5$	12.5	-
d/g	0.7	1%	$5 \times 10^4$	1.25	1.8
e/f	0.7	10%	$5 \times 10^5$	12.5	17.9



Figure 3.5: Microscope pictures taken at TUDelft Laboratory

### 3.1.5. Zeta potential and Conductivity

The zeta potential and conductivity were obtained from electrophoretic measurements using a Malvern Zetasizer 1000HS/3000HS (Figure 3.6). The zeta potential is given using the Smoluchowski equation [Chassagne et al., 2009]. Although the zeta potential is in theory not depending on sediment concentration, the sediment concentration should be low enough to ensure that there is no electrostatic interactions between particles [Mietta, 2010]. In this study, the sediment concentration was set to  $0.7 \text{ g l}^{-1}$  to ensure that there was no electrostatic interaction between sediment particles.

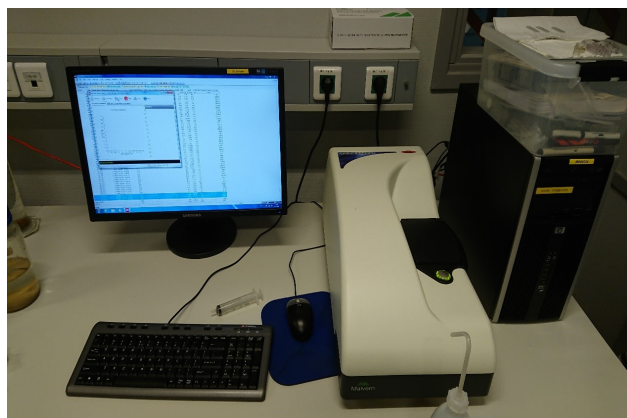


Figure 3.6: Malvern Zetasizer pictures taken at Deltares Laboratory.

### 3.1.6. LabsFLOC-2 camera system (Laboratory Spectral Flocculation Characteristics, version 2)

LabsFLOC-2 was developed by Manning [Benson & Manning, 2013, Manning & Dyer, 2002, Manning et al., 2017], and it utilizes a high magnification 2.0 MP Grasshopper monochrome digital video camera [Manning & Dyer, 2002] to observe individual flocs as they settle in a 350 mm high by 100 mm square Perspex settling column (Figure 3.7). The video camera, positioned nominally 75 mm above the base of the column, views all particles in the center of the column that pass within a 1 mm depth of field, 45 mm from the Sill TZM 1560 Telecentric (maximum pixel distortion of 0.6%), 0.66 (1:1.5) magnification, F4, macro lens fitted behind a 5 mm thick glass face-plate.

During sampling, a modified pipette is used to carefully extract a floc sub-sample from the Van Dorn chamber and is filled to produce a fluid head of 50 mm, which results in a video image control sample volume nominally of  $400 \text{ mm}^3$  (1 mm image depth and 8 mm nominal video image width, with a nominal 50 mm high suspension extracted with a modified pipette). This controlled volume permits in principle LabsFLOC-2 calculated floc mass to be compared and calibrated directly to ambient SSC.

The pipette sub-sample is immediately transferred to the LabsFLOC-2 settling chamber, whereby the aperture of the pipette was brought into contact with the settling column water surface and permitted the flocs to pass from the vertically held pipette to the chamber and settle solely under gravity, i.e. naturally and unassisted. Thus, the

flocs allowed to pass into the settling column were naturally segregated as they fell by the process of differential settling; i.e. the fastest falling aggregates would be observed first.

Settling flocs are viewed as silhouettes (to reduce image smearing) resulting from a CCS LDL-TP-43/35-BL, 43 x 35 mm, homogeneous blue (470 nm) back-illumination LED panel, located at the rear of the settling column. The video images are streamed in real time as AVI files to a laptop PC via a FireWire-B PCI card interface. The digital floc images are captured at a frame rate of 7.5 Hz (one frame is 0.04 s), at a resolution of  $1600 \times 1200$  pixels, with an individual pixel nominally representing  $5 \mu\text{m}$  (confirmed by independent calibration). The AVI files are not Codec compressed, so they could be analysed with MatLab software routines. During post-processing, the HR Wallingford Ltd DigiFloc software - version 1.0 [Benson & Manning, 2013, Manning et al., 2017], is then used to semi-automatically process the digital recordings to obtain floc size and settling velocity spectra.

The sphere-equivalent floc diameter,  $D_f$ , was calculated by measuring both major-axis and minor-axis of each observed two-dimensional floc image [Manning & Schoellhamer, 2013]:

$$D_f = (D_{major} \times D_{minor})^{0.5} \quad (3.2)$$

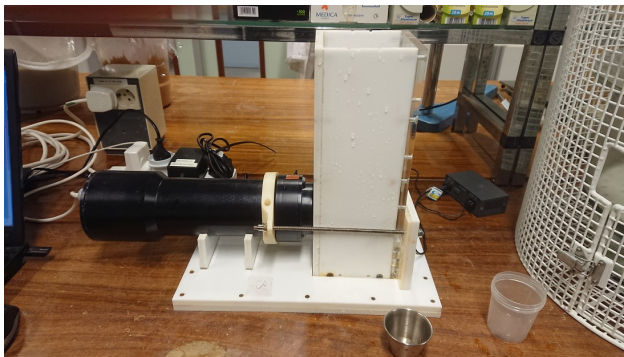


Figure 3.7: LabsFLOC-settling column pictures taken at Deltares Laboratory.

### 3.1.7. Experimental setup

In this study, the effect of different salt types (NaCl, MgCl<sub>2</sub> and CaCl<sub>2</sub>) and concentrations, different biological factors (EPS and living algae) were studied. The shear rate was set to certain values of 90 s<sup>-1</sup>. The different measurements are listed in Table 3.4. All measurements were carried out at room temperature and the water temperature was 20±2 °C.

The artificial sea salt used in the experiment consisted of four major components: NaCl, MgCl<sub>2</sub>, CaCl<sub>2</sub> and KCl. Because of the different proportions of cations in natural seawater, different salinity ranges were used for each cation: NaCl—0.1, 0.2, 0.3 mol l<sup>-1</sup>, MgCl<sub>2</sub>—0.01, 0.05, 0.1 mol l<sup>-1</sup> and CaCl<sub>2</sub>—0.005, 0.01, 0.02 mol l<sup>-1</sup>. In addition, regular sea water and artificial seawater also be considered in some comparative experiments.

Table 3.4: Experimental conditions

Num.*	SSC ( $\text{g l}^{-1}$ )	Salt ( $\text{mol l}^{-1}$ )		EPS ( $\text{ml l}^{-1}$ )	Algae (%)	Medium
1	0.7	-		-	-	Demi-water
2						Seawater
3	-	-		5	-	Demi-water
4	-	-		-	10	Demi-water
5	0.7	NaCl	0.1	-	-	Demi-water
6			0.2			
7			0.3			
8	0.7	MgCl <sub>2</sub>	0.01	-	-	Demi-water
9			0.05			
10			0.1			
11	0.7	CaCl <sub>2</sub>	0.005	-	-	Demi-water
12			0.01			
13			0.02			
14	0.7	NaCl	0.1	5	-	Demi-water
15			0.2			
16			0.3			
17	0.7	MgCl <sub>2</sub>	0.01	5		Demi-water
18			0.05			
19			0.1			
20	0.7	CaCl <sub>2</sub>	0.005	5		Demi-water
21			0.01			
21			0.02			
22	0.7	-	-	5	-	Seawater
23	0.7	-	-	-	10	Demi-water
24					1	
25					10	
26					1	
27	0.7	-	-	5	-	Seawater
28	0.7	-	-	-	10	Seawater
29	0.7	NaCl	0.5	-	1	Demi-water
30					5	
31					10	
32					20	
33					1	
34					5	
35					10	
36					20	
33	0.7	-	-	-	1	Seawater
34					10	
35					20	
36					30	

\* Some groups are not listed

## 3.2. In-situ observations

### 3.2.1. Changjiang Estuary Hydrodynamics

The Changjiang river is the third largest river in the world, with a total length of about 6,300 kilometers, second only to the amazon river in South America and the Nile river in Africa. Originating in the Tanggula mountains, the Changjiang river flows from west to east through 11 Chinese provinces, municipalities and autonomous regions, collecting hundreds of tributaries along the way and finally emptying into the east China sea. Yichang hydrologic station is a key hydrologic station in the middle reaches of the Changjiang river, and Datong hydrologic station is the nearest hydrologic station to the estuary, their hydrologic information was important to known the water and sediment input of the Changjiang Estuary. Years of monitoring data show that the average annual runoff of Yichang station and Datong station is about 430 and 893 billion cubic meters respectively, and annual sediment transport was 403 million tons and 368 million tons, respectively (1950–2015) [Changjiang Water Resources Commission, 2018]. The annual average runoff and sediment transport into the sea are the fifth and fourth in the world respectively [Milliman & Farnsworth, 2011]. The Changjiang river basin is a subtropical monsoon climate, with significant seasonal changes in rainfall. The annual flood season is from May to October, and the dry season is from November to next April. The runoff in the flood season and the dry season accounts for about 68% and 32% of the whole year respectively. The sediment transport in the flood season accounts for about 78% of the whole year [Changjiang Water Resources Commission, 2018]. The sediment minerals consist of illite (77.77%), chlorite (12.11%), kaolinite (8.53%) and montmorillonite (1.59%). With a  $D_{50}$  range being 7.7–11.5  $\mu\text{m}$  [Li et al., 2001].

Figure 3.8 shows the annual runoff and sediment load of Datong station in the past 60 years. The observation data shows the annual runoff is keeping stable, while the sediment load presents a decreasing trend. Since the 1970s and 1980s, the sediment load of Datong station gradually decreased from 450 million tons to about 300 million tons in 2000, especially, the sediment load was further reduced to less than 150 million tons after the Three Gorges Dam had been built up in 2003.

The Changjiang Estuary is a mesotidal estuary. The perennial average tidal range is about 2.7 m and the maximum tidal range is about 4.6 m. Tides are regular semid-

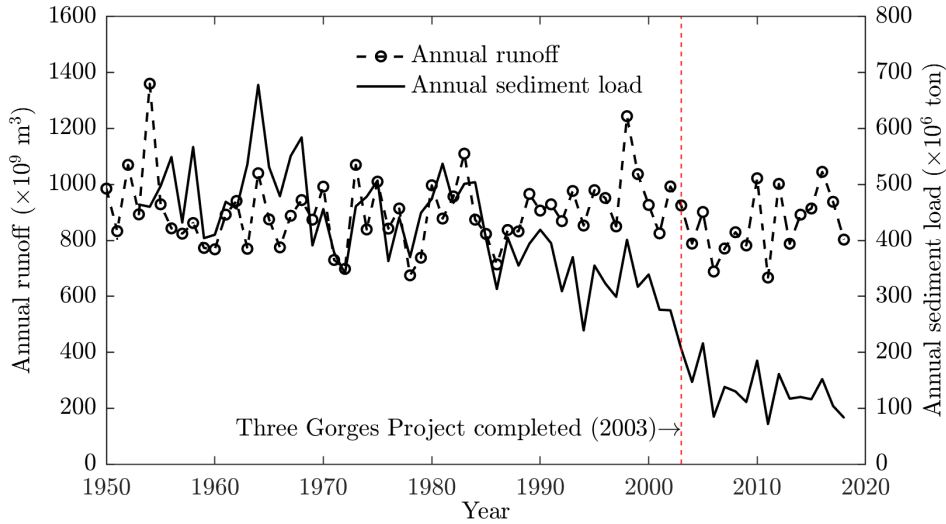


Figure 3.8: Annual river runoff, suspended sediment load, and median diameter of suspended sediment at Datong Gauging Stations (1950–2018).

urnal tides in the mouth outside, while tides are the irregular semidiurnal tides in the mouth inside. The average tidal cycle is 12 hours and 25 minutes, and the tidal current is mostly reciprocating due to the narrow topography. The channel appears regularly branching from Xuliujing to downstream: First, it is divided into the South Branch and the North Branch below Chongming Island, then the South Branch is further divided into the South Channel and the North Channel by Changxing Island and Hengsha Island, and the South Channel is divided into the South Passage and the North Passage by the Jiuduansha Shoals, thus forming a pattern of three bifurcations and four outlets. The site observation station of this study is in South Passage (Figure 3.9). Changjiang estuary is a high turbidity estuary with abundant sediment supply, suspended sediment mainly consists of fine sediment particles, which are dominated by silt [He et al., 2015].

In the South Passage, the annual mean tidal range is about 2.6 m. The average surface water current velocity can reach up to  $1 \text{ m s}^{-1}$  in surface water [Chen et al., 1988], and the depth-average velocity is higher in summer ( $0.76\text{--}0.96 \text{ m s}^{-1}$ ) than winter ( $0.43\text{--}0.78 \text{ m s}^{-1}$ ) [Yun, 2004]. The concentration of chlorophyll (which is a proxy for algae concentration) in the South passage has been given in [Chen et al., 1999] where it is indicated that the values are ranging from  $5$  to  $30 \text{ mg m}^{-3}$  ( $= 5$  to  $30 \text{ }\mu\text{g l}^{-1}$ )

in surface water. In the surface water, the average chlorophyll concentration range from year 1998 to year 2010 is 3 to 7  $\mu\text{g l}^{-1}$  near the study site, being high in late spring and summer while low in winter [Wang et al., 2015]. The suspended sediments in the Changjiang Estuary are mostly fine-grained particles (their amount can reach up to 95%). The average  $D_{50}$  of the dispersed suspended sediment is 7–11  $\mu\text{m}$ , whereas the median size range of the bottom sediment is 15–300  $\mu\text{m}$  (although there are spatial variations) [Liu et al., 2007a]. The Suspended Sediment Concentration (SSC) in the Changjiang Estuary varies greatly over time and space, ranging from 0.1 to 20  $\text{g l}^{-1}$ . The prevailing wind is in South-East direction in summer with the wind speed about 9.4  $\text{m s}^{-1}$ , while the prevailing wind is North-West wind about 7.4  $\text{m s}^{-1}$  [Yun, 2004].

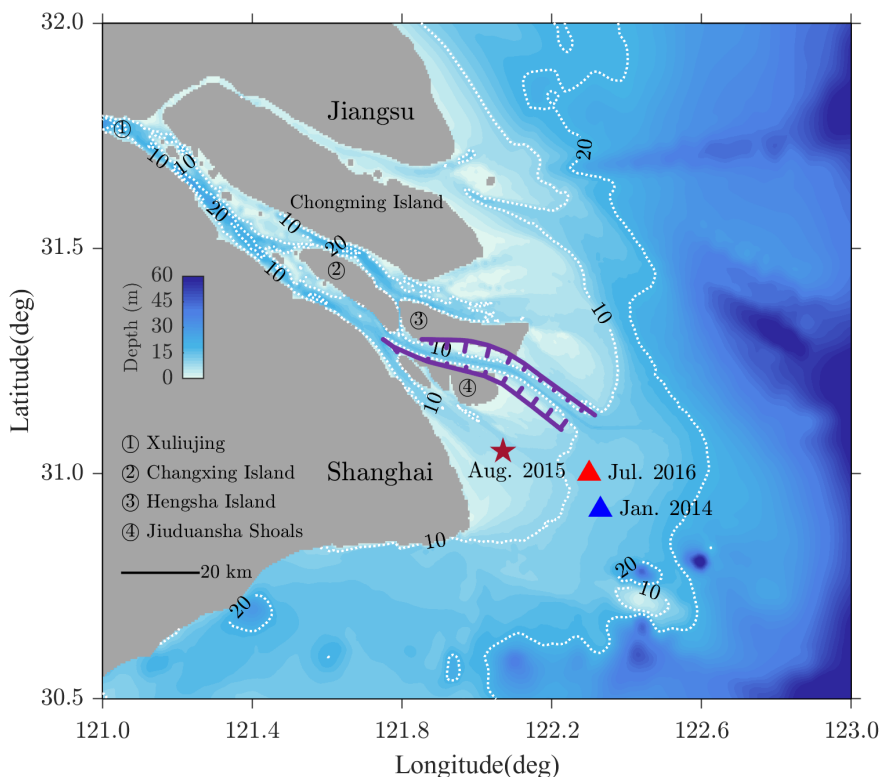


Figure 3.9: Map of the morphology of the Changjiang estuary and the study sites

### 3.2.2. Instruments

The field investigation equipment and parameters recorded are given in Table 3.5.

Table 3.5: Measurement methods

Time	Site	Flocs	Shear	SSC	Salinity	Temperature	Chlorophyll
2014-01	South Passage	LISST-100C	ADCP	OBS&Water sample	OBS&Water sample	OBS	Manta2 WQM
2015-08	South Passage	LISST-100C	ADCP	OBS&Water sample	OBS&Water sample	OBS	Manta2 WQM
2016-07	South Passage	LISST-100C	ADCP	OBS&Water sample	OBS&Water sample	OBS	Manta2 WQM

Flocs—and especially large ones—are so fragile by nature that in-situ monitoring is necessary [Chen & Eisma, 1995, Manning & Dyer, 1999]. The floc parameters were recorded by Sequoia Instruments—LISST (Laser In Situ Scattering and Transmissometry), which can measure the suspended particles by small Angle laser scattering, from which the volume concentration distribution of different particles size classes is obtained [Agrawal & Pottsmith, 2000]. LISST is widely used to observe the in-situ flocs parameters: Gartner et al. [2001] found that the LISST can estimate floc size within a 10% margin of error, the error increasing with increasing floc size. Reynolds et al. [2010] compared three different particle size methods—LISST, Coulter Counter and FlowCAM, and shown that the LISST was reliable that it can accurately measure standard samples as other methods. In addition to observe mineral sediment flocs, many researches indicate that the LISST also can record algae flocs [Anglès et al., 2008]. The LISST can be used for field observation at different water depths and different space regions and record PSD' s at short time intervals. Its subsequent data processing is very easy wich leads to the fact that the LISST instrument is widely used for in-situ observation [Curran et al., 2007, Fugate & Friedrichs, 2002, Guo et al., 2017, Guo & He, 2011, Markussen & Andersen, 2014, Mikkelsen & Pejrup, 2001]. The particle size range observed by the LISST-100C instrument is 2.5–500  $\mu\text{m}$ , with 32 size classes (Table 3.6).

Figure 3.10 shows the LISST device (a), the measurement chamber (b) and path reduction modules (PRM) (c). The total length of the instrument is about 800 mm, the diameter is about 150 mm, it weighs 12 kg in air. The PRM is used for reducing the optical path and to enable measurements in high suspended sediment concentration conditions.

An Acoustic Doppler Current Profiler (ADCP) was also used during the monitor-

Table 3.6: Size range of the LISST-100C

Size Classes	LISST-Type C						
	Lower ( $\mu\text{m}$ )	Upper ( $\mu\text{m}$ )	Median ( $\mu\text{m}$ )	Size Classes	Lower ( $\mu\text{m}$ )	Upper ( $\mu\text{m}$ )	Median ( $\mu\text{m}$ )
1	2.50	2.95	2.72	17	35.4	41.7	38.4
2	2.95	3.48	3.20	18	41.7	49.2	45.3
3	3.48	4.11	3.78	19	49.2	58.1	53.5
4	4.11	4.85	4.46	20	58.1	68.6	63.1
5	4.85	5.72	5.27	21	68.6	80.9	74.5
6	5.72	6.75	6.21	22	80.9	95.5	87.9
7	6.75	7.97	7.33	23	95.5	113	104
8	7.97	9.40	8.65	24	113	133	122
9	9.40	11.1	10.2	25	133	157	144
10	11.1	13.1	12.1	26	157	185	170
11	13.1	15.4	14.2	27	185	218	201
12	15.4	18.2	16.8	28	218	258	237
13	18.2	21.5	19.8	29	258	304	280
14	21.5	25.4	23.4	30	304	359	331
15	25.4	30.0	27.6	31	359	424	390
16	30.0	35.4	32.5	32	424	500	460



Figure 3.10: (a) The LISST-100C; (b) Observational area; (c) Path reduction modules (50% and 90%)

ing. This instrument is a type of sonar that records water current velocities over a range of depths. The ADCP working principle is based on Doppler shift, which enables a precise measurement of current speed and direction, with an accuracy of  $\pm 0.5\%/\pm 5\text{mm/s}$  [RD-Instruments, 1994]. In in-situ observations, the ADCP was fixed to the boat.

The OBS-3A (Optical Backscatter Sensor) that was used as well is an optical sensor that measures turbidity. Salinity and temperature are also recorded. The OBS sensor consists of an infrared-emitting diode (IRED) with a peak wavelength of 875 nm, four photodiodes, and a linear temperature transducer. The nephelometric turbidity units (NTUs) of water was measured by the infrared light backscattering, then the turbidity was converted into suspended sediment concentration by the correlation between NTUs and suspended sediment concentration measured in the lab [CAMPBELL SCIENTIFIC INC., 2018].

The amount of chlorophyll (chlorophyll-a) was recorded with a Manta2 instrument (Water Quality Multiprobe, Eureka Environmental Engineering Company). Fluorescence occurs when a molecule absorbs light at one wavelength and then emits that energy at a different wavelength. The fluorometric sensors emit light at a certain wavelength, and look for a very specific, different wavelength in return. The magnitude of the return light is relatable to the amount of molecules present. The measurement range of the Manta2 is from  $0.03\text{--}50\ \mu\text{g l}^{-1}$  (Medium sensitivity), the error is less than 3% of the scale range [Eureka Environmental Engineering, 2016].

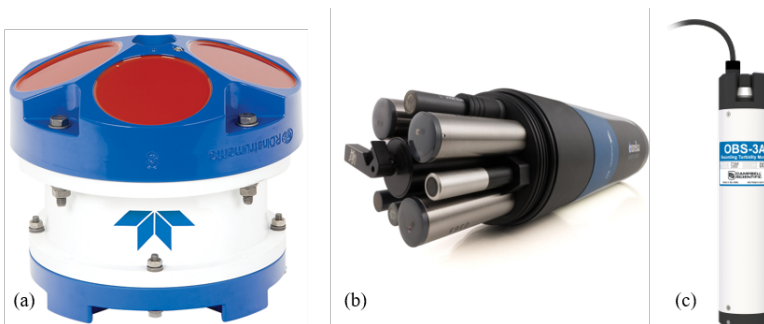


Figure 3.11: Pictures of instruments (a) ADCP; (b) Manta 2; (c) OBS

### 3.2.3. Monitoring campaigns

Three in-situ monitoring campaigns are presented in this study. For all the observation station was in South Passage of Changjiang Estuary—in January 2014, August 2015 and July 2016 (Figure 3.9). The recorded parameters were the same, but the monitoring was done at different tidal periods (Table 3.7). There were no storms during the short time before the observations.

3

All the instruments were attached together to make sure that all the detectors would measure at the same position. All the instruments were set to record at an interval of 1 second. A full vertical profile was measured every hour and the instruments were pulled slowly from bottom to surface at the speed of  $0.05 \text{ m s}^{-1}$ . At specific locations in the water column, corresponding to the positions where the water samples are taken (see underneath), the instruments were left for 2 min at the same position in order to acquire statistically significant data.

The hydrodynamic parameters were measured by ADCP (Acoustic Doppler Current Profiler, 300 kHz), which was set up 0.5 m under the ship with a 1.71 m blanking distance and a vertical resolution (bin size) of 0.5 m. Records of the water current direction and velocity were done in real time.

In addition, water samples were collected for calibration by 1.2L water sampler (horizontal trap sampler), then divided into two glass bottles, one for SSC analysis and another for chlorophyll analysis or primary particles analysis (the odd hours for chlorophyll analysis and even hours for another). We took these double water samples at 6 vertical heights (0H, 0.2H, 0.4H, 0.6H, 0.8H, 1H) per hour. In our definition, 0H represents the surface and 1H the bottom. The height corresponding to 1H was sampled 0.5 m above the bed. A water sample for each height was filtered through a  $0.45 \mu\text{m}$  cellulose acetate pre-weight filter paper, dried and weighted to estimate the sediment concentration distribution through the water column.

The chlorophyll analysis water sample was filtered through a  $0.45 \mu\text{m}$  ultra-fine glass fiber filter paper and stored at  $-20^\circ\text{C}$  for chlorophyll measurements in laboratory.

Table 3.7: Information of the in-situ measurements in the South Passage

Date&Periods	Tidal	Location	Weather	Instruments	Water samples
11 Jan. 2014 13:00 – 1:00 (+1)	Neap	E 122.33 N 30.92	Cloudy	Vertical sampling / h	6 cells / h
14 Aug. 2015 8:00 – 9:00 (+1)	Spring	E 122.07 N 31.05	Sunny	Vertical sampling / h	6 cells / h
20 Aug. 2015 8:00 – 9:00 (+1)	Neap	E 122.07 N 31.05	Sunny	Vertical sampling / h	6 cells / h
25 Jul. 2016 21:00 – 9:00 (+1)	Neap	E 122.30 N 31.00	Sunny	Vertical sampling / h	6 cells / h

### 3.3. Data processes

#### 3.3.1. Laboratory measurements data processes

Floc size and particle size distributions (PSDs) as estimated by the Malvern Mastersizer 2000 were used.

The median particle size ( $D_{50}$ ) of the Malvern Mastersizer was used to represent the mean floc size, which is defined as the particle size corresponding to 50% on the size cumulative curve.

In general, the flocculation rate  $R_{Floc}$  was estimated by:

$$R_{Floc} = (D_{max} - D_0) / (t_{max} - t_0) \quad (3.3)$$

where the  $D_{max}$  is the finally steady floc size,  $D_0$  is the initial floc size,  $t_{max}$  is the time to reach steady state and  $t_0$  is the initial time. As the floc size growth curves are nonlinear for long times, the initial flocculation rate was:

$$R_{Floc} = (0.9D_{max} - D_0) / (t_{max} - t_0) \quad (3.4)$$

#### 3.3.2. Hydrodynamics data processes

To estimate the shear stress in the water column, the velocity data should be converted into shear rate  $G$  [Guo et al., 2017, Pejrup & Mikkelsen, 2010]:

$$G(z, H, u_*) = \sqrt{\frac{(u_*^3 \times (1 - z/H))}{\nu \kappa z}} \quad (3.5)$$

where  $\nu$  is the kinematic viscosity of the water ( $\text{m}^2 \text{s}^{-1}$ ),  $H$  is the total water depth ( $\text{m}$ ),  $z$  is the height above bed,  $\kappa$  is Von Karman's constant (assumed to be 0.4) [Qian & Wan, 1983]. The friction velocity,  $u_*$  ( $\text{m s}^{-1}$ ) is given by:

$$u_* = \frac{u(z)\kappa}{\ln\left(\frac{z}{z_0}\right)} \quad (3.6)$$

where  $u(z)$  is the current velocity amplitude ( $\text{m s}^{-1}$ ) at position  $z$ .  $z_0$  is assumed to be constant and equal to 3 mm in accordance with the work of Guo et al. who investigated the same system in the same conditions [Guo et al., 2017].

The Kolmogorov microscale  $\eta$ , considered to be a characteristic length scale for floc size, is the smallest dissipating eddies length [van Leussen, 1999]. It can be estimated by:

$$\eta = (\nu^3 / \varepsilon)^{1/4} \quad (3.7)$$

where  $\varepsilon$  is the turbulent energy dissipation rate ( $\text{m}^2 \text{s}^{-3}$ ) which is linked to  $G$  given above by  $G = \sqrt{\varepsilon / \nu}$  [Camp, 1943].

### 3.3.3. Flocculation data processes

The in-situ PSD was acquired by LISST. First, the original data was processed by LISST-SOP (Version 5.00), from which the size volume concentration in 32 log-spaced size classes from 2.5–500  $\mu\text{m}$  was obtained. The flocculation data presented in this study is the average over a 2 min period to eliminate random fluctuations [Mikkelsen & Pejrup, 2001].

The total volume concentration (TVC) is calculated using:

$$TVC = \sum_{i=1}^{32} VC_i \quad (3.8)$$

where  $VC_i$  represent the volume concentration of  $i$  size class ( $\mu\text{l l}^{-1}$ ).

Unrealistic high values in both smallest and largest size classes can appear, usually caused by diffraction errors or leakage of signals, which should be ignored [Sequoia Scientific, 2011].

For simplicity, we will refer to all particles as “flocs” but it should be understood that particles at the lowest and largest size range can be composed, in majority, of single entities (like clay particles for the smallest sizes or algae particles for the largest sizes).

The density  $\Delta\rho$  of flocs was estimated from the LISST and OBS data, using equation [Fettweis, 2008, Verney et al., 2009]:

$$\Delta\rho = \rho_F - \rho_W = \left(1 - \frac{\rho_W}{\rho_P}\right) \frac{SSC}{V_F} \quad (3.9)$$

where  $\rho_F$  is the floc density,  $\rho_W$  is the water density,  $\rho_P$  is the sediment particle density which is estimated to  $2650 \text{ g l}^{-1}$ , SSC is the mass suspended sediment concentration obtained from the OBS and  $V_F$  is the floc volume concentration from LISST.

In the case of  $Re_* = \omega_s D_{50} \rho_W / \mu \leq 1$ , the settling velocity of flocs is calculated by the formula of Stokes' law. While in the case of  $Re_* > 1$ , the floc is in the Viscous Reynolds region, the settling velocity would be better to be calculated by Winterwerp Settling Formula [Winterwerp, 1998]:

$$\omega_s = \frac{D_{50}^2 \Delta\rho g}{18\mu} \quad (Re_* \leq 1) \quad (3.10)$$

$$\omega_s = \frac{D_{50}^2 \Delta\rho g}{18\mu(1 + 0.15Re_*^{0.687})} \quad (Re_* > 1) \quad (3.11)$$

where  $\mu$  is the viscosity of water,  $D_{50}$  is the media floc diameter and  $g$  is the gravity constant.

### 3.3.4. Chlorophyll data processes

The chlorophyll (chlorophyll-a) concentration (CC) can be calculated as follows [Knap et al., 1996]:

$$CC = (F_b - F_a - Blk_b + Blk_a) \frac{\tau}{(\tau - 1)} F_R \frac{V_{EXT}}{V_{FILT}} \quad (3.12)$$

where  $F_b$  is the fluorometric reading of sample with 90% acetone,  $F_a$  is the fluorometric reading of sample with 90% acetone and 10% HCl.  $Blk_b$  is the fluorometric reading

of pure 90% acetone,  $Blk_a$  is the fluorometric reading of pure 90% acetone with 10% HCl. Linear calibration factors ( $F_R$ ) are calculated as the slopes of the unacidified fluorometric readings vs. chlorophyll concentrations calculated spectrophotometrically. The acidification coefficient ( $\tau$ ) is calculated by averaging the ratio of the unacidified and acidified readings ( $\tau = (F_b - Blk_b) / (F_a - Blk_a)$ ) of pure chlorophyll.  $V_{EXT}$  is the extraction volume by acetone extraction method and  $V_{FILT}$  is the filtrate volume of the water sample.

### 3.3.5. Others

The suspended sediment concentration (SSC) of the collected water samples was measured by Filter drying—water sample for each height was filtered through a 0.45  $\mu\text{m}$  cellulose acetate pre-weight filter paper, dried and weighted to estimate the sediment concentration distribution through the water column. The organic matter (OM) was measured by calcination method—the sediment samples were burned at 450  $^{\circ}\text{C}$  for 6 hours and weighed.

The primary particles analysis was measured by Malvern Mastersizer 2000 laser granularity analyzer (measurement ranges from 0.02–2000  $\mu\text{m}$ , the repetition error is within 3%). Before the instrument measurements, the water sample was handled with hydrogen peroxide ( $\text{H}_2\text{O}_2$ ) and hydrochloric acid (HCl) to remove organic matter and carbonate. Hexametaphosphate ( $(\text{NaPO}_3)_6$ ) was then added as a dispersant and the sample was ultrasonically shaken (for 15 minutes).

# 4

A laboratory study on the  
behavior of estuarine  
sediment flocculation as  
function of salinity, EPS  
and living algae

*No cross no crown.*

Francis Quarles

## Abstract

The interactions between organic and inorganic particles in the context of flocculation is an on-going topic of research. Most current researches do not distinguish between the effects of EPS (produced by microorganisms) and living microorganisms (like algae). In this chapter, the effect of salinity, EPS and living algae on sediment flocculation are investigated separately. Several types of measurements were performed, which can be divided into the following categories: sediment at different salinities, sediment in the presence of EPS at different salinities, sediment in the presence of living algae at a given salinity. Results show that increasing salinity enhances slightly sediment flocculation. In the presence of EPS there was hardly any flocculation in demi-water, but the flocculation was significant in saline water. The living algae cells were shown to flocculate with themselves and form large flocs. These algae flocs can bind to sediment particles to form larger flocs, both in demi-water and sea water. Size-wise algae-sediment flocs were largest, EPS-sediment flocs came second, and salt-sediment flocs were smallest.

The contents of this chapter is based on the following manuscript:

**Z. Deng, Q. He, A. J. Manning, C. Chassagne**, *A laboratory study on the behavior of estuarine sediment flocculation as function of salinity, EPS and living algae*. (Submitted)

### 4.1. Introduction

Sediment that is found in natural estuarine aquatic environment is usually transported as part of entities called flocs [Droppo & Ongley, 1992, 1994]. The process of flocculation requires to be studied as flocculation, influenced by hydrodynamic and biogeochemical estuarine conditions, will modify sediment erosion, settling and transportation [Bianchi, 2007, Geyer et al., 2000, Jay et al., 2000].

In recent years, more and more researches focused on the biological processes related to flocculation. Flocculation between minerals and algae has been reported [Verspagen et al., 2006]. Microorganisms can attach to the sediment surface in combination with biological activities, such as growth, metabolism and decay [Grossart et al., 2006]. At the same time they can affect the flocculation processes due to their excretion of extracellular polymeric substances (EPS). EPS are typically polyelectrolytes

(polysaccharides), usually anionic like galacturonic acid [Plude et al., 1991]. Divalent cations (e.g.  $MgCl_2$  and  $CaCl_2$ ) can increase the EPS effects on flocculation [Park et al., 2010, Tan et al., 2008, 2014]. Bridging by cationic ions is enhanced when divalent cations are used (instead of monovalent ions like NaCl) [Mietta et al., 2009a].

Cohesive sediment organic matter mainly consists of EPS. EPS changes the properties of the sediment particle's surface hereby affecting the flocculation processes [Winterwerp & Van Kesteren, 2004]. Note that the effects of living organisms like (micro)algae on flocculation and the action of EPS on flocculation are generally not dissociated in researches on the topic. Some algae species can form large flocs due to their large cells size or cells chain length [de Lucas Pardo et al., 2013]. They can combine with sediment particles and form bio-sediment flocs which consist of sediment particles and algae particles [Deng et al., 2021, 2019]. The aim of this article is to distinguish between the effect of EPS in the absence of microalgae and the effect of microalgae on flocculation. To this end, a series of laboratory measurements were performed, where the effects of salinity, EPS and living algae on the estuarine sediment flocculation are reported. Three types of salts ( $NaCl$ ,  $MgCl_2$ ,  $CaCl_2$ ) were used, at three different concentrations (defined as “low”, “medium” and “high”). First, we investigated the variation of floc size and particle size distributions with different cation concentrations, then sediment added to EPS and mixed at different salinities was studied. Finally, we report the variation in particle size and particle size distribution of sediment with (micro)algae.

## 4.2. Sediment, EPS and algae flocs

In a first set of experiments, the time-dependence of sediment, EPS and algae flocs were investigated separately in demi-water. These samples are displayed in Figure 4.1 where the  $D_{50}$  and Particle Size Distribution (PSD) of the three samples measured by SLS are presented (see Chapter 3, section 3.1.1 for the measurement methodology).

The sediment flocculation in the absence of EPS and algae over a period of 120 min was limited as the  $D_{50}$  varied from 8 to 10.5  $\mu m$ . The PSD at start was a log-normal distribution and after 120 min a second peak appeared, one at about 6  $\mu m$  (about the  $D_{50}$  size of the primary particles) and the other at 20  $\mu m$ . This indicated that sediment flocculation in demi-water is very slow and incomplete.

The SLS measurement of EPS is shown to be unreliable. This is due to the fact

that EPS is composed of flexible elongated polymeric chains with a very large aspect ratio. These features lead to multiple peaks in the PSD, as the instrument is calibrated for the measurement of spherical particles.

The  $D_{50}$  of the 1% algae suspension fluctuated between 70 to 120  $\mu\text{m}$  as the sample remained very polydisperse. The  $D_{50}$  of the initial 10% algae sample is about 40  $\mu\text{m}$ , which is much larger than the  $D_{50}$  of the original sediment particles. Algae cells are shown to aggregate with themselves over time and form larger algae flocs, even in demi-water. It should be noted that the shear rate used in the measurement is usually higher than the ones experienced by algae in their natural environment. The algae particles flocculate faster than sediment particles, reaching a maximum floc size within 30 minutes. The change in the small and large peaks size indicate that the small algae cells tend to aggregate and form large flocs of the order of 70–100  $\mu\text{m}$  in size. The rather monomodal peak found at the end of the experiment seems to indicate that these flocs are rather spherical in shape. This sphericity is due to the constant shear experienced by these flocs during the measurements [Shakeel et al., 2020]. This type of shear is not often encountered in-situ where long-chain algae colonies are usually observed.

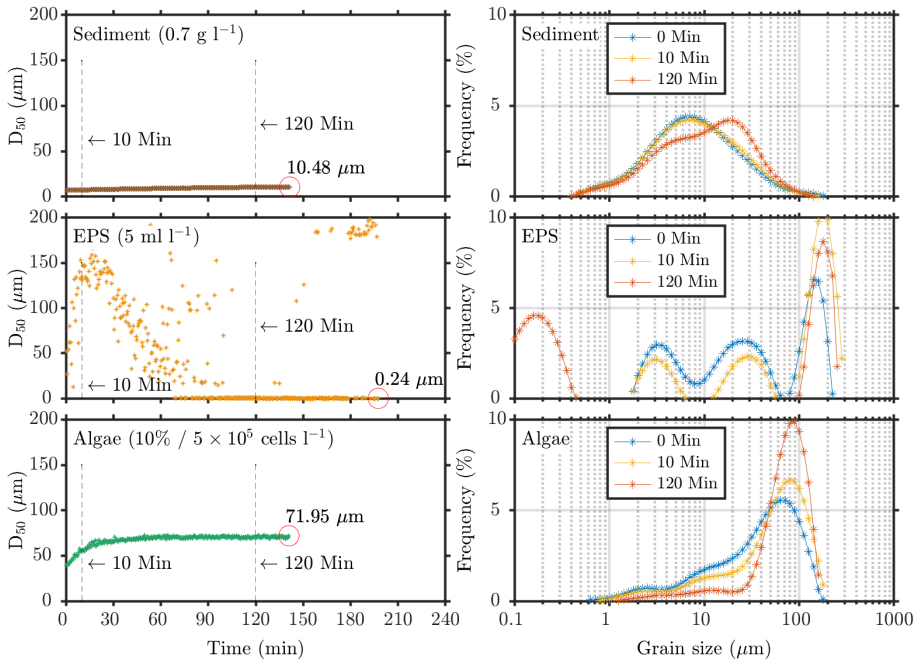


Figure 4.1: Floc size time evolution and distribution of sediment, EPS and living algae. The concentration of sediment was  $0.7 \text{ g l}^{-1}$ , EPS  $5 \text{ ml l}^{-1}$ , algae 10% and algae 1%, all of them in demi-water.

### 4.3. Salinity and EPS effects

#### 4.3.1. Evolution of the flocculation with salinity

The effects of different salts and salt concentrations on sediment flocculation is shown in Figure 4.2.

The floc size increased slowly with NaCl (ranging from 5.3  $\mu\text{m}$  to 8.5  $\mu\text{m}$ ) at 0.1  $\text{mol l}^{-1}$ , and higher NaCl concentrations led to higher flocculation rates and larger flocs. For the highest concentration used (0.3  $\text{mol l}^{-1}$ ) the  $D_{50}$  varied from 6.3  $\mu\text{m}$  to 11.2  $\mu\text{m}$ .

The  $\text{MgCl}_2$  led to faster flocculation than NaCl. The results show that the sediment particle size reached steady-state within 10 minutes. Contrary to expectation, and as is usually observed, see [Mietta et al. \[2009a\]](#), higher  $\text{MgCl}_2$  concentrations led to smaller steady-state sizes. A similar effect is observed with the other divalent salt used ( $\text{CaCl}_2$ ). This peculiar behavior indicates that flocculation with divalent salts is different from the classical DLVO theory (see Chapter 2, section 2.1.2 for a discussion about DLVO theory). Most probably chemical bindings are involved, but further analysis would be required to confirm this.

For flocculation with divalent salts, one can observe that the PSDs stays multi-modal with time: a tail is observed around 1  $\mu\text{m}$ , a main peak at about 10  $\mu\text{m}$  and a small fraction of the flocs has a size of about 100  $\mu\text{m}$ . The apparition of the peak at 100  $\mu\text{m}$  is linked to the fact that the highest size peak (around 10  $\mu\text{m}$ ) is narrowing over time, and hence the two individual size peaks can be seen separately.

Although the concentration of  $\text{CaCl}_2$  was lower than  $\text{MgCl}_2$ , the flocs grew faster than with  $\text{MgCl}_2$  leading to larger mean sizes of flocs. This indicates that besides cation concentration, the type of cation also influences the sediment flocculation. This is another indication that the flocculation occurring with divalent salts does not obey the classical DLVO theory. Following DLVO theory, for a same concentration and same valence of ions, flocculation should be the same.

#### 4.3.2. Evolution of sediment flocculation with EPS and salinity

In this section, the combined effect of EPS and salinity on flocculation is investigated. A fixed concentration of 5  $\text{ml l}^{-1}$  EPS was added to all samples and the salt type and concentration was varied. The results are shown in Figure 4.3.

The flocculation of sediment with EPS and salt led to larger steady-state floc sizes

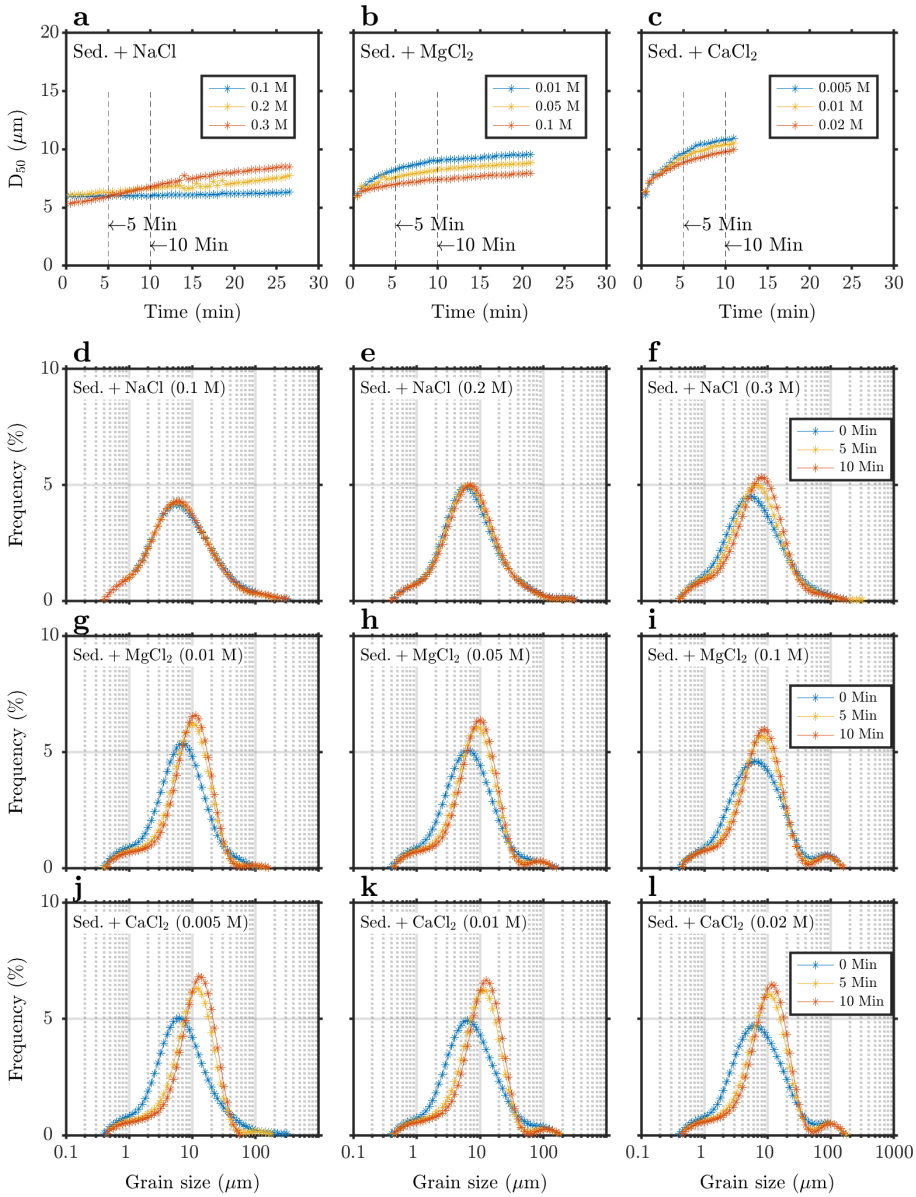


Figure 4.2: Effect of NaCl, MgCl<sub>2</sub> and CaCl<sub>2</sub> on floc size time evolution and distribution of sediment.

than in the experiments with only added salt. In the presence of sediment, for the shear rate used, EPS binds to the sediment to create flocs that are in good approximation spherical as can be deduced from the rather monomodal PSDs found.

The trends as function of salt type and concentration were similar to the ones observed in Figure 4.2, when no EPS was added: the flocs growth was slower with NaCl than with  $MgCl_2$  and  $CaCl_2$ . In contrast to what was observed in Figure 4.2, the steady-state floc size decreases with increasing salinity for all salts (hence: also with the monovalent salt NaCl). For the divalent salts, it is found that the time to reach the steady-state floc size is highest for the lowest salinity.

### 4.3.3. Experiments with sea water

In this section, the results presented in the two previous sections are compared with the results obtained from experiments done in artificial sea water.

Figure 4.4 and Figure 4.5 show the characteristics of flocs at different flocculation times. The horizontal bars represent the mean floc size ( $D_{50}$ ), the ends of the boxes  $D_{25}$  and  $D_{75}$  and the ends of the vertical lines are the  $D_{10}$  and  $D_{90}$  of PSDs. The results displayed with EPS at different salt types and concentrations are the same as the ones presented in the three previous sections.

Note that in demi-water, the floc size reached its steady-state only after 2 hours (Figure 4.1), while for all the other measurements it was within 30 minutes (Figure 4.2 and Figure 4.3). Therefore all PSDs shown at 30 minutes after the start of the experiments but the one for demi-water are at steady-state.

It is found that the mean floc size at steady-state is largest in the case of experiments done with sea salt. The cationic composition of sea water is roughly  $0.5 \text{ mol l}^{-1} \text{ Na}^+$ ,  $0.05 \text{ mol l}^{-1} \text{ Mg}^{2+}$  and  $0.01 \text{ mol l}^{-1} \text{ Ca}^{2+}$ . It would therefore appear, in light of the experiments shown in Figure 4.3, Figure 4.4 and Figure 4.5, that, in the presence of EPS, the kinetics of flocculation with sea salt is dependent on the flocculation with  $\text{Na}^+$ . Indeed, there is a marked difference in particle size between 10 and 30 min after the start of the experiments for both experiments with sea salt and with NaCl (much less with the other ions). On the other hand, the suspension with EPS in sea water has a wide spread in size.

Figure 4.6 shows the different initial flocculation rates obtained at different experimental conditions. The flocculation rate is defined as the slope of the  $D_{50}$  size as

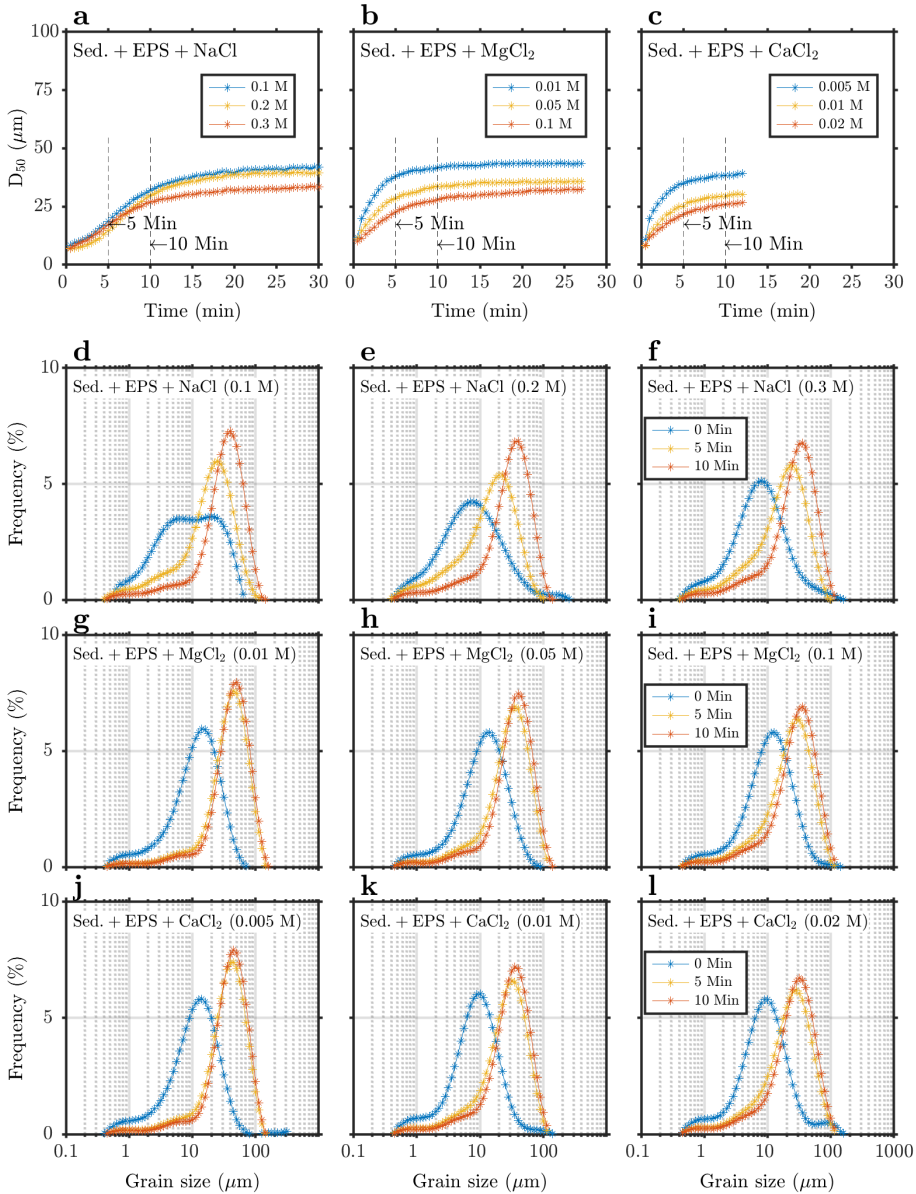


Figure 4.3: Effect of EPS combined with NaCl,  $\text{MgCl}_2$  and  $\text{CaCl}_2$  on floc size time evolution and distribution of sediment.

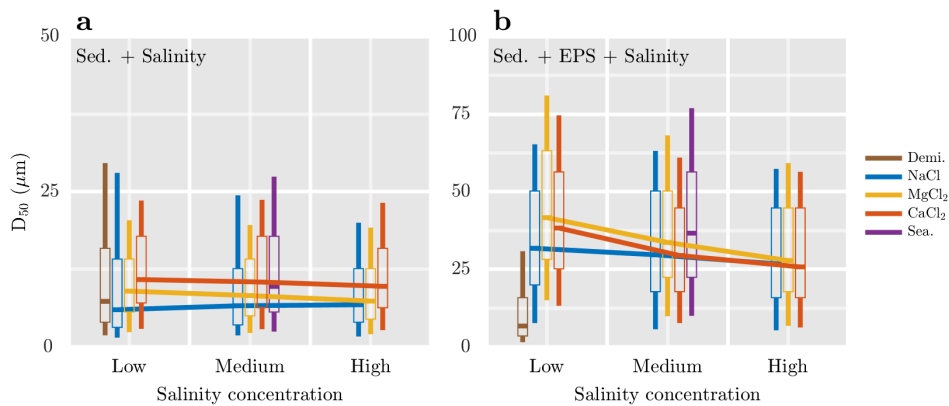


Figure 4.4: Floc size of sediment and sediment with EPS on the effect of salinity at 10 minutes.

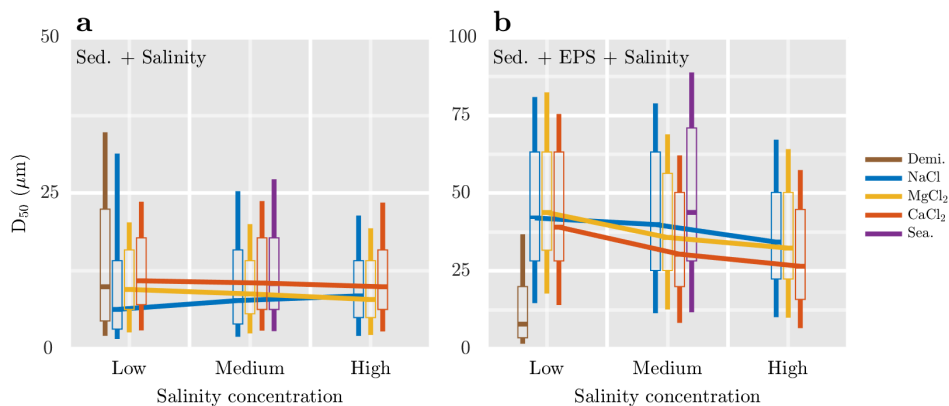


Figure 4.5: Floc size of sediment and sediment with EPS on the effect of salinity at 30 minutes.

function of time in the time interval  $[0, 10 \text{ min}]$ . Flocculation with  $\text{CaCl}_2$  is found to be the fastest, for any concentration when no EPS is present. The flocculation rate with sea salt is second highest when no EPS is present. In the presence of EPS, on the other hand, the flocculation rate with monovalent and divalent salts follows the trends discussed in section 4.3.2 and flocculation with sea salt is found the highest.

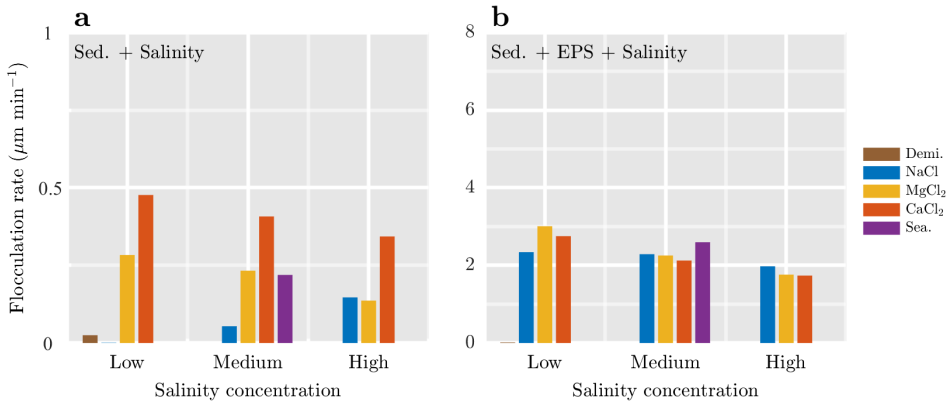


Figure 4.6: Flocculation rate of sediment and sediment with EPS at different salinities at 10 minutes.

Note that no experiment was performed at low and medium sea salt concentration and that the data for demi-water is plotted in the “low” column.

#### 4.3.4. Electrokinetic studies

To investigate the electrochemical properties of the sediment with EPS and salinity zeta potential and conductivity measurements were performed and are shown in Figure 4.7. The steady-state floc size does not depend on conductivity for the sediment + salt experiments and there is a slight decrease in floc size with conductivity for sediment + salt + EPS experiments. This trend is the same as the one observed in Figure 4.4, which follows from the fact that salinity and conductivity are correlated. The corresponding zeta potential is following the expected trend: it is decreasing with increasing conductivity (salinity). This reflects the fact that the overall surface charge of the flocs is screened by the electrolyte ions present in the water. This screening can also occur within a floc and be the reason why the  $D_{50}$  is decreasing with salinity as illustrated in Figure 4.8.

This behavior is possible as the flocs are made of clay particles aggregated with EPS composed of long-chain structures [Bolto & Gregory, 2007, Lee & Schlautman,

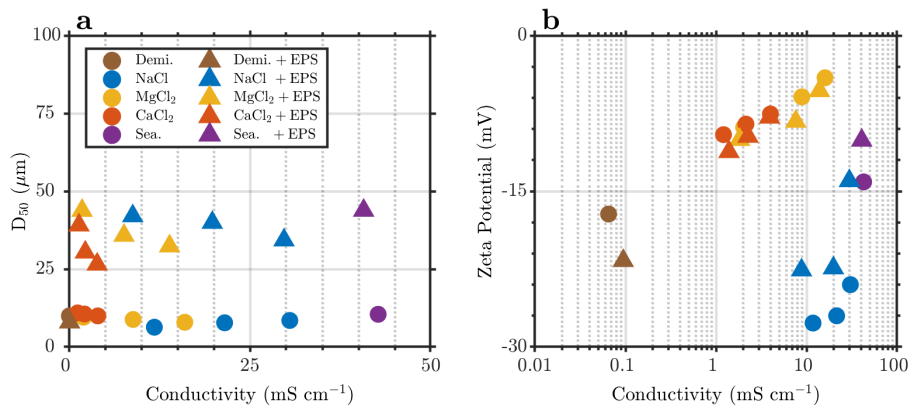


Figure 4.7: Floc size and zeta potential of sediment in presence of salt and EPS (indicated in the legends) as a function of conductivity.

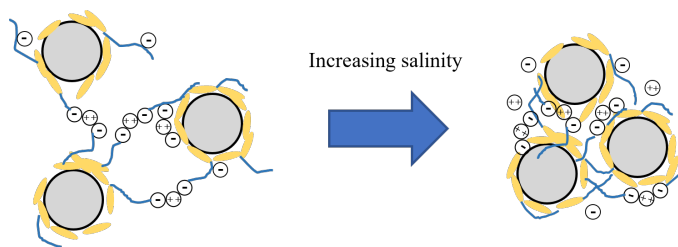


Figure 4.8: Upon an increase in salinity, the repulsion between the EPS chain surface groups is screened, leading to a smaller steady-state particle size and a smaller zeta potential (in absolute value).

2015] or galacturonic acid [Plude et al., 1991]. The repulsion between these chains within a floc is screened upon addition of salt.

The valence of ions is of influence on the flocculation. The monovalent salt NaCl led to higher zeta potential values (absolute values) than the divalent salts  $MgCl_2$  and  $CaCl_2$  for a same conductivity. This is to be understood as a consequence of the fact that the double layer thickness is proportional to the square of the valence of ions: the higher the valence, the thinner the double layer (for a same salinity) and hence a better screening of the surface charge and consequently a smaller (in absolute value) zeta potential.

Standard DLVO theory as described in Chapter 2, cannot be used to interpret the zeta potential results. According to DLVO theory, a zeta potential smaller than 25 mV in absolute value should lead to flocculation. This occurs for clay-salt systems [Mietta, 2010] but not for clay-polyelectrolyte systems [Shakeel et al., 2020] where steric interactions should be accounted for. In most research on sediment flocculation, it is usually found that an increase in salinity leads to a better flocculation (e.g., Kumar et al., 2010, Mietta et al., 2009a, van Leussen, 1999). This is true in the general sense, independently of zeta potential values, as salt ions screen surface charges whereby flocculation is promoted. Nonetheless the attractive force leading to flocculation could be of a different origin than van der Waals: steric and hydrogen bonding interactions are examples of interactions that can lead to flocculation. Steric interactions, on the other hand can also lead to (steric) repulsion—in which case flocculation is prevented [Napper, 1983]. This might explain why some researchers found that there was no correlation between flocculation and salinity [Chen & Eisma, 1995, Razaz et al., 2015, Verney et al., 2009]. Many studies report that organic matter enhances sediment flocculation [Chassagne, 2019, van Leussen, 1994], and that the presence of organic matter increases floc's strength [Shakeel et al., 2020]. We confirm, in this study, that EPS can lead to large flocs at high shear rates.

## 4.4. Experiments with living algae

### 4.4.1. Flocculation with living algae in demi-water

In the estuarine environment, the sediment PSD is affected by the ratio of algae concentration and sediment concentration (CC/SSC), see Chapters 5 and 6 and Deng

et al. [2021, 2019]. The symbol CC stands for Chlorophyll Concentration (which is linearly proportional to algae concentration) and SSC for Suspended Sediment Concentration. To remain as close as possible to in-situ experiments, flocculation was triggered in settling columns (see section 3.1.3). The measurements performed in these settling columns were used to discuss the effects of different living algae concentrations on flocculation/settling.

Figure 4.9 shows that the sediment suspension is hardly settling in demi-water, and the water kept turbid even after 24 hours. This result is in line with the results reported in section 4.3.2, where it was discussed that the depletion of ions in the water led to larger repulsion between particles. The living algae seemed to be settling little due to the fact that they tend to move to the surface for respiration and photosynthesis. In suspensions made of both sediment and algae a fast settling of particles is observed. Most of the sediment was settled after 5 hours with 10% living algae, and the sediment was settled after 24 hours with 1% living algae, though the living algae concentration (and hence CC/SSC) was very low.

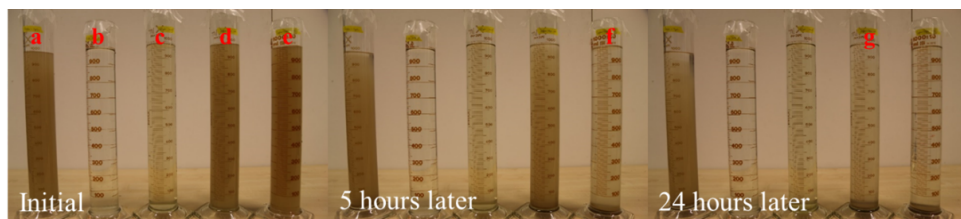


Figure 4.9: The settling column measurements of sediment, algae and sediment with algae in demi-water.

(a.  $0.7 \text{ g l}^{-1}$  sediment, b. 1% living algae, c. 10% living algae, d.  $0.7 \text{ g l}^{-1}$  sediment with 1% living algae (Group 1), e.  $0.7 \text{ g l}^{-1}$  sediment with 10% living algae (Group 2), f.  $0.7 \text{ g l}^{-1}$  sediment with 1% living algae 5 hours later, g.  $0.7 \text{ g l}^{-1}$  sediment with 10% living algae 24 hours later). The groups refer to Table 3.3.

In order to compare settling columns experiments with SLS experiments, four samples composed of different sediment and algae concentration were prepared and measured by SLS (Table 4.1 and Figure 4.11). The sample having the lowest CC/SSC ratio (of about  $1.8 \mu\text{g g}^{-1}$ ) is hereinafter called group 1 and is represented by the light blue curve. This group corresponds to group 1 in Figure 4.9 (same composition). This suspension had the lowest flocculation rate as the particle size did not reach its max-

imum value after 30 minutes. This is in agreement with what was observed in the settling column. When the living algae concentration was increased 10 times and sediment concentration kept constant ( $CC/SSC = 17.9 \mu\text{g g}^{-1}$ , hereinafter called group 2), represented by the dark blue curve, the flocculation rate increased and the maximum floc size was found to be  $71 \mu\text{m}$ . This group corresponds to group 2 in Figure 4.9 (same composition); this suspension indeed settled faster than group 1. When the sediment concentration and algae concentration were both decreased 10 times compared to group 2 (therefore yielding the same  $CC/SSC$  ratio, i.e.  $17.9 \mu\text{g g}^{-1}$ , hereinafter called group 3) represented by the yellow curve, the flocculation rate and maximum floc size were also high but smaller than group 2. The highest ratio group ( $178.6 \mu\text{g g}^{-1} CC/SSC$ , hereinafter called group 4) represented by the red curve led to a higher flocculation rate and larger maximum floc size than the other groups, even though the flocculation rate was smaller than the one of group 2.

The evolution of PSDs (sediment + algae) show different flocculation processes:

**At high CC (10% algae)**, a substantial increase in  $D_{50}$  is observed as a consequence of flocculation. The flocculation rate is highest for the sample with lowest  $CC/SSC$  ratio (group 2) but the largest floc size is obtained with the sample with highest  $CC/SSC$  ratio (group 4).

**At low CC (1% algae)**, two behaviors are observed:

(1) at low  $CC/SSC$  (group 1), not much flocculation is found, the  $D_{50}$  remains low. This is in line with the results found with 1% algae suspension (see Figure 4.1).

(2) at high  $CC/SSC$  (group 3), a significant increase in  $D_{50}$  is observed, which is the result of flocculation between algae and sediment.

These results confirm that a relevant parameter for studying flocculation is the  $CC/SSC$  ratio: when the  $CC/SSC$  ratio is high, large flocs are formed and vice-versa (irrespective of  $CC$  or  $SSC$  concentrations). The flocculation rate (group 2 vs group 4) is however highest for the sample with lowest  $CC/SSC$  (group 2). There are two reasons for this behavior: 1) algae do not aggregate at low concentration (see Figure 4.1); 2) high  $SSC$  lead to high collision frequency, so the flocculation is fastest when  $SSC$  is high. The  $SSC$  of group 2 is 10 times larger than the  $SSC$  of group 4.

The results are summarized in (Figure 4.11).

It is found that the steady-state floc size of group 1 ( $1.8 \mu\text{g g}^{-1} CC/SSC$ ) is smaller than all the others, confirming that the maximum floc size was limited by low  $CC/SSC$

Table 4.1: Set-ups of the SLS measurements

Group name	SSC $\text{g l}^{-1}$	Algae concentration			CC/SSC $\mu\text{g g}^{-1}$
		Volume	cells $\text{l}^{-1}$	(Estimated CC) $\mu\text{g l}^{-1}$	
Group 1	0.7	1%	$5 \times 10^4$	1.25	1.8
Group 2	0.7	10%	$5 \times 10^5$	12.5	17.9
Group 3	0.07	1%	$5 \times 10^4$	1.25	17.9
Group 4	0.07	10%	$5 \times 10^5$	12.5	178.6

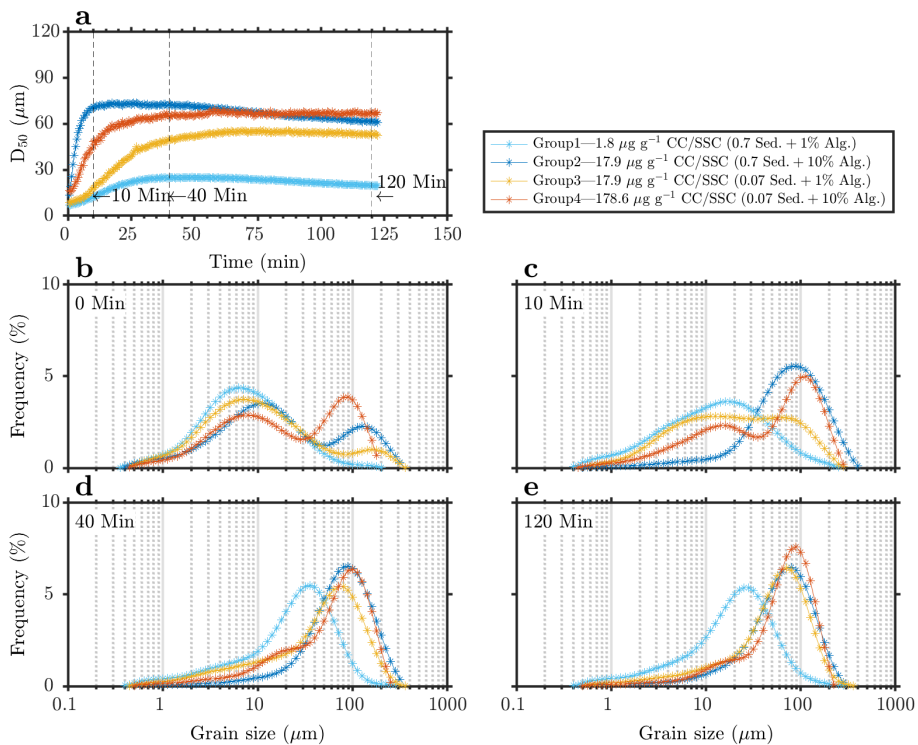


Figure 4.10: Floc size time evolution and distribution of sediment on the effect of algae.

despite the high SSC. The  $D_{90}$  of group 2 ( $17.9 \mu\text{g g}^{-1}$  CC/SSC) and group 4 ( $178.6 \mu\text{g g}^{-1}$  CC/SSC) were larger than group 1 ( $1.8 \mu\text{g g}^{-1}$  CC/SSC) and group 3 ( $17.9 \mu\text{g g}^{-1}$  CC/SSC), indicating that higher concentrations of living algae lead to larger particle sizes.

The flocculation rate of group 2 ( $17.9 \mu\text{g g}^{-1}$  CC/SSC) was much higher than the other groups. The flocculation rate of group 4 ( $178.6 \mu\text{g g}^{-1}$  CC/SSC) is higher than group 3 ( $17.9 \mu\text{g g}^{-1}$  CC/SSC). The flocculation rate of group 1 ( $1.8 \mu\text{g g}^{-1}$  CC/SSC) was lowest. The flocculation rate was higher with higher particles concentration (SSC), except for group 1 ( $1.8 \mu\text{g g}^{-1}$  CC/SSC), as said above. This highlight the fact that algae is the trigger for flocculation and that below a certain algae concentration neither algae cells with themselves, nor algae cells and sediment will flocculate.

Overall, it can be concluded that the maximum floc size is controlled by the value of CC/SSC, while the flocculation rate is controlled by SSC (above a certain CC threshold).

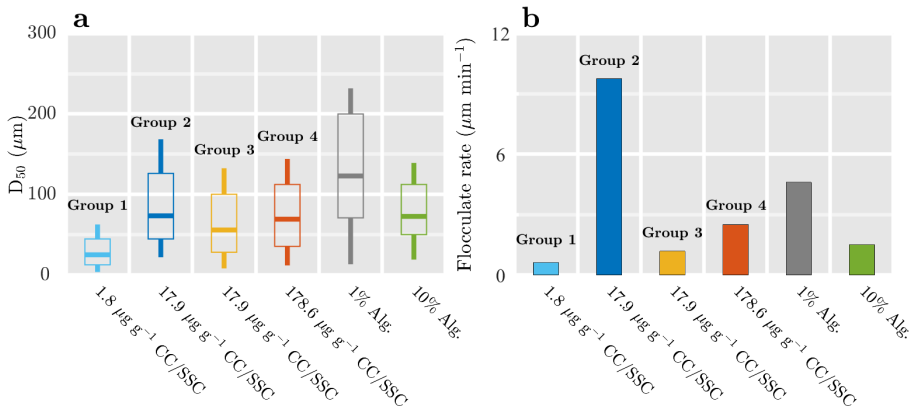


Figure 4.11: Floc size and flocculation rate as a function of algae.

The electrokinetic properties of the samples are shown in Figure 4.12. Higher living algae concentration give higher conductivity values, which indicated that the algae cells or their secreta (EPS) release ions. Higher zeta potential values (in absolute values) are found for the samples with lowest conductivity, which is expected based on standard DLVO theory. Note, however, that flocculation is not triggered by van der Waals attraction but by the binding of algae through electrostatic and steric forces to the sediment.

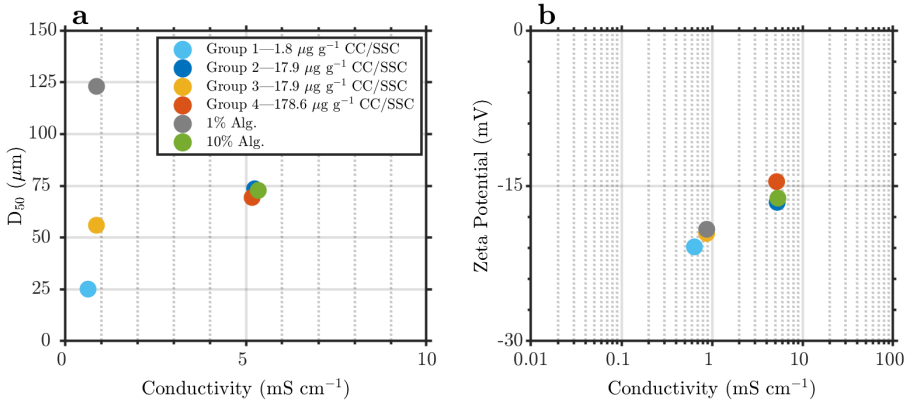


Figure 4.12: Floc size as a function of zeta potential and conductivity with sediment and algae.

#### 4.4.2. Flocculation with living algae in salt water

Figure 4.13 shows the time evolution of flocs with different SSC and different algae concentrations (CC/SSC) in NaCl ( $0.5 \text{ mol l}^{-1}$ , equal to approximately seawater NaCl concentration). In the absence of algae, the highest SSC leads to the largest floc sizes with NaCl (purple lines). In contrast to demi-water experiments, the high salinity ensures that the surface charge of the sediment particles is fully screened, making flocculation possible [Mietta, 2010]. In the presence of algae, it is found, as was discussed in the previous subsection, that the largest flocs are obtained for the suspensions with the highest CC/SSC (implying, for a given CC/algae concentration for samples with the lowest SSC). The flocculation rate, on the other hand is proportional to SSC: the highest the SSC, the fastest the flocculation. The highest floc sizes are observed 30 min after the start of the experiment, when a maximum floc size of about 60–80  $\mu\text{m}$  is reached. Higher algae concentrations do not lead to higher floc sizes and the floc size even decreases with algae concentration at longer times. The reason is most probably the reformation of algae chains under shear, the algae chains being extended at the beginning of the experiments while they tend to bind together while times passes and the concentration is increased. This effect is also visible on the experiments presented in Figure 4.13. When the algae concentration reached to 20% ( $1 \times 10^6 \text{ cells l}^{-1}$ ), the flocs had nearly a same size for two different SSC (green lines), which indicates that the flocs are algae-dominated when the algae concentration is high.

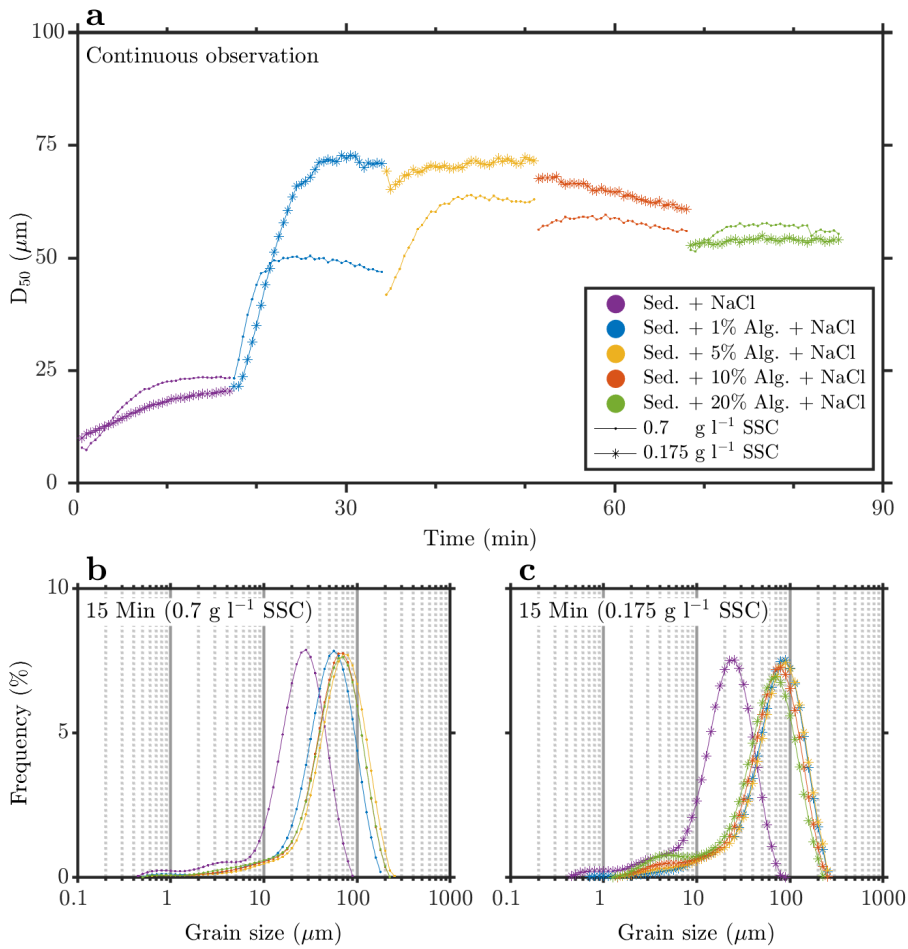


Figure 4.13: Floc size time evolution and distribution of different sediment concentration on the effect of different algae concentration in 0.5 M NaCl.

#### 4.4.3. Comparisons between EPS and living algae influences on flocculation

The effects of EPS and living algae are usually grouped under the generic term of “organic matter effects”. To distinguish between the two, several samples made in demi-water and sea water were compared. These samples were made of: (a) sediment (no added algae nor EPS), (b) algae (no added sediment nor EPS), (c) sediment with EPS and (d) sediment with algae. The results are shown in Figure 4.14.

In demi-water, the sediment and sediment with EPS suspensions (a and c) display no significant flocculation, while the sediment with algae and the pure algae suspensions (b and d) display similar flocculation kinetics and floc size. Note that the flocs formed by aggregation of algae cells reach a constant steady-state value whereas flocs formed by combining sediment and algae display a long-term time-dependent floc size. In sea water, all samples displayed flocculation except the pure sediment samples. Although the floc size of sediment did not significantly change from demi-water to sea water, the peak of sediment PSD in sea water was shaper than that in demi-water, which could indicate a slight flocculation effect in sea water. The fact that flocculation with EPS improved in seawater is consistent with section 4.3. The PSD of the samples with algae (green curves) shows that these samples are multimodal indicating the presence of some single algae cells or short-chains. The small peaks disappear when the algae is mixed with sediment particles (red curves) and the main peak moves from 25  $\mu\text{m}$  to 100  $\mu\text{m}$  over time, which indicates that flocculation occurs. The  $D_{50}$  in sea water is much larger than the one in demi-water for algae suspensions and larger for the sediment/algae suspensions, which indicates that sea water is especially beneficial to floc formation for algae cells.

Figure 4.15 only shows that the conductivity of sea water samples is higher than demi-water samples (which is to be expected) and that the zeta potential follows the expected trend that it is smallest at high conductivity.

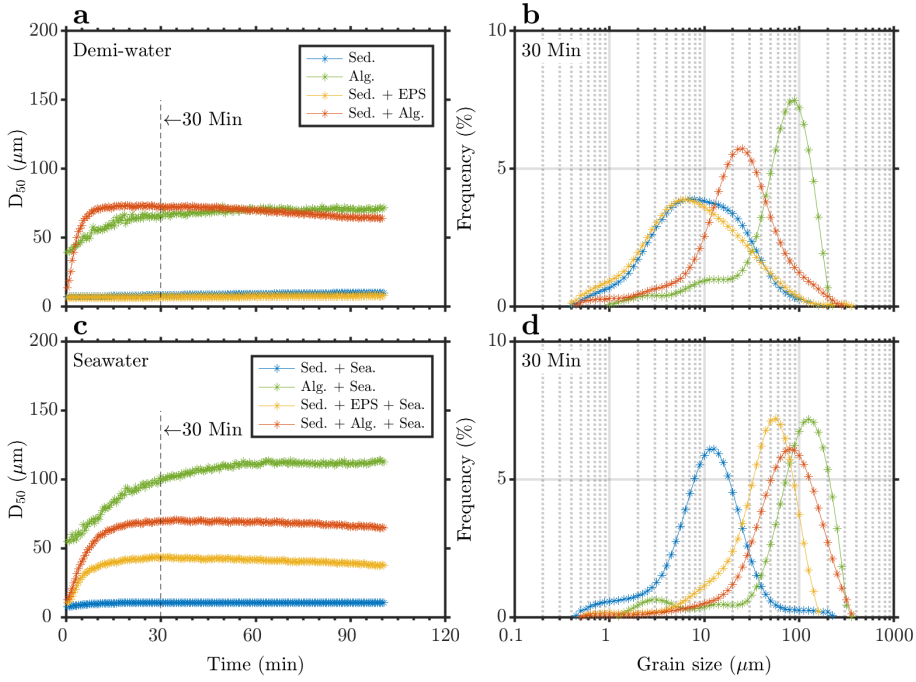


Figure 4.14: Floc size time evolution and distribution of sediment, sediment with EPS and sediment with algae on demi-water and sea water conditions.

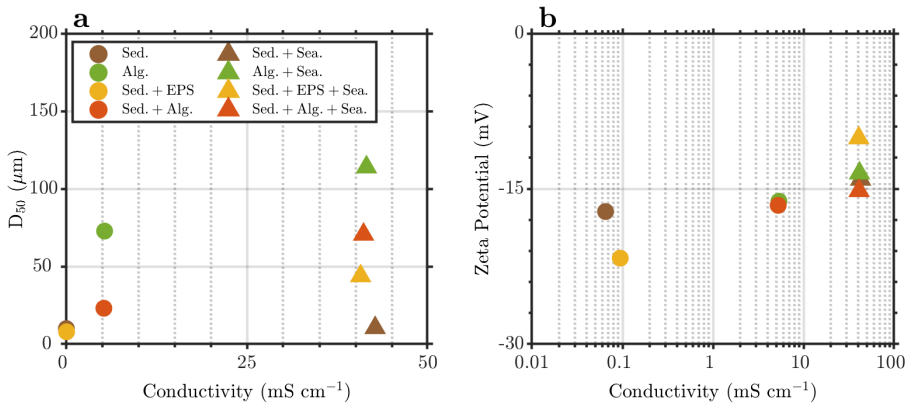


Figure 4.15: Floc size as a function of zeta potential and conductivity of all groups.

## 4.5. Evolutions of the algae-sediment flocculation

Experiments realized in artificial sea water are shown in Figure 4.16. In 4.16a, the time evolution of the  $D_{50}$  of different suspensions is shown, for a sediment concentration of  $0.7 \text{ g l}^{-1}$  (Table 3.4 of Chapter 3.). In contrast to flocculation with NaCl, flocculation with sea salt produces smaller flocs. One reason could be that due to the presence of divalent ions in sea salt, flocs get a denser structure than with monovalent NaCl. Additional measurements with algae in presence of divalent salt should help to confirm this. The  $D_{50}$  of the suspension with 30% algae shows that over time the mean particle size decreases at long times. This phenomenon is attributed to the shape of the flocs at this high algae concentration. The anisotropy of flocs is discussed in more detail in the next paragraph.

In order to investigate the morphological characteristics of algae-sediment flocs, video microscopy was used, more details can be seen in section 3.1.7. Figure 4.17a shows the steady state PSDs of the flocs as obtained from SLS (using the Malvern instrument, more details can be found in section 3.1.2). Figure 4.17b shows the PSDs obtained by video microscopy for the same samples, after that the images were analyzed by digital image processing. The SLS data shows that the peak of algae-sediment flocs increases with increasing algae concentration, while the peaks usually remain in the range 40–50  $\mu\text{m}$  using the video data.

Sample comparison is done in Figure 4.18. Several points can be made:

(1) The video technique is limited to the size range  $> 10 \mu\text{m}$ . This explains why no data is available with this technique for lower particle sizes.

(2) The software of the SLS device gives a smoothen PSD curve as output. The mathematical algorithm that smoothen the curve has been shown to “eliminate” data in an unwanted way [Ibanez Sanz, 2018].

(3) The model used to process the SLS data is based on the theory of spherical particles, with a given density. It can therefore not account properly for the complex diffraction pattern associated with algae.

Figure 4.19 shows the aspect ratio of algae-sediment flocs. There are some elongated particles (red circles) when the algae concentration is higher than 10%. When the algae concentration reaches to 30%, the aspect ratio (AR) appears to follow a trend:

$D_{50}$  increases when AR increases (red line). The video microscopy data therefore could confirm that the algae particles can aggregate into large flocs and lead to

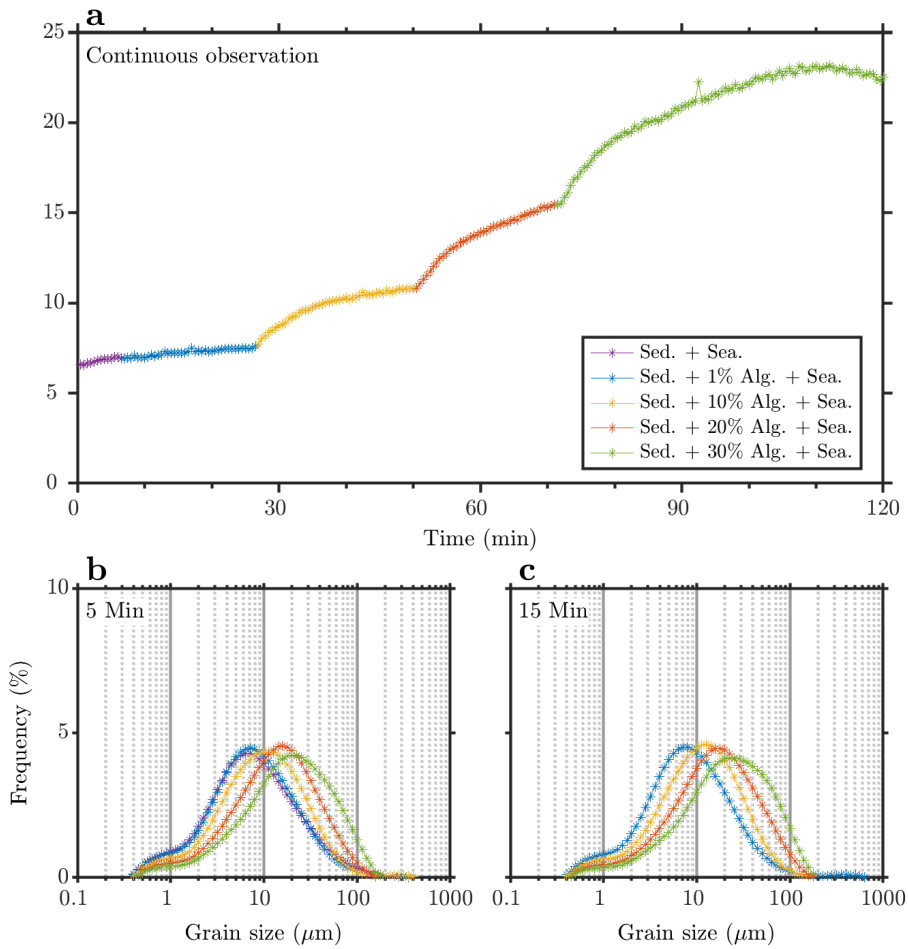


Figure 4.16: Floc size time evolution and distribution of suspensions having different sediment and algae concentrations in sea water. Figures b and c represent the PSD of suspensions given in a.

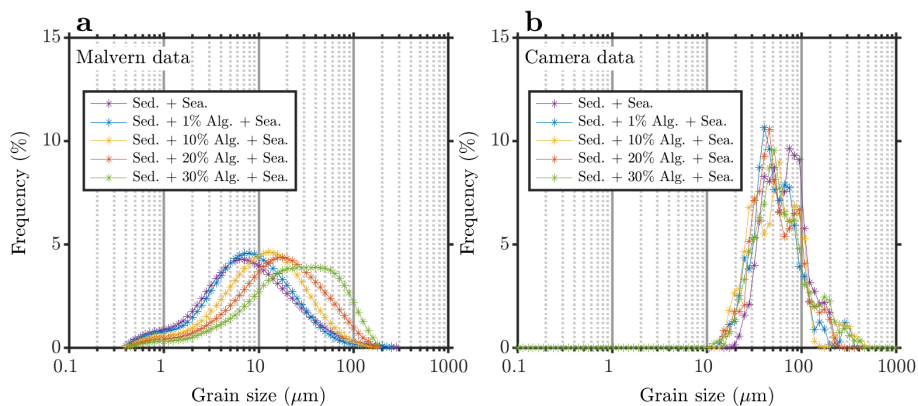


Figure 4.17: The comparisons of Malvern data and Camera data.

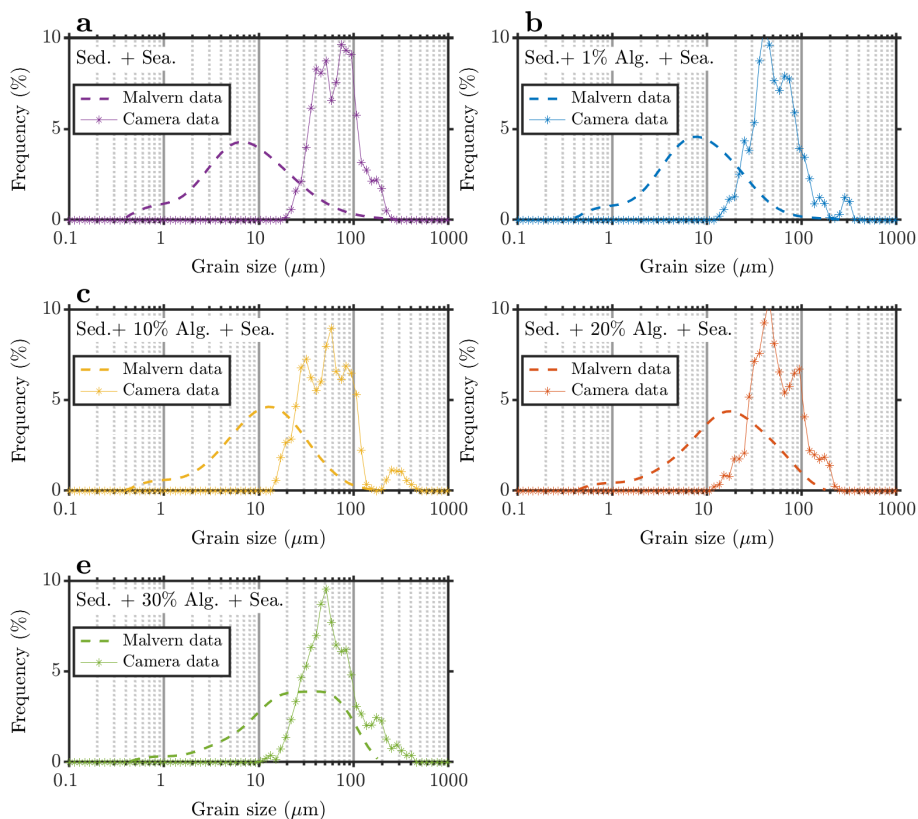


Figure 4.18: The comparisons of Malvern data and Camera data of different samples.

the formation of elongated aggregates. The anisotropy in shape can lead to additional problems in data interpretation, when SLS is used.

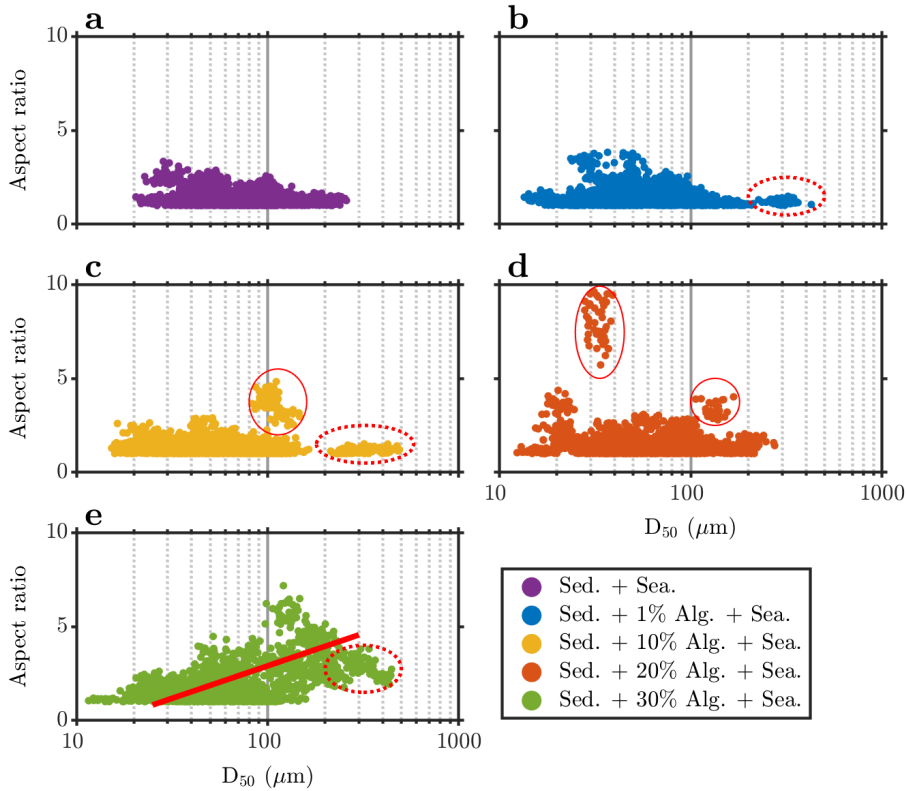


Figure 4.19: The aspect ratio (AR) as function of particle size from the camera data.

Figure 4.20 and Figure 4.21 show the effective density and settling velocity of algae-sediment flocs. From the observed trends, it can be concluded that:

(1) The effective density tends to decrease with increasing floc size while the settling velocity increases with increasing floc size.

(2) The effective density increases with increasing algae concentration for flocs smaller than 50  $\mu\text{m}$ , see the red dash circles. Many small flocs with high effective density and settling velocity appear with increasing algae concentration, indicating that the algae particles can bind to sediment particles and form dense flocs. This phenomenon is also observed in-situ: the floc effective density in summer (high algae concentration) is higher than the one in winter (low algae concentration).

(3) Algae cells also can form large flocs with themselves. Many flocs larger than 200  $\mu\text{m}$  appear with increasing algae concentration. These flocs have a small density, a high settling velocity and a large anisotropy.

Overall, algae can influence the flocculation by creating large flocs, but also by increasing the effective density of small flocs.

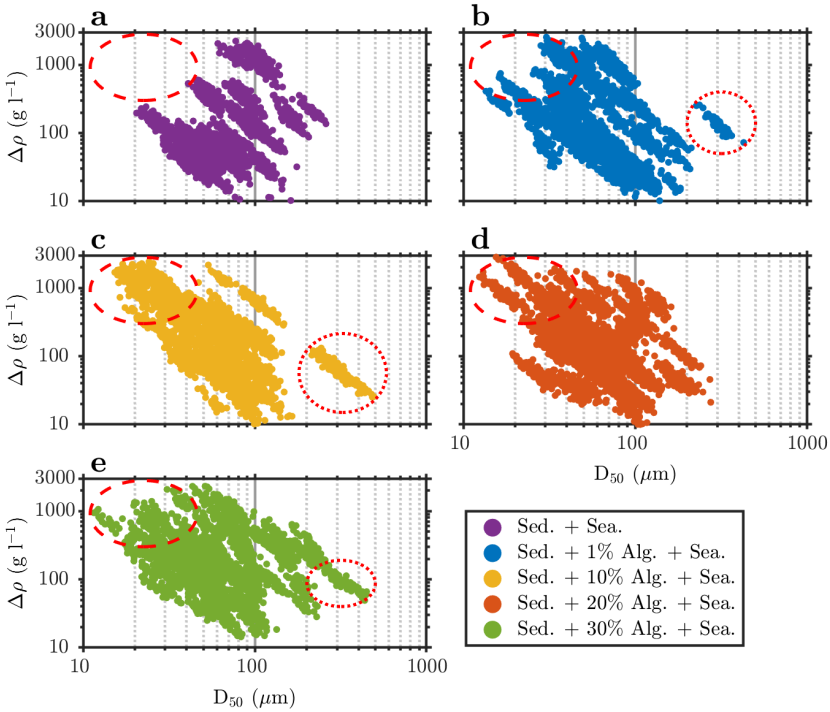


Figure 4.20: The effective density as function of particle size from the camera data.

Figure 4.22 shows a schematic illustration of the problem encountered in data analysis. The SLS technique most probably identifies large flocs as a collection of small (spherical) ones. As for video analysis, the most traditional way to define an equivalent diameter is given by Eq. (3.2), but the conformation of the elongated floc can introduce a significant uncertainty.

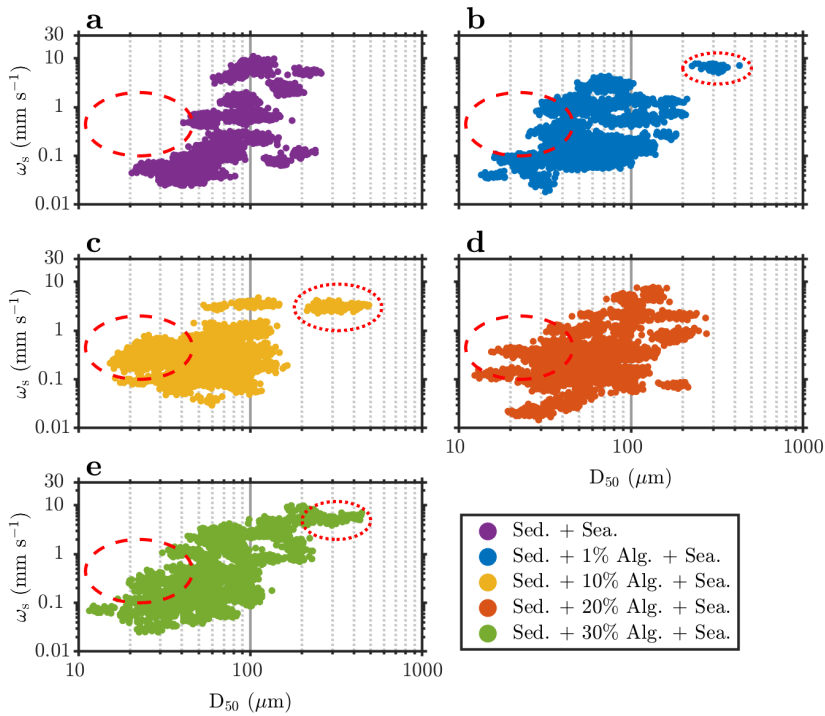


Figure 4.21: The settling velocity as function of particle size from the camera data.

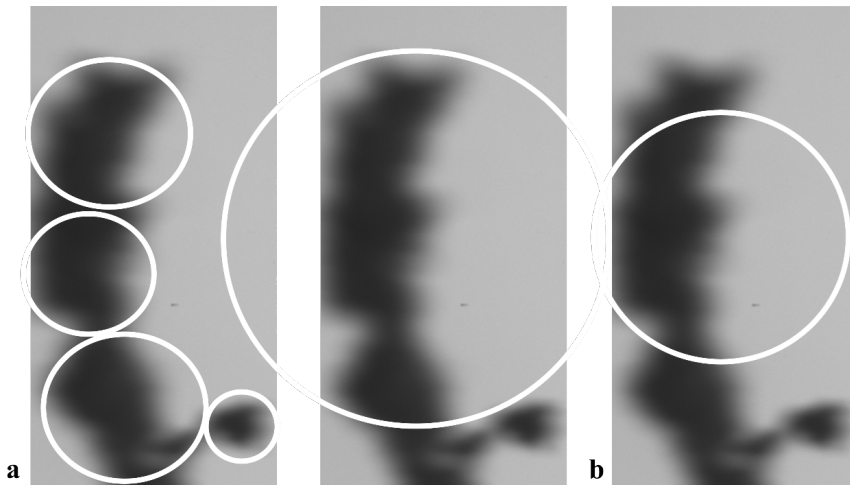


Figure 4.22: The different mean equivalent radius as found by (a) SLS data, and (b) video microscopy data analysis. In the case of video microscopy several equivalent radii could be defined, depending on the definition chosen.

## 4.6. Conclusions

The laboratory experiments presented in this article confirmed that the production of large flocs is correlated with the presence of EPS and living microalgae. Usually no distinction is made when organic matter effects are discussed. We show that while EPS, being a polyelectrolyte, acts as a traditional flocculant, microalgae can form large flocs as the microalgae cells aggregate with each other and also bind to sediment. This is in line with what has been found by analyzing in-situ monitoring data, see Chapters 5 and 6 and [Deng et al. \[2021, 2019\]](#), where the ratio CC/SSC was introduced. We confirm with the laboratory study that the ratio algae concentration (which is linearly proportional to CC) to sediment concentration (SSC) is driving floc properties. A continuous addition of algae to a suspension of sediment + algae that has reached a steady-state size results in a new flocculation. Flocs made of relative large amounts of algae are elongated. It should be noted that the algae effect is limited by sediment concentration, as high sediment concentration restricts sediment flocculation, which can also be related to the CC/SSC ratio. The flocculation rate is shown to be of the order of a few  $\mu\text{m}/\text{min}$  and a steady-state floc size (at constant shear rate) is obtained within 30 min for all experiments realized with organic matter.

In this chapter, the shear rate used was usually higher than the one encountered in natural environment conditions. This could lead to the fact that the effects of salinity (sediment + salt experiments) were smaller than the ones reported in other laboratory measurements [[Mietta et al., 2009a](#)], where different shear rates were used. The combination of cations with organic matter (EPS or algae) requires further investigation. We showed in particular that the combined action of salt and EPS does not follow the classical DLVO theory as EPS is also undergoing steric interactions, but that the presence of cations is required to promote flocculation.

Overall, salinity, EPS and living algae are parameters that all present in natural aquatic environments and their combined action makes flocculation processes complex. Further study is required to analyze the precise role of each parameter in combination with the others. A very schematic representation of the possible binding mechanisms is given in [Figure 4.23](#).

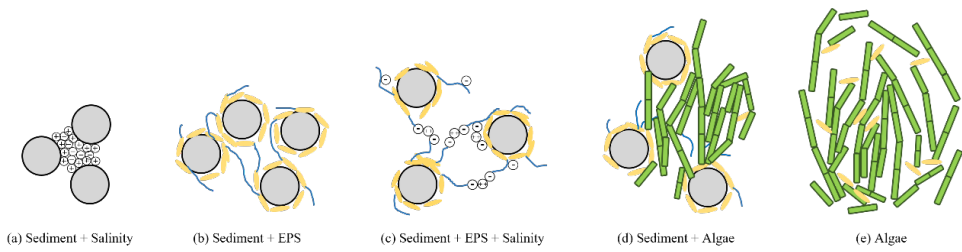


Figure 4.23: Different mechanisms of salinity, EPS and algae effects.



# 5

## The role of algae in fine sediment flocculation: in-situ and laboratory measurements

*Real knowledge is to know the extent of one's ignorance.*

Confucius

### Abstract

The precise interactions between organic and inorganic particles in the context of flocculation is an on-going topic of research. The suspended particulate matter (SPM) found in estuaries is composed of both organic and inorganic particles with specific particle size distributions (PSDs). These PSDs are a function of the hydrodynamic con-

ditions, suspended sediment concentration (SSC), organic matter composition, salinity and seasonal variations. A field campaign was carried out in August 2015 in the turbidity maximum zone of the Changjiang Estuary, where the SPM dynamics were recorded. The concentration of algae in the water column was indirectly measured through the chlorophyll concentration (CC). We show that there is a strong correlation between SSC and CC in the whole water column, for the whole tidal cycle. Additional flocculation experiments in the laboratory confirm that the largest observed flocs are predominantly organic-based, and that salinity alone could not induce the flocculation of the Changjiang mineral particles. A key parameter for the maximal floc size is the algae concentration to sediment concentration ratio. When this ratio is high, the  $D_{50}$  is high and vice-versa.

The contents of this chapter have been published in the article:

**Z. Deng, Q. He, Z. Safar, C. Chassagne**, *The role of algae in fine sediment flocculation: in-situ and laboratory measurements*, *Marine Geology* **71–84**, 413 (2019).

## 5.1. Introduction

Transport of fine-grained sediment in estuarine areas is a highly dynamic process, and is primarily controlled by river discharge, tidal energy and wave action as well as suspended matter load in the estuarine water. Flocculation and break-up are important processes of estuarine sediment transport as they govern the floc size, shape, strength, density, which in turn modifies the sediment settling velocity. The settling velocity is a main parameter for sediment transport and deposition models.

A lot of work has been done to study the physical flocculation/break-up mechanisms in estuaries [Cheng, 2004, Fennessy & Dyer, 1996, Mietta, 2010, Verney et al., 2009]. The influence of shear stresses and sample composition (clay type, chemistry) has been investigated, both in-situ and in the laboratory [Manning, 2010, Manning & Dyer, 1999, Mietta, 2010, Mikkelsen & Pejrup, 2001, Winterwerp, 1999]. More recently, the influence of microorganisms such as phytoplankton on sediment flocculation have been investigated [de Lucas Pardo, 2014, Fettweis & Lee, 2017, Huiming et al., 2011, Kjørboe et al., 1994, Lee et al., 2000, Maggi, 2009, 2013].

The present research was motivated by the following observation: we found, after

analyzing the results of our field campaign in the Changjiang Estuary, that most of the recorded particle size distributions were bimodal, with a small size peak around 20  $\mu\text{m}$  and a large particle peak around 200  $\mu\text{m}$ . Standard flocculation models, based on the population balance equation [Mietta, 2010, Nopens, 2005, Winterwerp, 1998, 2002] do not account for bimodal distributions. Recently, quite some work has been initiated on population balance equations accounting for both physical and bio-chemical effects [Lee et al., 2012, 2011, Shen et al., 2018, Verney et al., 2011]. All these models require several input parameters, in particular the collision efficiency and frequency, a break-up function and the number of microflocs (or primary particles) inside a macrofloc. Multimodal distributions can be achieved:

**Hypothesis 1** at steady-state for two types of particles (organic and inorganic for example), each type having different aggregation and break-up mechanisms and not significantly interfering with each other. This can happen for example in sediment-rich environments where organic-based flocs cannot “take-up” sediment anymore. Both mineral flocs and organic-based flocs have then their own aggregation/break-up mechanisms under shear.

**Hypothesis 2** by considering a same floc population having different modes of break-ups (binary/ternary), and/or accounting for floc erosion [Verney et al., 2011].

**Hypothesis 3** by having Population Size Distributions (PSD's) not yet at steady-state. An inflow of sediment particles in a water column containing organic matter for example can also be multimodal. If the aggregation between sediment and organic matter is optimal a monomodal distribution could be achieved at steady-state.

From in-situ data, it is difficult to distinguish which of the mechanisms is responsible for the observed multimodal distribution. Hypotheses 1 and 3 were tested in laboratory studies on sediment and algae where we could study PSD's reaching steady-state.

Based on the results of past research, it is known that algae, and in particular diatoms, combined with sediment, produce large aggregates [Droppo, 2001, Fettweis & Lee, 2017, Passow et al., 1994]. Diatoms are a common type of phytoplankton and are found in the whole water column in estuaries. Their concentration varies with the seasons and is highest usually in spring and summer in the Changjiang estuary [Zhu et al.,

2009]. These algae always coexist with sediment particles in estuaries. The relationship between algae and flocculation has been established for a long time. In the early 1960's, the aggregation of suspended particles with *Anabaenopsis* and their excreted substances has been studied [Walsby, 1968]. The earliest SEM picture of a floc composed of the algae *Cyanophyta* with sediment has been published in 1982 [Avnimelech et al., 1982]. This study also showed that the presence of *Cyanophyta* enhanced the flocculation ability of the sediment. Kiørboe et al. [Kiørboe et al., 1990, 1994] noticed from in-situ observations in the Danish Ise Fjord that sediment could aggregate with diatoms. As each algae species has different shape, size and surface properties, the flocculation involving one algae type or another create different flocs. For example, de Lucas Pardo [2014] investigated the flocculation involving two algae species (*Aphanizomenon* and *Aphanothece*). In the presence of clay particles and *Aphanizomenon*, filamentous small flocs were produced, whereas large isotropic flocs were produced in presence of *Aphanothece* and clay.

An important component in flocculation by algae is Extracellular Polymeric Substance (EPS) that is generated by the algae. This EPS is composed for a large part of polysaccharides (anionic or cationic carbohydrates) [Plude et al., 1991]. EPS plays a significant role as flocculating agent as EPS can bind onto anionic sediment particles by cationic bridging [Dontsova & Bigham, 2005]. The flocculation by different algae species and EPS sorts is an on-going topic of research. In order to improve the input parameters for flocculation models, a better understanding of the sediment/algae interaction is required [Chen et al., 2005, Fettweis et al., 2014, Maggi, 2009] In the present article, in view of the parametrization of our flocculation model, we answer the specific following questions, from in-situ measurements, for the Changjiang estuarine system:

1. How is the particle size distribution (PSD) evolving as function of depth and time?
2. What is the corresponding sediment/algae ratio?

From laboratory measurements, we investigate the following questions:

1. Can sediment particles aggregate without the presence of algae?
2. Can algae particles aggregate without the presence of sediment?

3. What is the evolution of the PSD as function of time, when sediment and algae are put in presence? Are the found PSD representative for the ones found in-situ?

## Study site

A whole tidal cycle sampling program was carried out from 14<sup>th</sup> to 22<sup>nd</sup> of August 2015 on a ship in the South passage of Changjiang Estuary (Figure 5.1). In this chapter, we analysed two successive tidal cycles: spring tide (08-14 to 08-15) and neap tide (08-20 to 08-21). For more details, please see chapter 3.

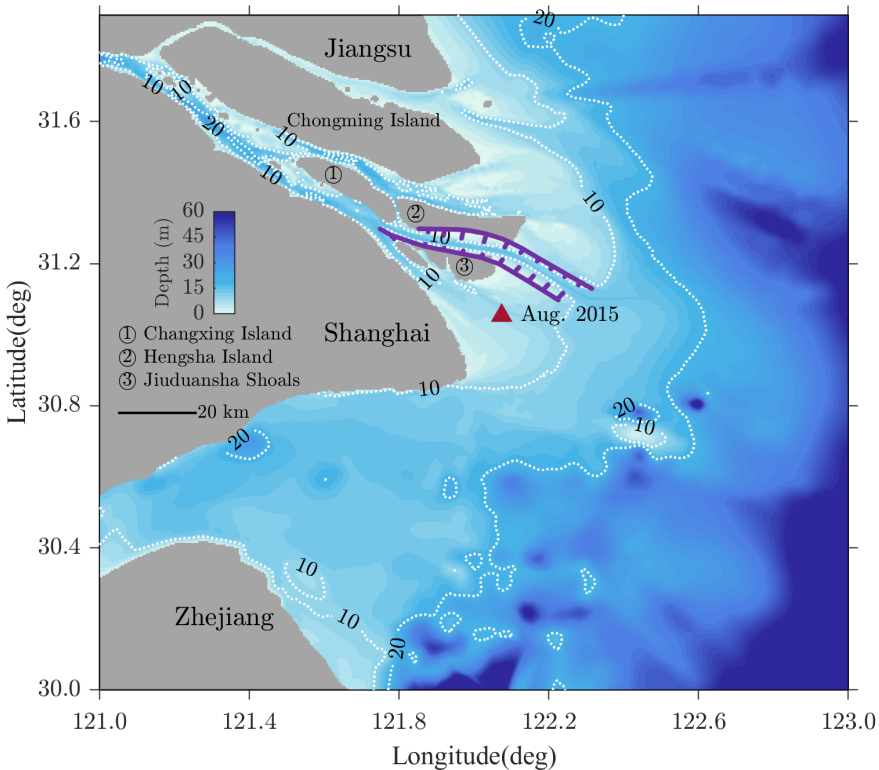


Figure 5.1: Study area of Changjiang Estuary. The local water depth of the study site (red star) is 5–9 m at spring tide and 5.3–8.3 m at neap tide.

## 5.2. Hydrodynamics and flocculation in a tidal period

### 5.2.1. In-situ versus laboratory OBS and chlorophyll estimations

The OBS response of clay particles of  $2\ \mu\text{m}$  is 50 times larger than the response of sand particles of  $100\ \mu\text{m}$  for the same concentration [Sutherland et al., 2000]. Hence, each sensor was calibrated using sediment from the site of interest. The calibration was done using filtration results performed on in-situ water samples, see Figure 5.2. In-situ measurements of chlorophyll were validated through laboratory (extraction) methods. The validation is also shown in Figure 5.2.

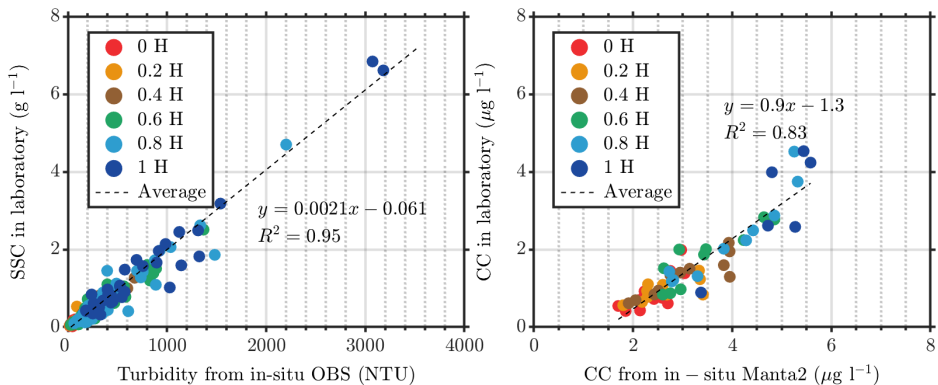


Figure 5.2: Calibration of the OBS (left) and Manta 2 (right). Analysis from the water samples in the laboratory are compared to in-situ measurements. Linear fits between turbidities and chlorophyll concentrations gave a coefficient of determination ( $R^2$ ) larger than 0.8 in both cases. The depth in the water column is represented by the H position, where 0H represents the surface and 1H the bottom.

The slope found for the sediment concentration measured in the laboratory versus the turbidity found in-situ is similar in spring and neap, indicating that the particle size distributions are not extremely different between these tides [Baker & Lavelle, 1984, Baker et al., 2001]. The relation between the chlorophyll concentrations measured in-situ and in the laboratory is fairly linear, with an average slope of 0.90, but with an offset at origin: when chlorophyll is found to be  $0\ \mu\text{g l}^{-1}$  in the laboratory, it has a value of  $2\ \mu\text{g l}^{-1}$  in-situ. The chlorophyll concentrations (CC) presented in the thesis were corrected using the laboratory calibration.

### 5.2.2. Hydrodynamics, and salinity

The depth average current velocity and shear stress distribution and salinity gradients are shown in Figure 5.3. Due to tidal asymmetry, the maximum current velocity appears at ebb tide, and can be up to  $1.5 \text{ m s}^{-1}$  at spring tide. At slack water, the current velocity is about  $0.4 \text{ m s}^{-1}$  on average in the water column. The shear rate at the bottom of the water column is larger than that at the surface of the water column and can reach  $50 \text{ s}^{-1}$ . The velocity and shear rate at spring tide are larger than at neap tide, but their distribution in the water column is similar.

At spring tide, salt sea water moves upstream and the salinity varies from 5 to 20 PSU. At neap tide, the salinity decreases and varies between 6 and 15 PSU. A low salinity surface plume is observed at ebb for spring tide. This is caused by the constant freshwater discharge which is spread out by the tidal current. The salinity is uniform during the flood period, being as large as 20 PSU, due to strong convection currents which are caused by oppositely directed river discharge and tidal current. At neap tide the salinity is uniformly distributed over the water column and remains on average below 12 PSU.

### 5.2.3. Suspended sediment, floc and chlorophyll characteristics

Distribution of sediment concentration and floc size and chlorophyll concentration are shown in Figure 5.3. The grey zones in the bottom figures indicate that no reliable LISST data could be obtained, due to the high SSC values.

The distribution of suspended sediment concentration (SSC) and chlorophyll concentration (CC) are clearly correlated. A more detailed description of the correlation will be given in section 5.5. Their distributions change with the tidal cycle. High SSC and CC concentrations appear at high shear stress, and their concentrations at the surface are lower than that at the bottom of the water column. The SSC was lower than  $1 \text{ g l}^{-1}$  in the upper half of the water column for both spring and neap tides. At spring/neap tide the SSC reached values between  $1\text{--}3 \text{ g l}^{-1}$  /  $0.5\text{--}2 \text{ g l}^{-1}$  for the lower half of the water column at maximum flood velocity. We note that even though the total sediment concentration (which varies from 0 to  $7 \text{ g l}^{-1}$ ) at spring tide is much higher than at neap tide (where it varies from 0 to  $2 \text{ g l}^{-1}$ ), the chlorophyll concentration is similar between spring tide and neap tide, being no more than  $7 \mu\text{g l}^{-1}$ .

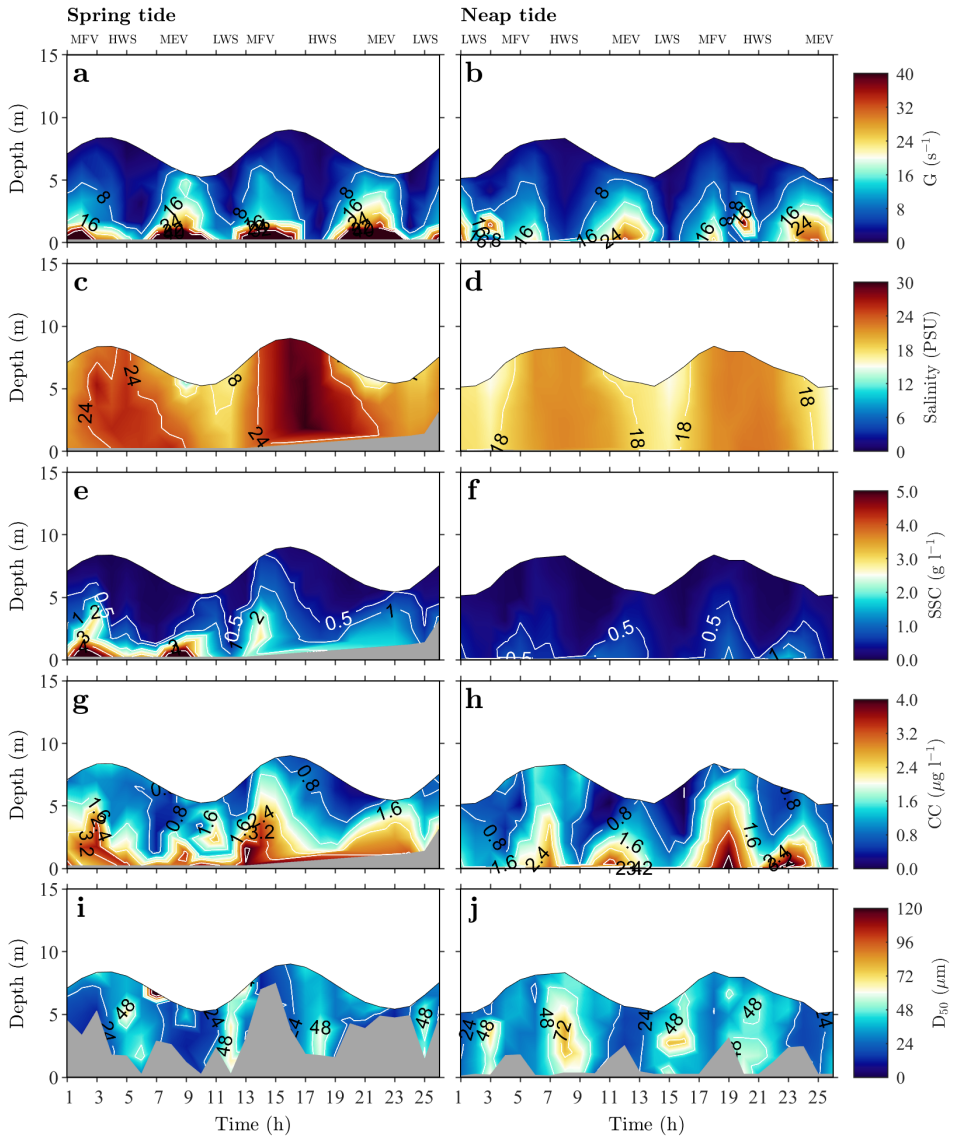


Figure 5.3: Distribution of shear stress, salinity, sediment concentration, chlorophyll concentration and floc size ( $D_{50}$ ) at spring and neap tide.

The mean floc size ( $D_{50}$ ) ranges from 20  $\mu\text{m}$  (high shear stress) to 120  $\mu\text{m}$  (low shear stress) with an average of 60  $\mu\text{m}$ . Large flocs of about 60 to 80  $\mu\text{m}$  are found at low shear rate conditions at slack water periods, for both high and low salinity conditions, at neap and spring tides. These flocs are distributed over the whole water column. At high water velocity, even though the largest SSC are then found, no large flocs are then observed in the upper half of the water column. The floc size could not be recorded in the lower part of the water column due to the high turbidity [Andrews et al., 2010].

In a natural environment, flocculation can be affected by many factors, such as shear stress, salinity, presence of organic matter, and so on [van Leussen, 1994]. The change in salinity is not likely to be one of these factors, as the overall salinity is too high to be responsible for a significant change in flocculation. Indeed, the overall salinity is about 5–20 PSU whereas salt-induced flocculation is promoted in the transition range between 0 PSU and 3 PSU [Chassagne et al., 2009, Guan & Chen, 1995, Guan et al., 1996]. The temperature is neither a factor, as the changes in temperatures are very small (the temperature varies between 25–30°C for all recording, not shown). In this section, we will distinguish between the evolution of the mean floc size  $D_{50}$  and its density as function of shear (section 5.3), the evolution of the full particle size distribution (section 5.4) and the role of algae (section 5.5). We will in particular show in section 5.5 that the ratio CC/SSC (chlorophyll concentration divided by suspended sediment concentration) is an interesting proxy.

### 5.3. Shear rate influence on the floc size and its density

Shear stress is usually the main factor influencing the size and density of flocs in a dynamic environment [Eisma, 1986, Manning & Dyer, 1999, Winterwerp, 2002]. Figure 5.4 shows the relationship between floc size and density with shear rate. As expected, the mean floc size decreases with increasing shear rate (Figure 5.5a). This is true for all shear rates, even the lowest ones, indicating that (1) the flocs are either breaking or restructuring to flocs of higher density and smaller size when the shear rate is increasing and/or (2) denser (mineral) particles are flowing in the water column or are resuspended from the bed. This is in line with the results found for the density as function of shear rate, see Figure 5.5b.

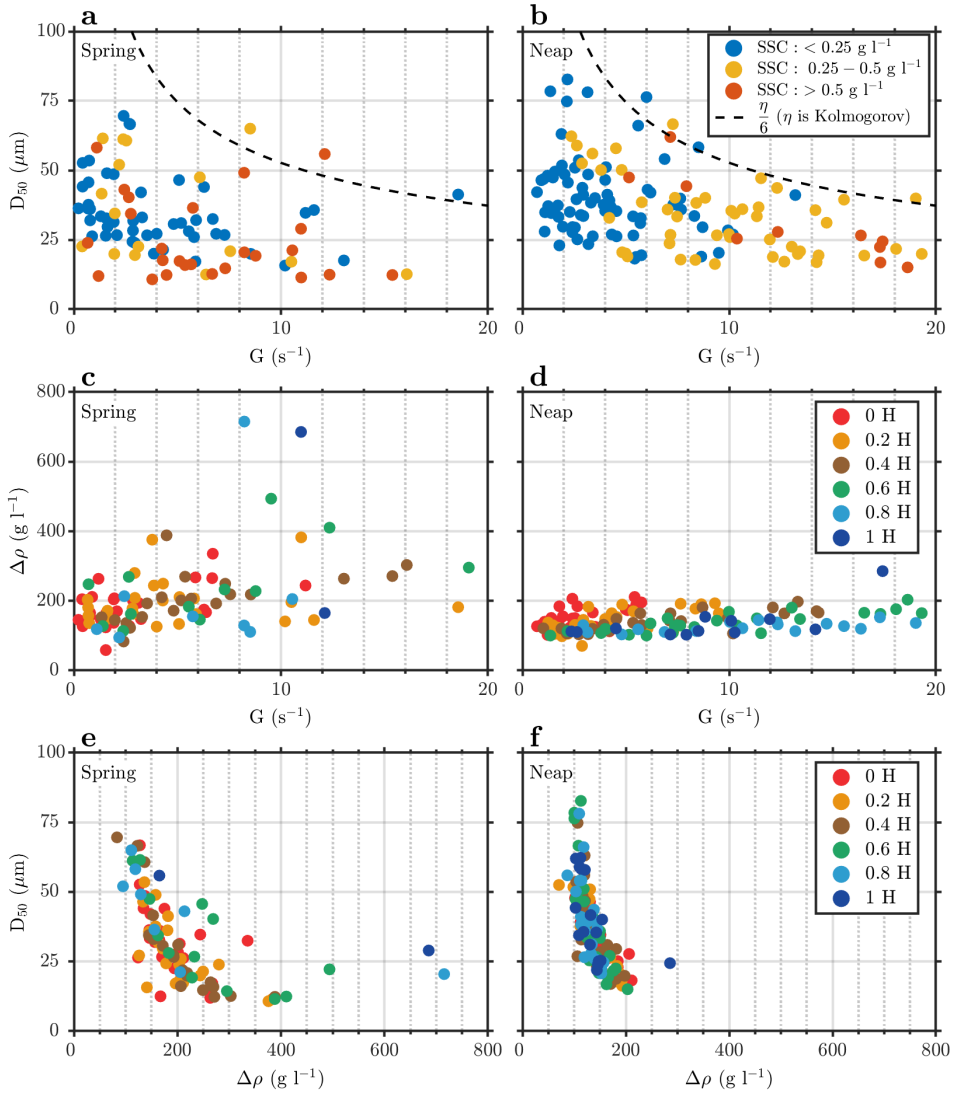


Figure 5.4: (a)  $D_{50}$  as function of shear for three SSC ranges; (b) density as function of shear for different depths and (c)  $D_{50}$  as function of effective density for different depths.

At spring tide, the floc effective density is increasing from below  $200 \text{ g l}^{-1}$  for the lowest shear rates ( $< 5 \text{ s}^{-1}$ ) to  $> 300 \text{ g l}^{-1}$  for shear rates above  $10 \text{ s}^{-1}$  indicating that denser particles are in suspension at high shears. At neap tide, there is no correlation between effective density and shear rate, and the effective density remains low (below  $200 \text{ g l}^{-1}$ ) for all shears, implying that mainly organic-rich particles are in suspension. From Figure 5.4c, it is observed that the smallest particles have the highest effective density, for all depths and shear rates, and that there is no correlation between  $D_{50}$  and depth. In the next subsection, we will see that correlations can nonetheless be found as function of depth and shear rates when the full particle size distribution (PSD) is studied.

## 5.4. Evolution of the particle size distribution at different

Figure 5.5 shows the full particle size distribution (PSD) in the water column, for different periods (termed MFV, HWS, MEV, LWS, see below). Both spring and neap periods display the same features. Several types of PSD's can be observed.

Three classes of particles are distinguished: (1) particles smaller than  $5 \mu\text{m}$  (2) particles in the range  $10\text{--}50 \mu\text{m}$  and (3) particles in the range larger than  $100 \mu\text{m}$ .

### 5.4.1. At Maximum Flood Velocity (MFV) and Maximum Ebb Velocity (MEV)

At MFV and MEV, The PSD is rather similar at all positions in the whole water column.

The small particles ( $< 5 \mu\text{m}$ ) are particularly abundant at all maximum velocities (MFV, MEV) and are a function of shear rate. Their concentration increases with depth, where the highest shear rates are found (see Figure 5.2). There are more of these small particles at spring than at neap tide, as the shear rates are higher at spring compared to neap tides. These particles also have a high density (see Figure 5.4c) and as they are found primarily close to the bed it would tend to prove that they are mineral sediment particles resuspended from the bed.

The particles of size  $10\text{--}50 \mu\text{m}$  and  $>100 \mu\text{m}$  are found over the whole water column in almost same proportion, except at the surface (0H, 0.2H) where there appears

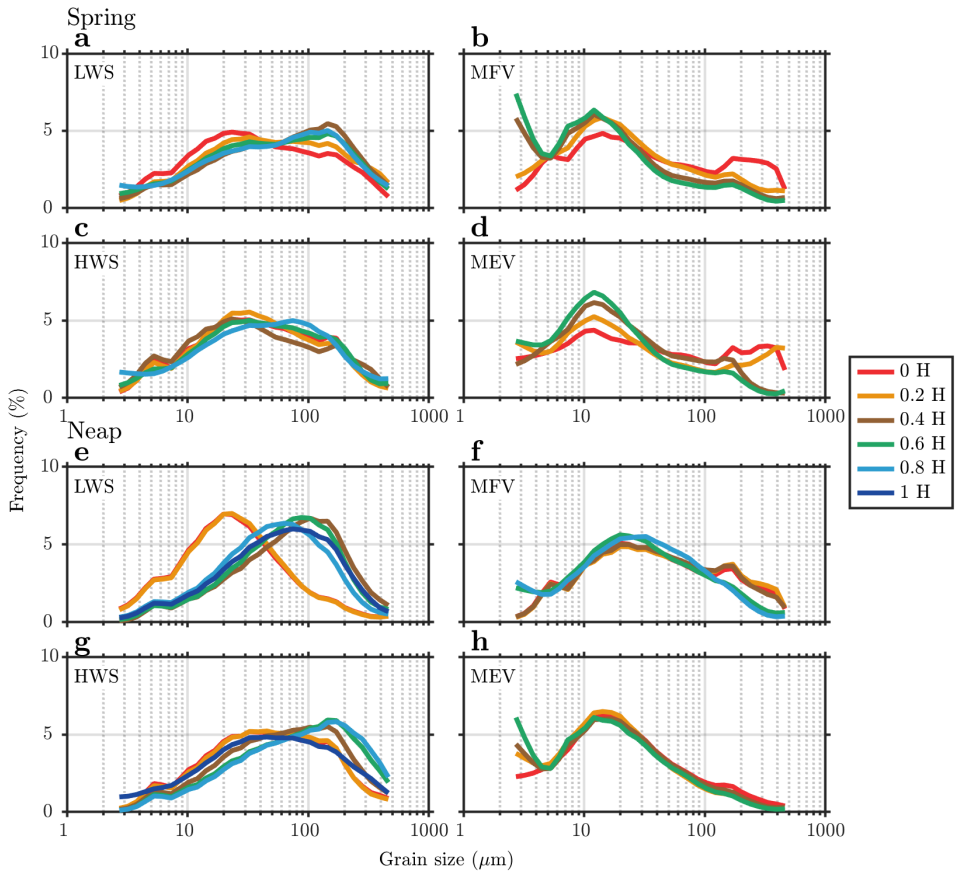


Figure 5.5: particle size distributions at different tidal periods.

to be more  $>100 \mu\text{m}$  particles. These large particles ( $> 100 \mu\text{m}$ ) are most probably algae, as their density should be low.

At MFV and MEV, the particles in the size range  $10\text{--}50 \mu\text{m}$  are dominant in volume-% compared to the other sizes, implying that the  $D_{50}$  will be in reasonably good approximation representative of that size fraction range, as can be seen in Table 5.1. From Table 5.1, it can however be noticed that the  $D_{50}$  is slightly biased by the presence of the largest particles from the range  $>100 \mu\text{m}$ , as the  $D_{50}$  at spring-MEV (where these large particles are significantly present, especially at the top of the water column) is larger than the  $D_{50}$  at spring-MFV, even though the peak in the size range  $10\text{--}50 \mu\text{m}$  is not varying. The same occurs for the  $D_{50}$  at neap-MFV (where the large particles are present) which it is larger than the  $D_{50}$  at neap-MEV, but in this case there is also a shift in the  $10\text{--}50 \mu\text{m}$  peak towards higher sizes for the particles at the bottom of the water column. This implies that at neap, the shear stresses are low enough to induce a particle size stratification in the water column.

Table 5.1: Mean water velocity, shear rate  $G$ , salinity  $\text{Sal}$ , suspended sediment concentration  $\text{SSC}$ , Chlorophyl- $a$  concentration  $\text{CC}$  and particle size  $D_{50}$ , averaged over the whole water column

		Velocity ( $\text{m s}^{-1}$ )	$G$ ( $\text{s}^{-1}$ )	Sal (PSU)	SSC ( $\text{g l}^{-1}$ )	CC ( $\mu\text{g l}^{-1}$ )	$D_{50}$ ( $\mu\text{m}$ )
Spring tide	MFV	1.2	14.5	13.8	1.8	2.3	17.1
	HWS	0.4	2.4	15.9	0.6	1.4	45.3
	MEV	1.5	17.6	12.7	0.7	1.1	23.4
	LWS	0.4	3.5	10.8	0.7	1.8	48.8
Neap tide	MFV	1.0	10.6	12.1	0.4	2.0	26.8
	HWS	0.4	3.2	12.5	0.2	1.1	54.1
	MEV	1.3	18.2	9.8	0.5	1.4	18.9
	LWS	0.4	5.1	8.7	0.2	0.7	50.7

At maximum velocity, with the  $D_{50}$  being in the range  $15\text{--}25 \mu\text{m}$ , it can be observed from Figure 5.5c that these particles have a wide spreading of density. This is the consequence of the fact that the suspended particles are a mixture of dense small particles (of size  $< 5 \mu\text{m}$ ), large particles with low density (of size  $> 100 \mu\text{m}$ ), and a significant amount of particles in the  $10\text{--}50 \mu\text{m}$  range, with variable density.

### 5.4.2. At High Water Slack (HWS) and Low Water Slack (LWS)

At HWS and LWS, the particles in the size range 10–50  $\mu\text{m}$  are not always dominant in volume (%) compared to the size range  $>100 \mu\text{m}$ . For instance, at Spring-LWS, a significant amount of particles are observed at the top of the water column (0H–0.2H) with a peak in size centered at about 20  $\mu\text{m}$  and a large amount of particles with a peak in size centered at about 200  $\mu\text{m}$  is observed at the bottom (0.8H–1H). There is a transition between the relative ratio of the two peaks (small / large particles) occurring between 0.4H and 0.6H, where the magnitude of the two peaks is the same. A similar trend is observed at neap, both for HWS and LWS.

At slack water, the shear stresses are low, and there is a shift of the  $D_{50}$  towards higher sizes compared to the maximum velocity case (see Table 5.1 and Figure 5.4a). The particles observed at slack must have therefore an effective density that is low enough to keep them in suspension. It can in particular be observed that large particles ( $> 100 \mu\text{m}$ ) are present at all depths at slack. This leads us to conclude that these particles are most probably algae and algae-rich particles.

There remains also a small background concentration of particles  $< 5 \mu\text{m}$  at all depths. These particles, whatever their density, remain primarily in suspension because their gravity-driven settling velocity is very low (their mass is very low).

At slack, with the  $D_{50}$  being in the range 45–55  $\mu\text{m}$ , it can be observed from Figure 5.5c that these particles have a narrow spreading in density, and that their density is very low. This is the consequence of the fact that the particles in suspension are predominantly algae and algae-rich particles.

## 5.5. Role of algae in the particle size distribution

We have found (see section 5.4) that the full PSD in the water column is tri- or bimodal, depending on the hydrodynamic conditions. We have identified the smallest class size ( $< 5 \mu\text{m}$ ) as being primarily composed of dense mineral sediment particles eroded from the bed and the largest class size ( $> 100 \mu\text{m}$ ) as being primarily composed of algae with a low density. It remains to be investigated what the middle size class 10–50  $\mu\text{m}$  is composed of. This raises the question whether and how mineral sediment interact with algae.

From Figure 5.5 we have seen that the PSD is primarily multimodal. As stated in

the introduction, a multimodal PSD can be due to several reasons. The smallest and the largest size classes ( $< 5 \mu\text{m}$  and  $> 100 \mu\text{m}$ ) are present for all hydrodynamic conditions. This could imply that these particles do not interact significantly (hypothesis 1) with the middle-class size  $10\text{--}50 \mu\text{m}$ , or that the PSD is has not reached a steady-state due to the changing hydrodynamic conditions or the new inflow of particles (hypothesis 3).

Hypothesis 1 was based on the fact that a same floc population could have different modes of break-ups (binary/ternary), however we discard this hypothesis in our case. Indeed, if only one type of particles would be present, one would expect that for similar shears, there would be a correlation between sediment concentration (SSC) and floc size, as the collision frequency increases with SSC [Eisma & Li, 1993, Law et al., 2013, Lee et al., 2000]. The correlation between  $D_{50}$  and SSC is not good, see Figure 5.6, and one can even argue that there is a small trend indicating that the  $D_{50}$  decreases with SSC. This trend has also been found by other authors [Manning & Schoellhamer, 2013]. This led us to conclude that the particles in the middle-class size  $10\text{--}50 \mu\text{m}$  (which is strongly correlated to the behavior of the  $D_{50}$ , as detailed in section 5.4) are composed of two types of particles: sediment and algae.

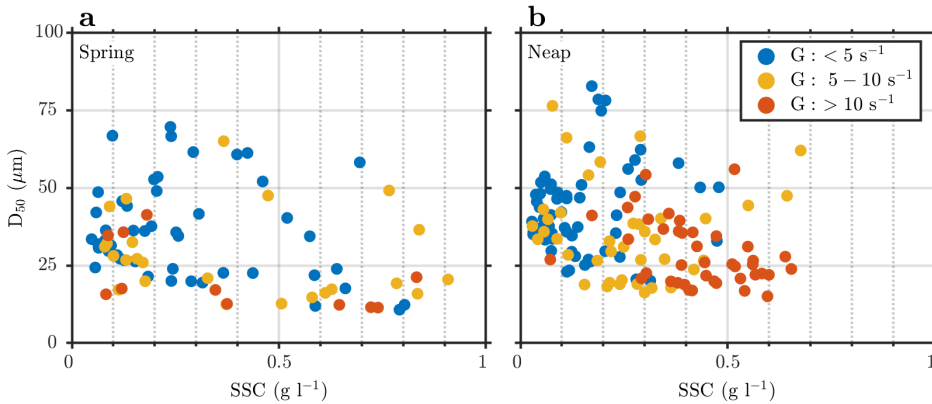


Figure 5.6: Variation of  $D_{50}$  with SSC for different shears.

As can be seen in Figure 5.3, the CC and SSC are strongly correlated. This correlation is better visible in Figure 5.7.

It is long known that sedimentation is a main cause for the distribution of phytoplankton in the water column [Barlow, 1955]. Phytoplankton particles can increase their density after excess photosynthesis [Thomas & Walsby, 1985, Visser et al., 1995],

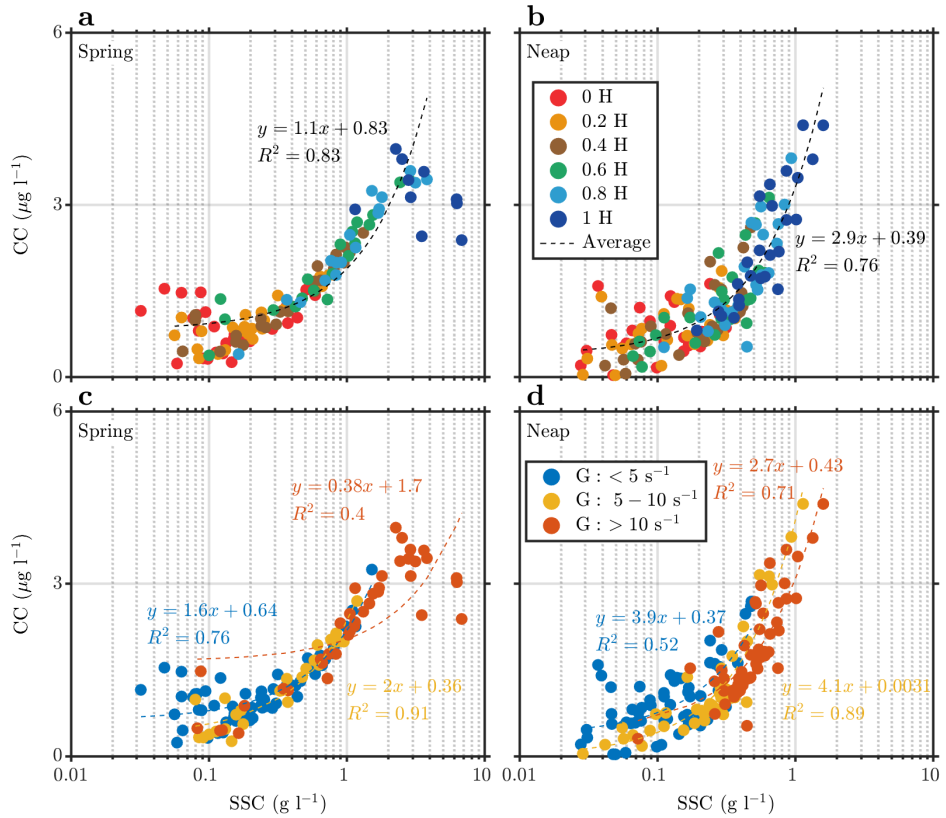


Figure 5.7: Relationship between chlorophyll concentration (CC) and suspended sediment concentration (SSC) for different shears.

hereby increasing their settling velocity. The settling velocity of phytoplankton is higher when it is combined to other suspended particles. Flocs, composed of extracellular polymer matter and diatoms have for instance been observed [Engel, 2000, Kiørboe et al., 1990, 1994]. Flocs, made of diatoms and sediment particles have also been reported [Avnimelech et al., 1982, Søballe & Threlkeld, 1988]. In our case, the algae particles can indeed be observed in the whole water column, as chlorophyll concentrations (CC) could be measured at all depths, see Figure 5.7. As the dependence of chlorophyll concentrations (CC) is linear with suspended sediment concentration (SSC) it enables us to define a CC/SSC ratio.

In section 5.5.1, we will study the relation between  $D_{50}$ , shear rate and depth as function of the CC/SSC ratio. In section 5.5.2, we will detail laboratory experiments, to check hypothesis 1 and 3.

### 5.5.1. Algae-sediment ratio in in-situ conditions

From Figure 5.7 it can be inferred that the chlorophyll (CC) to sediment (SSC) ratio is larger for neap than spring tide, which implies that for a given SSC there will be more algae in the suspension at neap (low shears) than at spring (high shears). This is in line with the results of section 5.2, where it was found that at neap the density of the particles in suspension is lower than at spring. This would agree with the fact that mineral-based aggregates are denser than algae-based aggregates: at spring, more mineral sediment can be transported in the water column, whereas at neap most of the mineral-based aggregates would be deposited and predominantly algae-based aggregates would remain in suspension.

The CC/SSC ratios are also different for different shear rates: the CC/SSC data is scattered at low shear rate, close to the top of the water column. In that part of the water column algae are dominant, and the sediment concentration is quite low. Considering the optical properties of algae, we raise the question whether the OBS can properly estimate the SSC concentrations in that part of the water column. As the water samples taken to be measured in the laboratory have been filtered, it is also possible that some biomass is lost in the process. This implies that the SSC correlation (in-situ/lab) shown in Figure 5.2 does not display significant outliers at low SSC. In the middle part of the water column, where higher shear rates ( $5-10 \text{ s}^{-1}$ ) and higher SSC are observed, the correlation between SSC and CC is significant, and the CC/SSC ratios are higher than

at the bottom of the water column.

The high SSC concentration close to the bottom is a result of the erosion of the bed due to the high shear ( $> 10 \text{ s}^{-1}$ ) at that position. As the deeper part of the eroded bed barely contains algae, this is the reason for the CC saturation value [Xu et al., 2016]. At neap, the SSC close to the bottom is much less than at spring tide, and only the upper layer (containing algae) of the bed is eroded, resulting in a better correlation between CC and SSC for any SSC.

The floc size as function of CC/SSC ratio is displayed in Figure 5.8. It is clear, from comparing Figure 5.8a and Figure 5.8b that the data is quite scattered for the measurements done at low shear, for the particles found at the top of the water column, i.e. 0H and 0.2H. This could, as indicated at the beginning of this section, correspond to the fact that at the top of the water column mainly algae are present and that the CC/SSC ratio is ill defined. At higher depths (0.4H–1H) the ratio CC/SSC is rather constant, at a value in the range  $2\text{--}4 \mu\text{g g}^{-1}$  at spring and  $2\text{--}5 \mu\text{g g}^{-1}$  at neap, indicating that there is more algae in the water column at neap than at spring. For this CC/SSC ratio the  $D_{50}$  varies between  $10\text{--}80 \mu\text{m}$ , the smallest  $D_{50}$  are found at high shear and the largest  $D_{50}$  at low shear, as expected.

Despite the limited amount of data points, one can observe that the largest  $D_{50}$  are found for the highest CC/SSC in the range  $1\text{--}5 \mu\text{g g}^{-1}$ . This is also the case for the data points above  $5 \mu\text{g g}^{-1}$ , even though the data is very scattered as discussed above. We wanted to confirm this by laboratory experiments. This is done in the next section.

### 5.5.2. Algae-sediment flocculation process in laboratory

From the data collected in-situ, it was not possible to assess (1) whether the  $D_{50}$  increases with CC/SSC ratio, (2) whether the algae-sediment mixture can reach a steady-state (hypothesis 3) and if algae-algae flocculation and sediment-sediment flocculation would occur significantly over algae-sediment flocculation (hypothesis 1). To verify these points, laboratory experiments were performed.

The experiments were done using Changjiang sediment, collected in the sediment bed. Even though the sediment samples might contain some (degraded) algae, the bottom shear stresses at the sampling site ensure that the sediment is very well mixed and a low content in algae is expected [Zhang et al., 2007, Zhu et al., 2011]. This is also confirmed from the analysis of the in-situ data, where we have shown that small and

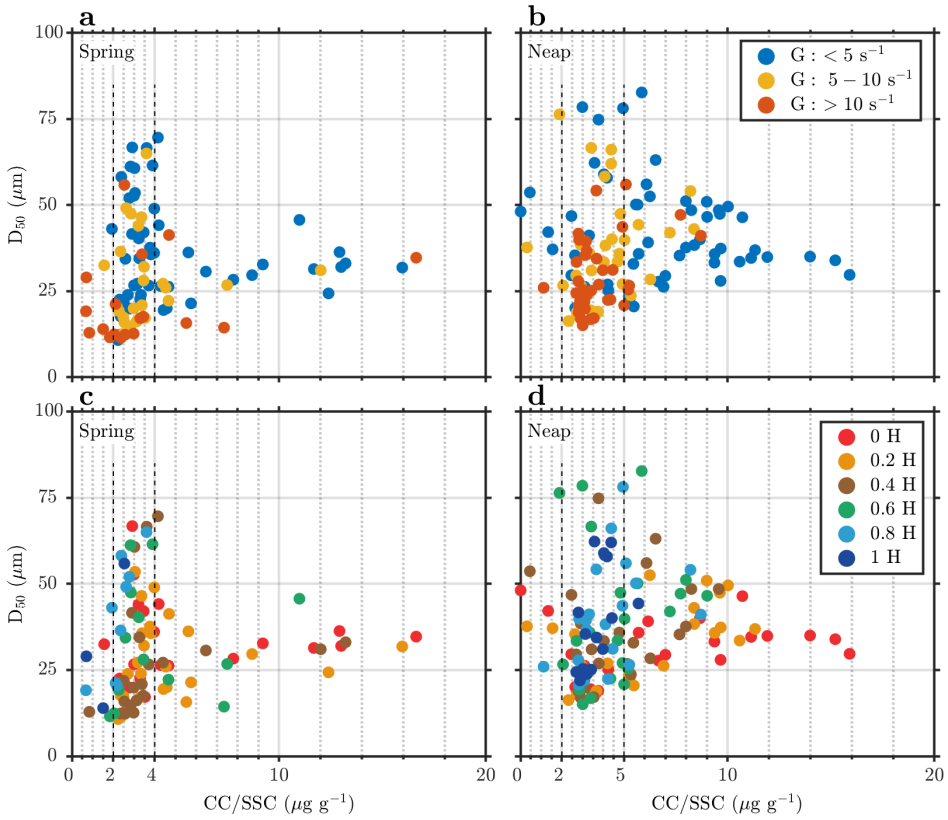


Figure 5.8: Relationship between floc size and CC/SSC ratio for different shears and different depths.

dense particles are resuspended from the bed at high shear (section 5.2).

It was first verified that the Changjiang sediment, collected in the sediment bed, has a limited flocculation ability. An amount of  $0.7 \text{ g l}^{-1}$  of this sediment, dispersed in artificial sea water was stirred (at 40 RPM, roughly equivalent to a shear rate of  $90 \text{ s}^{-1}$ ) in 1L jar, and particle size distributions were recorded for 3 hours by static light scattering. The mean particle size varied from  $7.1 \text{ }\mu\text{m}$  to  $10.48 \text{ }\mu\text{m}$  within 120 min and then remained constant, see Figure 5.9.

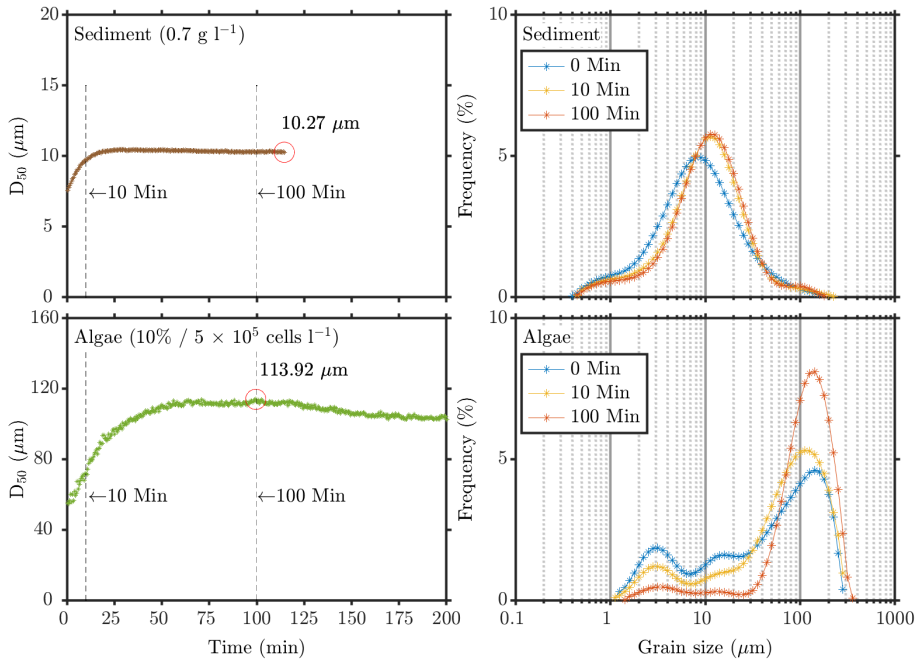


Figure 5.9: particle size distributions as function of time in artificial sea water, measured by static light scattering in the laboratory. (a)  $0.7 \text{ g l}^{-1}$  of Changjiang sediment and (b)  $5 \times 10^5 \text{ cells l}^{-1}$  of *Skeletonema costatum*.

In a second series of tests, *Skeletonema costatum* was studied [Riper et al., 1979, Smayda & Boleyn, 1966].  $5 \times 10^5$  cells were dispersed in artificial sea water in 1L jar, gently stirred (at 40 RPM), and particle size distributions were recorded for 5 hours by static light scattering. The mean particle size varied as indicated in Figure 5.9b.

The initial particle size distribution is in agreement with the shape of *Skeletonema costatum* as observed by microscope (Figure 5.10). A single *Skeletonema costatum*

cell is about 4–6  $\mu\text{m}$  wide. The *Skeletonema costatum* cultures produce distributions of single cells, but, by cell division or aggregation of cells with neighboring ones, 2 cell-long chains and sometimes 3, 4 or 5 cell-long chains can be observed. The chains length can reach lengths of 30  $\mu\text{m}$  [Capriulo et al., 1988, Gibson et al., 1993, Nayar et al., 2005]. In time, the cells flocculate or divide, creating particles of equivalent diameter of about 40–100  $\mu\text{m}$ .

The aggregates observed under microscope were never longer than 50  $\mu\text{m}$  because of the manipulation required to observe them by microscopy: longer aggregates are broken when the cover slip is slid over the sample.

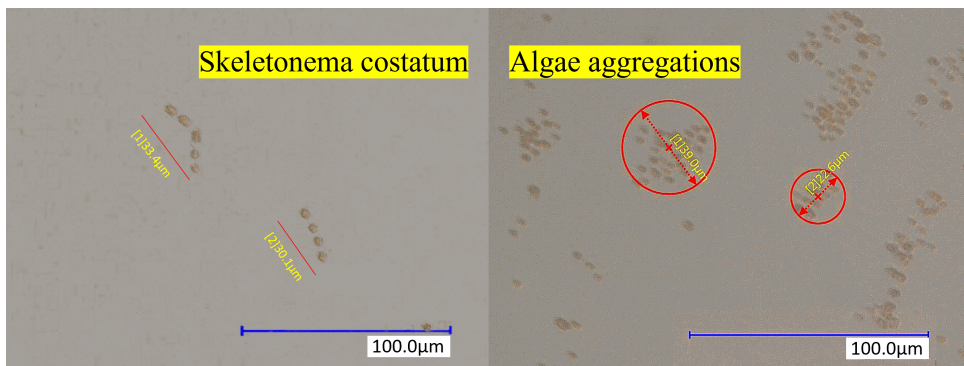


Figure 5.10: *Skeletonema costatum* and their aggregations.

In time, the mean particle size  $D_{50}$  (see insert in Figure 5.9) is significantly increasing, indicating that either the algae particles are flocculating, or their chains are growing. The larger peak of the distribution reaches a steady-state after 30 min. The concentration algae used in the laboratory experiments is comparable with the values obtained in-situ, as it was estimated that  $3 \times 10^3$  cells  $\text{l}^{-1}$  *Skeletonema costatum* corresponds to  $1 \mu\text{g l}^{-1}$  chlorophyll concentration in Changjiang estuary [Ministry of Environmental Protection of the People's Republic of China, 2014]. The estimated experimental chlorophyll concentration varies from  $1.25 \mu\text{g l}^{-1}$  to  $12.5 \mu\text{g l}^{-1}$ .

In the next series of tests, Changjiang sediment and *Skeletonema costatum* was mixed together and the time evolution of the PSD was recorded (Figure 5.11). From Figure 5.11a, it is clear that sediment-algae flocs can form rapidly when mixed, as the particle size curve shifts from bimodal to unimodal in 10 minutes. As the hydrodynamics in the jar are different from in-situ, the kinetics of aggregation might however be

different in-situ. From Figure 5.11b, it can be observed that the ratio of sediment and algae concentration plays a dominant role in determining the equilibrium particle size. The red and green curves correspond to the case where the CC/SSC ratio is the same (18  $\mu\text{g/g}$ ), but the algae and sediment concentrations are ten times higher for the red curve than the green curve. The same  $D_{50}$  is obtained in this case. When the CC/SSC is lower (CC/SSC = 1.8  $\mu\text{g g}^{-1}$ , blue curve compared to the red and green curves CC/SSC = 18  $\mu\text{g g}^{-1}$ ) the  $D_{50}$  is lower. It does not matter whether the CC/SSC (blue curve) is lower because there are less algae but same amount of sediment (red curve) or more sediment and same amount of algae (green curve). These results seem to indicate that when there is a relative abundance of algae compared to sediment particles, algae cells will aggregate with themselves to form large flocs (red and green curves), but that when the sediment concentration is substantial in comparison with the algae concentration, the limiting factor will be the sediment concentration (blue curve). Due to the binding of algae with sediment, there are no algae left to form large algae-algae aggregates.

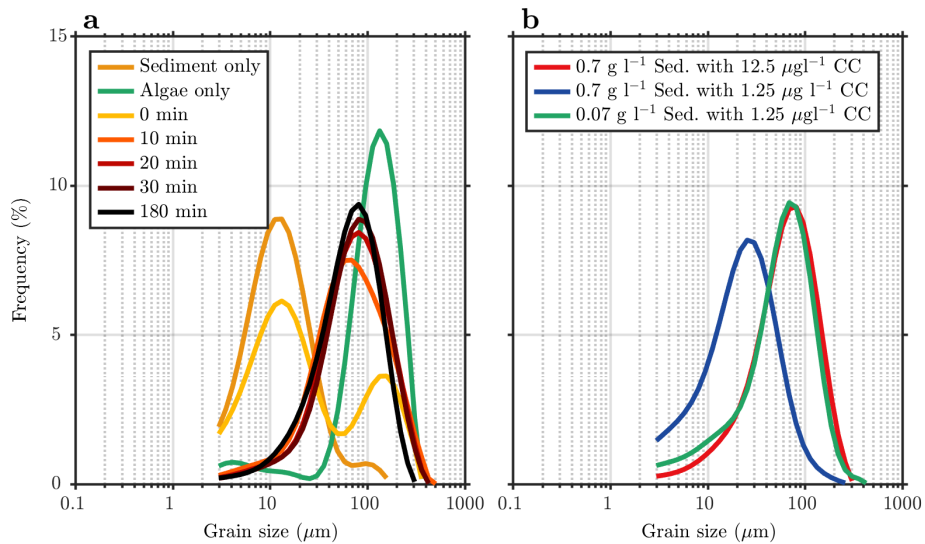


Figure 5.11: Aggregates of Changjiang sediment and *Skeletonema costatum*. (a) The PSD evolution of mixtures of sediment and algae. The time  $t=0$  corresponds to the moment sediment and algae particles are mixed. The concentration of sediment was  $0.7 \text{ g l}^{-1}$  and the concentration of algae was  $5 \times 10^4 \text{ cells l}^{-1}$  ( $1.25 \mu\text{g l}^{-1}$  CC) (b) Depending on the sediment to algae ratio, different equilibrium PSD are obtained.

We have shown that in the laboratory (1) the  $D_{50}$  increases with CC/SSC ratio

and (2) the algae-sediment mixture can reach a monomodal steady-state. There is a significant algae-algae flocculation but no sediment-sediment flocculation.

### 5.5.3. Link between in-situ observations and laboratory measurements

In section 5.4, we have identified 3 classes of particles in-situ: (1) particles smaller than 5  $\mu\text{m}$  (2) particles in the range 10–50  $\mu\text{m}$  and (3) particles in the range larger than 100  $\mu\text{m}$ . At the end of the same section, we have concluded that the particles smaller than 5  $\mu\text{m}$  are mineral sediment particles, resuspended from the bed at high shears and large particles (> 100  $\mu\text{m}$ ) are algae, which are present at all depths and all times, their largest relative amount being at slack. The in-situ and laboratory data are compared in Figure 5.12.

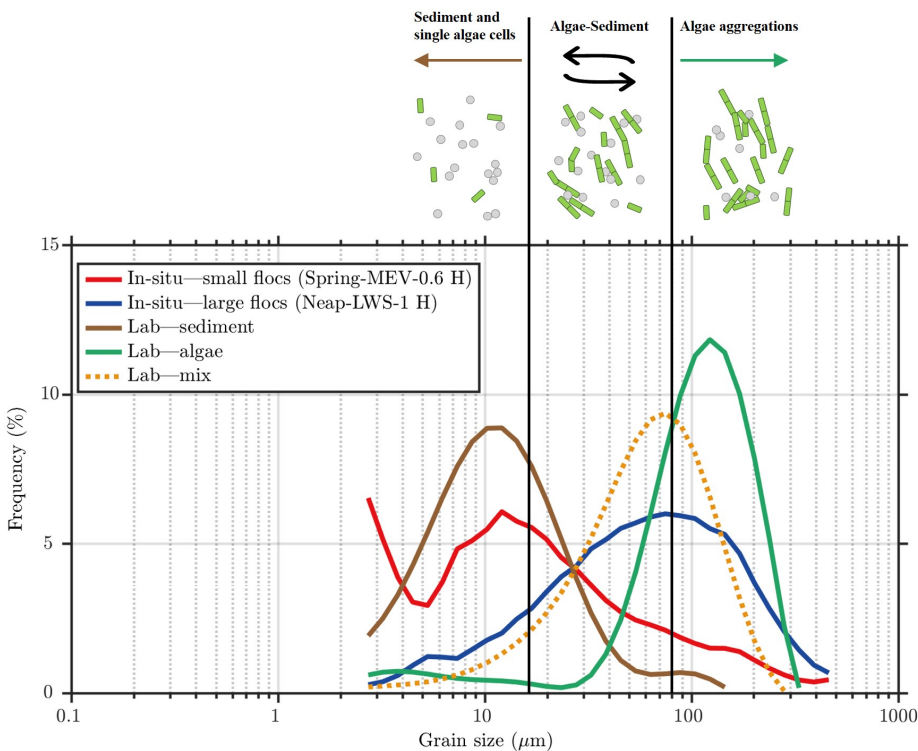


Figure 5.12: Comparison between in-situ and laboratory particle size distributions.

The peak in size of the mineral sediment taken from the bed and analysed in

the laboratory matches the peak in size corresponding to the middle fraction at spring (around 10–50  $\mu\text{m}$ ). This is consistent with the fact that at high shears, larger and denser particles (mineral sediment) can be eroded from the bed.

In the lab experiments, due to technical limitation (to avoid that particles would deposit in the pipes and at the bottom of the jar), the shear rate ( $90 \text{ s}^{-1}$ ) always larger than the in-situ shear rate ( $<60 \text{ s}^{-1}$ ). For this reason, and also because the diameter of the tubes was 6 mm it was not possible to obtain the largest floc sizes ( $> 500 \mu\text{m}$ ) observed in-situ. Nonetheless, see Figure 5.12, it can be observed that the peak in size obtained for algae at steady-state (around 200–300  $\mu\text{m}$ ) is very close to the peak for the highest particle size  $> 100 \mu\text{m}$  that is present in-situ at all depths and all times. This would tend to prove that this large particles in-situ are flocculated algae particles that have reached an equilibrium size.

The broad peak in size observed at LWS, for both spring and neap, at the bottom the water column (0.6H–1H) lays in the range 50–200  $\mu\text{m}$  and is in good agreement with the steady-state peak observed in the lab for  $\text{CC/SSC} = 1.8 \mu\text{g g}^{-1}$ . This  $\text{CC/SSC}$  is of the same order of magnitude than the  $\text{CC/SSC}$  ratio obtained in-situ (see Table 5.1). This would tend to prove that the particles corresponding to this in-situ peak are a mixture of algae and sediment. From the result found in 5.4.2 it is expected that for a lower  $\text{CC/SSC}$  ratio this peak in size would shift towards smaller sizes. This is indeed observed for the PSD's displayed in Figure 5.5, see also Table 5.1. The  $\text{CC/SSC}$  ratio at spring MFV and MEV is 1.2 and  $1.5 \mu\text{g g}^{-1}$ , where the  $D_{50}$  is 17 and 23  $\mu\text{m}$ , and it is 5.5 and  $3.5 \mu\text{g g}^{-1}$  at neap HWS and LWS where the  $D_{50}$  is 54 and 50  $\mu\text{m}$ .

## 5.6. Conclusions

By combining the analysis of in-situ data and laboratory experiments, it was found that the presence of algae (the species *Skeletonema costatum* was used for laboratory experiments as being representative for the dominant species in-situ) plays a major role in explaining the particle size distributions, and in particular the multimodal distribution observed in the Changjiang estuary. Three particle classes have been defined, corresponding to peaks in size observed in the particle size distributions: (1) particles smaller than 5  $\mu\text{m}$  (2) particles in the range 10–50  $\mu\text{m}$  and (3) particles in the range larger than 100  $\mu\text{m}$ . The algae was found in the whole water column, for any tidal condition, as chlorophyll concentration (a proxy for the algae concentration), CC, could

be measured at any depth. The suspended sediment concentration (SSC) was linearly linked to the CC which led us to study the CC/SSC ratio as function of shear, particle size and position in the water column. The discussion in section 5.5 can be summarized in a conceptual figure (Figure 5.13), where we divide the suspended sediment into three types: (mineral) sediment dominated, sediment-algae and algae dominated. All three types are present in the Changjiang estuary.

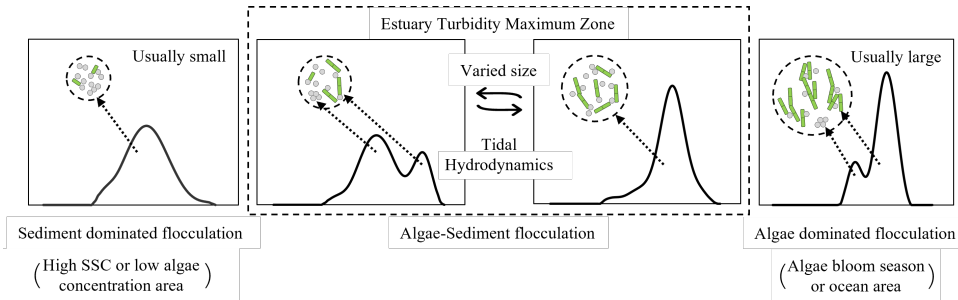


Figure 5.13: Schematic representation of algae-sediment flocculation in the Changjiang estuary.

In the absence of algae, sediment particles can flocculate due to the presence of salt but this flocculation will happen in the fresh to salt water transition region of the estuary. As demonstrated in the laboratory experiments, there will be no further flocculation of sediment flocs in saline water. The size of mineral sediment particles can be small ( $<5 \mu\text{m}$ ) as found at maximum velocities (see Figure 5.5), but there can also be a significant amount of mineral sediment in larger flocs ( $10 \mu\text{m}$  peak in Spring-MEV, see Figure 5.12) at high shears.

The primary algae cells, on the other hand, can easily flocculate with themselves, also in saline conditions as demonstrated in the laboratory experiments and this type of flocculation occurs in-situ, leading to the presence of large ( $> 100 \mu\text{m}$ ) flocs in the whole water column, at any hydrodynamic condition. The size of algae flocs (usually large) will depend on the algae species and the climate conditions. In the laboratory we demonstrated that the algae *Skeletonema costatum* has a dynamic particle size, as, in time, the algae cells flocculate or divide, creating larger particles. When mineral sediment and *Skeletonema costatum* are mixed together in the laboratory, the PSD changed rapidly from a bimodal PSD to a monomodal PSD. The  $D_{50}$  of this monomodal PSD (corresponding roughly to the in-situ middle peak size  $10\text{--}50 \mu\text{m}$  which is also in good approximation equal to the in-situ  $D_{50}$ ) is a function of the algae to sediment CC/SSC

ratio : the  $D_{50}$  is larger for a larger CC/SSC. In fact, from the laboratory experiments, we found that the presence of sediment is the limiting growth factor. The algae flocs are largest in the absence of sediment, and the more sediment (relative to the concentration of algae), the smaller the flocs.

In the Estuary Turbidity Maximum (ETM) Zone studied in the present article, depending on the tidal period, the shear stresses and the position in the water column, different particle size distributions were observed. These distributions ranged from small monomodal size peaks (sediment and single algae cells) to large monomodal size peaks (algae flocs), but with a predominance of monomodal and bimodal size peaks corresponding to sediment-algae flocs. Bimodal size distributions were also observed in the laboratory experiments for sediment-algae mixtures, but only at short times, as the optimized mixing of sediment and algae in the jar quickly led to a monomodal equilibrium particle size.

This leads us to conclude, in view of the hypothesis 1 and 3 given in the introduction, that in the ETM zone:

- there are two types of particles (sediment and algae), that most probably the large algae flocs ( $> 100 \mu\text{m}$ ) have been formed in a region devoid of sediment particles and the lowest size fraction ( $< 5 \mu\text{m}$ ) is composed of sediment particles eroded from the bed at high shears.

- the PSD's are usually not fully at steady-state as the middle size fraction (10–50  $\mu\text{m}$ ) is shifting in size according to shear and position in the water column. This middle size fraction is composed of sediment and algae particles and their relative amount is depending on the hydrodynamic condition and position in the water column.

Regarding the modelling of sediment-algae suspensions in the Changjiang estuary, all three particle sizes should be accounted for. A key parameter for predicting the position of the middle size peak is the CC/SSC ratio.

# 6

## Seasonal variation of floc population influenced by the presence of algae in the Changjiang (Yangtze River) Estuary

*He who would search for pearls must dive below.*

John Dryden

## Abstract

The variation of the floc population in the Changjiang Estuary has been studied for both winter and summer season as a function of the presence of living (micro)algae. The influence of algae has been characterized through the use of the chlorophyll concentration to suspended sediment concentration (CC/SSC) ratio. Two whole tidal cycle sampling campaigns were carried out and a full set of parameters (particle size distribution, particle concentration, salinity, velocities, chlorophyll concentration) was recorded as function of time for 6 vertical depths. It is found that the floc population can be described by three particle classes. The two most dynamic classes (microflocs and macroflocs) co-exist in the water column. It was nonetheless found, due to the correlation between CC/SSC and particle sizes that the system is at steady state, both in summer and in winter. This can be explained by the limited flocculation ability between the classes due to their segregation in the water column. In winter, macroflocs are found at the top of the water column but their amount and size are very reduced with a mean CC/SSC value of  $13 \pm 11 \mu\text{g g}^{-1}$ . In summer, algae-rich macroflocs are abundant at the top of the water column with a mean CC/SSC value of  $21 \pm 18 \mu\text{g g}^{-1}$ , especially at flood tide. Microflocs, on the other hand, have a higher density and are generally found deeper in the water column. At high water slack, both macroflocs and microflocs will settle but will never catch-up. The fact that the flocs are at steady-state in terms of flocculation is of importance for sediment transport modelling.

The contents of this chapter have been published in the article:

**Z. Deng, Q. He, C. Chassagne, Z. B. Wang**, *Seasonal variation of floc population influenced by the presence of algae in the Changjiang (Yangtze River) Estuary*, *Marine Geology*, 106600, 440 (2021).

## 6.1. Introduction

Flocculation of fine sediment particles, resulting in time and space-dependent settling velocities, plays an important role in the fine sediment dynamics in estuaries [van Leussen, 1988]. A large number of studies have been devoted to study flocculation, by field observations [Alldredge & Gotschalk, 1989, Braithwaite et al., 2010, Fennessy & Dyer, 1996, Guo et al., 2017, Li et al., 2017], laboratory measurements [Guan et al., 1996, Manning & Dyer, 1999, Wan et al., 2015] and modelling [Khelifa & Hill, 2006,

Mietta et al., 2011, Winterwerp, 1998].

Many factors can influence sediment flocculation and studies have concentrated on the influence of shear rate [Keyvani & Strom, 2014, Manning & Dyer, 1999], SSC and salinity [Eisma & Irion, 1993, Fettweis et al., 2010, 2007, Karbassi et al., 2014, Manning et al., 2010a,b, Mietta et al., 2009a, Pérez et al., 2016, van Kessel et al., 2011]. It has long been recognized that in natural environments, organic matter is always part of flocs [Eisma et al., 1991]. In that review article, the authors confirm that the kinetics for flocculation are related to the tidal cycle, and that microscope observations have shown that flocs consist of mineral particles held together by organic matter (organic matter with or without hard parts of organisms). They state that in west-European estuaries there is no evidence for an influence of salinity on in situ floc size distributions. A same result was found for our site of interest, i.e. the Changjiang Estuary [Guo et al., 2017] and the Seine estuary [Verney et al., 2009]. As salt-induced flocculation is a slow process it will only be dominant in the case that no other flocculating agent is present (like polyelectrolytes, stemming from industry or produced by microorganisms) [Mietta et al., 2009a,b]. Salinity can however influence the binding of organic matter to mineral clay [Wilkinson et al., 2017].

Polyelectrolytes like Extracellular Polymeric Substances (EPS) have been shown to drive flocculation [Droppo, 2001, Furukawa et al., 2014, Lee et al., 2017, Paterson & Hagerthey, 2001, Tolhurst et al., 2002, Uncles et al., 2010]. EPS primarily consists of carbohydrates, proteins, nucleic acids, and polymers, which can absorb fine sediment particles and change their surface property [Ni et al., 2009, Sheng & Yu, 2006]. When we refer to algae-induced flocculation in this article, it is implied that EPS-induced flocculation (whereby the algae can produce EPS) is also accounted for. There is a strong correlation between algae bloom season and flocculation, when higher temperature and higher light intensity promote algae activity and EPS secretion enhance sediment particles flocculation [Chen et al., 2005, Fettweis & Baeye, 2015, Lee et al., 2017, Shen et al., 2018, van der Lee, 2000]. Most research associated to algae effects usually focus on the algae bloom season (spring season, from March to June). We wanted to investigate the role of algae in different seasons (summer and winter). One of the purposes of the present article is to compare floc size distribution in summer and winter, related to microalgae content of the flocs.

Most studies also rely on observations made using instrument at a fixed position

above bed. In our study, we performed measurements as function of both depth and time in order to highlight the vertical variation in particle distributions and their composition in terms of algae content.

In our previous study, realized in summer [Deng et al., 2019], we already found that the living microorganisms (algae) have a specific influence on flocculation in summer, outside the algae bloom season, as function of different hydrodynamics conditions and position in the water column. It was shown that the algae particles could participate in the flocculation process and a key parameter—the sediment to chlorophyll concentrations ratio (CC/SSC)—was introduced that reflected the dependence of flocculation on algae concentration. In particular, it was concluded from the study that large algae flocs ( $> 100 \mu\text{m}$ ) were formed in a region devoid of sediment particles whereas the lowest size fraction ( $< 5 \mu\text{m}$ ) is composed of sediment particles eroded from the bed at high shear. The particle size distribution (PSD) but also composition in the water column is therefore dynamic and changes with depth and hydrodynamic conditions. As sediment transport models are relying on estimation of the particle density (to assess their settling velocity), it is important to study the variations of floc properties in space and time.

In the present study, we compare the algae influence on flocculation in different seasonal conditions (summer and winter), and show how the floc properties such as effect density and settling velocity are changing with the seasons. Most of sediment accretion occurs in the flood season (summer) while erosion occurs in the dry season (winter) in the Estuary Turbidity Maximum (ETM) area of Changjiang Estuary [Li et al., 2018]. It will therefore be interesting to compare the dependence of CC/SSC ratio on shear, particle size and position in the water column in winter and in summer. Typical questions we like to answer are:

–How is the floc size evolving as function of season and tidal cycle in the whole water column?

–How are floc properties (size, effective density, settling velocity) linked with algae-sediment ratio?

## Study site

Two whole tidal cycle sampling programs were carried out from 10<sup>th</sup> to 11<sup>th</sup> of January 2014 and 25<sup>th</sup> to 26<sup>th</sup> of July 2016 on a ship in the South passage of Changjiang

Estuary (Figure 6.1), which is located in East China. There were no storms in the short period before the observations. For more details, please see chapter 3.

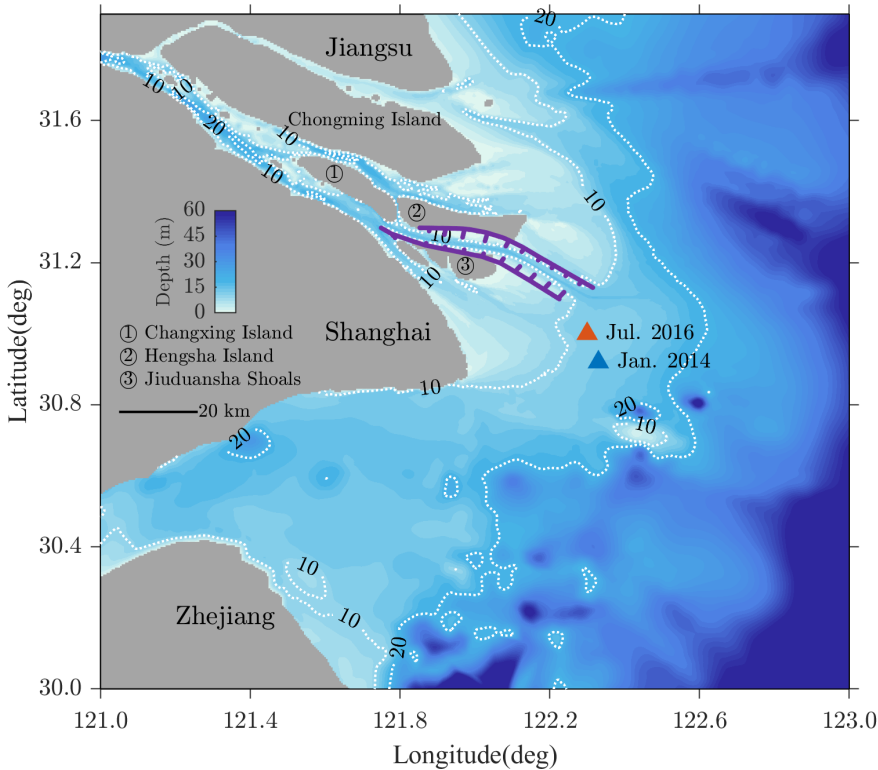


Figure 6.1: Map of the morphology of the Changjiang estuary and the study sites in summer (July in 2016) and winter (January in 2014).

## 6.2. Seasonal variations

Each of the two surveys started from flood tide to ebb tide, lasted for 13 hours, and included a whole tidal cycle with four periods: Low Water Slack (LWS), Maximum Flood Velocity (MFV), High Water Slack (HWS) and Maximum Ebb Velocity (MEV).

The water depths as function of time demonstrated the tidal asymmetry that the flood periods are about 4 hours while the ebb periods are about 6 hours both in winter and summer surveys. Because the observation station was further away from the coast

in winter, the water depth in winter (11–12.5 m) was deeper than in summer (7.5–11 m). The water depth variation amplitudes in winter were smaller than in summer. The tidal range in winter was smaller than in summer, which means that the hydrodynamics in winter are less energetic. This was also reflected in the shear rate (Figure 6.2a, b). The shear rate ranged from 0.1–20 s<sup>-1</sup> in winter, and from 0.4–50 s<sup>-1</sup> in summer. The shear rate in summer was always higher than in winter for the same tidal period. In addition, the shear rates remained at a high value at flood period and ebb period. The SSC correlated with shear rate both in winter and summer surveys. The maximum SSC usually appeared at the high shear rate periods (MFV and MEV). Although the SSC in bottom water was lower during the summer survey than during the winter survey, the SSC in upper water was higher than during the winter survey (> 0.05 g l<sup>-1</sup>).

The salinity in winter was higher than in summer because of a smaller river discharge in winter (Figure 6.2c, d). The salinity in winter ranged from 18.5 to 27.3 PSU (it increased with rising tide), which means that the water column was mainly affected by sea water. The salinity ranged in summer from 4.8 to 22.0 PSU meaning that the water column was always affected by both fresh and sea water. The vertical gradient of salinity indicated different stratifications in winter and summer: water is better mixed in winter than in summer. The stratification corresponded with high CC/SSC in summer at the top of the water column, probably due to favorable algae growth conditions during that period. These flocs are mainly advected from the sea at flood tide [Zhao & Gao, 2019].

The temperature in winter (7–10 °C) was lower than in summer (25–29 °C) (Figure 6.2e, f). The salinity is shown to correlate with the water density for both the winter and the summer survey period: a high salinity corresponds to a high water density and vice-versa. There is no correlation between SSC and water density as there is no correlation between SSC and salinity, a feature that was already observed in diverse estuaries worldwide and this estuary in particular [Eisma et al., 1991, Guo et al., 2017].

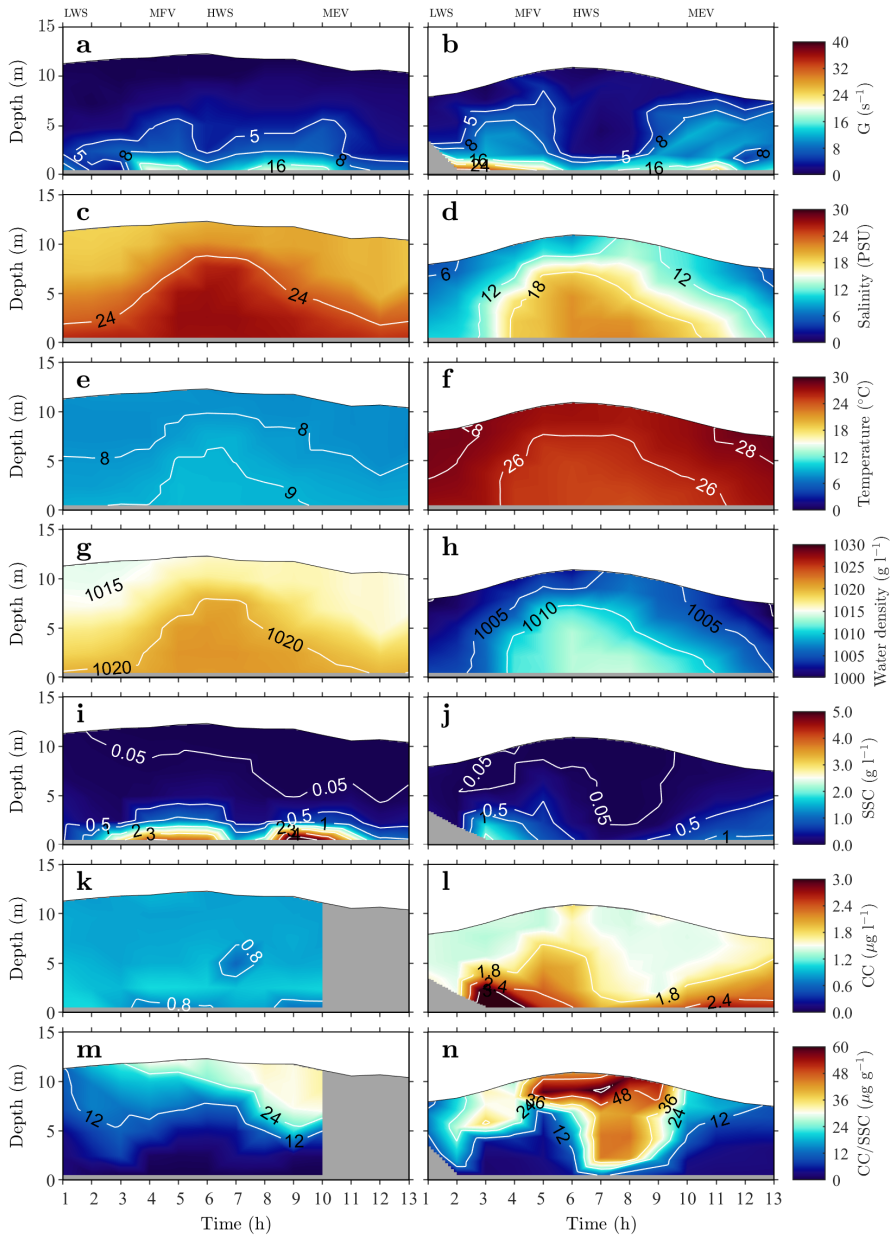


Figure 6.2: Vertical distribution of shear stress (a, b), salinity (c, d), Temperature (e, f), water density (g, h), sediment concentration (i, j), chlorophyll concentration (k, l) and algae-sediment ratio (m, n).

(Left: 2014-01 winter season, Right: 2016-07 summer season.

LWS: 1–2 h, MFV: 4–5 h, HWS: 6–7 h, MEV: 10–11 h)

### 6.3. Mean flocculation properties in winter and in summer surveys

In Figure 6.3 it is shown that the median flocculation size ( $D_{50}$ ) in winter (13–65  $\mu\text{m}$ ) is smaller than in summer (13–359  $\mu\text{m}$ ). Studies in the same area have shown that Particulate Organic Carbon (POC) correlates positively with chlorophyll, and that the amount of POC is reduced in winter as compared to summer [Zhao & Gao, 2019]. This is in line with the results presented in Figure 6.2k, l, where the CC is lower in winter as compared to summer. Flocculation induced by particulate organic matter (as represented by POC) is therefore reduced in winter. Floccs of higher size can only be observed if their effective density is low enough so that their residence time in the water column is significant—this can only be achieved if floccs contain a substantial amount of algae.

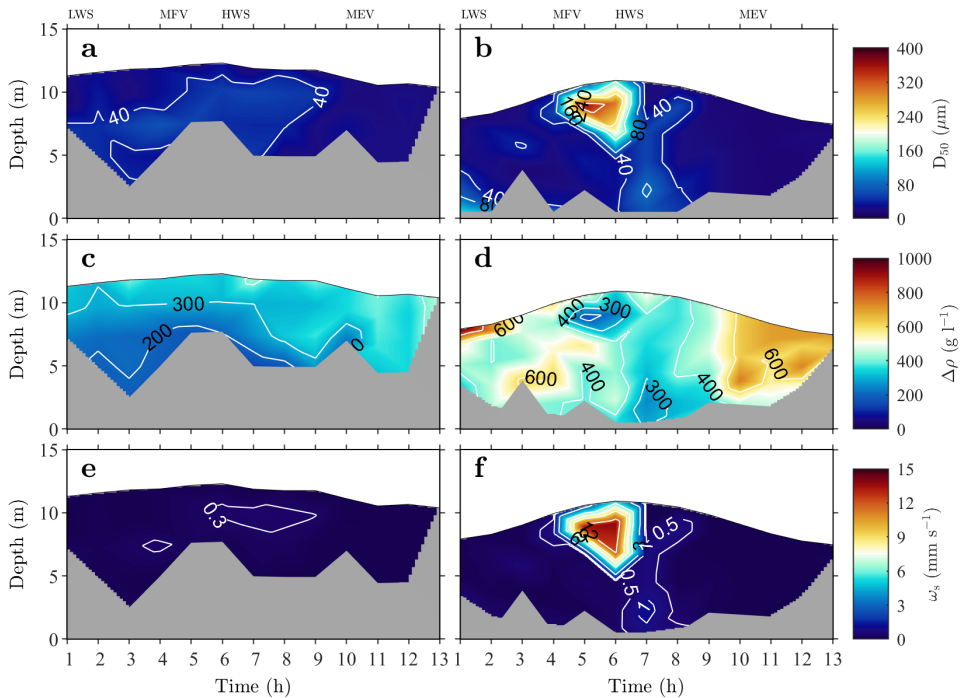


Figure 6.3: Vertical distribution of mean flocculation size (a, b), effective density (c, d) and settling (e, f) velocity.  
(Left: 2014-01 winter season, Right: 2016-07 summer season, LWS: 1–2 h, MFV: 4–5 h, HWS: 6–7 h, MEV: 10–11 h)

The effective floc density map shows that large particles are found in the upper layer, especially at HWS. These particles have a higher settling velocity than other particles found at the same time in the water column, but have a similar density. Particles of higher density are found (in all layers) when the shear rate is higher than in other periods (both around 8–12 h in winter and in summer). The mean floc size has a positive correlation with effective density in summer: large flocs usually have a smaller density, and vice versa. This is better represented in Figure 6.4. This result is consistent with many other studies where the relation between density and size is an exponentially decreasing function [Manning et al., 2006, Manning & Dyer, 1999, Mikkelsen et al., 2007]. The mean effective density of flocs in winter appears to be a little smaller in winter than that in summer. This is counter-intuitive if one assumes that flocs in summer are composed of more algae than in winter (which is confirmed by comparing the CC/SSC ratio in both seasons). However, as discussed in the previous section, the shear rates were overall higher in summer than in winter. This has two effects:

1—the high shear rate in summer leads to more sediment resuspension during MFV, whereby this sediment is flocculated by biological agents (EPS secreted by algae). Even silt-size particles could be trapped in these flocculated structures, leading to flocs with higher density. These flocs even reach the surface water (except for HWS periods), see section 6.4.2. As is shown in Figure 6.8, the sediment that is in surface water in winter contains more clay-size particles than in summer, which is due to both lower shear rates and lower organic material content in that season compared to summer.

2—There can be a reformation of flocs under shear (a reduction in volume while sediment mass is preserved) resulting in a higher density in summer [Guo, 2018, Sterling et al., 2004, Verney et al., 2009, Winterwerp, 1998]. This hypothesis is debatable as reformation is depending strongly on residence time and the nature of the organic matter that composes the floc. The composition of organic matter is known to be different in summer and winter [Hart et al., 1990, Morrissey et al., 2014]. The organic matter in summer is usually composed of living algae and their EPS, which can capture effectively mineral sediment particles, leading to higher particle density than in winter. In winter the organic matter is scarce and usually composed of debris and dead organic matter or EPS [Craig et al., 1989, Grey et al., 2001].

The settling velocity is positively correlated with  $D_{50}$  and large flocs have a larger settling velocity than small flocs; this is to be expected since the settling velocity is de-

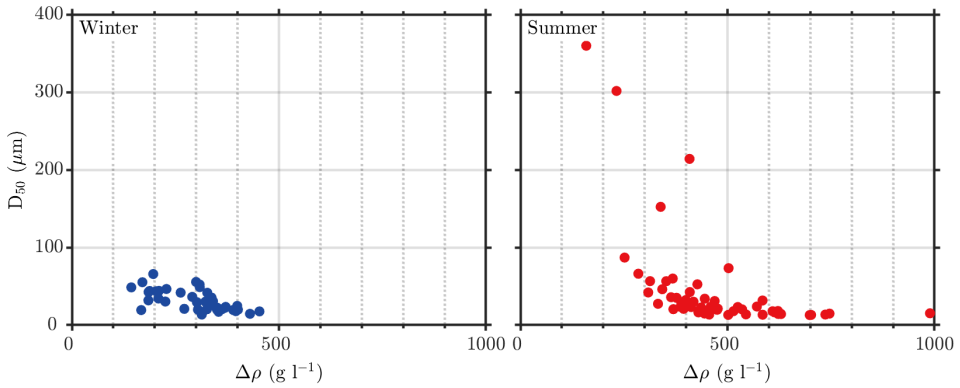


Figure 6.4: Correlation between effective density with mean floc size.

pending on the particle size squared, whereas it is only linearly correlated with density, see Eq. (3.11) and that density is within the limited range 140–990  $\text{g l}^{-1}$ .

6

### 6.3.1. Variations with shear rate, salinity and SSC

In the Changjiang Estuary, the correlations between  $D_{50}$  and salinity/SSC are poor. In addition, the shear rate displays an overall negative relationship with  $D_{50}$ , that is, large flocs usually appear at low shear rate periods (HWS), but the coefficient of determination is poor ( $R^2 < 0.5$ ) both in winter and summer. These poor correlations are in line with previous studies [Deng et al., 2019, Guo et al., 2017].

Table 6.1 shows the variations of floc properties and velocity, salinity and SSC in winter and summer, and comparisons to other results of North Passage (NP) in Changjiang Estuary in summer season [Guo et al., 2017]. The main difference was that there were larger flocs ( $> 100 \mu\text{m}$ ) in summer in the South Passage (SP) compared to the North Passage, especially in surface water, this can be seen by comparing Figure 6.3 with Fig.2 in Guo et al. [2017]. As the study area chosen in the South Passage was closer to the sea, the salinity was overall higher and the shear rate lower than in Guo et al. [2017].

### 6.3.2. Variation with CC and CC/SSC in the tidal cycle

The chlorophyll concentration (CC) was relatively uniform over the whole water depth with a mean value of  $0.9 \pm 0.1 \mu\text{g l}^{-1}$  ( $0.6\text{--}1.0 \mu\text{g l}^{-1}$ ) in winter and it was more

Table 6.1: Characteristics of flocs and velocity, salinity, SSC, CC and CC/SSC in the South Passage (winter and summer) and North Passage (summer)

Parameters	Winter	Summer	NP*
Floc size $D_{50}$ ( $\mu\text{m}$ )	32±13	45±64	43±10
Density $\Delta\rho$ ( $\text{g l}^{-1}$ )	143–453	159–989	60–450
Settling $\omega_s$ ( $\text{mm s}^{-1}$ )	0.02–0.4	0.05–14	0.08–0.3
Current Velocity ( $\text{m s}^{-1}$ )	0.5±0.2	0.9±0.4	1.4
Salinity (PSU)	18.5–27.3	4.8–22.0	2–11
SSC ( $\text{g l}^{-1}$ )	0.6±1.2	0.3±0.4	0.24±0.12
CC ( $\mu\text{g l}^{-1}$ )	0.9±0.1	1.8±0.5	-
CC/SSC ( $\mu\text{g g}^{-1}$ )	13±11	21±18	-

\* Data from Guo et al. [2017].

stratified with higher concentrations towards the bed with a mean value of  $1.5\pm 0.5 \mu\text{g l}^{-1}$  in summer ( $1.3\text{--}3.7 \mu\text{g l}^{-1}$ ). It was observed that the CC in the bottom water is always higher than at the surface (also in winter). We will show (see Figure 6.11 and section 6.5.2) that a large amount of algae are binding to mineral clay by differential settling during the HWS period. This leads to an accumulation of algae and algae debris at the bed.

The CC/SSC ratio is shown in Figure 6.2m, n. The ranges of CC/SSC were around  $0.1\text{--}33.2 \mu\text{g g}^{-1}$  in winter and  $1.5\text{--}61.6 \mu\text{g g}^{-1}$  in summer, the higher values in upper water layer can reflect the vertical variation of algae activities. The correlation of CC with SSC in summer was already discussed in [Deng et al., 2019]. Even though the dataset presented here is of another summer (2015 in Deng et al. [2019] and 2016 in the present article), we found that the same conclusions hold. The CC/SSC ratio plot illustrates that the algae percentage is higher in surface water, reflect that the algae (CC) is not always distribute with sediment (SSC), they tend to stay in surface water, due to their buoyancy or phototaxis. From Figure 6.2m, n, one finds that a threshold value for CC/SSC is around  $10\text{--}20 \mu\text{g g}^{-1}$ . Above this value, it is expected that flocs will be predominantly governed by the organic matter (algae), as bimodal PSD are found. These type of flocs are found at the top of the water column where algae can benefit from photosynthesis [Reynolds, 2006]. During the summer survey the algae-dominated

flocs start to populate the whole water column in the period HWS to ebb tide. At low hydrodynamic activity the buoyant algae particles in the water column are less likely to flocculate with mineral sediment particles which will be predominantly found at the bottom of the water column.

The trends for  $D_{50}$  as function of CC/SSC are shown in Figure 6.5. As was already observed in a previous study [Deng et al., 2019], there is no correlation between  $D_{50}$  and CC/SSC in the summer period (in 2015). It is confirmed that no overall trend is observed between  $D_{50}$  and CC/SSC in summer (in 2016), nor in winter. There is however a marked increase in  $D_{50}$  with CC/SSC ratio corresponding with low density particles at 5–6 h in summer 2016, which indicates that the algae play a significant role in large flocs formation during flood tide, when a lot of algae particles are imported from the seaside. The details of algae effects on floc PSDs will be discussed in section 6.4 and 6.5.

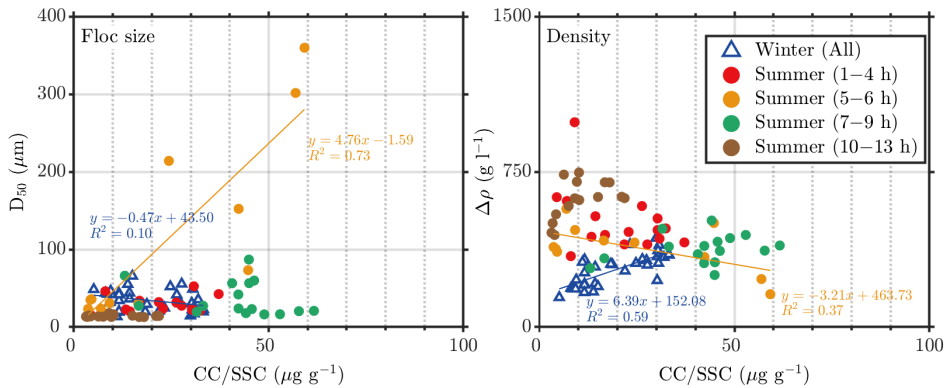


Figure 6.5:  $D_{50}$  and effective density as function of CC/SSC for winter and summer conditions.

The density is better correlated with CC/SSC as can be seen in the Figure 6.5. The decreasing trend observed in summer can be understood as a higher CC/SSC is then linked to a higher CC and therefore a lower density (as in summer, SSC is relatively constant over the whole water column, see Figure 6.2j). A higher CC/SSC ratio in winter corresponds to a lower SSC (as in winter, CC is relatively constant over the whole water column, see Figure 6.2k), but as in winter there is a very low CC and SSC, the correlation between density and CC/SSC is not to be trusted. The density is nonetheless much lower than in summer for the same CC/SSC. We will come back to

this point in section 6.4.2.

## 6.4. Particle Size Distributions (PSDs) in winter and summer surveys

Large flocs usually form at the upper part of the water column between MFV and HWS both in winter and summer (Figure 6.3a, b). The vertical variation of flocs PSDs is however different in winter and summer when one takes a closer look at the PSDs at different layers, see Figure 6.6. Flocs are usually smaller in surface water (0H) than in middle water (0.4H) in winter at LWS (2 h) and MFV (4 h) whereas they are small in summer for these periods. This implies that the flocculation processes are different in winter and summer. Large flocs are hardly formed in summer in LWS (2 h), due to higher shear rates. Large flocs are formed at low shear rate both in winter and summer at HWS (6 h). In particular, large flocs can be form in the middle and surface water in summer HWS. This phenomenon will be discussed in the following section.

### 6.4.1. Variation within the tidal cycle

The PSD in winter at MFV is different from the other periods: at MFV the larger peak of the PSD is found at 150  $\mu\text{m}$ , whereas at the other periods it is around 20  $\mu\text{m}$ . This behavior can be ascribed to small sand particles that are eroded during maximum currents. In comparison, during summer, the bed is more stabilized because of the presence of EPS and thus no large peak in MFV is observed. The largest peak in summer is always around 20  $\mu\text{m}$  at LWS, MFV and MEV, however a second peak, around 100  $\mu\text{m}$ , is distinguishable in three figures indicating the presence of particles in that size range. This confirms the fact that in summer more organic particles, at all depths, are present. At HWS (6 h), two PSDs are observed. Between [0H–0.6H], the PSD peaks at about 20  $\mu\text{m}$  (with the peak having an asymmetric shape towards the highest sizes—again indicating the presence of larger particles). Between [0.6H–1H] the PSD peaks at 30–50  $\mu\text{m}$  and does not display any large PSD asymmetry, but a significant amount particles in the range 100–400  $\mu\text{m}$ . This transition seems to be in line with the change in salinity at HWS: clay-algae particles are probably trapped under the pycnocline (see Figure 6.3j) whereas algae-rich particles are located above (resulting in a large CC/SSC ratio, see Figure 6.3i). This trapping mechanism has also been reported by other authors

[Lee et al., 2016, Ren & Wu, 2014, Yao et al., 2016]. The evolution of the PSD around the changes in salinity gradients is shown in more details in Figure 6.7, reflecting the very dynamic PSD's around HWS.

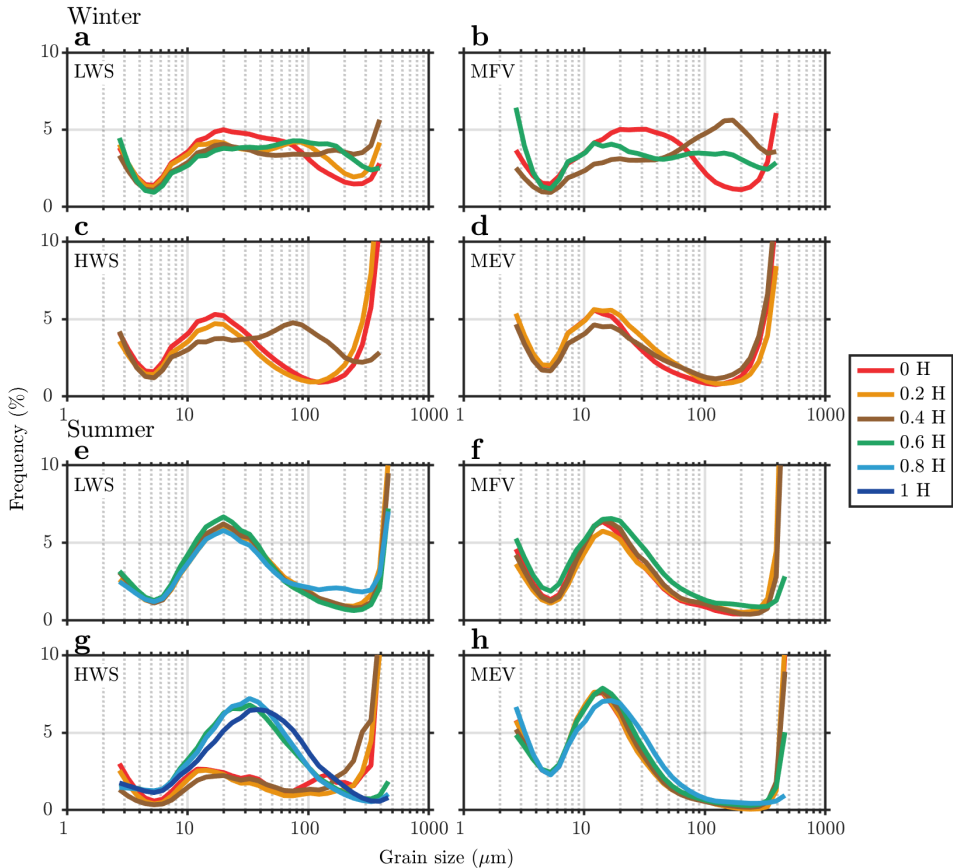


Figure 6.6: Vertical variations of floc size distribution measured by LISST in different tidal phases, at neap tide. The measurements are presented for LWS (2 h), MFV (4 h), HWS (6 h) and MEV (10 h).

#### 6.4.2. Particle characteristics at the top of the water column

The PSD of the particles collected at the top of the water column (in the surface water) was further investigated by comparing the PSD measured in-situ and the PSD obtained in the laboratory on samples treated so as to remove organic matter. These laboratory samples are labelled “primary particles” (pp. in short). The results are presented in Figure 6.8. It is found that primary particles in summer ( $D_{50} = 6 \mu\text{m}$ ) have

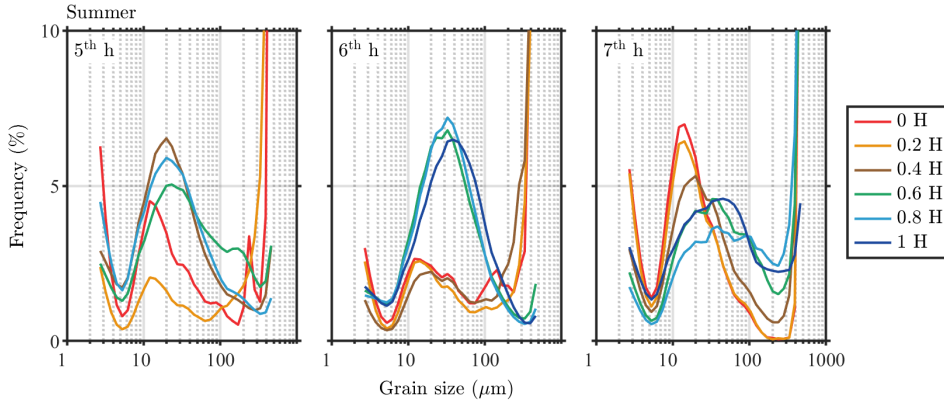


Figure 6.7: Vertical variations of flocs PSDs in summer during the period 5–7 hours.

the same mean size than in winter ( $D_{50} = 5 \mu\text{m}$ ).

The PSD of the treated samples from the winter survey displays the presence of more fine clay-size particles ( $< 1 \mu\text{m}$ ) than in the samples from the summer survey. The difference can be explained by the fact that in summer fine particles are more likely to be captured by organic matter and hence be found at deeper depths. In winter fine particles (devoid of organic material) can populate the whole water column. This very fine material cannot properly be recorded by LISST, as the lower size range of the LISST is  $2 \mu\text{m}$ . A remarkable amount of large particles are found in the surface water in-situ, both in summer and winter. These particles are usually not expected to be found in surface waters if they are pure mineral particles (with a density close to  $2600 \text{ g l}^{-1}$ ). We nonetheless found, after treating the summer samples so as to remove organic matter, that large particles can still be found (see Figure 6.8, summer, dashed lines). The nature of these particles is not known, they might be skeletons of diatoms. Particles were monitored by LISST and OBS, from which particle densities were deduced using Eq. (3.10). As LISST cannot properly measured the fine material in the size range ( $< 2 \mu\text{m}$ ) and that a significant amount of fine particles in that size range is found in suspension in winter, the estimation of the density is biased. This results in the fact that flocs in summer appear to have a higher density than flocs formed in winter as discussed at the end of section 6.3.2.

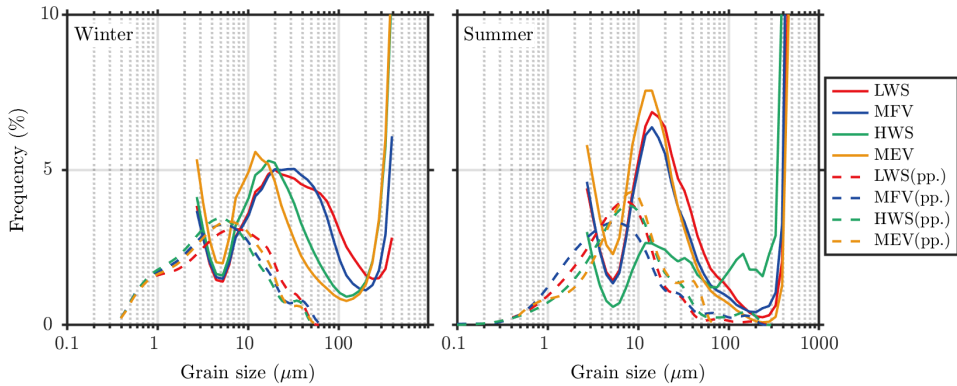


Figure 6.8: Surface water size distribution of both dispersed (“pp”, i.e. measured in the lab after deflocculation) and flocculated particles (as measured in-situ) in different tidal phases.

## 6.5. Floc classes

Following what other authors do, we subdivided the PSD into 3 classes: single-grain: particles of size  $< 5 \mu\text{m}$ , microflocs: particles of size  $> 5 \mu\text{m}$  and size  $< 200 \mu\text{m}$  and macroflocs of size  $> 200 \mu\text{m}$  [Mikkelsen et al., 2006]. It is expected, in light of the discussion in the previous sections, that single-grain particles are predominantly mineral based, macroflocs are composed in majority of organic material and microflocs are a combination of mineral sediment and algae.

### 6.5.1. Variation with CC/SSC

No correlation was found between CC/SSC and the  $D_{50}$  estimated from the whole PSD's. We here study the dependence of the  $D_{50}$  of each size class. The  $D_{50}$  of each class  $D_{50}$  as function of CC/SSC is given in Figure 6.9. From the figure, it can be seen that there is a correlation between  $D_{50}$  and CC/SSC:  $D_{50}$  of microflocs is decreasing with CC/SSC whereas the  $D_{50}$  of macroflocs is increasing. The volume-% of microflocs/macroflocs also display a clear trend with CC/SSC: the higher the CC/SSC, the more macroflocs are present in the water column. It was furthermore verified (not shown) that the relative volume-% of macroflocs is decreasing with SSC. This is in line with the laboratory tests performed in Deng et al. [2019], where it was shown that the CC/SSC ratio is driving the steady-state size of the flocs: at higher CC/SSC ratio, larger flocs are obtained, irrespective of the amount of sediment or flocculant in presence. Al-

gae sediment flocculation reaches a steady-state within 30 min in jar test experiments [Deng et al., 2019], for a large range of SSC (0.07–0.7 g l<sup>-1</sup>) and a high shear rate (90 s<sup>-1</sup>). This would hint to the fact that micro and macroflocs are (on average) at proper conditions that large flocs can be formed in HWS of summer, due to the HWS periods last about 2 hours with low shear rate.

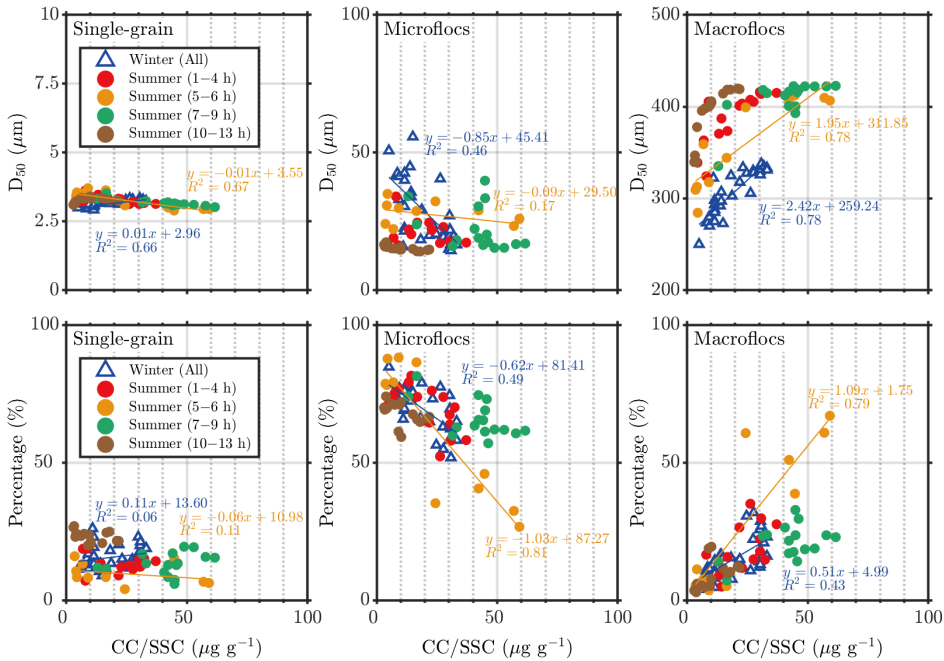


Figure 6.9: Relationship between the mean size  $D_{50}$  and volume-% of each class with CC/SSC.

### 6.5.2. Transfer between classes

In sediment transport modelling, like in numerical programs such as TELEMAC [Blumberg et al., 1996, Blumberg & Mellor, 1987], DELFT3D [Lesser et al., 2004, 2000] or ECOMSED [Sherwood et al., 2018], two or three classes of particles are usually defined that are associated with a concentration and a settling velocity. In the present article, we like to discuss the spatial and temporal variation of the concentrations of the classes in terms of the relative volume fraction of these classes that can be obtained from LISST data.

In section 6.5.1, it was shown that the CC/SSC ratio is correlated to the size of

the micro and macroflocs, which, as we discussed is an indication that the system is at steady-state.

Despite the fact that the system is at steady-state (in terms of flocculation), the PSD is very dynamic and shifts between unimodal and bimodal depending on hydrodynamic conditions. This shift is related to the relative volume-% of micro and macroflocs. A bimodal peak appears when the two classes (microflocs and macroflocs) have a comparable relative volume fraction (volume-%). The evolution of the volume-% of the three classes and CC/SSC are given in Figure 6.10 as function of time. The water column is divided in three: surface (0H–0.2H), middle (0.4H–0.6H) and bottom (0.8H–1H). One can see that there is a slight increasing trend in CC/SSC from 11.6 to 33.2  $\mu\text{g g}^{-1}$  in surface water while no significant trend is found in other water layers during the tidal period in winter. The CC/SSC ratio increases at flood tide in summer, at all depths (from 9 to 57.8  $\mu\text{g g}^{-1}$ ), where a relative increase of the volume-% of macroflocs compared to the volume-% microflocs can also be observed, which indicates that algae-rich particles are brought in the water column from the sea. This is coherent with the observation made by Wu [2015] who observed that the dominant species to be found at the observation station is *Skeletonema costatum* which is found predominantly in sea water.

It is well-known that algae can aggregate in large flocs at the top of the water column where they use sunlight to perform photosynthesis [Maggi & Tang, 2015, Takabayashi et al., 2006]. Subsequently, the algae-dominated flocs populate the whole water column in the period HWS to ebb tide (see Figure 6.7 and Figure 6.11), slowly sinking to the bottom of the water column. As the biomineral flocs are forming and settling, the CC/SSC ratio, which is about 50  $\mu\text{g g}^{-1}$  at depths  $> 7$  m increases below 7 m from 0 to 50  $\mu\text{g g}^{-1}$  over time. This is to be linked with the observations shown in Figure 6.2, where it was found that CC iso-lines are decreasing towards the bed over time in that time period. This implies that a significant amount of algae is reaching the seafloor, and that macroflocs are algae-dominated. It is known that algae flocs have a dynamic settling velocity, as algae can adapt their buoyancy by photosynthetically-produced oxygen, therefore the CC/SSC ratio remained high both in surface (0H) and middle water (0.4H), despite the settling of algae-based flocs [Fernández-Méndez et al., 2014].

The overall  $D_{50}$  is also changing over depth in time. At 6 h, during HWS, the

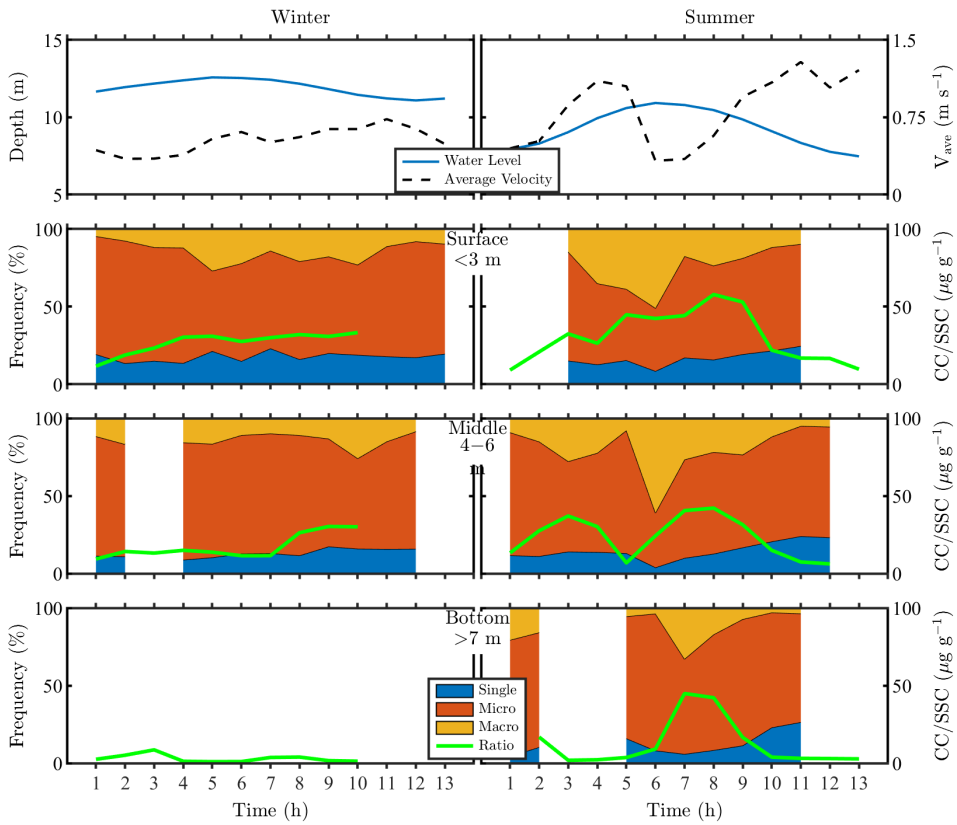


Figure 6.10: Time series of three floc fractions with CC/SSC ratio in winter and summer season in surface, middle and bottom water layers.

largest  $D_{50}$  is shifting towards the middle depth, but its value is lower than at 5 h. At 7 h, the  $D_{50}$  is small everywhere, despite the fact that macroflocs are observed in the bottom layer: as the SSC is high in the bottom layer microflocs are the most abundant type of floc present, hereby reducing the overall  $D_{50}$ . As was observed in Figure 6.6, Figure 6.7 and Figure 6.8, the PSDs remain however bimodal, confirming the presence of large particles at any depth.

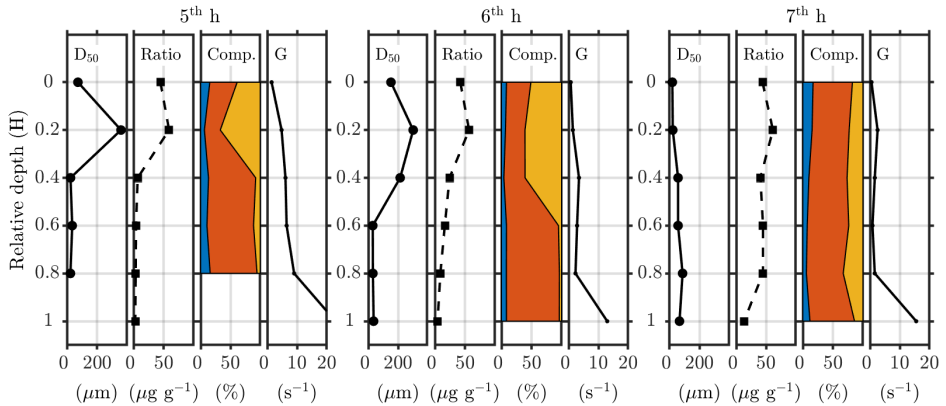


Figure 6.11: Vertical variations of  $D_{50}$ , CC/SSC ratio, floc size fractions and shear rate in summer during the period 5–7 hours.

It has been shown in [Deng et al. \[2019\]](#) that if the water column is well-mixed bimodal PSD's shift towards unimodal PSD's, as microflocs flocculate with macroflocs. This raises the question of residence in the water column, and the collision probability between micro and macroflocs. The variations in PSDs with depth in the period 5–7 hours (see Figure 6.11) was discussed above, where the clear difference between the PSDs found in the water column at [0H–0.4H] and [0.6H–1H] was attributed to the presence of a pycnocline: the residence time of algae flocs at specific depths are not only dependent on hydrodynamics but also on density—this is especially the case for algae-rich flocs which have smaller density than sediment dominated flocs. During HWS the algae flocs settle down, as do the mineral sediment particles and both have then no chance to meet as the slow settling algae flocs leaving the pycnocline do not catch-up with the faster settling sediment flocs that are found at lower depth. This can in part explain why multimodal PSDs are quite often observed in the system. Therefore, despite finding bimodal distributions, the flocculation ability between classes is very

reduced and it can be concluded that the system is in good approximation at steady-state.

## 6.6. Conclusions

In this article, the seasonal variation of particle size distributions (PSD) were studied in relation with the presence of living organic matter (algae). The presence of algae lead to both unimodal and bimodal PSDs. When the PSD is bimodal two floc fractions (microflocs and macroflocs) can clearly be distinguished. These two classes of flocs have different properties that can be studied as function of relevant parameters (shear, CC/SSC ratio, seasonality). The existence of these two classes of particles makes it therefore problematic to reduce the study of the PSD to the study of its  $D_{50}$  and it was shown that no correlation could be found between the relevant parameters (CC/SSC in particular) and  $D_{50}$ .

A clear difference is found between the winter and the summer surveys. Both the algae production and the shear are low in winter, leading to the suspension of smaller flocs with lower density than in summer (the average floc size is  $32 \pm 13 \mu\text{m}$  in winter and  $45 \pm 64 \mu\text{m}$  in summer, the range density of flocs is  $143\text{--}453 \text{ g l}^{-1}$  in winter and  $159\text{--}989 \text{ g l}^{-1}$  in summer). The flocs are composed of small amount of clay and organic particles in winter. In winter, more fine mineral sediment ( $< 2 \mu\text{m}$ ) are found at the top of the water column than in summer. In summer, the flocs are larger by two orders of magnitude and can contain both clay and silt particles, which makes them having a higher density than in winter, as in-situ monitoring techniques cannot properly assess the very fine ( $< 2 \mu\text{m}$ ) clay fraction suspended in winter. Moreover, as the shear rates were higher in summer also, close to the bottom, larger silt and sand particles could be suspended compared to winter.

A good correlation is found between the presence of algae (through the measurement of chlorophyll concentration) and the presence of large, buoyant flocs at the top of the water column in summer, where algae perform their photosynthesis. The algae appear predominantly during the flood tide period. Large flocs, i.e. macroflocs, (with high CC/SSC ratio) are then formed during the early flood period in the surface water. These flocs then settle to the middle water layer and finally reach the bottom water layer during the HWS period. At the same time, microflocs with a higher density than macroflocs are found deeper in the water column. During HWS both macroflocs and

microflocs settle down but cannot flocculate as they never catch-up due to the difference in settling rates. This is the reason why, in line with the work of Soulsby et al. [2013], who studied Northern European estuaries, it can be concluded that the floc population can be treated as if at steady state in the Changjiang Estuary. This finding is of importance for the modelling of sediment transport in this estuary, as the relative concentration of the microflocs/macroflocs populations at a given depth is then solely governed by their settling rates and local hydrodynamic conditions [Manning et al., 2011, 2010a, Spearman et al., 2011, Spencer et al., 2010].

The algae-sediment interaction in the estuarine system is shown in Figure 6.12. The key factor to study the changes in size, density and relative abundance of flocs are the CC/SSC ratio, which is related to the volume-% fraction of micro and macroflocs. The full PSD's are changing with tidal conditions and position in the water column, in line with our previous study [Deng et al., 2019]. In addition, due to the sensitivity of algae to their living environment, the floc characteristics may vary from one location to another in the estuary. For example, in our previous study, where the observation position was closer to the channel, the biological effect was weaker, and combined with a strong estuarine tidal action, the distribution of floc sizes and settling velocities were comparable during flood tide and ebb tide. In the present study the observation location was closer to the open sea, the algae activity was relatively strong, and hence a strong tidal asymmetry in floc size was observed, that is, flocs properties were clearly different at flood and ebb tide.

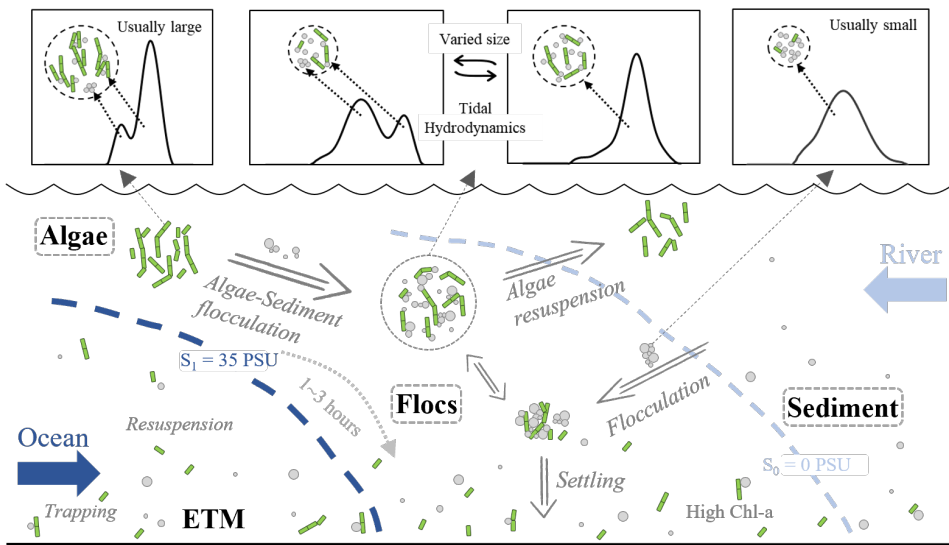


Figure 6.12: Algae-Sediment flocculation processes in estuary.



# 7

## Conclusions and recommendations

In this study, the characteristics of sediment flocculation and the process of sediment flocculation under various influencing factors were analyzed by combining laboratory experiments and in-situ observation. Detailed descriptions of the study and the conclusions have been given in Chapters 4,5 and 6. In this chapter, we provide a general overview of the conclusions. Besides, the possible applications and recommendations for future studies are also discussed.

### 7.1. Findings of this study

This study improved the knowledge about biologically influenced processes during flocculation. The flocculation mechanisms between sediment and algae are studied. Different flocculation mechanisms and processes were found by laboratory measurements and in-situ observations, demonstrating the crucial role of biology on sediment flocculation in a natural environment (Figure 7.1).

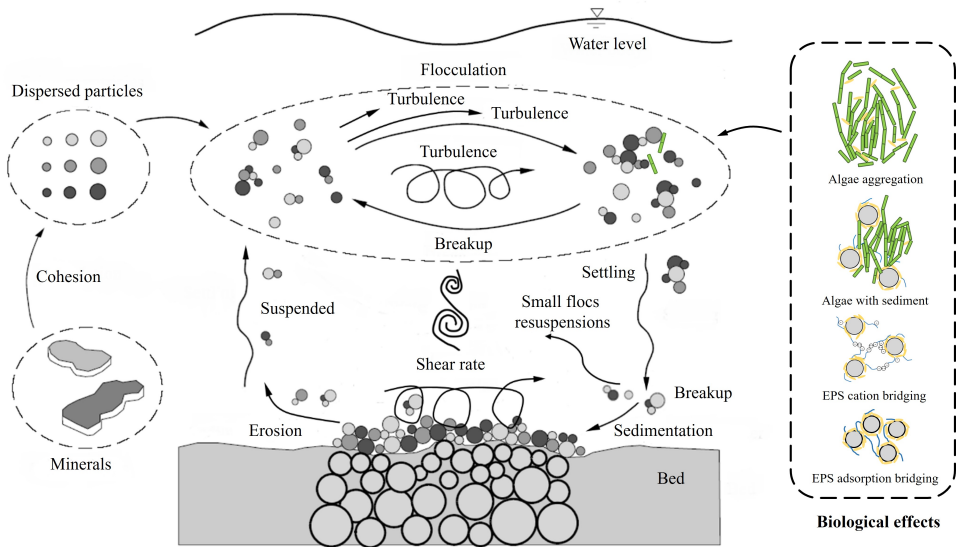


Figure 7.1: Flocculation processes with the addition of biological effects.

### Answers to the research questions:

#### 1. What are the effects of biological components (algae, EPS) and salinity on flocculation? What are the different mechanisms of algae and EPS?

In the laboratory experiment, different types of flocculation processes were identified under the effects of algae, EPS and salinity: (1) Algae particles can form large flocs by themselves, and their mean particle size can reach up to 100  $\mu\text{m}$ , which is larger than the monomer length of the microalgae *Skeletonema costatum* (about 30  $\mu\text{m}$ ). When algae and sediment particles are mixed, the floc size distribution (PSD) presents a bimodal curve, whereby the smaller peak corresponds to the sediment particle size (about 10  $\mu\text{m}$ ). The larger peak corresponds to the size of algae or algae flocs (about 100  $\mu\text{m}$ ). With the progress of flocculation, the bimodal curve gradually merged into a unimodal curve, and the overall floc size increased. The time to reach an equilibrium flocculation state was about 10 to 40 minutes, the width of the particle size distribution was between 10 to 100  $\mu\text{m}$ , and the equilibrium floc size was in the range 20–70  $\mu\text{m}$ . (2) EPS can only promote flocculation in the presence of cations. The floc size changes little with EPS in fresh water, while the effect of EPS on flocculation is remarkable in saline condition—the equilibrium particle size of flocs then increases from about 10  $\mu\text{m}$

to 40  $\mu\text{m}$ , and the flocculation time to reach equilibrium state is about 10 minutes. The flocculation rate of EPS coexisting with divalent salt ( $\text{MgCl}_2$  and  $\text{CaCl}_2$ ) or seawater is higher than that of monovalent salt ( $\text{NaCl}$ ). The flocs formed by EPS are smaller than those formed by algae. (3) Salinity alone can promote sediment flocculation, and the flocculation effect of divalent cations ( $\text{MgCl}_2$  and  $\text{CaCl}_2$ ) is larger than that of monovalent cations ( $\text{NaCl}$ ). The salt-induced flocculation rate is slow, and the time to reach the equilibrium state is long. It usually takes more than 60 minutes, and the variation of floc size is small with a slight increase in the range 10–20  $\mu\text{m}$ . The floc size formed by salinity is smaller than that caused by algae and EPS.

The effects and mechanisms of algae, EPS and salinity on flocculation are significantly different. Algae and EPS can significantly promote the flocculation of sediment, and the flocculation time is short, while salinity has a weak influence, with smaller flocs and longer flocculation time. The presence of algae changes the floc's composition, and large algae-sediment flocs are formed by the combination of algae-algae flocs with sediment particles. EPS, acts as a binder by bridging under the action of cations, and can form large flocs with high strength that withstands high shear rates. Salinity changes the electrokinetic surface charge of sediment particles. Thus the flocs are formed by the standard DLVO interaction, but these flocs are fragile and it is difficult to form large flocs under high shear rate. The three factors can of course combine to lead to the formation of flocs.

## **2. How does the algae population interact with hydrodynamics in an estuarine area? How to assess the biological parameters in natural environment?**

Both in-situ observations and laboratory experiments show an interaction between algae and sediment. In field observations, there is a significant correlation between algae concentration (CC) and suspended sediment concentration (SSC) in the studied estuarine area. In contrast to other aquatic environments where the chlorophyll concentration is higher in the upper layer of water, both chlorophyll concentration and suspended sediment concentration show a trend that increases with the increase of water depth. This is caused by the combined flocculation and transport of algae and sediment particles under the high suspended sediment concentration and strong vertical mixing. In this study, the ratio of chlorophyll concentration to suspended sediment concentration is taken as the parameter to represent the algae to suspended sediment ratio, which

is abbreviated CC/SSC. The algae-sediment ratio not only reflects the intensity of biological effects, but also can shed light on the location and period of the tide where sediment flocculation is dominated by algae effects. In laboratory experiments, high algae-sediment ratio promotes the flocculation process, and the flocs formed have a large particle size and fast flocculation rate. The temporal and spatial distribution of algae-sediment ratio in estuaries corresponds to algae biological activities: the algae-sediment ratio in summer is higher than that in winter. The highest ratio is about  $60 \mu\text{g g}^{-1}$ , and the seawards ratio is larger than the coastal area one, reflecting that algae are predominantly found at sea. The distribution of algae-sediment ratio is different during the tidal cycle: in summer, the algae-sediment ratio in the water surface is high during ebb as well as flood, and the biological activity is stronger, while in winter, the high algae-sediment ratio only appears during ebb, due to the decrease of sediment concentration. In addition, the algae-sediment ratio increases significantly in the middle and bottom layers of water at the end of flood tide in summer, which reflects that the algae is settling during the sediment flocculation process.

The distribution of algae-sediment ratio is expected to reflect the seasonal and tidal variation of the biological activity. The use of the algae-sediment ratio should therefore account for the fact that biological activity is low in winter, so the high algae-sediment ratio is caused by the low suspended sediment concentration in the surface water, and the biological flocculation is not significant. It was observed that in the early period of ebb in summer, the algae-sediment ratio in the water surface is also large due to high levels of algae but the limited supply of suspended mineral sediment implied that the floc size was small with high algae-sediment ratio.

### **3. What are the roles of biological parameters on sediment flocculation in estuarine areas?**

Most of the algae particles in the Changjiang Estuary are distributed in the part where the flocs are larger than  $100 \mu\text{m}$  and have dynamic interaction with sediment particles. When the algae concentration is high (the algae-sediment ratio is high), the floc particle size distribution (PSD) will give a bimodal curve with double peaks of sediment particles and algae particles. This bimodal PSD interchanges with unimodal PSD curves in the range  $10\text{--}100 \mu\text{m}$ , in time and space under the interaction of runoff and tidal current influences. The effective density and settling velocity of flocs in this

size range are related to the flocculation kinetics. Current sediment transport models use constant sediment settling velocity. These models should in fact account for dynamic settling velocities of flocs. It is expected that the algae-sediment ratio could be a useful parameter for deriving a time-dependent settling velocity. Flocs can be divided into three components according to their particle size distribution: Single-grain ( $< 5 \mu\text{m}$ ), Microflocs ( $5\text{--}200 \mu\text{m}$ ) and Macroflocs ( $> 200 \mu\text{m}$ ). With the increase of algae-sediment ratio, the abundance of single-grain components remains unchanged, while the frequency of microflocs decreases and that of macroflocs increases. This implies that the main algae effect is to combine microflocs and transform them into macroflocs. The algae-sediment flocculation process in estuaries is mainly affected by shear rate. Overall, water shear rate controls the upper limit of floc size in a tidal cycle, and the maximum floc size is about  $\eta/6$  ( $\eta$  is Kolmogorov microscale). The overall floc size varies within a tidal cycle. The floc is small at the maximum flood/ebb tide periods while the floc is large during the slack water periods. During flood tide, the water shear rate is high, and flocs will form a bimodal curve under the strong biological effect, in which the sediment peak is in the range of  $10\text{--}30 \mu\text{m}$ , and the biological algae peak remains in the range of  $100\text{--}200 \mu\text{m}$  due to the high strength of these flocs. This kind of large flocs with bimodal PSD appears during the flood tide when many algae are brought in from the seaside. The floc size can reach  $160 \mu\text{m}$ , which is similar to the size of algae flocs obtained in laboratory experiments. During the period around highwater slack, low shear rate is maintained for about 2–3 hours, and the algae particles and sediment particles are fully mixed under relatively stable hydrodynamic conditions forming a unimodal large PSD with a mean particle size of about  $40\text{--}80 \mu\text{m}$ . The flocculation process is then close to steady-state. Salinity and other factors have no significant influence on algae-sediment flocculation process in estuarine area.

#### **4. How do the seasonal and tidal variations affect flocculation in the presence of biological activity? How does algae-sediment flocculation affect sediment transport and deposition in the estuarine area?**

Because the concentration of algae in summer is higher than that in winter (chlorophyll concentration is about  $1\text{--}8 \mu\text{g l}^{-1}$ ), the effect of algae is mainly reflected in summer. The variation of flood and ebb tide indicate different flocculation processes: during flood, the algae-sediment ratio increases in the upper layer of the water column

(within 2m of water depth) due to algae particles brought in with seawater, and algae-sediment flocculation occurs in the early period, forming bimodal flocs with low density and high settling velocity. In the following 2–3 hours, the large flocs gradually settled to the middle and bottom layers of water, and the floc size distribution changed from bimodal to unimodal, and the floc size decreased due to the influence of high shear rate. In the early of ebb tide period (within 1–2 hours after high water slack period), the chlorophyll concentration in the surface layer of water does not decrease due to the resuspension of algae, and the suspended sediment concentration decrease significantly due to the settling of many sediment particles. Thus the algae-sediment ratio in water body increases while the floc size decreases. During ebb, although algae also participated, the flocculation efficiency decreased and the biological effect weakened due to the decrease of suspended sediment concentration and seawater retreat. So there are no large flocs and the PSD does not show double peaks. The large flocs during ebb usually appear in low shear rate periods, especially around low water slack, and the floc size is smaller than that in flood tide period. Therefore, the sediment settling velocity in ebb tide period is smaller than that in flood tide period. Therefore, algae promoted the asymmetry of sediment settling during ebb and flood tide, an important factor causing net sediment transport toward the estuary during a tidal cycle.

7

In winter, the algae concentration is low (chlorophyll concentration is less than  $1 \mu\text{g l}^{-1}$ ), and the biological effect is weak as well. Therefore, the sediment flocculation process is dominated by hydrodynamic forces, and there are no algae-sediment flocs and the sediment floc PSD is not bimodal. Large flocs usually appear at the slack water period and small flocs appear at the periods of maximum flood/ebb velocity. There is no significant biological effects on sediment settling in winter.

Seasonal variation and tidal cycle variation of sediment flocculation under biological effect in the Changjiang Estuary influence the sediment settling processes, affecting sediment transport in the Changjiang Estuary.

To sum up, the combination of laboratory experiment and in-situ observation results is helpful to deeply understand flocculation kinetics. This study establishes the relationship between sediment transport and ecological cycle in estuarine area. The coupling phenomenon between algae and sediment showed that sediment flocculation not only affected the evolution of estuarine geomorphology, but is also an important

process in estuarine ecological cycle (Figure 7.2).

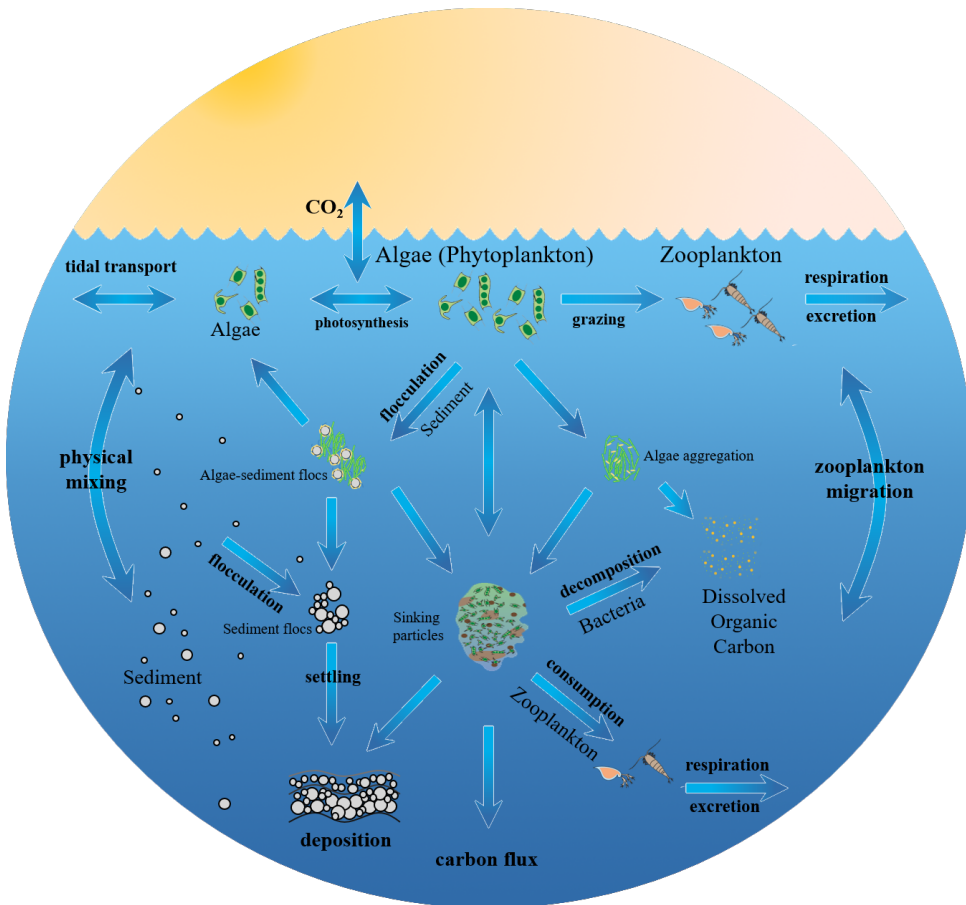


Figure 7.2: Function of flocculation in ecological cycle. Adapted from JGOFS [2001].

## 7.2. Applications

The results obtained from this research confirms that combining laboratory experiments and in-situ observations is fruitful, as it enables to study a system from a small scale to a large scale. Although there are some different conditions between laboratory and in-situ, it was found that some important parameters (like equilibrium floc size) obtained from lab and field agree with each other. It is therefore recommended for other researches focusing on process knowledge to continue working with these different systems/scales.

In contrast to biological studies that focus on algae bloom seasons, this study provides detailed information on algae concerning its spatial and temporal variations (seasonal and within a tidal cycle), and its influence on sediment flocculation.

### 7.3. Recommendations for future work

The present study is still limited in terms of what can be done for laboratory experiments and in-situ observations. The experience accumulated during the present PhD work can help improving experimental designs. For example:

- 1) In laboratory experiments, the observation equipment for flocculation should be improved.

In chapters 4 and 5, where sediment flocculation is discussed, flocculation was triggered in a beaker with a stirrer and pumped through the equipment with a tube of about 5 mm diameter. The shear rate evaluated from the transport of flocs within the tube and the confined region within the tube are likely to produce flocs that are not fully representative for in-situ flocs. Flocculation would be better studied by combining a variety of observation devices such as camera, settling cylinders, etc. in addition to light scattering particle sizers.

- 2) For in-situ observations, more extensive temporal and spatial bio-flocculation observations are still lacking. More extensive and detailed observations of biological influences are needed.

Due to the large extent of the Changjiang estuary and the obvious differences in water-sediment characteristics in different areas, the observation range can be expanded. For example, measurements could be taken closer to the upstream river, or closer to the downstream outer sea, or at other locations with different hydrological conditions, etc., to better study different bio-flocculation characteristics under different conditions. As the biological condition varies significantly with the environment, different seasons can have different effects. Although this study has considered winter and summer variations, more results from different seasons are required to provide a full spectrum of the effect of biological processes on sediment flocculation. Since the hydrodynamic conditions and sediment composition of estuaries vary from region to region, the generalization of the results of the present study is somewhat limited. Therefore, the study of bio-sediment flocculation processes in different estuaries is recommended.

In the present study, only chlorophyll (chlorophyll-a) was used as a proxy for algae concentration. It is recommended that in future studies, more biological parameters

such as algal species, abundance, nutrient, oxygen content, light, temperature, etc., are added to the observations. The analysis of the correlation between these parameters are expected to give a more profound understanding of biological sediment flocculation.

- 3) In terms of modelling studies, the results from this study are relevant so as to pinpoint the role of microalgae in flocculation and its temporal and spatial variation. Settling velocity should be made temporally and spatially varying and account for the role of living matter in flocculation.

Previous theories included physical parameters such as shear, suspended sediment concentration and salinity, which are relatively easy to quantify. Biological processes on the other hand are quite dynamic as they are associated to the lifetime of a microorganism. Thus sediment flocculation process needs to consider various factors synthetically.

Finally, with urban and landscape development, ecological issues are becoming more and more important. As stated above, sediment transport and biological activity are inextricably linked. Therefore, a broader vision and a more integrated approach for sediment transport research are required.

# References

- Adachi, Y., Kobayashi, A., & Kobayashi, M. (2012). Structure of Colloidal Floes in relation to the Dynamic Properties of Unstable Suspension. *International Journal of Polymer Science*, 2012, 1–14.
- Agrawal, Y. C. & Pottsmith, H. C. (2000). Instruments for particle size and settling velocity observations in sediment transport. *Marine Geology*, 168(1-4), 89–114.
- Allredge, A. L. & Gotschalk, C. C. (1989). Direct observations of the mass flocculation of diatom blooms: Characteristics, settling velocities and formation of diatom aggregates. *Deep Sea Research Part A. Oceanographic Research Papers*, 36(2), 159–171.
- Aly, S. M. & Letey, J. (1988). Polymer and Water Quality Effects on Flocculation of Montmorillonite. *Soil Science Society of America Journal*, 52(5), 1453–1458.
- Andrews, S., Nover, D., & Schladow, S. G. (2010). Using laser diffraction data to obtain accurate particle size distributions: The role of particle composition: Laser diffraction data processing. *Limnology and Oceanography: Methods*, 8(10), 507–526.
- Anglès, S., Jordi, A., Garcés, E., Masó, M., & Basterretxea, G. (2008). High-resolution spatio-temporal distribution of a coastal phytoplankton bloom using laser in situ scattering and transmissometry (LISST). *Harmful Algae*, 7(6), 808–816.
- Avnimelech, Y., Troeger, B. W., & Reed, L. W. (1982). Mutual flocculation of algae and clay: Evidence and implications. *Science*, 216(4541), 63–65.
- Bainbridge, Z. T., Wolanski, E., Álvarez-Romero, J. G., Lewis, S. E., & Brodie, J. E. (2012). Fine sediment and nutrient dynamics related to particle size and floc formation in a Burdekin River flood plume, Australia. *Marine Pollution Bulletin*, 65(4-9), 236–248.

- Baker, E. T. & Lavelle, J. W. (1984). The effect of particle size on the light attenuation coefficient of natural suspensions. *Journal of Geophysical Research*, 89(C5), 8197.
- Baker, E. T., Tennant, D. A., Feely, R. A., Lebon, G. T., & Walker, S. L. (2001). Field and laboratory studies on the effect of particle size and composition on optical backscattering measurements in hydrothermal plumes. *Deep Sea Research Part I: Oceanographic Research Papers*, 48(2), 593–604.
- Bar-Or, Y. & Shilo, M. (1988a). Cyanobacterial flocculants. In *Methods in Enzymology*, volume 167 (pp. 616–622). Elsevier.
- Bar-Or, Y. & Shilo, M. (1988b). The role of cell-bound flocculants in coflocculation of benthic cyanobacteria with clay particles. *FEMS Microbiology Letters*, 53(3-4), 169–174.
- Barlow, J. P. (1955). Physical and Biological Processes Determining the Distribution of Zooplankton in a Tidal Estuary. *The Biological Bulletin*, 109(2), 211–225.
- Benson, T. & Manning, A. J. (2013). DigiFloc: The development of semi-automatic software to determine the size and settling velocity of flocs. *HR Wallingford Report DDY0427-Rt001*.
- Bergaya, F. & Lagaly, G., Eds. (2013). *Handbook of Clay Science*. Number Volume 5A-B in Developments in Clay Science. Amsterdam: Elsevier, second edition edition.
- Bianchi, T. S. (2007). *Biogeochemistry of Estuaries*. Oxford ; New York: Oxford University Press.
- Biggs, S., Habgood, M., Jameson, G. J., & Yan, Y.-d. (2000). Aggregate structures formed via a bridging flocculation mechanism. *Chemical Engineering Journal*, 80(1-3), 13–22.
- Blanchard, G., Guarini, J., Richard, P., Gros, P., & Mornet, F. (1996). Quantifying the short-term temperature effect on light-saturated photosynthesis of intertidal microphytobenthos. *Marine Ecology Progress Series*, 134, 309–313.
- Blum, J. L. (1956). The ecology of river algae. *The Botanical Review*, 22(5), 291–341.

- Blumberg, A. F., Ji, Z.-G., & Ziegler, C. K. (1996). Modeling outfall plume behavior using far field circulation model. *Journal of Hydraulic Engineering*, 122(11), 610–616.
- Blumberg, A. F. & Mellor, G. L. (1987). A description of a three-dimensional coastal ocean circulation model. In N. S. Heaps (Ed.), *Coastal and Estuarine Sciences*, volume 4 (pp. 1–16). Washington, D. C.: American Geophysical Union.
- Bob, M. & Walker, H. W. (2001). Enhanced adsorption of natural organic matter on calcium carbonate particles through surface charge modification. *Colloids and Surfaces A: Physicochemical and Engineering Aspects*, 191(1-2), 17–25.
- Bolto, B. & Gregory, J. (2007). Organic polyelectrolytes in water treatment. *Water Research*, 41(11), 2301–2324.
- Bouyer, D., Liné, A., & Do-Quang, Z. (2004). Experimental analysis of floc size distribution under different hydrodynamics in a mixing tank. *AIChE Journal*, 50(9), 2064–2081.
- Braithwaite, K. M., Bowers, D. G., Nimmo Smith, W. A. M., Graham, G. W., Agrawal, Y. C., & Mikkelsen, O. A. (2010). Observations of particle density and scattering in the Tamar Estuary. *Marine Geology*, 277(1-4), 1–10.
- Burban, P.-Y., Lick, W., & Lick, J. (1989). The flocculation of fine-grained sediments in estuarine waters. *Journal of Geophysical Research*, 94(C6), 8323.
- Camp, T. R. (1943). Velocity gradients and internal work in fluid motion. *J. Boston Soc. Civ. Eng.*, 30, 219–230.
- CAMPBELL SCIENTIFIC INC., I. (2018). OBS-3A Turbidity and Temperature Monitoring System.
- Capriulo, G. M., Schreiner, R. A., & Dexter, B. L. (1988). Differential growth of *Euplores vannus* fed fragmented versus unfragmented chains of *Skeletonema costatum*. *Marine Ecology Progress Series*, (pp. 205–209).
- Castro, P. & Huber, M. E. (2016). *Marine Biology*. New York, NY: McGraw-Hill Education, tenth edition edition.

- Chai, C., Yu, Z., Song, X., & Cao, X. (2006). The Status and Characteristics of Eutrophication in the Yangtze River (Changjiang) Estuary and the Adjacent East China Sea, China. *Hydrobiologia*, 563(1), 313–328.
- Changjiang Water Resources Commission, G. (2018). Changjiang river sediment bulletin (in Chinese).
- Chassagne, C. (2019). *Introduction to Colloid Science*. Delft Academic Press.
- Chassagne, C. & Ibanez, M. (2012). Electrophoretic mobility of latex nanospheres in electrolytes: Experimental challenges. *Pure and Applied Chemistry*, 85(1), 41–51.
- Chassagne, C., Mietta, F., & Winterwerp, J. (2009). Electrokinetic study of kaolinite suspensions. *Journal of Colloid and Interface Science*, 336(1), 352–359.
- Chen, J. (1995). Sediment dynamics and evolution of the mouthbar and subaqueous delta in the Yangtze estuary. *Resources & Environment in the Yangtze Valley*.
- Chen, J., Li, D., Chen, B., Hu, F., Zhu, H., & Liu, C. (1999). The processes of dynamic sedimentation in the Changjiang Estuary. *Journal of Sea Research*, 41(1), 129–140.
- Chen, J., Shen, H., Yun, C., et al. (1988). Process of dynamics and geomorphology of the Changjiang Estuary. *Shanghai Science and Technology Press, Shanghai*.
- Chen, M. S., Wartel, S., & Temmerman, S. (2005). Seasonal variation of flocculation characteristics on tidal flats, the Scheldt estuary. *Hydrobiologia*, 540(1), 181–195.
- Chen, S. & Eisma, D. (1995). Fractal geometry of in situ flocs in the estuarine and coastal environments. *Netherlands Journal of Sea Research*, 33(2), 173–182.
- Chen, S., Eisma, D., & Kalf, J. (1994). In situ distribution of suspended matter during the tidal cycle in the elbe estuary. *Netherlands Journal of Sea Research*, 32(1), 37–48.
- Cheng, J. (2004). The characteristic of suspended fine sediment flocs in Changjiang estuary (in Chinese). Master's thesis, East China Normal University.
- Colijn, F. & van Buurt, G. (1975). Influence of light and temperature on the photosynthetic rate of marine benthic diatoms. *Marine Biology*, 31(3), 209–214.

- Comte, S., Guibaud, G., & Baudu, M. (2006). Biosorption properties of extracellular polymeric substances (EPS) resulting from activated sludge according to their type: Soluble or bound. *Process Biochemistry*, 41(4), 815–823.
- Costerton, J. W., Cheng, K. J., Geesey, G. G., Ladd, T. I., Nickel, J. C., Dasgupta, M., & Marrie, T. J. (1987). Bacterial biofilms in nature and disease. *Annual Reviews in Microbiology*, 41(1), 435–464.
- Craig, D., Ireland, R. J., & Bärlocher, F. (1989). Seasonal variation in the organic composition of seafoam. *Journal of Experimental Marine Biology and Ecology*, 130(1), 71–80.
- Curran, K., Hill, P., Milligan, T., Mikkelsen, O., Law, B., Durrieu de Madron, X., & Bourrin, F. (2007). Settling velocity, effective density, and mass composition of suspended sediment in a coastal bottom boundary layer, Gulf of Lions, France. *Continental Shelf Research*, 27(10-11), 1408–1421.
- de Lucas Pardo, M. (2014). *Effect of Biota on Fine Sediment Transport Processes: A Study of Lake Markermeer*. PhD thesis, TU Delft, Delft University of Technology.
- de Lucas Pardo, M. A., Bakker, M., van Kessel, T., Cozzoli, F., & Winterwerp, J. C. (2013). Erodibility of soft freshwater sediments in Markermeer: The role of bioturbation by meiobenthic fauna. *Ocean Dynamics*, 63(9-10), 1137–1150.
- Deng, Z., He, Q., Chassagne, C., & Wang, Z. B. (2021). Seasonal variation of floc population influenced by the presence of algae in the Changjiang (Yangtze River) Estuary. *Marine Geology*, 440, 106600.
- Deng, Z., He, Q., Safar, Z., & Chassagne, C. (2019). The role of algae in fine sediment flocculation: In-situ and laboratory measurements. *Marine Geology*, 413, 71–84.
- Domozych, D. S. (2007). Exopolymer Production by the Green Alga *Penium margaritaceum*: Implications for Biofilm Residency. *International Journal of Plant Sciences*, 168(6), 763–774.
- Dontsova, K. M. & Bigham, J. M. (2005). Anionic Polysaccharide Sorption by Clay Minerals. *Soil Science Society of America Journal*, 69(4), 1026.

- Dronkers, J., van Leussen, W., Puls, W., Kuehl, H., & Heymann, K. (1988). Settling velocity of mud flocs: Results of field measurements in the elbe and the weser estuary. In J. Dronkers & W. van Leussen (Eds.), *Physical Processes in Estuaries* (pp. 404–424). Springer Berlin Heidelberg.
- Droppo, I. G. (2001). Rethinking what constitutes suspended sediment. *Hydrological Processes*, 15(9), 1551–1564.
- Droppo, I. G., D'Andrea, L., Krishnappan, B. G., Jaskot, C., Trapp, B., Basuvaraj, M., & Liss, S. N. (2015). Fine-sediment dynamics: Towards an improved understanding of sediment erosion and transport. *Journal of Soils and Sediments*, 15(2), 467–479.
- Droppo, I. G. & Ongley, E. D. (1992). The state of suspended sediment in the freshwater fluvial environment: A method of analysis. *Water Research*, 26(1), 65–72.
- Droppo, I. G. & Ongley, E. D. (1994). Flocculation of suspended sediment in rivers of southeastern Canada. *Water Research*, 28(8), 1799–1809.
- Dyer, K. R. (1989). Sediment processes in estuaries: Future research requirements. *Journal of Geophysical Research*, 94(C10), 14327.
- Dyer, K. R. & Manning, A. J. (1999). Observation of the size, settling velocity and effective density of flocs, and their fractal dimensions. *Journal of Sea Research*, 41(1-2), 87–95.
- Eisma, D. (1986). Flocculation and de-flocculation of suspended matter in estuaries. *Netherlands Journal of Sea Research*, 20(2-3), 183–199.
- Eisma, D. (1991). Particle size of suspended matter in estuaries. *Geo-Marine Letters*, 11(3-4), 147–153.
- Eisma, D., Bernard, P., Cadée, G. C., Ittekkot, V., Kalf, J., Laane, R., Martin, J., Mook, W., van Put, A., & Schuhmacher, T. (1991). Suspended-matter particle size in some West-European estuaries; part II: A review on floc formation and break-up. *Netherlands Journal of Sea Research*, 28(3), 215–220.
- Eisma, D. & Irion, G. (1993). Suspended Matter and Sediment Transport. In W. Salomons, B. L. Bayne, E. K. Duursma, & U. Förstner (Eds.), *Pollution of the North Sea* (pp. 20–35). Berlin, Heidelberg: Springer Berlin Heidelberg.

- Eisma, D. & Li, A. (1993). Changes in suspended-matter floc size during the tidal cycle in the dollard estuary. *Netherlands Journal of Sea Research*, 31(2), 107–117.
- Engel, A. (2000). The role of transparent exopolymer particles (TEP) in the increase in apparent particle stickiness ( $\alpha$ ) during the decline of a diatom bloom. *Journal of Plankton Research*, 22(3), 485–497.
- Eureka Environmental Engineering, I. (2016). Manta 2 Water Quality Multiprobe Manual.
- Fennessy, M. J. & Dyer, K. R. (1996). Floc population characteristics measured with INSSEV during the Elbe estuary intercalibration experiment. *Journal of Sea Research*, 36(1-2), 55–62.
- Fennessy, M. J., Dyer, K. R., & Huntley, D. A. (1994). Inssev: An instrument to measure the size and settling velocity of flocs in situ. *Marine Geology*, 117(1-4), 107–117.
- Fernández-Méndez, M., Wenzhöfer, F., Peeken, I., Sørensen, H. L., Glud, R. N., & Boetius, A. (2014). Composition, Buoyancy Regulation and Fate of Ice Algal Aggregates in the Central Arctic Ocean. *PLoS ONE*, 9(9), e107452.
- Fettweis, M. (2008). Uncertainty of excess density and settling velocity of mud flocs derived from in situ measurements. *Estuarine, Coastal and Shelf Science*, 78(2), 426–436.
- Fettweis, M. & Baeye, M. (2015). Seasonal variation in concentration, size, and settling velocity of muddy marine flocs in the benthic boundary layer. *Journal of Geophysical Research: Oceans*, 120(8), 5648–5667.
- Fettweis, M., Baeye, M., Van der Zande, D., Van den Eynde, D., & Joon Lee, B. (2014). Seasonality of floc strength in the southern North Sea. *Journal of Geophysical Research: Oceans*, 119(3), 1911–1926.
- Fettweis, M., Francken, F., Van den Eynde, D., Verwaest, T., Janssens, J., & Van Lancker, V. (2010). Storm influence on SPM concentrations in a coastal turbidity maximum area with high anthropogenic impact (southern North Sea). *Continental Shelf Research*, 30(13), 1417–1427.

- Fettweis, M. & Lee, B. J. (2017). Spatial and Seasonal Variation of Biomineral Suspended Particulate Matter Properties in High-Turbid Nearshore and Low-Turbid Offshore Zones. *Water*, 9(9), 694.
- Fettweis, M., Nechad, B., & Van den Eynde, D. (2007). An estimate of the suspended particulate matter (SPM) transport in the southern North Sea using SeaWiFS images, in situ measurements and numerical model results. *Continental Shelf Research*, 27(10), 1568–1583.
- Filippa, L., Freire, L., Trento, A., Álvarez, A. M., Gallo, M., & Vinzón, S. (2011). Laboratory evaluation of two LISST-25X using river sediments. *Sedimentary Geology*, 238(3-4), 268–276.
- Foree, E. G. & McCarty, P. L. (1970). Anaerobic decomposition of algae. *Environmental science & technology*, 4(10), 842–849.
- Fox, J. M., Hill, P. S., Milligan, T. G., & Boldrin, A. (2004). Flocculation and sedimentation on the Po River Delta. *Marine Geology*, 203(1-2), 95–107.
- Fugate, D. C. & Friedrichs, C. T. (2002). Determining concentration and fall velocity of estuarine particle populations using ADV, OBS and LISST. *Continental Shelf Research*, 22(11-13), 1867–1886.
- Fugate, D. C. & Friedrichs, C. T. (2003). Controls on suspended aggregate size in partially mixed estuaries. *Estuarine, Coastal and Shelf Science*, 58(2), 389–404.
- Furukawa, Y., Reed, A. H., & Zhang, G. (2014). Effect of organic matter on estuarine flocculation: A laboratory study using montmorillonite, humic acid, xanthan gum, guar gum and natural estuarine flocs. *Geochemical Transactions*, 15, 1.
- Gao, X. & Song, J. (2005). Phytoplankton distributions and their relationship with the environment in the Changjiang Estuary, China. *Marine Pollution Bulletin*, 50(3), 327–335.
- Gartner, J. W., Cheng, R. T., Wang, P.-F., & Richter, K. (2001). Laboratory and field evaluations of the LISST-100 instrument for suspended particle size determinations. *Marine Geology*, 175(1-4), 199–219.

- Geyer, W. R., Hill, P. S., & Kineke, G. C. (2004). The transport, transformation and dispersal of sediment by buoyant coastal flows. *Continental Shelf Research*, 24(7-8), 927–949.
- Geyer, W. R., Morris, J. T., Prah, F. G., & Jay, D. A. (2000). Interaction between physical processes and ecosystem structure: A comparative approach. *Estuarine science: a synthetic approach to research and practice*, (pp. 177–206).
- Gibbs, R. J. (1985). Estuarine flocs: Their size, settling velocity and density. *Journal of Geophysical Research*, 90(C2), 3249.
- Gibson, C. E., McCall, R. D., & Dymond, A. (1993). *Skeletonema subsalsum* in a freshwater irish lake. *Diatom Research*, 8(1), 65–71.
- Goldberg, S. (1991). Flocculation of Illite/Kaolinite and Illite/Montmorillonite Mixtures as Affected by Sodium Adsorption Ratio and pH. *Clays and Clay Minerals*, 39(4), 375–380.
- Gratiot, N. & Manning, A. J. (2004). An experimental investigation of floc characteristics in a diffusive turbulent flow. *Journal of Coastal Research*, (pp. 105–113).
- Gregory, J. (2005). *Particles in Water: Properties and Processes*. CRC Press, zeroth edition.
- Gregory, J. & Barany, S. (2011). Adsorption and flocculation by polymers and polymer mixtures. *Advances in Colloid and Interface Science*, 169(1), 1–12.
- Grey, J., Jones, R. I., & Sleep, D. (2001). Seasonal changes in the importance of the source of organic matter to the diet of zooplankton in Loch Ness, as indicated by stable isotope analysis. *Limnology and Oceanography*, 46(3), 505–513.
- Grossart, H.-P., Czub, G., & Simon, M. (2006). Algae-bacteria interactions and their effects on aggregation and organic matter flux in the sea. *Environmental Microbiology*, 8(6), 1074–1084.
- Guan, X. & Chen, Y. (1995). Experimental study on dynamic formula of sand coagulation sinking in stationary water in Changjiang estuary (in Chinese). *Ocean Engineering*, 13(1), 46–50.

- Guan, X., Chen, Y., & Du, X. (1996). Experimental study on mechanism of flocculation in Yangtze estuary (in Chinese). *Journal of Hydraulic Engineering*, 1(6), 70–80.
- Guo, C. (2018). *Cohesive Sediment Flocculation and Settling Processes and the Controlling Mechanisms (in Chinese)*. PhD thesis, East China Normal University, Shanghai.
- Guo, C., He, Q., Guo, L., & Winterwerp, J. C. (2017). A study of in-situ sediment flocculation in the turbidity maxima of the Yangtze Estuary. *Estuarine, Coastal and Shelf Science*, 191(Supplement C), 1–9.
- Guo, L. & He, Q. (2011). Freshwater flocculation of suspended sediments in the Yangtze River, China. *Ocean Dynamics*, 61(2-3), 371–386.
- Hart, B. T., Bailey, P., Edwards, R., Hortle, K., James, K., McMahon, A., Meredith, C., & Swadling, K. (1990). Effects of salinity on river, stream and wetland ecosystems in Victoria, Australia. *Water Research*, 24(9), 1103–1117.
- He, Q., Guo, L., Liu, H., & Wang, Y. (2015). Changjiang Estuary Sediment Transport Dynamics. In *Ecological Continuum from the Changjiang (Yangtze River) Watersheds to the East China Sea Continental Margin*, Estuaries of the World (pp. 47–69). Springer, Cham.
- He, Q. & Sun, J. (2009). The Netz-phytoplankton community in Changjiang(Yangtze) River Estuary and adjacent waters. *Acta ecologica sinica/Shengtai Xuebao*, 29(7).
- Herbert, R. (1999). Nitrogen cycling in coastal marine ecosystems. *FEMS Microbiology Reviews*, 23(5), 563–590.
- Higgins, M. J. & Novak, J. T. (1997). The effect of cations on the settling and dewatering of activated sludges: Laboratory results. *Water Environment Research*, 69(2), 215–224.
- Hu, K., Ding, P., Wang, Z., & Yang, S. (2009). A 2D/3D hydrodynamic and sediment transport model for the Yangtze Estuary, China. *Journal of Marine Systems*, 77(1-2), 114–136.
- Huiming, Z., Hongwei, F., & Minghong, C. (2011). Floc architecture of bioflocculation sediment by ESEM and CLSM. *Scanning*, 33(6), 437–445.

- Hunt, J. R. (1980). Prediction of Oceanic Particle Size Distributions from Coagulation and Sedimentation Mechanisms. In M. C. Kavanaugh & J. O. Leckie (Eds.), *Particulates in Water*, volume 189 (pp. 243–257). WASHINGTON, D. C.: AMERICAN CHEMICAL SOCIETY.
- Hunter, K. A. & Liss, P. S. (1979). The surface charge of suspended particles in estuarine and coastal waters. *Nature*, 282(5741), 823–825.
- Hunter, K. A. & Liss, P. S. (1982). Organic matter and the surface charge of suspended particles in estuarine waters I: Surface electrical charge. *Limnology and Oceanography*, 27(2), 322–335.
- Ibanez Sanz, M. E. (2018). *Flocculation and Consolidation of Cohesive Sediments under the Influence of Coagulant and Flocculant*. PhD thesis, Delft University of Technology.
- Jarvis, P., Jefferson, B., Gregory, J., & Parsons, S. A. (2005). A review of floc strength and breakage. *Water Research*, 39(14), 3121–3137.
- Jay, D. A., Geyer, R., & Montgomery, D. R. (2000). An ecological perspective on estuarine. *Estuarine science: a synthetic approach to research and practice*, (pp. 149).
- Jeldres, R. I., Fawell, P. D., & Florio, B. J. (2018). Population balance modelling to describe the particle aggregation process: A review. *Powder Technology*, 326, 190–207.
- JGOFS (2001). U.S. Joint Global Ocean Flux Study (U.S. JGOFS) Brochure.
- Jiang, G., Yao, Y., & Tang, Z. (2002). Analysis of influencing factors on fine sediment flocculation in the Changjiang Estuary. *Acta Oceanologica Sinica*, 21(3), 385–394.
- Jorand, F., Zartarian, F., Thomas, F., Block, J. C., Bottero, J., Villemin, G., Urbain, V., & Manem, J. (1995). Chemical and structural (2D) linkage between bacteria within activated sludge flocs. *Water Research*, 29(7), 1639–1647.
- Karbassi, A. R., Heidari, M., Vaezi, A. R., Samani, A. R. V., Fakhrace, M., & Heidari, F. (2014). Effect of pH and salinity on flocculation process of heavy metals during

- mixing of Aras River water with Caspian Sea water. *Environmental Earth Sciences*, 72(2), 457–465.
- Keyvani, A. & Strom, K. (2014). Influence of cycles of high and low turbulent shear on the growth rate and equilibrium size of mud flocs. *Marine Geology*, 354, 1–14.
- Khelifa, A. & Hill, P. S. (2006). Models for effective density and settling velocity of flocs. *Journal of Hydraulic Research*, 44(3), 390–401.
- Kiemle, S. N., Domozych, D. S., & Gretz, M. R. (2007). The extracellular polymeric substances of desmids (Conjugatophyceae, Streptophyta): Chemistry, structural analyses and implications in wetland biofilms. *Phycologia*, 46(6), 617–627.
- Kjørboe, T., Andersen, K. P., & Dam, H. G. (1990). Coagulation efficiency and aggregate formation in marine phytoplankton. *Marine Biology*, 107(2), 235–245.
- Kjørboe, T., Lundsgaard, C., Olesen, M., & Hansen, J. L. (1994). Aggregation and sedimentation processes during a spring phytoplankton bloom: A field experiment to test coagulation theory. *Journal of Marine Research*, 52(2), 297–323.
- Knap, A. H., Michaels, A., Close, A. R., Ducklow, H., & Dickson, A. G. (1996). Protocols for the Joint Global Ocean Flux Study (JGOFS) Core Measurements.
- Kosmulski, M. & Dahlsten, P. (2006). High ionic strength electrokinetics of clay minerals. *Colloids and Surfaces A: Physicochemical and Engineering Aspects*, 291(1-3), 212–218.
- Kranenburg, C. (1994). The fractal structure of cohesive sediment aggregates. *Estuarine, Coastal and Shelf Science*, 39(6), 451–460.
- Kruyt, H. R. (1949). *Colloid Science*. Technical report, Elsevier Pub. Co.,.
- Kruyt, H. R., Jonker, G., & Overbeek, J. (1952). *Colloid Science. Vol. 1. Irreversible Systems*. Elsevier Publishing Co.
- Kumar, R. G., Strom, K. B., & Keyvani, A. (2010). Floc properties and settling velocity of San Jacinto estuary mud under variable shear and salinity conditions. *Continental Shelf Research*, 30(20), 2067–2081.

- Lai, H., Fang, H., Huang, L., He, G., & Reible, D. (2018). A review on sediment bioflocculation: Dynamics, influencing factors and modeling. *Science of The Total Environment*, 642, 1184–1200.
- Lau, Y. L. (1994). Temperature effect on settling velocity and deposition of cohesive sediments. *Journal of Hydraulic Research*, 32(1), 41–51.
- Law, B. A., Milligan, T. G., Hill, P. S., Newgard, J., Wheatcroft, R. A., & Wiberg, P. L. (2013). Flocculation on a muddy intertidal flat in Willapa Bay, Washington, Part I: A regional survey of the grain size of surficial sediments. *Continental Shelf Research*, 60, S136–S144.
- Lee, B. & Schlautman, M. (2015). Effects of Polymer Molecular Weight on Adsorption and Flocculation in Aqueous Kaolinite Suspensions Dosed with Nonionic Polyacrylamides. *Water*, 7(11), 5896–5909.
- Lee, B. J., Fettweis, M., Toorman, E., & Molz, F. J. (2012). Multimodality of a particle size distribution of cohesive suspended particulate matters in a coastal zone: A MULTIMODAL PSD OF COHESIVE SEDIMENTS. *Journal of Geophysical Research: Oceans*, 117(C3), n/a–n/a.
- Lee, B. J., Hur, J., & Toorman, E. A. (2017). Seasonal variation in flocculation potential of river water: Roles of the organic matter pool. *Water*, 9(5), 335.
- Lee, B. J., Toorman, E., & Fettweis, M. (2014). Multimodal particle size distributions of fine-grained sediments: Mathematical modeling and field investigation. *Ocean Dynamics*, 64(3), 429–441.
- Lee, B. J., Toorman, E., Molz, F. J., & Wang, J. (2011). A two-class population balance equation yielding bimodal flocculation of marine or estuarine sediments. *Water Research*, 45(5), 2131–2145.
- Lee, D. G., Bonner, J. S., Garton, L. S., Ernest, A. N., & Autenrieth, R. L. (2000). Modeling coagulation kinetics incorporating fractal theories: A fractal rectilinear approach. *Water Research*, 34(7), 1987–2000.
- Lee, J., Liu, J. T., Hung, C. C., Lin, S., & Du, X. (2016). River plume induced variability of suspended particle characteristics. *Marine Geology*, 380, 219–230.

- Leppard, G. G. (1992). Size, morphology and composition of particulates in aquatic ecosystems: Solving speciation problems by correlative electron microscopy. *The Analyst*, 117(3), 595.
- Lesser, G., Roelvink, J., van Kester, J., & Stelling, G. (2004). Development and validation of a three-dimensional morphological model. *Coastal Engineering*, 51(8-9), 883–915.
- Lesser, G. R., Van Kester, J., & Roelvink, J. A. (2000). *On-Line Sediment Transport within Delft3D-FLOW*. Technical report, Deltares (WL).
- Li, D. & Ganczarczyk, J. J. (1990). Structure of activated sludge flocs. *Biotechnology and Bioengineering*, 35(1), 57–65.
- Li, D., Li, Y., & Xu, Y. (2017). Observations of distribution and flocculation of suspended particulate matter in the Minjiang River Estuary, China. *Marine Geology*, 387, 31–44.
- Li, H., Tang, H., Shi, X., Zhang, C., & Wang, X. (2014). Increased nutrient loads from the Changjiang (Yangtze) River have led to increased Harmful Algal Blooms. *Harmful Algae*, 39, 92–101.
- Li, J., He, Q., Xiang, W., Wan, X., & Shen, H. (2001). Fluid mud transportation at water wedge in the Changjiang Estuary. *Science in China Series B: Chemistry*, 44(S1), 47–56.
- Li, Y., Jia, J., Zhu, Q., Cheng, P., Gao, S., & Wang, Y. P. (2018). Differentiating the effects of advection and resuspension on suspended sediment concentrations in a turbid estuary. *Marine Geology*, 403, 179–190.
- Lick, W., Huang, H., & Jepsen, R. (1993). Flocculation of fine-grained sediments due to differential settling. *Journal of Geophysical Research*, 98(C6), 10279.
- Lick, W. & Lick, J. (1988). Aggregation and Disaggregation of Fine-Grained Lake Sediments. *Journal of Great Lakes Research*, 14(4), 514–523.
- Liu, H., He, Q., Meng, Y., Wang, Y., & Tang, J. (2007a). Characteristics of surface sediment distribution and its hydrodynamic responses in the Yangtze River estuary (in Chinese). *ACTA GEOGRAPHICA SINICA-CHINESE EDITION*-, 62(1), 81.

- Liu, Q., Li, J., Dai, Z., & Li, D. (2007b). Flocculation process of fine-grained sediments by the combined effect of salinity and humus in the Changjiang Estuary. *ACTA OCEANOLOGICA SINICA-ENGLISH EDITION*, 26(1), 140.
- Lupi, F. M., Fernandes, H. M. L., Sá-Correia, I., & Novais, J. M. (1991). Temperature profiles of cellular growth and exopolysaccharide synthesis by *Botryococcus braunii* Kütz. UC 58. *Journal of Applied Phycology*, 3(1), 35–42.
- Maggi, F. (2005). *Flocculation Dynamics of Cohesive Sediment*. PhD thesis, Technische Universiteit Delft, Delft.
- Maggi, F. (2009). Biological flocculation of suspended particles in nutrient-rich aqueous ecosystems. *Journal of Hydrology*, 376(1), 116–125.
- Maggi, F. (2013). The settling velocity of mineral, biomineral, and biological particles and aggregates in water. *Journal of Geophysical Research: Oceans*, 118(4), 2118–2132.
- Maggi, F. & Tang, F. H. M. (2015). Analysis of the effect of organic matter content on the architecture and sinking of sediment aggregates. *Marine Geology*, 363, 102–111.
- Mandelbrot, B. B. (1982). *The Fractal Geometry of Nature*. San Francisco: W.H. Freeman.
- Manning, A. J. (2010). Video Observations of Flocculated Sediment from Three Contrastingly Different Natural Environments in the USA. In *PiE 2010 Particles in Europe Villefranche-sur-Mer, France 14-17 November 2010*, volume 10 (pp. 44).
- Manning, A. J., Bass, S. J., & Dyer, K. R. (2006). Floc properties in the turbidity maximum of a mesotidal estuary during neap and spring tidal conditions. *Marine Geology*, 235(1-4), 193–211.
- Manning, A. J., Baugh, J. V., Spearman, J. R., Pidduck, E. L., & Whitehouse, R. J. S. (2011). The settling dynamics of flocculating mud-sand mixtures: Part 1—Empirical algorithm development. *Ocean Dynamics*, 61(2-3), 311–350.
- Manning, A. J., Baugh, J. V., Spearman, J. R., & Whitehouse, R. J. S. (2010a). Flocculation settling characteristics of mud: Sand mixtures. *Ocean Dynamics*, 60(2), 237–253.

- Manning, A. J. & Dyer, K. R. (1999). A laboratory examination of floc characteristics with regard to turbulent shearing. *Marine Geology*, 160(1), 147–170.
- Manning, A. J. & Dyer, K. R. (2002). The use of optics for the in situ determination of flocculated mud characteristics. *Journal of Optics A: Pure and Applied Optics*, 4(4), S71–S81.
- Manning, A. J., Friend, P. L., Prowse, N., & Amos, C. L. (2007). Estuarine mud flocculation properties determined using an annular mini-flume and the LabSFLOC system. *Continental Shelf Research*, 27(8), 1080–1095.
- Manning, A. J., Langston, W. J., & Jonas, P. J. C. (2010b). A review of sediment dynamics in the Severn Estuary: Influence of flocculation. *Marine Pollution Bulletin*, 61(1-3), 37–51.
- Manning, A. J. & Schoellhamer, D. H. (2013). Factors controlling floc settling velocity along a longitudinal estuarine transect. *Marine Geology*, 345, 266–280.
- Manning, A. J., Whitehouse, R. J. S., & Uncles, R. J. (2017). Suspended Particulate Matter: The Measurement of Floccs. In R. J. Uncles & S. B. Mitchell (Eds.), *Estuarine and Coastal Hydrography and Sediment Transport* (pp. 211–260). Cambridge: Cambridge University Press.
- Markussen, T. N. & Andersen, T. J. (2014). Flocculation and floc break-up related to tidally induced turbulent shear in a low-turbidity, microtidal estuary. *Journal of Sea Research*, 89, 1–11.
- McAnally, W. H. & Mehta, A. J. (2001). *Coastal and Estuarine Fine Sediment Processes*. Number 3 in Proceedings in Marine Science. Amsterdam ; New York: Elsevier.
- McCave, I. N. (1984). Size spectra and aggregation of suspended particles in the deep ocean. *Deep Sea Research Part A. Oceanographic Research Papers*, 31(4), 329–352.
- Mehta, A. J. & Partheniades, E. (1975). An investigation of the depositional properties of flocculated fine sediments. *Journal of Hydraulic Research*, 13(4), 361–381.

- Mhashhash, A., Bockelmann-Evans, B., & Pan, S. (2018). Effect of hydrodynamics factors on sediment flocculation processes in estuaries. *Journal of Soils and Sediments*, 18(10), 3094–3103.
- Mietta, F. (2010). *Evolution of the Floc Size Distribution of Cohesive Sediments*. PhD thesis, TU Delft, Delft University of Technology.
- Mietta, F., Chassagne, C., Manning, A. J., & Winterwerp, J. C. (2009a). Influence of shear rate, organic matter content, pH and salinity on mud flocculation. *Ocean Dynamics*, 59(5), 751–763.
- Mietta, F., Chassagne, C., Verney, R., & Winterwerp, J. C. (2011). On the behavior of mud floc size distribution: Model calibration and model behavior. *Ocean Dynamics*, 61(2-3), 257–271.
- Mietta, F., Chassagne, C., & Winterwerp, J. C. (2009b). Shear-induced flocculation of a suspension of kaolinite as function of pH and salt concentration. *Journal of Colloid and Interface Science*, 336(1), 134–141.
- Mikkelsen, O. & Pejrup, M. (2001). The use of a LISST-100 laser particle sizer for in-situ estimates of floc size, density and settling velocity. *Geo-Marine Letters*, 20(4), 187–195.
- Mikkelsen, O. A. (2002). Examples of spatial and temporal variations of some fine-grained suspended particle characteristics in two Danish coastal water bodies. *Oceanologica Acta*, 25(1), 39–49.
- Mikkelsen, O. A., Hill, P. S., & Milligan, T. G. (2006). Single-grain, microfloc and macrofloc volume variations observed with a LISST-100 and a digital floc camera. *Journal of Sea Research*, 55(2), 87–102.
- Mikkelsen, O. A., Hill, P. S., & Milligan, T. G. (2007). Seasonal and spatial variation of floc size, settling velocity, and density on the inner Adriatic Shelf (Italy). *Continental Shelf Research*, 27(3-4), 417–430.
- Mikutta, R., Mikutta, C., Kalbitz, K., Scheel, T., Kaiser, K., & Jahn, R. (2007). Biodegradation of forest floor organic matter bound to minerals via different binding mechanisms. *Geochimica et Cosmochimica Acta*, 71(10), 2569–2590.

- Milliman, J. D. & Farnsworth, K. L. (2011). *River Discharge to the Coastal Ocean: A Global Synthesis*. Cambridge: Cambridge University Press.
- Ministry of Environmental Protection of the People's Republic of China (2014). China Inshore Waters Environment Quality Bulletin.
- Morrissey, E. M., Gillespie, J. L., Morina, J. C., & Franklin, R. B. (2014). Salinity affects microbial activity and soil organic matter content in tidal wetlands. *Global Change Biology*, 20(4), 1351–1362.
- Nabzar, L., Pefferkorn, E., & Varoqui, R. (1988). Stability of polymer—clay suspensions. The polyacrylamide—sodium kaolinite system. *Colloids and Surfaces*, 30(3-4), 345–353.
- Napper, D. H. (1983). *Polymeric Stabilization of Colloidal Dispersions*. Number 3 in Colloid Science. London ; New York: Academic Press.
- Nayar, S., Goh, B. P. L., & Chou, L. M. (2005). Dynamics in the size structure of *Skeletonema costatum* (Greville) Cleve under conditions of reduced photosynthetically available radiation in a dredged tropical estuary. *Journal of Experimental Marine Biology and Ecology*, 318(2), 163–182.
- Ni, B., Fang, F., Xie, W., Sun, M., Sheng, G., Li, W., & Yu, H. (2009). Characterization of extracellular polymeric substances produced by mixed microorganisms in activated sludge with gel-permeating chromatography, excitation–emission matrix fluorescence spectroscopy measurement and kinetic modeling. *Water Research*, 43(5), 1350–1358.
- Nopens, I. (2005). Modelling the activated sludge flocculation process: A population balance approach. *PhD Thesis, Ghent University, Belgium*.
- Otsubo, Y. (1992). Effect of particle size on the bridging structure and elastic properties of flocculated suspensions. *Journal of Colloid and Interface Science*, 153(2), 584–586.
- Pan, L. A., Zhang, J., & Zhang, L. H. (2007). Picophytoplankton, nanophytoplankton, heterotrophic bacteria and viruses in the Changjiang Estuary and adjacent coastal waters. *Journal of Plankton Research*, 29(2), 187–197.

- Park, C., Fang, Y., Murthy, S. N., & Novak, J. T. (2010). Effects of floc aluminum on activated sludge characteristics and removal of 17- $\alpha$ -ethinylestradiol in wastewater systems. *Water Research*, 44(5), 1335–1340.
- Partheniades, E. (1991). Effect of bed shear stresses on the deposition and strength of deposited cohesive muds. In R. H. Bennett, W. R. Bryant, M. H. Hulbert, W. A. Chiou, R. W. Faas, J. Kasprowicz, H. Li, T. Lomenick, N. R. O'Brien, S. Pamukcu, P. Smart, C. E. Weaver, & T. Yamamoto (Eds.), *Microstructure of Fine-Grained Sediments: From Mud to Shale* (pp. 175–183). New York, NY: Springer New York.
- Partheniades, E. (1993). Turbulence, flocculation and cohesive sediment dynamics. *Coastal and Estuarine Studies*, (pp. 40–40).
- Passow, U. (2002). Transparent exopolymer particles (TEP) in aquatic environments. *Progress in Oceanography*, 55(3-4), 287–333.
- Passow, U., Alldredge, A. L., & Logan, B. E. (1994). The role of particulate carbohydrate exudates in the flocculation of diatom blooms. *Deep Sea Research Part I: Oceanographic Research Papers*, 41(2), 335–357.
- Paterson, D. M. & Hagerthey, S. E. (2001). Microphytobenthos in Constrasting Coastal Ecosystems: Biology and Dynamics. In I. T. Baldwin, M. M. Caldwell, G. Heldmaier, O. L. Lange, H. A. Mooney, E.-D. Schulze, U. Sommer, & K. Reise (Eds.), *Ecological Comparisons of Sedimentary Shores*, volume 151 (pp. 105–125). Berlin, Heidelberg: Springer Berlin Heidelberg.
- Pearson, H. W., Mara, D. D., Mills, S. W., & Smallman, D. J. (1987). Physico-Chemical Parameters Influencing Faecal Bacterial Survival in Waste Stabilization Ponds. *Water Science and Technology*, 19(12), 145–152.
- Pejrup, M. & Mikkelsen, O. A. (2010). Factors controlling the field settling velocity of cohesive sediment in estuaries. *Estuarine, Coastal and Shelf Science*, 87(2), 177–185.
- Pérez, L., Salgueiro, J. L., Maceiras, R., Cancela, Á., & Sánchez, Á. (2016). Study of influence of pH and salinity on combined flocculation of *Chaetoceros gracilis* microalgae. *Chemical Engineering Journal*, 286, 106–113.

- Plude, J. L., Parker, D. L., Schommer, O. J., Timmerman, R. J., Hagstrom, S. A., Joers, J. M., & Hnasko, R. (1991). Chemical Characterization of Polysaccharide from the Slime Layer of the Cyanobacterium *Microcystis flos-aquae* C3-40. *Applied and Environmental Microbiology*, 57(6), 1696.
- Porter, K. G. (1973). Selective Grazing and Differential Digestion of Algae by Zooplankton. *Nature*, 244(5412), 179–180.
- Qian, N. & Wan, Z. (1983). *Mechanics of Sediment Transport*. Beijing: Science Press.
- R. F. Hicks, G. (1988). Sediment rafting: A novel mechanism for the small-scale dispersal of intertidal estuarine meiofauna. *Mar. Ecol. Prog. Ser.*, 48, 69–80.
- Rand, B. & Melton, I. E. (1977). Particle interactions in aqueous kaolinite suspensions. *Journal of Colloid and Interface Science*, 60(2), 308–320.
- Razaz, M., Kawanisi, K., & Nistor, I. (2015). Tide-driven controls on maximum near-bed floc size in a tidal estuary. *Journal of Hydro-environment Research*, 9(3), 465–471.
- RD-Instruments (1994). Acoustic Doppler Current Profilers User's Manual.
- Ren, J. & Wu, J. (2014). Sediment trapping by haloclines of a river plume in the Pearl River Estuary. *Continental Shelf Research*, 82, 1–8.
- Reynolds, C. S. (2006). *Ecology of Phytoplankton*. Cambridge: Cambridge University Press.
- Reynolds, R. A., Stramski, D., Wright, V. M., & Woźniak, S. B. (2010). Measurements and characterization of particle size distributions in coastal waters. *Journal of Geophysical Research*, 115(C8).
- Riley, G. A. (1963). Organic aggregates in seawater and the dynamics of their formation and utilization. *Limnology and Oceanography*, 8(4), 372–381.
- Riper, D. M., Owens, T. G., & Falkowski, P. G. (1979). Chlorophyll Turnover in *Skeletonema costatum*, a Marine Plankton Diatom. *PLANT PHYSIOLOGY*, 64(1), 49–54.

- Rosen, M. J. (2004). *Surfactants and Interfacial Phenomena*. Hoboken, NJ, USA: John Wiley & Sons, Inc.
- Round, F. E. (1981). *The Ecology of Algae*. Cambridge [Eng.]; New York: Cambridge University Press.
- Sahin, C. (2014). Investigation of the variability of floc sizes on the Louisiana Shelf using acoustic estimates of cohesive sediment properties. *Marine Geology*, 353, 55–64.
- Sequoia Scientific, I. (2011). The Influence of Particles Outside the Size Range of the LISST. <http://www.sequoiasci.com/article/the-influence-of-particles-outside-the-size-range-of-the-lisst/>.
- Serra, T. & Casamitjana, X. (1998). Structure of the Aggregates During the Process of Aggregation and Breakup Under a Shear Flow. *Journal of Colloid and Interface Science*, 206(2), 505–511.
- Serra, T., Colomer, J., & Logan, B. E. (2008). Efficiency of different shear devices on flocculation. *Water Research*, 42(4-5), 1113–1121.
- Shakeel, A., Safar, Z., Ibanez, M., van Paassen, L., & Chassagne, C. (2020). Flocculation of clay suspensions by anionic and cationic polyelectrolytes: A systematic analysis. *Minerals*, 10(11), 999.
- Shao, Y., Yan, Y., & Maa, J. P.-Y. (2011). In Situ Measurements of Settling Velocity near Baimao Shoal in Changjiang Estuary. *Journal of Hydraulic Engineering*, 137(3), 372–380.
- Shen, X., Toorman, E. A., Lee, B. J., & Fettweis, M. (2018). Biophysical flocculation of suspended particulate matters in Belgian coastal zones. *Journal of Hydrology*, 567, 238–252.
- Sheng, G. & Yu, H. (2006). Characterization of extracellular polymeric substances of aerobic and anaerobic sludge using three-dimensional excitation and emission matrix fluorescence spectroscopy. *Water Research*, 40(6), 1233–1239.

- Sheng, G., Yu, H., & Li, X. (2010). Extracellular polymeric substances (EPS) of microbial aggregates in biological wastewater treatment systems: A review. *Biotechnology Advances*, 28(6), 882–894.
- Sherwood, C. R., Aretxabaleta, A. L., Harris, C. K., Rinehimer, J. P., Verney, R., & Ferré, B. (2018). Cohesive and mixed sediment in the Regional Ocean Modeling System (ROMS v3.6) implemented in the Coupled Ocean–Atmosphere–Wave–Sediment Transport Modeling System (COAWST r1234). *Geoscientific Model Development*, 11(5), 1849–1871.
- Smayda, T. J. & Boleyn, B. J. (1966). Experimental observations on the flotation of marine diatoms. II. *Skeletonema costatum* and *Rhizosolenia setigera*: Flotation of marine diatoms. *Limnology and Oceanography*, 11(1), 18–34.
- Søballe, D. M. & Threlkeld, S. T. (1988). Algal-clay flocculation in turbid waters: Variations due to algal and mineral differences: With 4 figures in the text. *SIL Proceedings, 1922-2010*, 23(2), 750–754.
- Sobeck, D. C. & Higgins, M. J. (2002). Examination of three theories for mechanisms of cation-induced bioflocculation. *Water Research*, 36(3), 527–538.
- Son, M. & Hsu, T. J. (2009). The effect of variable yield strength and variable fractal dimension on flocculation of cohesive sediment. *Water Research*, 43(14), 3582–3592.
- Sondi, I., Bišćan, J., & Pravdić, V. (1996). Electrokinetics of Pure Clay Minerals Revisited. *Journal of Colloid and Interface Science*, 178(2), 514–522.
- Soulsby, R. L., Manning, A. J., Spearman, J., & Whitehouse, R. J. S. (2013). Settling velocity and mass settling flux of flocculated estuarine sediments. *Marine Geology*, 339, 1–12.
- Spearman, J. R., Manning, A. J., & Whitehouse, R. J. S. (2011). The settling dynamics of flocculating mud and sand mixtures: Part 2—numerical modelling. *Ocean Dynamics*, 61(2-3), 351–370.
- Spencer, K. L., Manning, A. J., Droppo, I. G., Leppard, G. G., & Benson, T. (2010). Dynamic interactions between cohesive sediment tracers and natural mud. *Journal of Soils and Sediments*, 10(7), 1401–1414.

- Spicer, P. T. & Pratsinis, S. E. (1996). Coagulation and fragmentation: Universal steady-state particle-size distribution. *AIChE Journal*, 42(6), 1612–1620.
- Sterling, M. C., Bonner, J. S., Ernest, A. N., Page, C. A., & Autenrieth, R. L. (2004). Characterizing aquatic sediment–oil aggregates using in situ instruments. *Marine Pollution Bulletin*, 48(5-6), 533–542.
- Stolzenbach, K. D. & Elimelech, M. (1994). The effect of particle density on collisions between sinking particles: Implications for particle aggregation in the ocean. *Deep Sea Research Part I: Oceanographic Research Papers*, 41(3), 469–483.
- Stone, M. (2000). *The Role of Erosion and Sediment Transport in Nutrient and Contaminant Transfer*. Number 263 in IAHS Publication. Wallingford: International Association of Hydrological Sciences.
- Sutherland, T. F., Lane, P. M., Amos, C. L., & Downing, J. (2000). The calibration of optical backscatter sensors for suspended sediment of varying darkness levels. *Marine Geology*, 162(2), 587–597.
- Swenson, J., Smalley, M. V., & Hatharasinghe, H. L. M. (1998). Mechanism and Strength of Polymer Bridging Flocculation. *Physical Review Letters*, 81(26), 5840–5843.
- Takabayashi, M., Lew, K., Johnson, A., Marchi, A., Dugdale, R., & Wilkerson, F. P. (2006). The effect of nutrient availability and temperature on chain length of the diatom, *Skeletonema costatum*. *Journal of Plankton Research*, 28(9), 831–840.
- Tan, D., Yong, Y., Tan, H., Kamarulzaman, A., Tan, L., Lim, A., James, I., French, M., & Price, P. (2008). Immunological profiles of immune restoration disease presenting as mycobacterial lymphadenitis and cryptococcal meningitis. *HIV Medicine*, 9(5), 307–316.
- Tan, X., Hu, L., Reed, A. H., Furukawa, Y., & Zhang, G. (2014). Flocculation and particle size analysis of expansive clay sediments affected by biological, chemical, and hydrodynamic factors. *Ocean Dynamics*, 64(1), 143–157.
- Tang, J. (2007). Characteristics of Fine Cohesive Sediment's Flocculation in the Changjiang Estuary and Its Adjacent Sea Area (in Chinese). Master's thesis, East China Normal University, Shanghai.

- Thill, A., Moustier, S., Garnier, J.-M., Estournel, C., Naudin, J.-J., & Bottero, J.-Y. (2001). Evolution of particle size and concentration in the Rhône river mixing zone. *Continental Shelf Research*, 21(18-19), 2127–2140.
- Thomas, D. N., Bass, S. J., & Fawcett, N. (1999). Flocculation modelling: A review. *Water Research*, 33(7), 1579–1592.
- Thomas, R. H. & Walsby, A. E. (1985). Buoyancy Regulation in a Strain of Microcystis. *Microbiology*, 131(4), 799–809.
- Tolhurst, T. J., Gust, G., & Paterson, D. M. (2002). The influence of an extracellular polymeric substance (EPS) on cohesive sediment stability. In *Proceedings in Marine Science*, volume 5 (pp. 409–425). Elsevier.
- Tsai, C. & Hwang, S. (1995). Flocculation of sediment from the Tanshui River estuary. *Marine and Freshwater Research*, 46(1), 383.
- Tsujimoto, Y., Chassagne, C., & Adachi, Y. (2013). Comparison between the electrokinetic properties of kaolinite and montmorillonite suspensions at different volume fractions. *Journal of Colloid and Interface Science*, 407, 109–115.
- Uncles, R. J., Bale, A. J., Stephens, J. A., Frickers, P. E., & Harris, C. (2010). Observations of Floc Sizes in a Muddy Estuary. *Estuarine, Coastal and Shelf Science*, 87(2), 186–196.
- van der Lee, W. T. B. (2000). Temporal variation of floc size and settling velocity in the Dollard estuary. *Continental Shelf Research*, 20(12-13), 1495–1511.
- van Kessel, T., Winterwerp, H., Van Prooijen, B., Van Ledden, M., & Borst, W. (2011). Modelling the seasonal dynamics of SPM with a simple algorithm for the buffering of fines in a sandy seabed. *Continental Shelf Research*, 31(10), S124–S134.
- van Leussen, W. (1988). Aggregation of particles, settling velocity of mud flocs a review. In J. Dronkers & W. van Leussen (Eds.), *Physical Processes in Estuaries* (pp. 347–403). Berlin, Heidelberg: Springer Berlin Heidelberg.
- van Leussen, W. (1994). *Estuarine Macroflocs and Their Role in Fine-Grained Sediment Transport*. PhD thesis, University of Utrecht.

- van Leussen, W. (1997). The Kolmogorov microscale as a limiting value for the floc sizes of suspended fine-grained sediments in estuaries. *Cohesive sediments*, (pp. 45–62).
- van Leussen, W. (1999). The variability of settling velocities of suspended fine-grained sediment in the Ems estuary. *Journal of Sea Research*, 41(1-2), 109–118.
- van Maren, D. S. & Winterwerp, J. C. (2013). The role of flow asymmetry and mud properties on tidal flat sedimentation. *Continental Shelf Research*, 60, S71–S84.
- Verney, R., Lafite, R., & Brun-Cottan, J.-C. (2009). Flocculation potential of Estuarine particles: The importance of environmental factors and of the spatial and seasonal variability of suspended particulate matter. *Estuaries and Coasts*, 32(4), 678–693.
- Verney, R., Lafite, R., Claude Brun-Cottan, J., & Le Hir, P. (2011). Behaviour of a floc population during a tidal cycle: Laboratory experiments and numerical modelling. *Continental Shelf Research*, 31(10), S64–S83.
- Verspagen, J., Visser, P., & Huisman, J. (2006). Aggregation with clay causes sedimentation of the buoyant cyanobacteria *Microcystis* spp. *Aquatic Microbial Ecology*, 44, 165–174.
- Visser, P. M., Ibelings, B. W., & Mur, L. R. (1995). Autumnal sedimentation of *Microcystis* spp. as result of an increase in carbohydrate ballast at reduced temperature. *Journal of Plankton Research*, 17(5), 919–933.
- Walsby, A. E. (1968). Mucilage secretion and the movements of blue-green algae. *Protoplasma*, 65(1-2), 223–238.
- Wan, Y., Wu, H., Roelvink, D., & Gu, F. (2015). Experimental study on fall velocity of fine sediment in the Yangtze Estuary, China. *Ocean Engineering*, 103, 180–187.
- Wang, Y., Jiang, H., Jin, J., Zhang, X., Lu, X., & Wang, Y. (2015). Spatial-Temporal Variations of Chlorophyll-a in the Adjacent Sea Area of the Yangtze River Estuary Influenced by Yangtze River Discharge. *International Journal of Environmental Research and Public Health*, 12(5), 5420–5438.
- Wang, Y. P., Voulgaris, G., Li, Y., Yang, Y., Gao, J., Chen, J., & Gao, S. (2013). Sediment resuspension, flocculation, and settling in a macrotidal estuary: Flocculation

- and Settling in Estuary. *Journal of Geophysical Research: Oceans*, 118(10), 5591–5608.
- Wells, M. L. & Goldberg, E. D. (1993). Colloid aggregation in seawater. *Marine Chemistry*, 41(4), 353–358.
- Wilén, B. M., Lund Nielsen, J., Keiding, K., & Nielsen, P. H. (2000). Influence of microbial activity on the stability of activated sludge flocs. *Colloids and Surfaces B: Biointerfaces*, 18(2), 145–156.
- Wilkinson, N., Metaxas, A., Bricchetto, E., Wickramaratne, S., Reineke, T. M., & Dutcher, C. S. (2017). Ionic strength dependence of aggregate size and morphology on polymer-clay flocculation. *Colloids and Surfaces A: Physicochemical and Engineering Aspects*, 529, 1037–1046.
- Winterwerp, J. C. (1998). A simple model for turbulence induced flocculation of cohesive sediment. *Journal of Hydraulic Research*, 36(3), 309–326.
- Winterwerp, J. C. (1999). *On the Dynamics of High-Concentrated Mud Suspensions*. PhD thesis, TU Delft, Delft University of Technology.
- Winterwerp, J. C. (2002). On the flocculation and settling velocity of estuarine mud. *Continental Shelf Research*, 22(9), 1339–1360.
- Winterwerp, J. C., Manning, A. J., Martens, C., de Mulder, T., & Vanlede, J. (2006). A heuristic formula for turbulence-induced flocculation of cohesive sediment. *Estuarine, Coastal and Shelf Science*, 68(1-2), 195–207.
- Winterwerp, J. C. & Van Kesteren, W. G. M. (2004). *Introduction to the Physics of Cohesive Sediment Dynamics in the Marine Environment*. Burlington: Elsevier Science.
- Wood, E. J. F. (2014). *Microbiology of Oceans and Estuaries*. Amsterdam: Elsevier Science.
- Wu, B. (2015). *Study of algal distribution pattern and its correlation with environmental factors in Yangtze River Estuary area (in Chinese)*. PhD thesis, East China Normal University, Shanghai.

- Xia, X. M., Li, Y., Yang, H., Wu, C. Y., Sing, T. H., & Pong, H. K. (2004). Observations on the size and settling velocity distributions of suspended sediment in the Pearl River Estuary, China. *Continental Shelf Research*, 24(16), 1809–1826.
- Xu, Y., Li, X., Wang, H., & Zhang, B. (2016). Characteristics of a macrozoobenthic community in the sea adjacent to the Yangtze River estuary during the wet season. *Biodiversity Science*, 24(7), 811–819.
- Yao, H. Y., Leonardi, N., Li, J. F., & Fagherazzi, S. (2016). Sediment transport in a surface-advected estuarine plume. *Continental Shelf Research*, 116, 122–135.
- Yeh, K. (1988). *The Influence of Cations on Activated Sludge Behavior*. PhD thesis, Virginia Polytechnic Institute and State University.
- Yeung, A. K. C. & Pelton, R. (1996). Micromechanics: A New Approach to Studying the Strength and Breakup of Floes. *Journal of Colloid and Interface Science*, 184(2), 579–585.
- Yokoi, H. (2002). Flocculation properties of pectin in various suspensions. *Bioresource Technology*, 84(3), 287–290.
- Yokoi, H., Natsuda, O., Hirose, J., Hayashi, S., & Takasaki, Y. (1995). Characteristics of a biopolymer flocculant produced by *Bacillus* sp. PY-90. *Journal of Fermentation and Bioengineering*, 79(4), 378–380.
- Yun, C. (2004). *Recent Developments of the Changjiang Estuary (in Chinese)*. Beijing: China Ocean Press.
- Zhang, J., Wu, Y., Jennerjahn, T. C., Ittekkot, V., & He, Q. (2007). Distribution of organic matter in the Changjiang (Yangtze River) Estuary and their stable carbon and nitrogen isotopic ratios: Implications for source discrimination and sedimentary dynamics. *Marine Chemistry*, 106(1-2), 111–126.
- Zhang, J., Zhang, Q., Maa, J. P. Y., & Qiao, G. (2013). Lattice Boltzmann simulation of turbulence-induced flocculation of cohesive sediment. *Ocean Dynamics*, 63(9-10), 1123–1135.
- Zhang, Z. (1996). Studies on basic characteristics of fine sediment in Changjiang Estuary (in Chinese). *Journal of Sediment Research*, 1(01), 67–73.

- Zhao, L. & Gao, L. (2019). Dynamics of dissolved and particulate organic matter in the Changjiang (Yangtze River) Estuary and the adjacent East China Sea shelf. *Journal of Marine Systems*, 198, 103188.
- Zhu, Z., Ng, W., Liu, S., Zhang, J., Chen, J., & Wu, Y. (2009). Estuarine phytoplankton dynamics and shift of limiting factors: A study in the Changjiang (Yangtze River) Estuary and adjacent area. *Estuarine, Coastal and Shelf Science*, 84(3), 393–401.
- Zhu, Z., Zhang, J., Wu, Y., Zhang, Y., Lin, J., & Liu, S. (2011). Hypoxia off the Changjiang (Yangtze River) Estuary: Oxygen depletion and organic matter decomposition. *Marine Chemistry*, 125(1-4), 108–116.
- Zinkevich, V., Bogdarina, I., Kang, H., Hill, M. A. W., Tapper, R., & Beech, I. B. (1996). Characterisation of exopolymers produced by different isolates of marine sulphate-reducing bacteria. *International Biodeterioration & Biodegradation*, 37(3-4), 163–172.
- Zou, S., Gu, Y., Xiao, D., & Tang, C. Y. (2011). The role of physical and chemical parameters on forward osmosis membrane fouling during algae separation. *Journal of Membrane Science*, 366(1-2), 356–362.

# List of symbols

$a_{i,j}$	Collision efficiency	[-]
$b$	Empirical parameter	[-]
$d$	Media particle size of dispersed particles	[ $\mu\text{m}$ ]
$f_{i,j}$	Frequency of particle collision	[-]
$g$	Gravitational acceleration	[ $\text{m s}^{-2}$ ]
$n_j$	Number of flocs of a given size	[-]
$p$	Empirical parameter	[-]
$r$	Radius of the pipe	[mm]
$s_f$	Stirring rotations per second	[-]
$t_0$	Initial time	[s]
$t_{max}$	Time to reach steady state	[s]
$u$	Current velocity	[ $\text{m s}^{-1}$ ]
$u_*$	Friction velocity	[ $\text{m s}^{-1}$ ]
$z$	Height above bed	[m]
$B_i$	Dispersion frequency	[-]
$Blk_b$	Fluorometric of pure 90% acetone	[-]
$Blk_a$	Fluorometric of pure 90% acetone with 10% HCl	[-]
$C$	Salt concentration	[-]
$C_D$	Drag coefficient	[-]
$D_0$	Initial floc size	[ $\mu\text{m}$ ]
$D_{50}$	Floc media size	[ $\mu\text{m}$ ]
$D_f$	Floc size	[ $\mu\text{m}$ ]
$D_{major}$	Major-axis of each observed two-dimensional floc image	[ $\mu\text{m}$ ]
$D_{minor}$	Minor-axis of each observed two-dimensional floc image	[ $\mu\text{m}$ ]
$D_{max}$	Finally steady floc size	[ $\mu\text{m}$ ]
$E$	Empirical parameter	[-]
$F_a$	Fluorometric of sample with 90% acetone and 10% HCl	[-]
$F_b$	Fluorometric of sample with 90% acetone	[-]

$F_R$	Linear calibration factors	[-]
$G$	Shear rate	[s <sup>-1</sup> ]
$H$	Total water depth	[m]
$K$	Boltzmann constant	[J K <sup>-1</sup> ]
$L_j$	A given size of flocs	[-]
$N_f$	Three-dimensional fractal dimension	[-]
$N_p$	Two-dimensional fractal dimension	[-]
$Q$	Discharge	[m <sup>3</sup> s <sup>-1</sup> ]
$R_{Floc}$	Flocculation rate	[μm s <sup>-1</sup> ]
$Re$	Particle Reynolds number	[-]
$SSC$	Suspended Sediment Concentration	[g l <sup>-1</sup> ]
$T$	Absolute temperature	[K]
$TVC$	Total volume concentration	[μl l <sup>-1</sup> ]
$V_{EXT}$	Extraction volume by acetone extraction method	[l]
$V_F$	Total Floc volume concentration	[μl l <sup>-1</sup> ]
$V_{FILT}$	Filtrate volume of the water sample	[l]
$VC$	Volume concentration	[μl l <sup>-1</sup> ]
$\alpha$	Coefficients related to particle shape	[-]
$\beta$	Coefficients related to particle shape	[-]
$\gamma$	Coefficients related to particle shape	[-]
$\epsilon$	Turbulent energy dissipation rate	[-]
$\zeta$	Zeta potential	[μV]
$\eta$	Kolmogorov micro scale	[m]
$\kappa$	Von Karman's constant	[-]
$\mu$	Dynamic viscosity of water	[Pa s]
$\nu$	Kinematic viscosity of water	[m <sup>2</sup> s <sup>-1</sup> ]
$\rho_F$	Density of floc	[g l <sup>-1</sup> ]
$\rho_P$	Density of dispersed sediment particles	[g l <sup>-1</sup> ]
$\rho_W$	Density of water	[g l <sup>-1</sup> ]
$\tau$	Acidification coefficient	[-]
$\phi$	Electric surface potential	[-]
$\omega_s$	Floc settling velocity	[mm s <sup>-1</sup> ]
$\Delta\rho$	Floc effective density	[g l <sup>-1</sup> ]

# List of acronyms

ADCP	Acoustic Doppler Current Profiler
AR	Aspect Ratio
BM	Brownian Motion
CC	Chlorophyll Concentration
DLVO	Derjaguin, Landau, Verwey and Overbeek
DNA	Deoxyribonucleic acid
DS	Differential Settling
EPS	Extracellular Polymeric Substances
ETM	Estuary Turbidity Maximum
FPP	Fultoportula process
HPLC	High-Performance Liquid Chromatography
HWS	High Water Slack
IFPP	Intercalary fultoportula process
IREL	Infrared-emitting diode
IRPP	Intercalary rimoportula process
LISST	Laser In-Situ Scattering and Transmissometry
LWS	Low Water Slack
MFV	Maximum Flood Velocity
MEV	Maximum Ebb Velocity
NP	North Passage
NTU	Nephelometric Turbidity Units
OBS	Optical Back-Scatter sensor
OM	Organic Matter
PBE	Population Balance Equations
PRM	Path Reduction Modules
PSD	Particle Size Distribution
PSU	Practical Salinity Units
RPM	Rotations Per Minute
SH	Shear
SLS	Static Light Scattering
SP	South Passage
SPM	Suspended Particle Matter
SSC	Suspended Sediment Concentration
TEP	Transparent Exopolymer Particles
TFPP	terminal fultoportula process
TRPP	terminal rimoportula process
TS	Turbulent Shear
VDW	Van der Waals' force
WQM	Water Quality Multiprobe



# Acknowledgements

## FUNDERS AND INSTITUTIONS

This dissertation was supported by an agreement for joint supervision and dual diploma of doctoral research between Delft University of Technology (TUD) and East China Normal University (ECNU). The Doctoral Education was well performed under the joint supervision and responsibility of the two universities. Following financial sponsorships are acknowledged: the Natural Science Foundation of China (NSFC; 51320105005, 51739005, 41876091), the Chinese Scholarship Council (CSC), and other relevant funds.

## RELEVANT INVOLVED

I would like to thank all the people who, directly or indirectly, have contributed to the completion of my PhD degree.

First of all, I would like to thank my promoters, Prof. dr. Qing He and Prof. dr. Zheng Bing Wang. Prof. He gave me the opportunity to study for my PhD, and she has been very supportive throughout my PhD career, giving me many opportunities to practice and improve. Particularly in my research project, there were often many difficulties as I often had to try schemes that I had never tried before, but she was always there to support my planned scheme and make my research possible. In addition to the scientific gains, I have also benefited from other aspects, such as the vision and perspective on science, skills of communication, speech and eloquence, etc. Prof. Wang gave me a lot of help in the Netherlands, especially in the process of applying for joint degree. In addition, Prof. Wang gave me lots of constructive suggestions in scientific research. I really appreciate the way they trusted my work and the freedom I had during the project. In particular, I really thanks to Prof. dr. Han Winterwerp, his invitation letter let me able to go to TUDelft, he also gave me a lot of advice although he was retired when I was in TUDelft.

Next, I would like to express a warm thanks to my daily supervisor (co-promotor), Prof. dr. Claire Chassagne. First of all, I would like to thank her for her constant supervision, encouragement and enthusiastic about helping me with the many tedious and

complicated administrative documents in the Netherlands, without which I would not have been able to complete my joint-PhD degree. Secondly, her disciplinary background from colloid chemistry helped me immensely in my research and brought new knowledge and ideas to my study of sediment flocculation. She also guided me through the theoretical knowledge of colloid chemistry to refine my flocculation theory. She also actively helped me establish contacts with various scholars and often invites me to participate in seminars, collaborative experiments, etc. Finally, she is a very, very enthusiastic and nice person. She helped me with all my problems, especially with the editing of my essays and thesis. In addition, she helped me to integrate into Dutch life by inviting me to dinners and social events. I also would like to thank Claire for all the nice conversations in both research and daily life. Especially, many other professors have provided valuable feedback on my research work, such as Prof. Andy Manning, Prof. Peter Hermes, etc.

I sincerely appreciate SKLEC which is a platform full of opportunities and challenges. I also want to thank my advisors Leicheng Guo, Xianye Wang, Jian Shen, their expertise made it possible for me to do my research with less effort. And Prof. Fang Shen, who provided professional advice, equipment and personnel for my research in biological research. Thank Prof. Zhanghua Wang, Prof. Weiguo Zhang, Prof. Daoji Li, Prof. Lei Gao, Prof. Zhuoyi Zhu and all the other teachers for giving me suggestions and answering my questions in my research career. Thank Guo'an Zhang, Wei Li, Junhong Li, Can Jin, Xiaoli Huo, Li Tan and Hong Jiang for their administrative support. Thank Jinghua Gu, Wenxiang Zhang for their help in field instrument use; thank Ruiming Wu and Lingxiang Wang for their technical support. Specially, I sincerely thank all the Sediment research Group (424/313) officemates: Jie Zhao, Lei Zhu, Weiming Xie, Dai Zhang, Chao Guo, Qin Zhu for shearing their research experiments and research skills knowledge, especially, Chao Guo guided me to use LISST and flocculation and Dai Zhang help me a lot in daily life. And thank Yu Chen, Chaofeng Xing, Jianliang Lin, Chunyan Zhu, Jie Jiang, Yu Qiao, Yi Shen, Shuai Liu, Yuning Zhang, Jianwei Sun, Zhonghao Zhao, Shang Yu, Xuefeng Wu, Simin Zhou, Zhongquan Hou, Qinze Chen, and other colleagues for their accompany in everyday life and support, and our unforgettable experience in the field campaign! Thank Xiaodao Wei, Yangyang Liu, Xuerong Sun for their support in chlorophyll experiments, and other SKLEC students for everyday moments shared with them.

I would like to thank TUDelft and Deltares that provide me with platforms to finish the experiments research work. Special thanks to Prof. dr. Thijs van Kessel for Dutch translation, and other professors for useful discussions. Also, thanks a lot to my colleagues in the Netherlands—Zeinab Safar, Alex, Chunyan Zhu, Sabine and many other colleagues in Water Lab and Deltares for the good vibes. I would like to especially thank Zeinab Safar, she helped me a lot with my research in the Netherlands, especially with the experimental research part. Talking to her also gives me a lot of knowledge about flocculation since our research topics are similar. And Chunyan Zhu, before arriving in the Netherlands, she helped me apply for housing, school procedures, etc. In addition, as a student of Prof. Wang, she helped me a lot in my studies and life, and brought me to many friends, such as Zhiling Zhang. And my friends who played volleyball with me, you brought me a rich extracurricular life, especially Xueyuan Wu, Xiaoyu Xu, Xuehan Jiang, Xuchao Yu and other friends, not only organized a lot of activities, but also took me on trips around, which made me feel that my life in the Netherlands is no longer lonely. And thank other people who helped me with my life when I first came to TUDelft, such as Na Li and others. Finally, thanks to the secretaries who handled my paperwork.

And in the end, I would like to thank my family for their support and help. The time spent on my PhD studies was very long, but they have given me the greatest support and encouragement, which helped me to persevere in times of difficulties.



# List of Publications

## Journal articles

- Z. Deng**, Q. He, C. Chassagne, Z. B. Wang, *Seasonal variation of floc population influenced by the presence of algae in the Changjiang (Yangtze River) Estuary*, *Marine Geology* **106600**, 440 (2021).
- Z. Deng**, Q. He, Z. Safar, C. Chassagne, *The role of algae in fine sediment flocculation: in-situ and laboratory measurements*, *Marine Geology* **71–84**, 413 (2019).
- C. Chassagne, Z. Safar, **Z. Deng**, Q. He, A. J. Manning, *Flocculation in Estuaries: Modeling, Laboratory and In-situ Studies*, in: *Sediment Transport - Recent Advances* (2021).
- Z. Deng**, Q. He, A. J. Manning, C. Chassagne, *A laboratory study on the behavior of estuarine sediment flocculation as function of salinity, EPS and living algae*. (Submitted)
- Z. Deng**, Q. He, C. Xing, L. Guo, X. Wang, *Sediment depositional characteristics of North Passage in the Yangtze River Estuary*, *Marine Sciences* **112–122**, 40 (2016). (in Chinese)
- Z. Deng**, Q. He, Q. Yang, J. Lin, *Observations of in situ flocs character in the Modaomen Estuary of the Pearl River*, *Haiyang Xuebao* **152–161**, 37 (2015). (in Chinese)
- S. Yu, Q. He, Y. Chen, **Z. Deng**, *Response of suspended sediment particle size to sediment reduction in the Yangtze Estuary turbidity maximum zone*, *Journal of Sediment Research* **60–67**, 46 (2021). (in Chinese)
- J. Lin, Q. He, Q. Yang, **Z. Deng**, *Study on sediment flocculation mechanism at Modaomen in the Pearl River Estuary in flood season*, *Journal of Sediment Research* **304–313**, 42 (2017). (in Chinese)
- C. Xing, Q. He, L. Guo, **Z. Deng**, *Application of ASM at the bottom observation of suspended sediment concentration*, *Journal of Sediment Research* **46–51**, 06 (2015). (in Chinese)
- C. Xing, Q. He, **Z. Deng**, X. Wang, L. Guo, *Study of sediment grain sizes and sources for the short cores collected from the North Passage of Yangtze estuary*, *Marine Geology & Quaternary Geology* **9–17**, 35 (2015). (in Chinese)

## Conference proceedings, abstracts and talks

- Oral presentation.** Flocculation influenced by the presence of algae in the Changjiang Estuary. 2021 The 16<sup>th</sup> International Conference on Cohesive Sediment Transport Processes (INTERCOH 2021).
- Oral presentation.** Seasonal variation of sediment flocculation and the modeling thereof as function of biochemical factors. 2017 The 14<sup>th</sup> International Conference on Cohesive Sediment Transport Processes (INTERCOH 2017).
- Oral presentation.** Biomass effects on cohesive sediment flocculation—a case study in the Yangtze Estuary, China. Physics of Estuaries and Coastal Seas Conference 2016 (PECS 2016).
- Poster.** Flocculation influenced by the presence of algae in the Changjiang Estuary. The 7<sup>th</sup> International Conference on Estuaries and Coasts (ICEC 2021).

# Curriculum Vitæ

Zhirui Deng was born on the 10<sup>th</sup> September 1990 in Guangxi, China. After high school, he started his studies in Marine Resources of Biology and Environment at Marine School of Sun Yat-Sen University from 2009 to 2013. In June 2013, he awarded the Bachelors' Degree in Science.

Since September of 2013, he was recommended to directly continue his PhD study in Estuarine and Coastal Research at the Department—State Key Laboratory of Estuarine and Coastal Research (SKLEC) of East China Normal University (ECNU), promoted by Prof. dr. Qing He. He received the funding of Chinese Scholarship Council (CSC) and became a joint-doctoral PhD student Department of Hydraulic Engineering at TU Delft since October 2016, under the supervision of dr. ir. Claire Chassagne and Prof. dr. ir. Zheng Bing Wang. His research topic is the sediment dynamics and flocculation processes based on in-situ observations and laboratory measurements.